40211

National Library of Canada | Bibliothèque nationale du Canada

CANADIAN THESES ON MICROFICHE | THÈSES CANADIENNES SUR MICROFICHE

NAME OF AUTHOR/*NOM DE L'AUTEUR* JANICE ELIZABETH KUSTER

TITLE OF THESIS/*TITRE DE LA THÈSE* COMPARATIVE STRUCTURE AND FUNCTION OF COMPOUND EYES OF CICINDELIDAE and CARABIDAE (COLEOPTERA): Evolution of Scotopic and Photopic Eyes and Fine Structure of Photopic cicindelid Eyes.

UNIVERSITY/*UNIVERSITÉ* University of Alberta

DEGREE FOR WHICH THESIS WAS PRESENTED/*GRADE POUR LEQUEL CETTE THÈSE FUT PRÉSENTÉE* Ph.D

YEAR THIS DEGREE CONFERRED/*ANNÉE D'OBTENTION DE CE GRADE* 1978

NAME OF SUPERVISOR/*NOM DU DIRECTEUR DE THÈSE* DR. D.A. CRAIG

Permission is hereby granted to the NATIONAL LIBRARY OF CANADA to microfilm this thesis and to lend or sell copies of the film.

The author reserves other publication rights, and neither the thesis nor extensive extracts from it may be printed or otherwise reproduced without the author's written permission.

L'autorisation est, par la présente, accordée à la BIBLIOTHÈQUE NATIONALE DU CANADA de microfilmer cette thèse et de prêter ou de vendre des exemplaires du film.

L'auteur se réserve les autres droits de publication; ni la thèse ni de longs extraits de celle-ci ne doivent être imprimés ou autrement reproduits sans l'autorisation écrite de l'auteur.

DATED/*DATÉ* June 15, 1978 SIGNED/*SIGNÉ* Janice E. Kuster

PERMANENT ADDRESS/*RÉSIDENCE FIXE* 1512 - 1333 Bloor Street, East
Mississauga, Ontario
L4Y 3T6

NOTICE

The quality of this microfiche is heavily dependent upon the quality of the original thesis submitted for microfilming. Every effort has been made to ensure the highest quality of reproduction possible.

If pages are missing, contact the university which granted the degree.

Some pages may have indistinct print especially if the original pages were typed with a poor typewriter ribbon or if the university sent us a poor photocopy.

Previously copyrighted materials (journal articles, published tests, etc.) are not filmed.

Reproduction in full or in part of this film is governed by the Canadian Copyright Act, R.S.C. 1970, c. C-30. Please read the authorization forms which accompany this thesis.

THIS DISSERTATION
HAS BEEN MICROFILMED
EXACTLY AS RECEIVED

AVIS

La qualité de cette microfiche dépend grandement de la qualité de la thèse soumise au microfilmage. Nous avons tout fait pour assurer une qualité supérieure de reproduction.

S'il manque des pages, veuillez communiquer avec l'université qui a conféré le grade.

La qualité d'impression de certaines pages peut laisser à désirer, surtout si les pages originales ont été dactylographiées à l'aide d'un ruban usé ou si l'université nous a fait parvenir une photocopie de mauvaise qualité.

Les documents qui font déjà l'objet d'un droit d'auteur (articles de revue, examens publiés, etc.) ne sont pas microfilmés.

La reproduction, même partielle, de ce microfilm est soumise à la Loi canadienne sur le droit d'auteur, SRC 1970, c. C-30. Veuillez prendre connaissance des formules d'autorisation qui accompagnent cette thèse.

LA THÈSE A ÉTÉ
MICROFILMÉE TELLE QUE
NOUS L'AVONS REÇUE

THE UNIVERSITY OF ALBERTA

COMPARATIVE STRUCTURE AND FUNCTION OF COMPOUND EYES OF CICINDELIDAE AND CARABIDAE (COLEOPTERA): EVOLUTION OF SCOTOPIC AND PHOTOPIC EYES AND FINE STRUCTURE OF PHOTOPIC CICINDELID EYES

by

© JANICE ELIZABETH KUSTER

A THESIS

SUBMITTED TO THE FACULTY OF GRADUATE STUDIES AND RESEARCH

IN PARTIAL FULFILMENT OF THE REQUIREMENTS FOR THE DEGREE

OF DOCTOR OF PHILOSOPHY

DEPARTMENT OF ENTOMOLOGY

EDMONTON, ALBERTA

FALL, 1978

THE UNIVERSITY OF ALBERTA

FACULTY OF GRADUATE STUDIES AND RESEARCH

The undersigned certify that they have read, and recommend to the Faculty of Graduate Studies and Research, for acceptance, a thesis entitled Comparative Structure and Function of Compound Eyes of Cicindelidae and Carabidae (Coleoptera): Evolution of Scoptic and Photopic Eyes and Fine Structure of Photopic cicindelid Eyes submitted by Janice Elizabeth Kuster in partial fulfilment of the requirements for the degree of Doctor of Philosophy in Entomology.

D A Craig
.....
Supervisor

Mara E. Zalik
.....

B K McLeod
.....

.....

Stanley D Carlson
.....
External Examiner

Date May 24th 1978

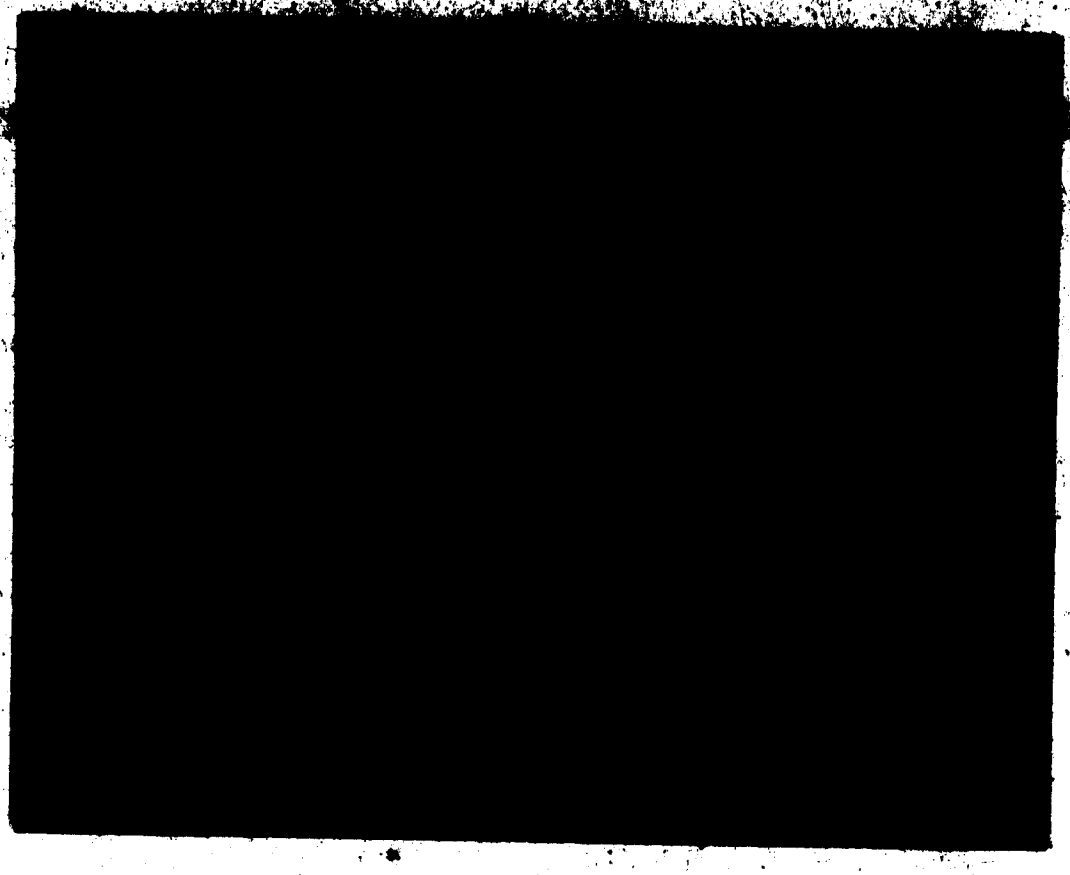

Frontal section through the head of a Cicindela tranquebarica Herbst adult stained with Mallory's triple stain.

Scale = 300 µm

ABSTRACT

Compound eyes of males of Amblychella schwarzi W. Horn, Omus californicus californicus W. Horn, Megacephala carolina mexicana Gray, and Cicindela tranquebarica Herbst, North American Cicindelidae, were examined by light, Nomarski interference, and scanning electron microscopies. Using a "goniometric field of view" apparatus, angles of visual fields were determined then plotted on Mollweide homolographic projections. This included deriving a formula to calculate monoscopic, stereoscopic, and blind regions both in steradians and as a percentage surface area of the homolographs. Eyes of A. schwarzi adults have both the largest monoscopic and blind areas; those of C. tranquebarica adults, the largest stereoscopic areas of the visual field.

Intergeneric statistical analyses were made using data from visual field areas and from measurements of eye structures. Comparisons based on eye size showed two groups: small eyes, nocturnal A. schwarzi and nocturnal O. californicus; and large eyes, crepuscular M. carolina and diurnal C. tranquebarica adults. Three categories for eye function were shown: scotopic A, A. schwarzi and M. carolina; scotopic B, O. californicus; and photopic, C. tranquebarica adults. Photopic eyes also occur in these

other cicindelids examined: C. belfragei Saylé, C. limbata nympha Casey, C. limbalis Klug, C. repanda repanda Dejean, and C. longilabris Say. However, eyes of crepuscular adults of C. lepida Dejean are scotopic A, although [redacted] beetles are in the large eye group. The plesiot[redacted]r state of eye structure and function in [redacted]ts is scotopic A; the apotypic state is photopic. C. lepida adults have secondarily evolved scotopic A eyes.

Cicindelid eye structure and function was compared with that of two representatives of their probable sister taxon, the Carabidae. Adult nocturnal Pterostichus melanarius Illiger are small-eyed and in the scotopic B functional category; diurnal Elaphrus americanus Dejean are large-eyed and photopic. It is concluded that scotopy and photopy have evolved through parallelism in these sister taxa.

All beetle eyes examined are eucone and have a "subcorneal layer" between corneal lenses and crystalline cones. They have a distal rhabdomere composed of microvilli only from retinula cell seven, a more proximal, rectangular fused rhabdom formed from six retinula cells, and a basal eighth retinula cell with a spherical rhabdomere. Eyes of diurnal and crepuscular beetles are large and bulbous with interfacetal mechanoreceptors.

The cellular fine structure of photopic eyes of

C. tranquebarica was further examined by scanning electron and transmission electron microscopies. The subcorneal layer has lamellae of endocuticle consisting of microfibrils having a chitin core with protein deposits along their lengths. In surface view this layer consists of concave polygons. Extensions of the crystalline thread form inter-retinular fibers containing microtubules between retinula cells 1/2, 3/4, 5/6, and 7/1. Two primary pigment cells are devoid of pigment granules, but are rich in rough endoplasmic reticulum. Proximal to each retinula cell nucleus are two basal bodies, one perpendicular to the other. The proximal basal body extends two fibrillar feet which fuse to form a horizontally banded ciliary rootlet which extends the retinula length peripheral to the rhabdom. Multivesicular and onion bodies are near the proximal rhabdom and onion bodies are also in some of the 16 secondary pigment cells. Other secondary pigment cells contain pigment granules and some contain vesicles surrounded by microtubules.

Interfacetal mechanoreceptors have a single biopolar innervation with a typical dendritic sheath, tubular body, cilium, outer and inner sheath cells, and an axon surrounded by a neurilemma sheath cell.

Structures are discussed in relation to their function in the eye. It is postulated that the opsins of visual

pigments may be synthesized in either the primary pigment and/or retinula cells. Visual proteins are probably hydrolyzed in multivesicular and onion bodies. Lipid droplets surrounding the ocular sclerite may store vitamin A_1, the precursor of the visual chromophore.

"When we reflect on these facts, here given much too briefly, with respect to the wide, diversified, and graduated range of structure in the eyes of the lower animals; and when we bear in mind how small the number of all living forms must be in comparison with those which have become extinct, the difficulty ceases to be very great in believing that natural selection may have converted the simple apparatus of an optic nerve, coated with pigment and invested by transparent membrane, into an optical instrument as perfect as is possessed by any member of the Articulate Class."

-- Darwin (1859)

ACKNOWLEDGEMENTS

Creative scientific research demands imagination, intuition, and reason from the investigator (Beveridge, 1950). Formulation of new hypotheses and analyses of experimental results rely on new associations and fresh ideas from a varied store of memories and experiences. To this end, the researcher is dependent not only upon himself, but his colleagues to provide stimulation for inventive research and for applying new information to the current paradigm (Kuhn, 1970) in his area of specialization.

I acknowledge Dr. R. Freitag, Department of Biology, Lakehead University, for introducing me to the diversity of entomology during my association with him as a research assistant in my undergraduate years. I thank my supervisor, Dr. D.A. Craig, for his generous and full cooperation during the course of my graduate experiences. For discussions concerning my progress and for critically reading the manuscript, I thank my committee members: Dr. G.E. Ball and Dr. B.K. Mitchell, Department of Entomology, and Dr. S.E. Zalik, Department of Zoology.

Several people were involved in collection of beetles used in this investigation. I thank Dr. G.E. Ball for collection of *Megacephala carolina mexicana* Gray in Mexico, and D.H. Kavanaugh, California Academy of Science, for field

assistance at Point Reyes National Seashore, California to collect Omus californicus californicus W. Horn adults. Also I thank Dr. E.L. Sleeper, California State University, Long Beach, for his enthusiasm for my project and his student, W.E. Mispagel for a memorable collection of Amblycheila schwarzi W. Horn adults in the Mohave Desert of Southern California. For an interesting discussion and display of his world cicindelid collection, I thank W.D. Sumlin III of Riverside, California. I thank R.R. Murray, Texas A & M University for specimens of Cicindela belfragei Sallé, my colleague G.J. Hilchie for specimens of Cicindela lepida Dejean, and K.A. Shaw for local field assistance.

For expert consultation on transmission electron microscope techniques and for the use of his facilities, I thank Dr. S.K. Malhotra of the University of Alberta, his research associate, Dr. J.C. Tu, for his assistance in freeze-etch experiments, and his technician, H.W. Batz, for maintenance of the microscopes. I also acknowledge the skillful operation of the scanning electron microscope by G.D. Braybrook of the Department of Entomology. I thank Dr. D.D. Cass, Department of Botany, for use of his photomicroscope with Nomarski interference optics and Dr. R.A. Burwash, Department of Geology, for discussions of optical minerology and use of the polarizing petrographic microscope.

Gratefully acknowledge Dr. [illegible] Evans, Department of Entomology, for the use of his experimental goniometric apparatus. I extend my appreciation also to Dr. [illegible] Department of [illegible] for assistance in choosing appropriate computer statistical tests for analysis of numerical data; Dr. E.H. Pinnington, Department of Physics, for a discussion in optics of lenses, and J.A. Brooke, Department of Mathematics, for teaching me the rigors of solid angle geometry. Also I thank J.S. Scott, Department of Entomology, for photographing the frontispiece and for darkroom technical advice.

For stimulating conversations on aspects of examination of cellular ultrastructure I thank Dr. D.J. Peteya, Department of Zoology, and Cpt. Ruth Lynn Hooper Ph.D., LAIR, Presidio of San Francisco. I also thank my colleagues, Dr. H. Goulet, and K.R. Parker, for their discussions in systematic and biochemical aspects of entomology. For their emotional awareness throughout this study, I appreciate my family; and close friends: T.P. Carter and D.A. Hildebrandt.

This research was funded by a Gulf Oil Canada Limited Graduate Student Fellowship and by the Department of Entomology, The University of Alberta.

TABLE OF CONTENTS

Chapter

Chapter Page

LIST OF TABLES

LIST OF FIGURES

LIST OF ABBREVIATIONS

The following important abbreviations have been used in the thesis besides those specified in the text:

α:	level of statistical significance
ATP:	adenosine triphosphate
cm:	centimeter
Fig.:	figure
h:	hour
km:	kilometer
kV:	kilovolt
LM:	light microscopy
mm:	millimeter
n:	sample size or refractive index
NAD:	nicotinamide adenine dinucleotide
NIM:	Nomarski interference microscopy
nm:	nanometer = $1(10^{-9})$m
SEM:	scanning electron microscopy
sp.:	species
TEM:	transmission electron microscopy
μm:	micrometer = $1(10^{-6})$m
$\bar{x} \pm$ SE:	mean of a sample $\pm$ standard error
τ:	lambda = wavelength

1. General Introduction

Eyes stimulated by various wavelengths of light, elicit neuronal responses and provide animals with vision. Adult insects have evolved a compound eye composed of functional groups termed ommatidia, each with a lens and retinal structural component. Selected reviews on insect eye structure include: Fernández-Morán, 1958; Ruck, 1964; Trujillo-Cenóz, 1966; Gribakin, 1969 (in Russian); and Trujillo-Cenóz, 1972. Reviews discussing structural and physiological aspects of insect vision are: Buddenbrock, 1935; Goldsmith, 1964; Bernhard, 1965; Wolken, 1968; Mazokin-Porshnyakov, 1969; and Goldsmith and Bernard, 1974. Neurophysiological central nervous system information processing for vision, including intensity-evaluating systems, colour-selecting systems, and pattern recognition systems are reviewed in the proceedings of a symposium by Wehner (1972) which I reviewed elsewhere (Kuster, 1973). Current biophysical explanations of photoreceptor optics are discussed by Bernhard et al. (1972), and in the proceedings for a workshop by Snyder and Menzel (1975). Included in the latter treatment is an explanation of the mechanism for polarized light detection in compound eyes. Biochemical and physiological aspects of visual pigments involving the chromophore, 11-cis retinal (vitamin A_1 aldehyde), bonded to an opsin

(protein) as the photochemical intermediate in the transduction mechanism to all-trans retinal plus opsin are discussed in the proceedings of a symposium edited by Langer (1973). A comprehensive review on most apsects of insect vision is in a recent book edited by Horridge (1975).

No scientist by training or inclination, can experiment and be critical in all the heterogeneous aspects of vision research. Considering this premise, the first part of this thesis answers questions concerning structure and function of cicindelid compound eyes as an adaptation to the environments in which they live. Eyes of males of one species of each of the four North American genera of Cicindelidae (Coleoptera) were examined. Beetles used were adults of Amblycheila schwarzi W. Horn; Omus californicus californicus W. Horn; Megacephala carolina mexicana Gray; Cicindela tranquebarica Herbst. Since adults of Cicindela lepida Dejean and Cicindela belfragei Sallé have apparently become secondarily crepuscular, their eye structures are also described to determine if these eyes have evolved in response to this behavioural adaptation.

The question arises as to why tiger beetles were chosen for a detailed examination of eye structure and function from an evolutionary approach. This bias is based on my hypothesis that since there is a behavioural transformation series from a plesiotypic (ancestral) nocturnal to crepuscular to the apotypic (derived) diurnal diel activity

within the four North American genera of cicindelids (Chapter 2), that there may also be a parallel transformation series in structure and function of their compound eyes. I therefore believe this to be an appropriate family to work with in attempting to infer evolution of eye structure and function in relation to diel activity.

The only detailed research on larval stemmata and adult compound eye structure and function of some species of Cicindela is that by Friedrichs (1931). On questioning the structural attributes of eyes of individuals of other cicindelid genera, he wrote (translated from German):

> "It would be particularly interesting to establish in what manner the eyes of these nocturnal and crepuscular cicindelines have been adapted to their way of life: it may well be assumed that superposition [scotopic] eyes with pigment displacement have been formed, while the day-running or flying cicindelines possess apposition [photopic] eyes (like Cicindela)."

To answer some of Friedrichs' questions, this presentation provides the following:

1. Descriptions of a method for quantifying stereoscopic and monoscopic visual field areas and a discussion of their behavioural significance (Chapter 3).
2. Descriptions of the cellular organization of these beetles based on histological examination (Chapter 4).
3. Descriptions of the relationships between visual field areas and eye structure to eye size groups (Chapter 4).

4. Descriptions of the relationships between eye structure and function by grouping structures of these compound eyes into scotopic and photopic functional categories (Chapter 4).
5. Descriptions of the relationships between eye size groups, functional eye categories, and diel time of activities in terms of a reconstructed phylogeny of the Cicindelidae (Chapter 4).

Structure and function of cicindelid eyes are then compared to eyes of individuals of their probable sister group, the Carabini, to determine if carabids with similar diel activity have evolved similar eye structures. To answer this question, eyes of adults of nocturnal Pterostichus melanarius Illiger, and diurnal Elaphrus americanus Dejean are described. Eye structure is then related to eye size groups and eye functional categories of the cicindelids and the phylogeny of these sister taxa (Chapter 4).

From examination of the fine structural cellular organization for vision in eyes of Cicindela tranquebarica Herbst adults, conclusions are made in Chapter 5 concerning function of this derived cicindelid eye.

Although Eakin (1966; 1972) discussed evolution of the structure of invertebrate photoreceptors at the class level, and Wolken (1975) considered evolution of photoprocesses and photoreceptors in invertebrate and vertebrate phyla, most literature on insect compound eye structure and

function, gives only descriptions of single species. Studies on eyes are therefore required in closely related genera and species. By intergeneric and interspecific comparisons of cicindelid and carabid beetle compound eyes, this investigation begins to fill this void in understanding the evolution of insect eyes. Although not as detailed as this study, there have been other contributions toward this end. Scott (1937) discussed the relationship of eye shape and number of ommatidia to diel activity and feeding behaviour for several families in many insect orders. Pritchard (1966) compared angles of visual fields, interommatidjal angle, diameter of corneal lenses, and pigment distribution of adult anisopteran dragonflies belonging to 64 Australian species. These observations were discussed in relation to their role in prey capture and diel activity. Japanese workers have estimated diel activity of insects based on internal structures of insect eyes: several families of Lepidoptera (Yagi and Koyama, 1963a; 1963b); bombycid and saturniid moth genera (Koyama, 1964); genera of lamellicorn leaf-chafer beetles (Gokan, 1973); and cerambycid beetle genera (Koyama et al., 1975). By examining compound eye structure, Yagi (1953) determined the taxonomic position of the Hesperiidae (Lepidoptera). Yagi (1951) stated that the pseudopupil provides valid evidence for the relationship of various families of Lepidoptera. He postulated that the origin of a species begins from the differences of the sense organ which perceives the mate and

since visual cues are dominant in butterfly courtship, the origin of a species begins with a change in eye structure! From a reconstructed phylogeny of the brachyceran and cyclorrhaphan Diptera, Wada (1975) used 48 species of 26 families to discuss evolutionary trends of two retinal structural types. However, he did not correlate diel activity or mechanisms of prey capture to eye structure as this study attempts to do.

2. Taxonomic and Ecological Considerations

Within the order Coleoptera, suborder Adephaga, there are four North American genera of Cicindelidae (Amblycheila, Omus, Megacephala, and Cicindela) grouped into the tribes Megacephalini and Cicindelini (Schaupp, 1883; Horn, 1908-1915; translated by Willis, 1969; Leng, 1920; 1926; Bradley, 1930; Arnett, 1946; Hatch, 1953; and Arnett, 1968). However, earlier workers include Amblycheila and Omus in the tribe Mantichorini, Megacephala in Megacephalini; and Cicindela in Cicindelini (Lacordaire, 1843; 1854; and Thompson, 1857). The dendrogram (Fig. 1) represents a reconstructed phylogeny, based on the classification of Horn (1926), to show cladistic relationships of the taxa studied by me. The compound eye structure and function is incorporated into this phylogenetic framework (Section 4.4.6).

Adults of genera included in the subtribe Omina are nocturnal and have relatively small heads and small eyes (Schaupp, 1883; Vaurie, 1955), while adult megacephalines are crepuscular with large heads and bulbous eyes (Horn, 1908-1915). Secondarily, adult omines are incapable of flight. Adult cicindelines are diurnal and have large heads with prominent eyes and are generally capable of flight though there are some exceptions (Leng, 1902; Horn, 1908-1915; and Arnett, 1968).

Reconstructed Phylogeny of North American Genera of Cicindelidae, Based on Horn, 1926.

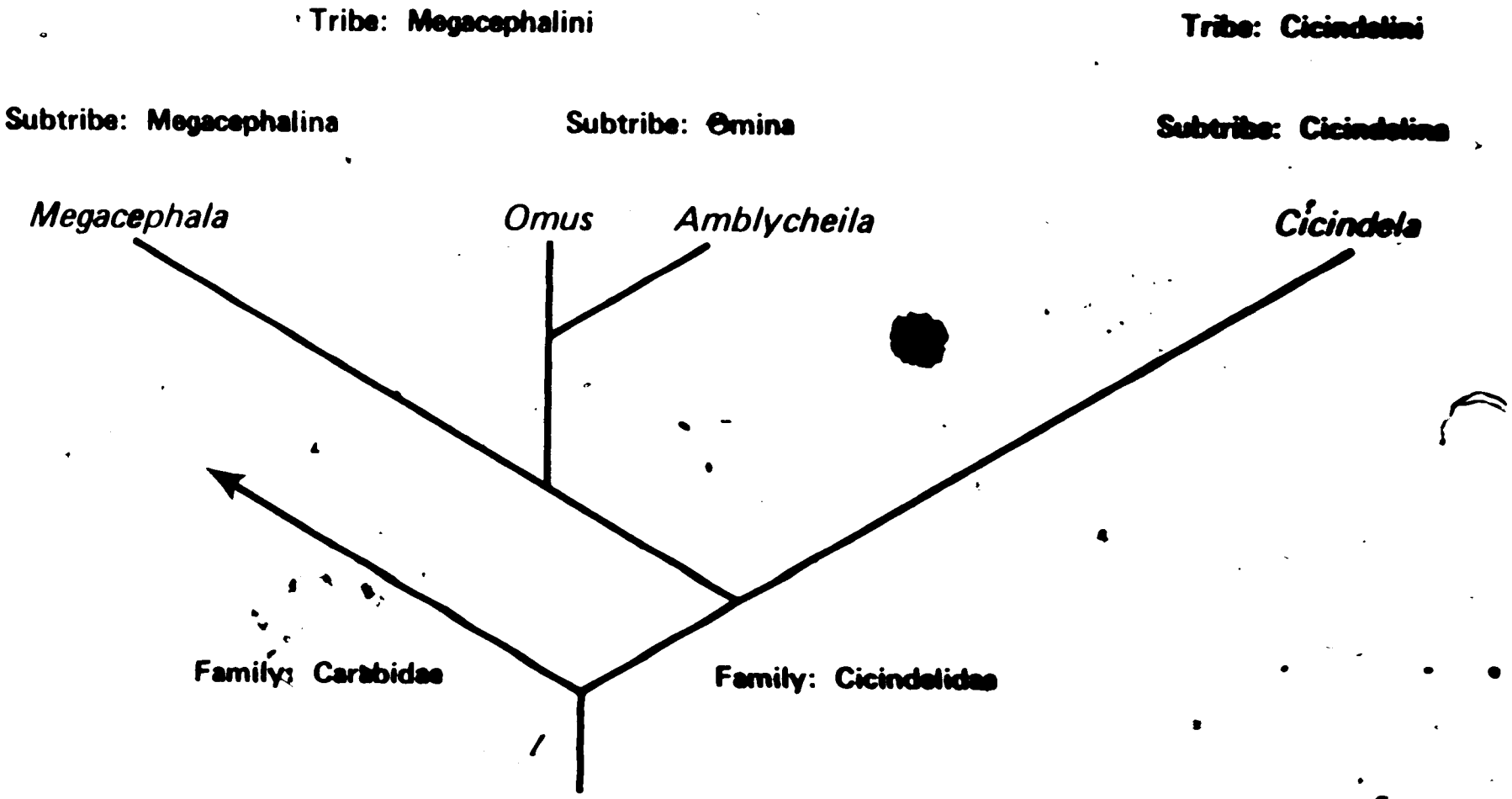

Adults of Amblycheila are nocturnal (Snow, 1877; Brous, 1877; Schaupp, 1883; Horn, 1908-1915; Vaurie, 1955; and Kuster, 1976), however, during warm and humid days they have been observed to leave their self-dug holes or their shelter in kangaroo rat burrows (Williston, 1877; Horn, 1908-1915; translated by Lawton, 1972). Amblycheila adults are flightless and inhabit semi-arid regions at high altitude (Vaurie, 1955). Adults of A. schwarzi W. Horn (Fig. 2) were identified using the Keys of Horn (1926) and Vaurie (1955). On a June night solitary adults were collected among boulders in the quartz, monzonite granite, canyon wash of Upper Covington Flat in Joshua Tree National Monument, Riverside County, California (Kuster, 1976).

Adults of Omus are generally nocturnal (Edwards, 1875; Schaupp, 1883; Leng, 1902; and Horn, 1908-1915), but are diurnal during the spring mating season (Horn, 1908-1915). Mark, release, and recapture records of adult O. audouini Reiche and of O. dejeani Reiche indicate that these beetles are active during all hours (Maser and Beer, 1971). Adults hide under stones, wood, bark, or soil, usually on dry substrates far from water (Horn, 1908-1915). Adults of Omus californicus californicus W. Horn (Fig. 3) used here were identified using keys of Horn (1926; 1930). Specimens were trapped by pitfall in Sonoma County, California, 4 km southeast of Anguin, by D.H. Kavanaugh, and I collected others at near darkness in June at the forest/beach interface of McClures Beach, Point Reyes National Seashore, Marin County,

Figs. 2-5. Dorsal aspect of four adult cicindelid beetles used in this investigation.

Scale = 5 mm

Fig. 2. Amblycheila schwarzi W. Horn.

Fig. 3. Omus californicus californicus W. Horn.

Fig. 4. Megacephala carolina mexicana Gray.

Fig. 5. Cicindela tranquebarica Herbst.

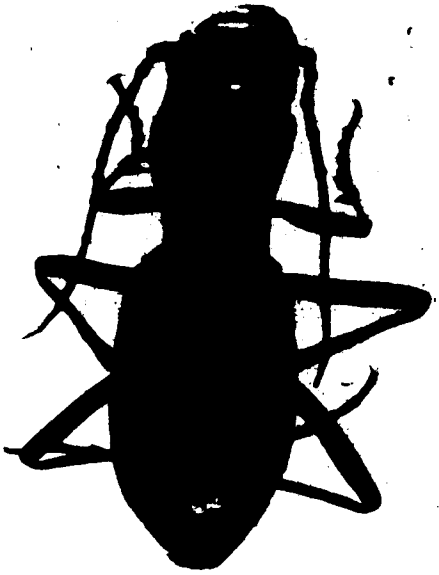

2

3

4

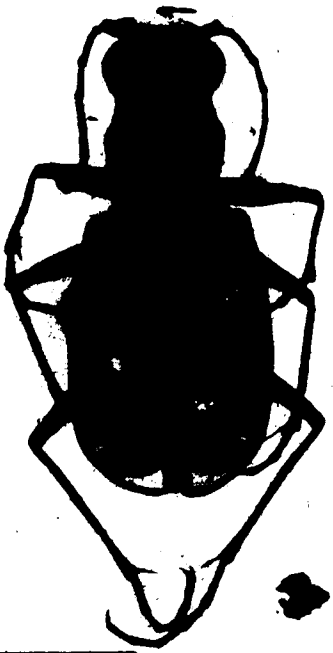

5

California.

As their name denotes, adults of Megacephala have large heads, and large eyes. These beetles are active during twilight hours (Horn, 1908-1915) and many are attracted to lights (Graves and Pearson, 1973). In the mid-summer mating season, they may be diurnal (Horn, 1908-1915). During periods of repose, individuals inhabit holes dug by themselves along grassy meadows, or natural cracks in the earth. They make little use of their wings (Horn, 1908-1915). Adults of Megacephala carolina mexicana Gray (Fig. 4) were identified using keys of Horn (1903; 1926). During July, specimens were collected at dusk by G.E. Ball in the state of Oaxaca, Mexico, 10 km north of Valle Nacional.

Adults of Cicindela, the most derived cicindelid genus, are brightly colored beetles with large heads and prominent eyes (Schaupp, 1883; Leng, 1902; Horn, 1908-1915; Bradley, 1930; and Wallis, 1961). They are active on clear warm days, but during the night and on cloudy days, hide in shallow burrows dug in the substrate (Davis, 1921). Species have radiated into open sandy, clay, or alkali habitats along ocean shores, lake shores, river banks, and mud flats (Leng, 1902; Horn, 1908-1915; and Wallis, 1961). The principal diurnal species used in this study was Cicindela tranquebarica Herbst (Fig. 5), but eyes of adult C. limbata nympha Casey, C. limbalis Klug, C. repanda repanda Dejean, and C. longilabris Say were also examined. Specimens were identified using the keys of Wallis (1961) and Willis (1968).

Adults were collected from May to September in open sandy areas on sunny days at Edmonton, Devon, and Bon Accord, Alberta. Since adult Cicindela lepida Dejean exhibit bimodal activity rhythms of day and twilight, their eyes were also studied. G.J. Hilchie collected specimens at twilight and in daylight on sand dunes at Empress, Alberta.

Eyes of Cicindela belfragei Sallé adults were also examined to help clarify their taxonomic position. Earlier workers placed this taxon and Cicindela pilatei Guérin-Ménéville in a separate genus, Dromochorus (Guérin-Ménéville, 1845; Sallé, 1877; Lacordaire, 1854; Thompson, 1857; Gemminger and de Harold, 1868; Casey, 1897; Leng, 1902; Lantz, 1905; Schilder, 1953; and Rivalier, 1954). Other workers considered these two species to belong to Cicindela (Schaupp, 1883; Horn, 1886; Horn, 1908-1915; 1926; Leng, 1920; and Bradley, 1930), but the subgenus Dromochorus is now accepted by Arnett, 1968; Gaumer and Murray, 1971; and Graves and Pearson, 1973. These adult beetles are crepuscular and flightless, running at dawn and twilight in grass near sandy roadsides in the southern United States (Jones, 1884; Knaus, 1900; Leng, 1902; Lantz, 1905; and Graves and Pearson, 1973). Specimens of Cicindela belfragei Sallé were collected by R.R. Murray in Hamilton County, Texas, 7.5 km north of Hamilton.

For comparison of eye structure and function in relation to diel time of activity and to phylogeny, two carabids were also studied. I collected brachypterous, nocturnal

Pterostichus melanarius Illiger adults by pit fall during July in mixed boreal forest leaf litter along the McIntyre River on the campus of Lakehead University, Thunder Bay, Ontario. Eyes of a more derived carabid, Elaphrus americanus Dejean were also examined. Like most adults of Cicindela, these beetles are heliophilous and capable of flight. In July, on the sandy shores of Black Sturgeon Lake, 144 km north of Dorion, Ontario, I collected several individuals. Both carabids were identified using the keys of Lindroth (1961; 1963).

3. Calculation and Significance of Visual Field Areas of Some cicindelid Beetle Compound Eyes

3.1 Introduction

Although insect compound eyes are immobile and laterally positioned on the head, they have the capacity for both monoscopic (monocular) and stereoscopic (binocular) vision. Depth perception, or binocular vision is usually achieved via overlap of visual fields of both eyes. Estimation of depth is more precise when the image of the object is projected on symmetrical visual cells in the left and right eye. It is therefore assumed that predatory insects attack when the victim is centered between their eyes (Mazokhin-Porshnyakov, 1969; Horridge, 1977a).

Many experimental methods have been devised to quantify visual field areas and to demonstrate binocular visual ability in insects. Baldus (1926) shone light into eyes of nymphs of the dragonfly species Aeschna cyanea Müll. and from the position of bilateral pseudopupils, drew visual axes of individual ommatidia extending from the eyes to the protracted labium. He showed that maximum depth perception occurred between the extended labial hooks and concluded that focal length for binocular vision had evolved with labium length to provide an efficient prey capture mechanism. Again using pseudopupils, Seitz (1968) concluded

that adults of Calliphora erythrocephala Meig. (Calliphoridae) have a visual field of 190° horizontally and 198° vertically. Using angular measurements from serial paraffin sections, Butler (1973a) demonstrated that adults of Periplaneta americana L. (Blattidae) have a vertical visual field of 198° with a 40° dorsal overlap, and a horizontal visual field of 240° with a 65° anterior and 56° posterior overlap. Mazokin-Porshnyakov (Table 8; 1969) summarizes angular values of binocular visual fields of seven insects obtained by various authors.

Hocking (1964) examined hand-cut sections from the estimated horizontal axis of adult eyes of 28 species of insects in 13 orders. Using an ocular goniometer, he measured horizontal axial angles and vertical axial angles of these eyes. Via trigonometric manipulations of these angles, he calculated the horizontal field of view, horizontal binocular field, and vertical binocular field. Of the insects investigated, the mean angle of vision in a horizontal plane was 157°, 68% forward; 32% backwards. Generally, he concluded that an angle of blindness exists posteriorly extending nearly 40° on either side of the midline. Between the frons there are 20° of binocular vision and 10° dorsally and 3° to 4° below the insect head. The insect's mean total field of vision in steradians is 10.5 and the mean binocular visual field is 1.6 steradians (12.56 steradians = 1 unit sphere).

Maldonado and Barrós-Pita (1970) concluded that female

mantid eyes have an area for fine estimation of distance for prey capture. This area is termed the "fovea" by analogy to the structure in vertebrate eyes. Individuals of the mantis Stagmatoptera biocellata were mounted between goniometers; one behind and one lateral to the insect. The eye was symmetrically illuminated by bifurcated Fiber-lite and the angles of the pseudopupil was observed, then mapped on eye surface projections. Once pseudopupil area was determined, various regions of the eye were painted and successful prey capture responses recorded. Additional experiments by Barrós-Pita and Maldonado (1970) concluded that the fovea had a smaller radius of curvature and a greater concentration of ommatidia. They postulated that the fovea of one eye working with the complementary fovea of the other eye enabled precise estimation of catching distance through binocular vision. Further research by Lévin and Maldonado (1970) concluded that the foveal regions of the mantid eyes are generally precisely aligned with the victim before successful prey capture. Horridge (1977a) reviews the function of foveae in other predatory insect eyes and Sherk (1978) relates fovea position to adult prey capture mechanisms in dragonflies.

Investigations of ommatidial and interommatidial angles have clearly demonstrated binocular vision by insect eyes. By plotting interommatidial angles in vertical and horizontal planes of eyes of adult Apis mellifera L. (Apidae), Baumgärtner (1928) and Portillo (1936) discovered that the

angles are smaller in the centre and larger at the periphery of the eye. Resolving power of central ommatidia is two to three times higher than that of peripheral ommatidia. For a review of angular dimensions of fields of vision and interommatidial angle values for various insects, see Autrum and Widerman (1962). Using measurements from eye sections, Goldsmith (Table III; 1964) indicates overlap of adjacent ommatidial visual fields. Bernhard et al. (Table I, 1972) tabulated the interommatidial angle (angle of divergence) and acceptance angle (opening angle of the ommatidium) of many insects. Methods to obtain these data include: eye-scalps, pseudopupils, and intracellular electrophysiological recordings. These authors concluded that visual fields of neighbouring ommatidia overlap since the ommatidial acceptance angle is greater than the interommatidial angle. Burkhardt et al. (1973) proposed a mathematical model for the structure of visual fields of insect eyes based on interommatidial angles between adjacent ommatidia. Frontal areas of the visual field were projected from measurements of "critical angle" for one and both eyes of Aequiaster polytechnicus Bu. (Diopsidae); for both eyes of A. lindaueri Bu., A. exneri Bu., and A. frischi Bu. adults. Only angles of visual fields and not visual field areas were calculated. These researchers suggested that maximum depth perception occurs at the distance equal to half the span between the eyes projected in the forward direction. Current methods for calculation of interommatidial

angle and width of field of view of an ommatidium are explained by Horridge (1977b). Other investigators have determined the visual field of individual retinula cells and proven an electrophysiological basis for angular sensitivity (Washizu et al., 1964; Burkhardt et al., 1966; Tunstall and Horridge, 1967; Horridge et al., 1970; Eheim and Wehner, 1972; Horridge, Giddings, and Stange, 1972; Snyder, 1972; Goldsmith and Bernard, 1974; and Horridge et al., 1976).

Future models for determining absolute visual field angles and areas will probably be based on the concept of "neural superposition" (Kirschfeld, 1967). This term is used when axons of different ommatidia that see the same point of visual space are received by a single lamina cartridge. Accurate limits of monoscopic and stereoscopic perception will be calculated from detailed examination of central neuronal interconnections of both eyes in the lamina ganglionaris, medulla, lobula (and lobula plate). Such histological information will then be coupled with simultaneous intraneuronal electrophysiological recordings from both eyes initiated by varied wavelength, intensity, and angles of electromagnetic radiation.

Homann (1928) was the first to use techniques similar to those used here. He suspended the cephalothorax of adults of Epiblemum sp. and of Evarcha sp. (Araneae: Salticidae) on a universal joint between two perpendicular goniometric rings. Observed through a microscope, the cephalothorax was rotated through 180° and angular measurements of the

three pairs of ocelli were recorded after each 10° rotation. Visual field angles then were plotted on a hemispherical projection. The hemisphere represented the cephalothorax with the visual fields occupying areas on the hemisphere. Although no mathematical details were given concerning the derivation of the projection, it appears to be pseudo-orthographic with one standard parallel and meridian. He made no attempt to quantify visual field areas. However, he graphed frontal, dorsal, and lateral stereoscopic and monoscopic areas of the visual field, and importantly, demonstrated differences in visual abilities between these two genera of salticid spiders.

The purpose of the following experiments is to provide a method of comparing visual field areas of eyes of individuals of the four North American genera of Cicindelidae. A model is presented which maps visual field areas of one and both compound eyes on Mollweide homolographs. Formulae are derived to compute surface areas of monoscopic, stereoscopic visual fields, and blind regions both in steradians, and as a percentage of surface area of the unit sphere homolographs. This technique transforms the shape of any compound eye into a spherical representation for qualitative and quantitative comparisons of visual field areas. Since none of the eyes are spherical, and this model is based on a unit sphere, the results have inherent mathematical distortion. But this distortion can be assumed to be constant for each eye examined and since the experimental treatments

are similar, this model can be used for intergeneric comparisons. The areas of visual fields of individuals of genera of tiger beetles are discussed in relation to eye size and shape, antennal length, other structural ratios, and pertinent behavioural activities.

3.2 Materials and Methods

For scanning electron microscope (SEM) examination of eyes, beetle heads were washed in Tide ^{R} laundry detergent, rinsed in distilled water, then fixed in 5% formalin. After dehydration in ethanol, heads were cleared in xylol and air-dried overnight (Hollenberg and Erickson, 1973). The heads were carbon and gold coated to a thickness of 15 to 20 nm using an Edwards 12E vacuum evaporator, then examined with a Cambridge Stereoscan S4, Scanning Electron Microscope (SEM) at accelerating voltages of 20 to 30 kV. Observations were recorded on Kodak Plus-X Pan Professional PXP-120 roll film. Number of ommatidia were counted from enlarged SEM photomicrographs and from double replicas of celloidin casts of eyes made from a silicone rubber mould (Lawko, 1971). Measurements of structures were made with an ocular micrometer in a Wild M5 dissecting microscope.

Visual field angles were determined using a "goniometric field of view" apparatus. This instrument was designed by Dr. W.G. Evans, Department of Entomology, to measure angles of infrared detection of sense organs on Melanophila acuminata De Geer (Bruprestidae). Modifications

to this instrument made visual field angle measurements possible. A goniometer is an instrument for measuring angles and in this apparatus (Fig. 6), two disc goniometers of 360° were used. To obtain angles of visual fields, three male heads (bh) from each species of the four genera were individually mounted on a pin on the horizontal bar (hb). The 0° reading, both on the ocular goniometer (og) and stage goniometer (sg) were recorded when the cross hairs in the ocular lens (ol) were positioned at the exact centre of the compound eye. The ocular goniometer (og) was then rotated in 10° increments through 180°. For each 10° rotation of the ocular goniometer (og), the [illegible] was rotated 10° using the horizontal bar (hb) to once again place the centre of the eye on the cross hairs. The vertical bar (vb) was rotated until the margin of the last facet at the ocular sclerite was in the centre of the cross hairs. The angle of rotation indicating the visual field angle was recorded directly from the stage goniometer (sg) as indicated by the pointer (pt). Two rotations of the vertical bar (vb) in opposite directions were necessary so that two readings were recorded for each 10° rotation of the ocular goniometer (og). The two angles represent one visual field angle above, and one angle below the centre of the eye which are separated by 180°. For example, at rotation of the ocular goniometer (og) equal to 20°, the stage goniometer (sg) angles represent the angle of the field of vision 20° below the centre of the eye (i.e., towards the mouth of the beetle)

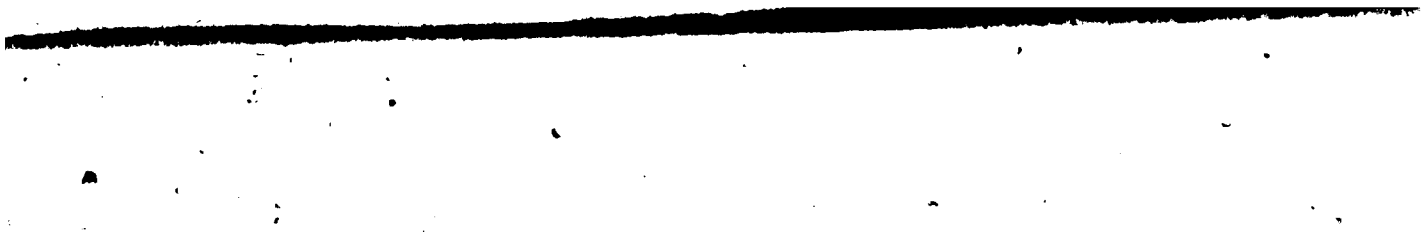

Fig. 6. Goniometric field of view apparatus, showing beetle head (bh); horizontal bar (hb); vertical bar (vb); pointer (pt); stage goniometer (sg); ocular lens (ol) with cross hairs; and ocular goniometer (og).

Scale = 10 cm

and its 180° complement (the angle of the field of vision 20° above the centre of the eye towards the posterior vertex of the beetle head). In this way, visual field angles for the total circumference of the eyes were recorded from the stage goniometer (sg), after the rotation of the ocular goniometer (og) and the compound eye through 180° in 10° increments.

The visual field angles were then plotted on Mollweide homolographic projections (Mollweide, 1806; 1807). A homolograph is an equal-area map projection capable of showing the entire surface of a unit sphere in the form of an ellipse (Fig. 17). All latitudes are represented as straight lines which are more widely spaced at the equator than at the poles. Distances of latitudes from the equator are determined by the laws of equal surfaces, and their values have been tabulated (Deetz and Adams, 1945) between the limits 0 at the equator and 1 for the pole. The central meridian is one half the length of the equator. All meridians are parts of elliptical arcs except the meridian of 90° on either side of the central meridian which appears in the projection as a circle. The mathematical description and theory for construction of the Mollweide homolograph projection are given in Melluish (1931), Mainwaring (1942), and Deetz and Adams (1945).

Such representations of visual fields were drawn for one eye and then both eyes. Two projections were drawn for both eyes: one displaying forward visual field areas; the

other, dorsal visual field areas. The surface areas of the visual field area of one eye and monoscopic, stereoscopic, and blind regions for the two projections of both eyes were quantified in steradians and as a percentage surface area of the unit sphere homolographs. A steradian is a unit of measurement of solid angle that is expressed as the solid angle subtended at the centre of the sphere by a portion of the surface whose area is equal to the square of the radius of the sphere. One steradian = 1/4 π of the solid angle around a point, and there are 4π steradians on the surface of the unit sphere of radius equal to one (Weast, 1975).

To calculate the visual field areas from the homolographs, the following formulae were derived: From Fig. 7, the surface area of an infinitesimal strip centered on the coordinat[illegible] ϕ) on the unit sphere (radius = 1)

$$= \cos\theta \cdot d\theta d\phi$$

From Fig. 8, the surface area of the stippled strip

$$= \Delta(\theta_1\theta_2, \phi_1\phi_2)$$

$$= \int_{\phi_1}^{\phi_2} \int_{\theta_1}^{\theta_2} \cos\theta \cdot d\theta d\phi$$

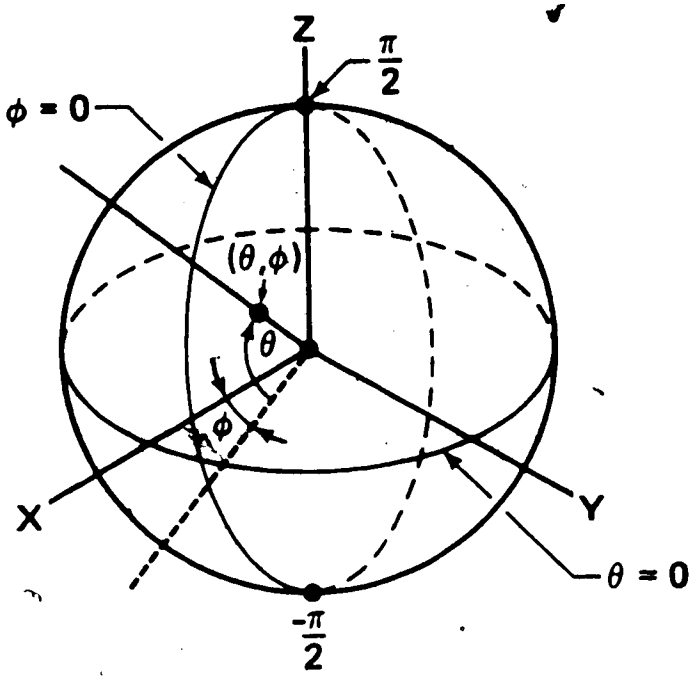

7

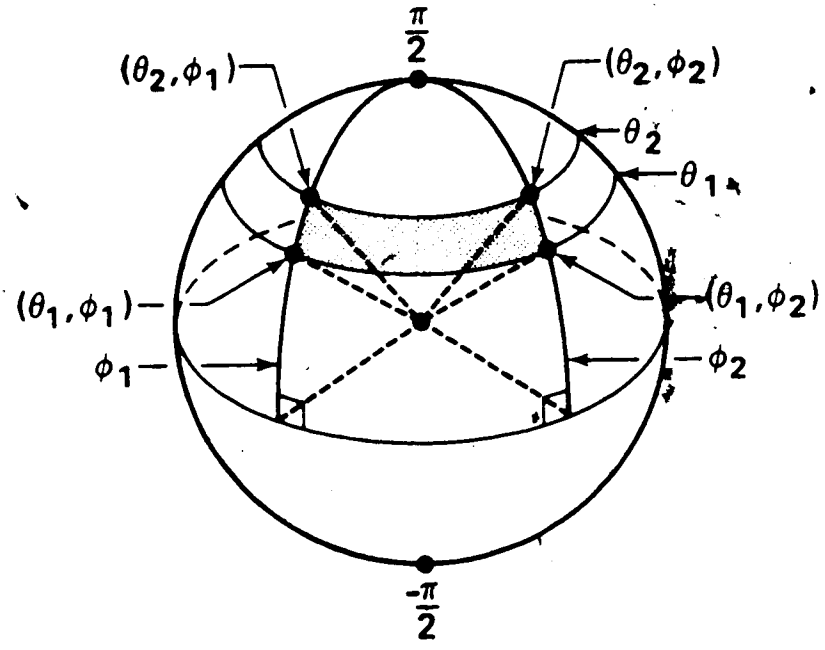

$$0 \leq \phi_1 < \phi_2 \leq 2\pi$$

$$\frac{-\pi}{2} \leq \theta_1 < \theta_2 \leq \frac{\pi}{2}$$

8

$$= \int_{\phi_1}^{\phi_2} d\theta \int_{\theta_1}^{\theta_2} \cos \, d\theta$$

$$= (\phi_2 - \phi_1)(\sin \theta_2 - \sin \theta_1)$$

Applying this formula to the homolographs, surface areas in steradians of 10° strips

$$= \begin{pmatrix} \text{average longitude} \\ \text{angle of } \phi_1 \text{ in radians} \end{pmatrix} + \begin{pmatrix} \text{average longitude} \\ \text{angle of } \phi_2 \text{ in radians} \end{pmatrix}$$

$$\cdot \begin{pmatrix} \sin \\ \text{latitude} \\ \text{angle } \theta_2 \end{pmatrix} - \begin{pmatrix} \sin \\ \text{latitude} \\ \text{angle } \theta_1 \end{pmatrix}$$

where ϕ_1 and ϕ_2 are evaluated at latitude θ_1 and θ_2; where $\theta_2 = \theta_1 + 10°$ and where ϕ_1 and ϕ_2 were measured directly from the goniometric apparatus (Tables 3 and 5).

$$= A_{\theta_1}^{\theta_1+10°} = \left(\frac{\phi_1(\theta_1) + \phi_2(\theta_2)}{2} + \frac{\phi_2(\theta_1) + \phi_2(\theta_2)}{2} \right) \frac{\pi}{180}$$

$$\cdot (\sin \theta_2 - \sin \theta_1)$$

Surface areas in steradians of one eye visual field area or monoscopic, stereoscopic, or blind regions

= sum of surface areas of each 10° strip from -90° to +90°

$$= A_{-90°}^{-80°} + A_{-80°}^{-70°} \ldots + A_{+80°}^{+90°}$$

$$= \sum_{j=-90°}^{+90°} A_{(10_j)°}^{(10_j+10)°}$$

Surface areas of the visual fields as percentages of the surface area of the unit sphere surface area where the surface area of a unit sphere = 4π

$$= \frac{100}{4\pi} \sum_{j=-90°}^{+90°} A_{(10_j)°}^{(10_j+10)°}$$

3.3 Results

The character state of compound eye size has been used by several authors (Chapter 2) to characterize genera of Cicindelidae. Adult eyes of the two nocturnal genera, Amblycheila and Omus are comparatively very small (Figs. 9, 10); eyes of the crepuscular genus, Megacephala (Fig. 11) are large, and adults of the diurnal genus, Cicindela (Fig. 12) have the largest and most bulbous eyes. The vertex (v) of C. tranquebarica is very concave (Fig. 12) while the vertices of adult M. carolina is slightly concave (Fig. 11), but O. californicus (Fig. 10) and A. schwarzi

Figs. 9-12. SEM of the frontal aspect of heads of four cicindelid beetles, showing variation in eye size and degree of convexity or concavity of the vertex (v).

Scale = 500 µm

Fig. 9. Amblycheila schwarzi.

Fig. 10. Omus californicus.

Fig. 11. Megacephala carolina.

Fig. 12. Cicindela tranquebarica.

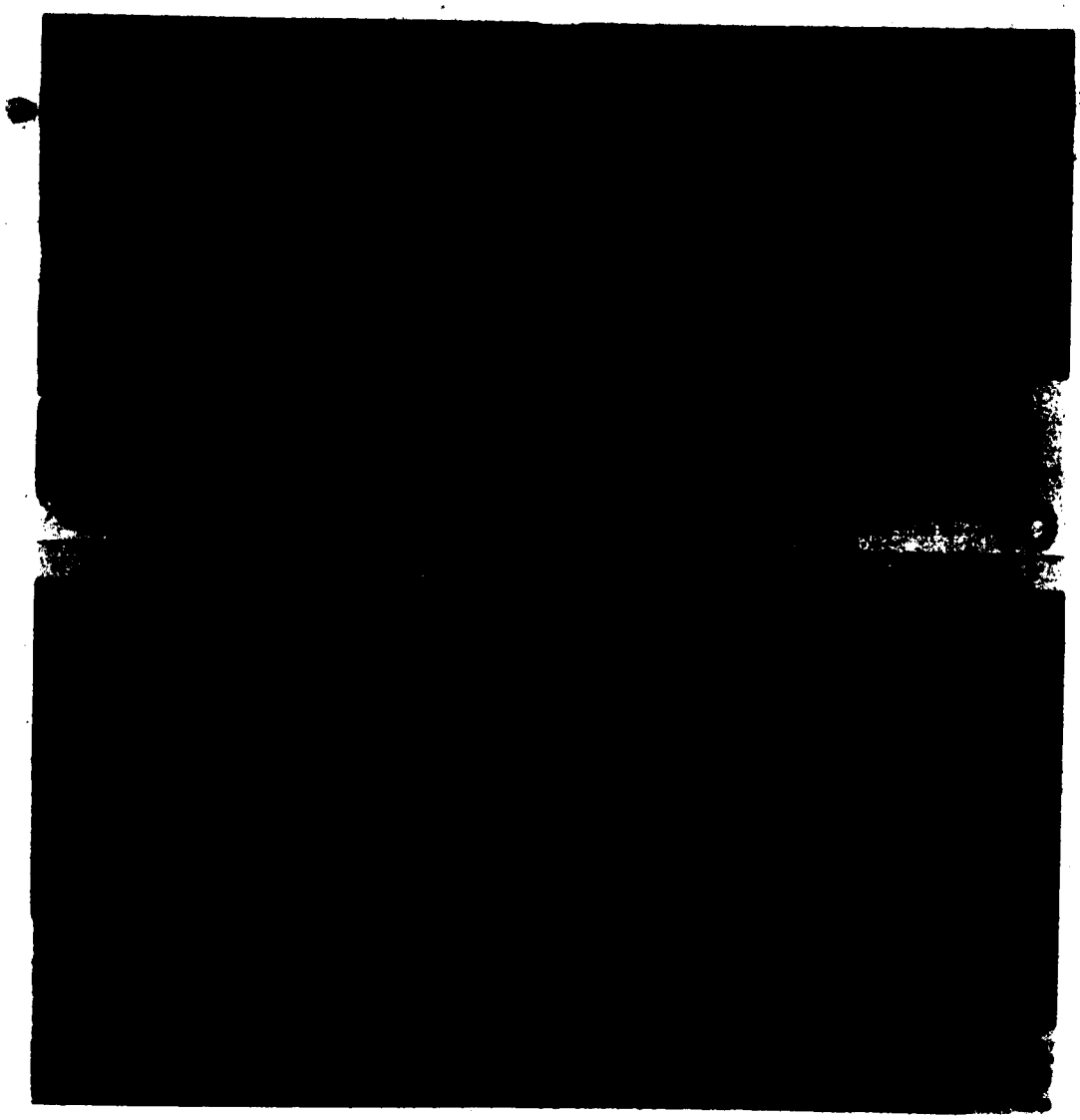

adults (Fig. 9) have convex vertices. Eyes of A. schwarzi adults (Fig. 13) are almost spherical while O. californicus eyes are elliptical in shape (Fig. 14). Eyes of adult M. carolina (Fig. 15) and of C. tranquebarica (Fig. 16; Kuster, 1975) are cordate, with the indentation positioned at the vertex. Figs. 13-16 show that representative compound eyes of all four genera are convex and outer surfaces consist of convex, hexagonal corneal lenses (l). A ring of cuticle, the ocular sclerite (os), defines the border of the eyes.

Table 1 shows that adults of nocturnal cicindelids have fewer ommatidia than have adults of diurnal-crepuscular beetles. Adults of A. schwarzi have long antennae and fewer ommatidia per mm of antennal length than nocturnal O. californicus adults; M. carolina adults fewer than diurnal C. tranquebarica adults. Eye size is related to other structural ratios in Table 2. In representatives of nocturnal genera, eyes span less than one-third the head widths, but in crepuscular and diurnal genera, eyes occupy approximately one-half the head widths. From values comparing eye height to head height, neither eyes of A. schwarzi nor O. californicus adults extend above the vertex while both eyes of M. carolina and C. tranquebarica do. It is possible therefore to assume that both C. tranquebarica and M. carolina adults see above the head, but that vision above the vertex is less in eyes of A. schwarzi and O. californicus adults. Ratios of head width to pronotum width indicate

Figs. 13-16. Lateral view of compound eyes of cicindelid beetles, showing hexagonal corneal lenses (l) and ocular sclerites (os).

Scale = 200 µm

Fig. 13. *Amblycheila schwarzi*.

Fig. 14. *Omus californicus*.

Fig. 15. *Megacephala carolina*.

Fig. 16. *Cicindela tranquebarica*.

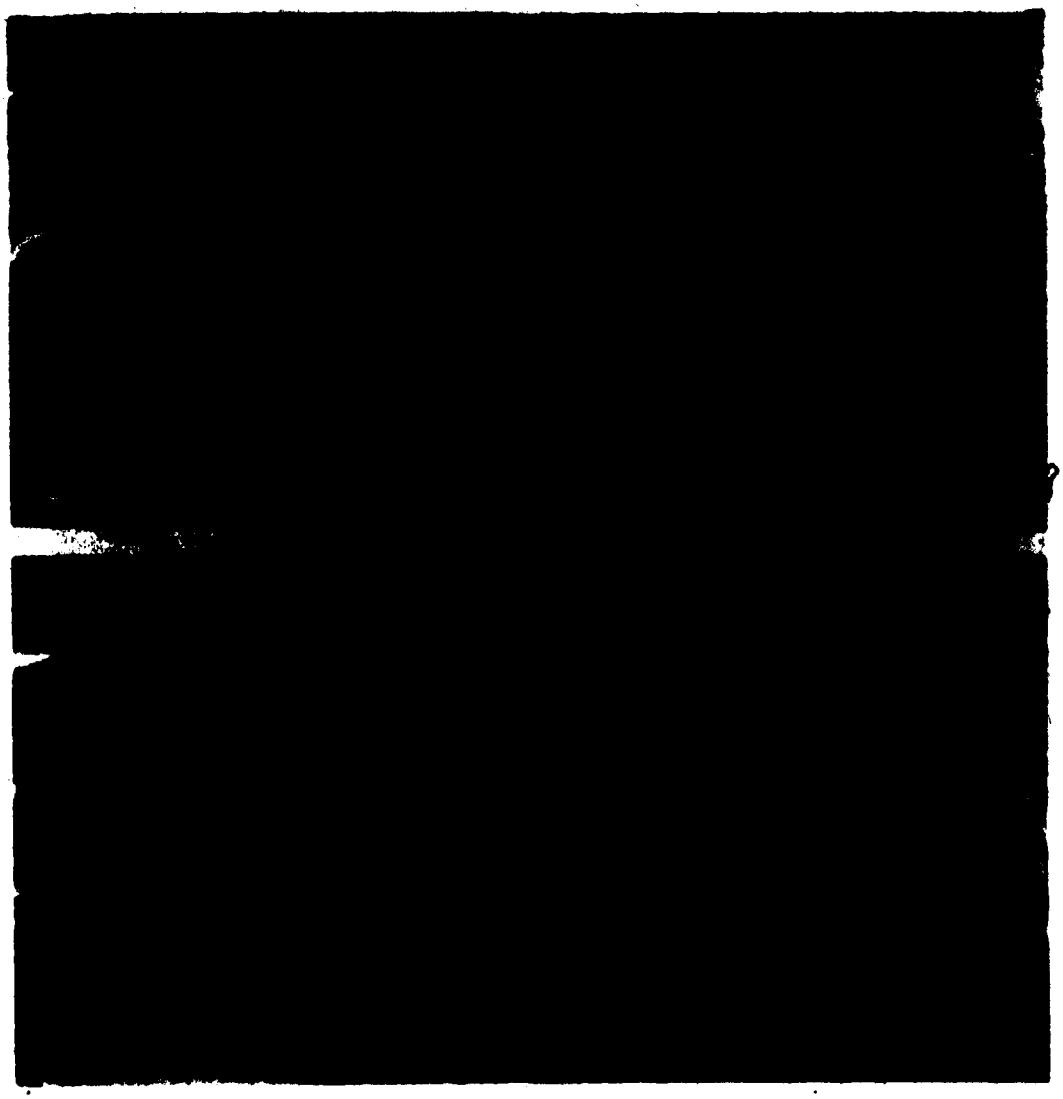

Table 1. Relationships between the number of ommatidia and the antennal length of some cicindelid beetles.
The values are $\bar{x} \pm$ SE for n = 5 for each species.

Measurement	*Amblycheila schwarzi*	*Omus californicus*	*Megacephala carolina*	*Cicindela tranquebarica*
Diel time of activity	Nocturnal	Nocturnal	Crepuscular	Diurnal
Number of ommatidia	1,700 ± 12	1,500 ± 9	4,200 ± 25	4,000 ± 19
Antennal length (mm)	18.98 ± 0.30	8.98 ± 0.22	12.98 ± 0.22	8.00 ± 0.31
$\frac{\text{Number of ommatidia}}{\text{Antennal length}}$	89.60 ± 0.79	167.17 ± 1.98	323.79 ± 3.54	498.53 ± 9.23

Table 2. Structural ratios expressed as percentages measured from four cicindelid beetles.

Values are $\bar{x} \pm SE$ for $n = 5$ for each species.

Percent	*Amblycheila schwarzi*	*Omus californicus*	*Megacephala carolina*	*Cicindela transmississippica*
Diel time of activity	Nocturnal	Nocturnal	Crepuscular	Diurnal
Eye width / Head width	23.70 ± 0.21	26.88 ± 1.00	41.50 ± 0.43	55.10 ± 0.14
Eye height / Head height	91.18 ± 0.15	92.58 ± 0.85	105.54 ± 1.73	112.60 ± 1.62
Head width / Pronotum width	84.30 ± 0.31	85.80 ± 0.99	104.70 ± 0.14	108.48 ± 1.54
Head width / Elytra width	66.90 ± 1.41	66.10 ± 1.10	76.20 ± 0.95	63.90 ± 1.27

that neither adults of A. schwarzi nor O. californicus can see behind their pronota. However, both representatives of M. carolina and C. tranquebarica have this ability. None of these adult tiger beetles can see behind their elytral margins.

Table 3 lists mean visual field angles which were measured using the goniometric field of view apparatus for the left compound eye of three individuals of one species in each cicindelid genus. Structural reference points are indicated on the table and 0° represents the horizontal centre of the compound eye. Data were plotted on Mollweide homolograph projections (Figs. 17-20). The larger the data point, the wider the field of vision, so comparatively, the gradation A. schwarzi, O. californicus, M. carolina, C. tranquebarica represents the smallest to the largest visual field area of one eye. Data from Table 3 were then plotted on homolographs representing the forward visual field for both compound eyes (Figs. 21-24). Centres of the left and right eyes are labelled CL and CR respectively, and structural reference points are indicated. For one and both eye homolographs, Table 4 quantifies forward visual field areas in steradians and also as a percentage surface area of the unit sphere. Monoscopic, stereoscopic, and blind surface areas are tabulated. An example follows to clarify visual field area calculations. The surface area in steradians of the 10° strip bounded by $\theta_1 = 0°$ and $\theta_2 = +10°$ for Cicindela tranquebarica (Table 3, Fig. 20)

Table 3. Mean visual field angles for the left compound eye of one species of each of the four North American genera of cicindelid beetles.

Degrees of Rotation	Angles of the Visual Field for One Eye: ← ϕ_1 →	← ϕ_2 →	Degrees of Rotation
	Vertex		
	A. O. M. C.	C. M. O. A.	
+90	128 122 148 143	143 148 122 128	+90
+80	117 118 145 142	138 144 115 126	+80
+70	116 117 140 143	132 134 111 127	+70
+60	111 117 146 153	133 126 104 122	+60
+50	108 115 146 153	121 113 101 113	+50
+40	111 112 154 155	119 116 98 112	+40
+30	106 111 142 146	119 118 94 99	+30
+20	102 101 134 156	120 114 92 97	+20
+10	97 106 123 142	120 114 89 89	+10
0	92 103 106 125	118 110 94 80	0
-10	92 110 104 122	120 111 96 97	-10
-20	90 116 98 116	125 113 90 94	-20
-30	89 111 95 114	112 111 89 93	-30
-40	88 96 92 116	110 106 92 92	-40
-50	85 107 95 117	109 109 96 88	-50
-60	86 107 95 118	112 106 93 86	-60
-70	85 104 97 104	113 102 94 83	-70
-80	90 101 105 103	111 105 99 86	-80
Mouth -90	93 102 106 102	102 106 102 93	-90 Neck

A. = *Amblycheila schwarzi*

O. = *Omus californicus*

M. = *Megacephala carolina*

C. = *Cicindela tranquebarica*

ϕ_1 = longitude to the left of 90°

ϕ_2 = longitude to the right of 90°

Figs. 17-20. Mollweide homolographs of total visual field of left compound eyes of one representative species of each of the four cicindelid beetle genera. Centre of left eyes represented as CL.

Fig. 17. Amblycheila schwarzi.

Fig. 18. Omus californicus.

Fig. 19. Megacephala carolina.

Fig. 20. Cicindela tranquebarica.

17

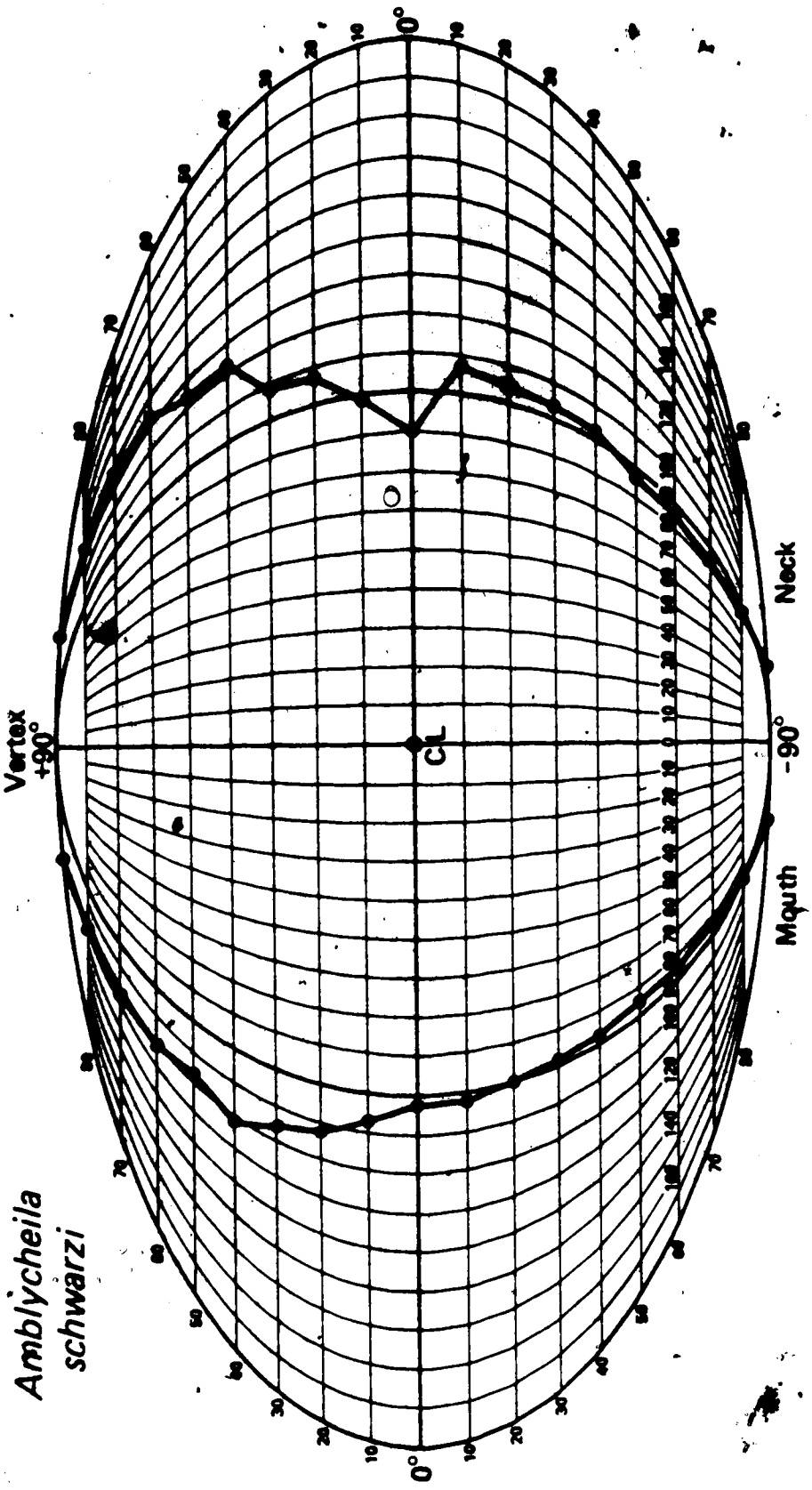

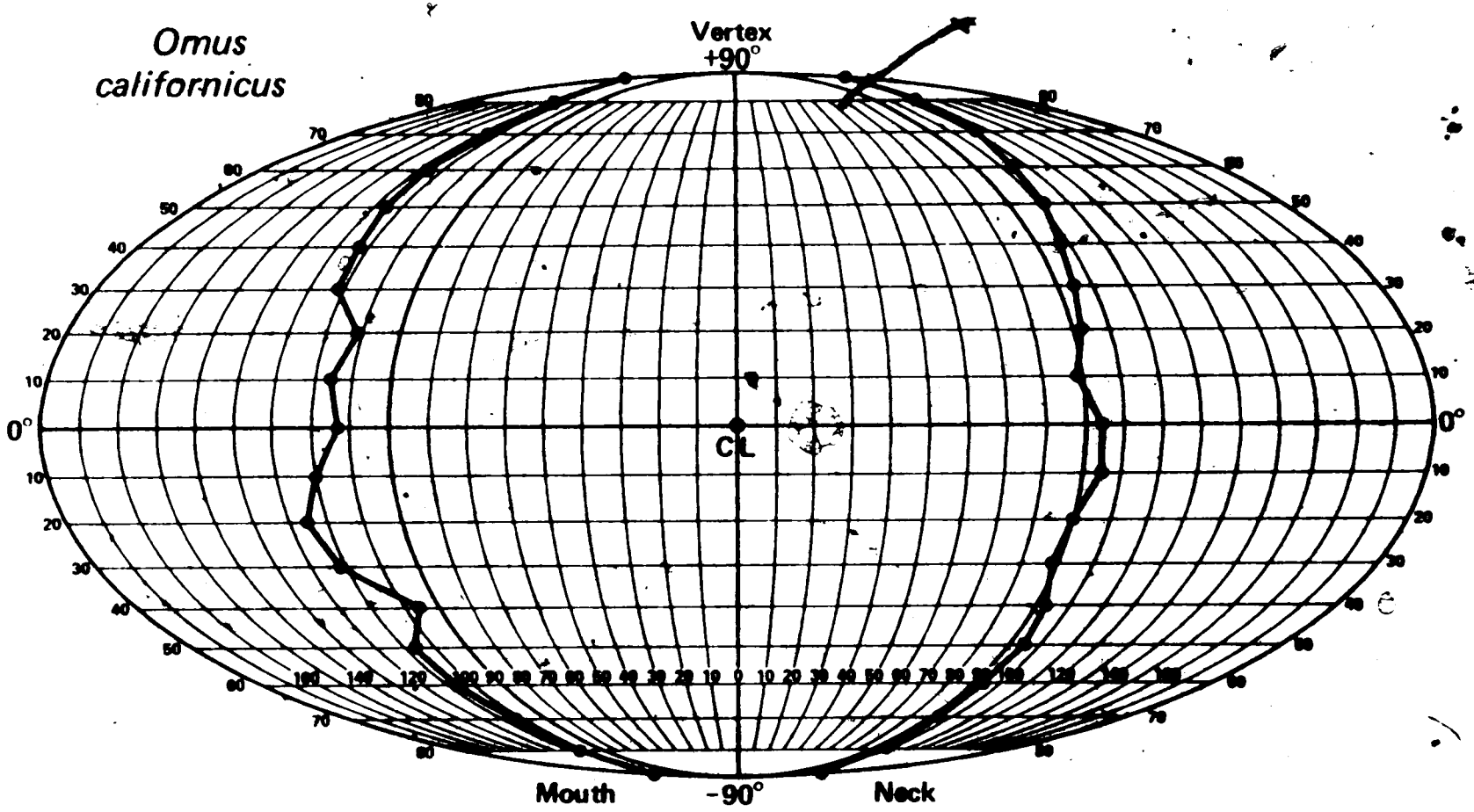
Omus californicus
Vertex
+90°
0°
0°
CL
Mouth
-90°
Neck

Megacephala carolina

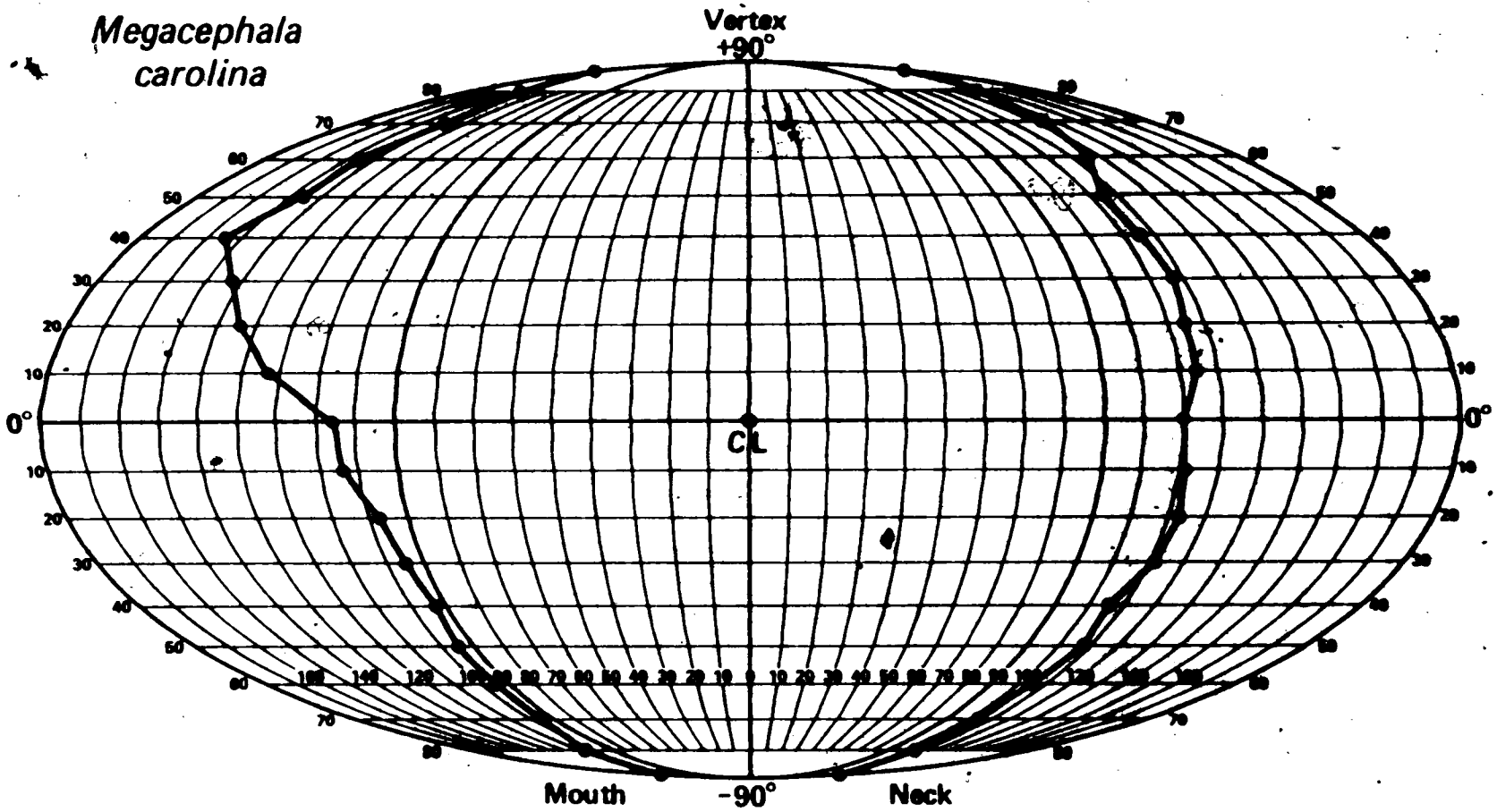

Cicindela tranquebarica

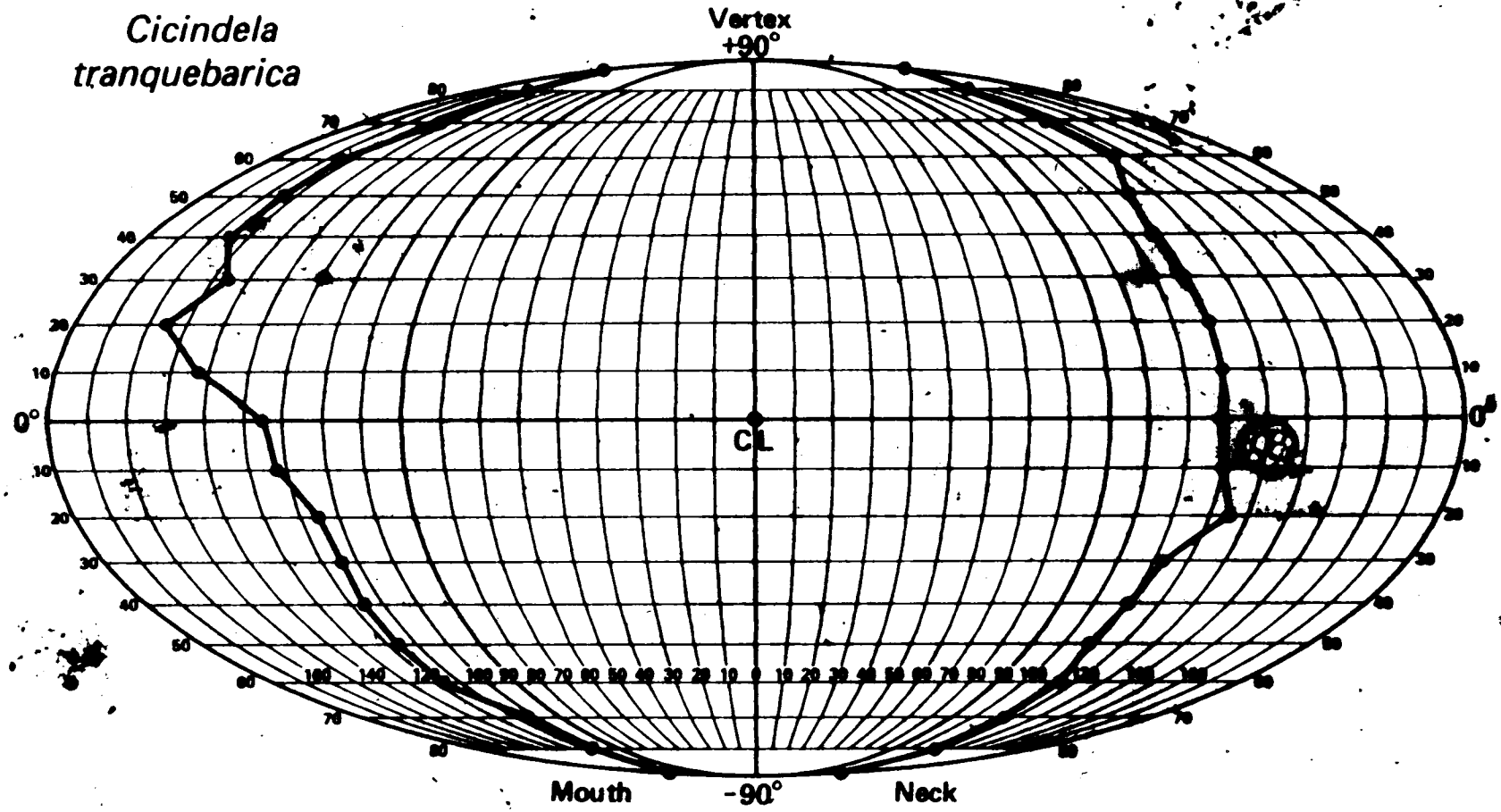

Figs. 21-24. Mollweide homolographs of frontal visual fields of both compound eyes of cicindelid beetles. Centres of right (CR) and left eyes (CL) are indicated. Stereoscopic visual field area stippled, blind area black; and remaining area monoscopic.

Fig. 21. Amblycheila schwarzi.

Fig. 22. Omus californicus.

Fig. 23. Megacephala carolina.

Fig. 24. Cicindela tranquebarica.

Amblycheila schwarzi

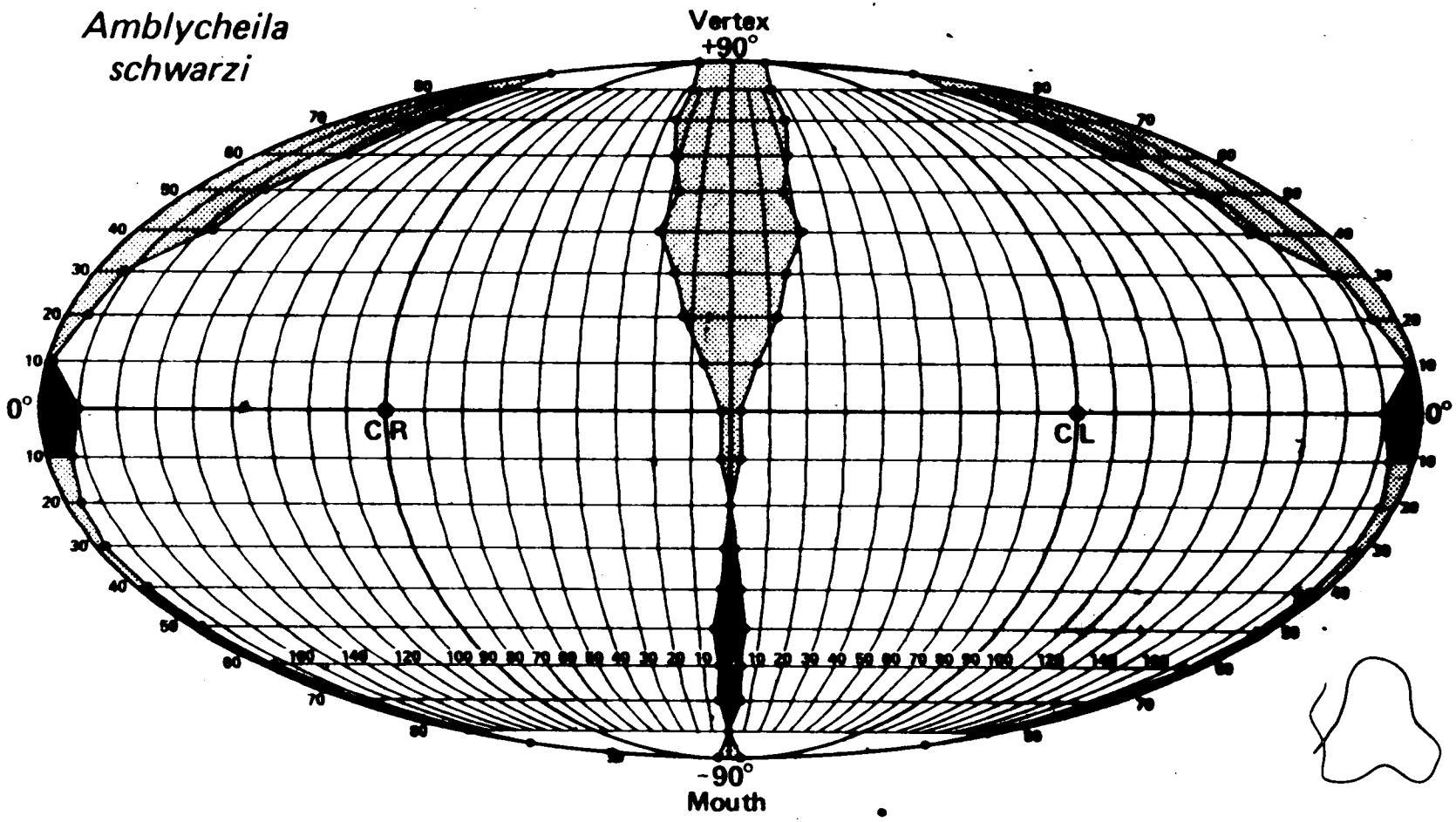

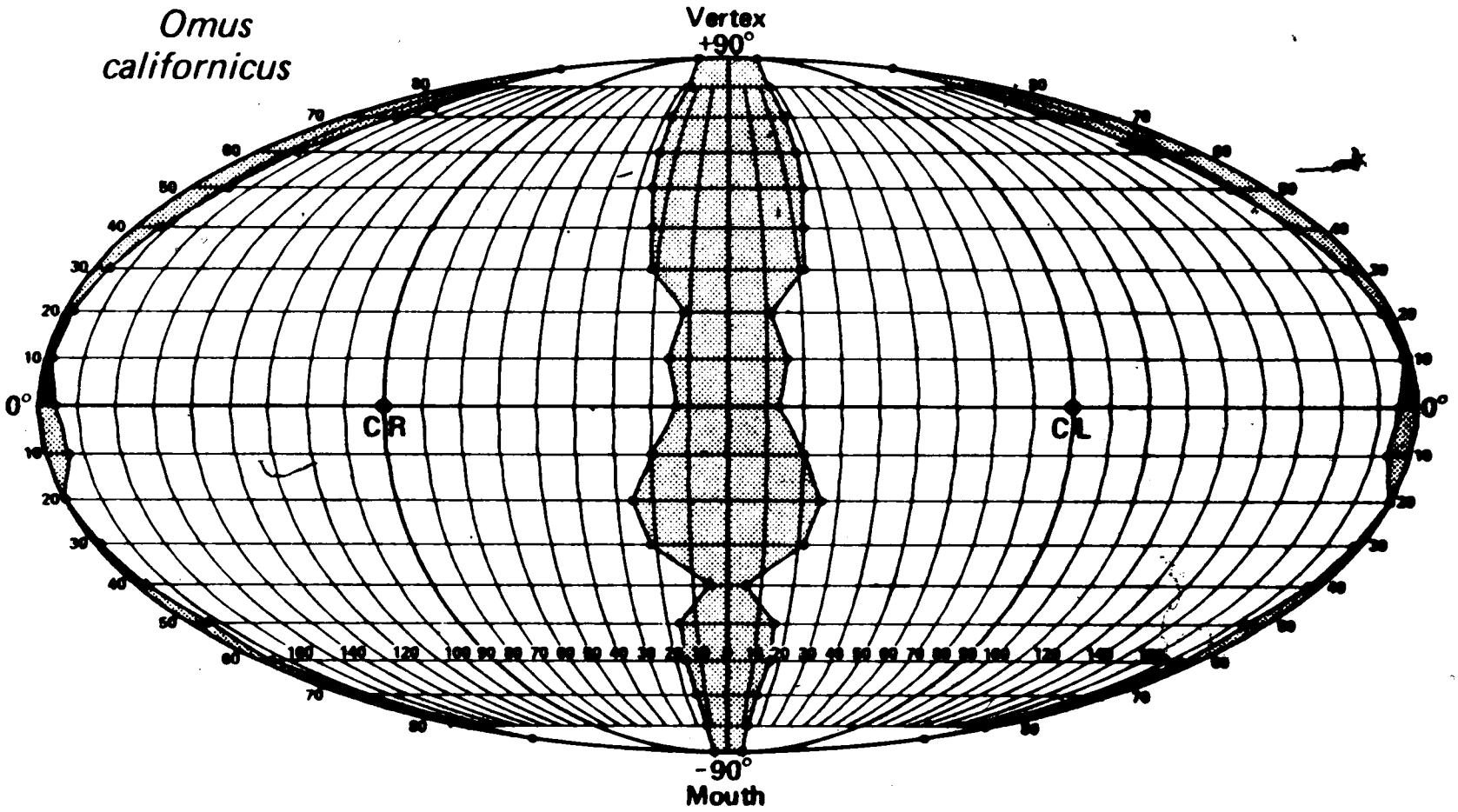
Omus californicus
Vertex
+90°
0°
CR
CL
0°
-90°
Mouth

Megacephala carolina

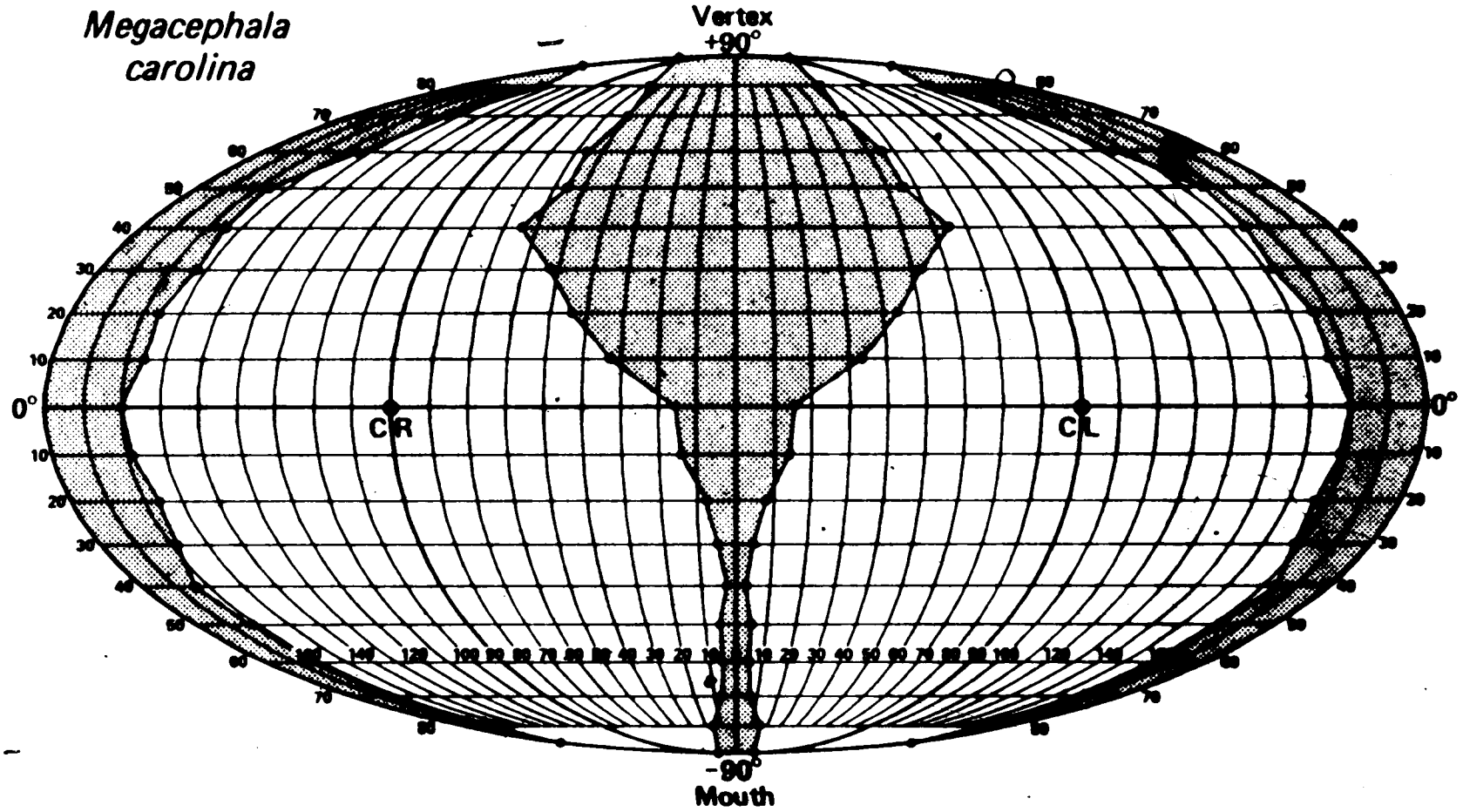

Cicindela tranquebarica

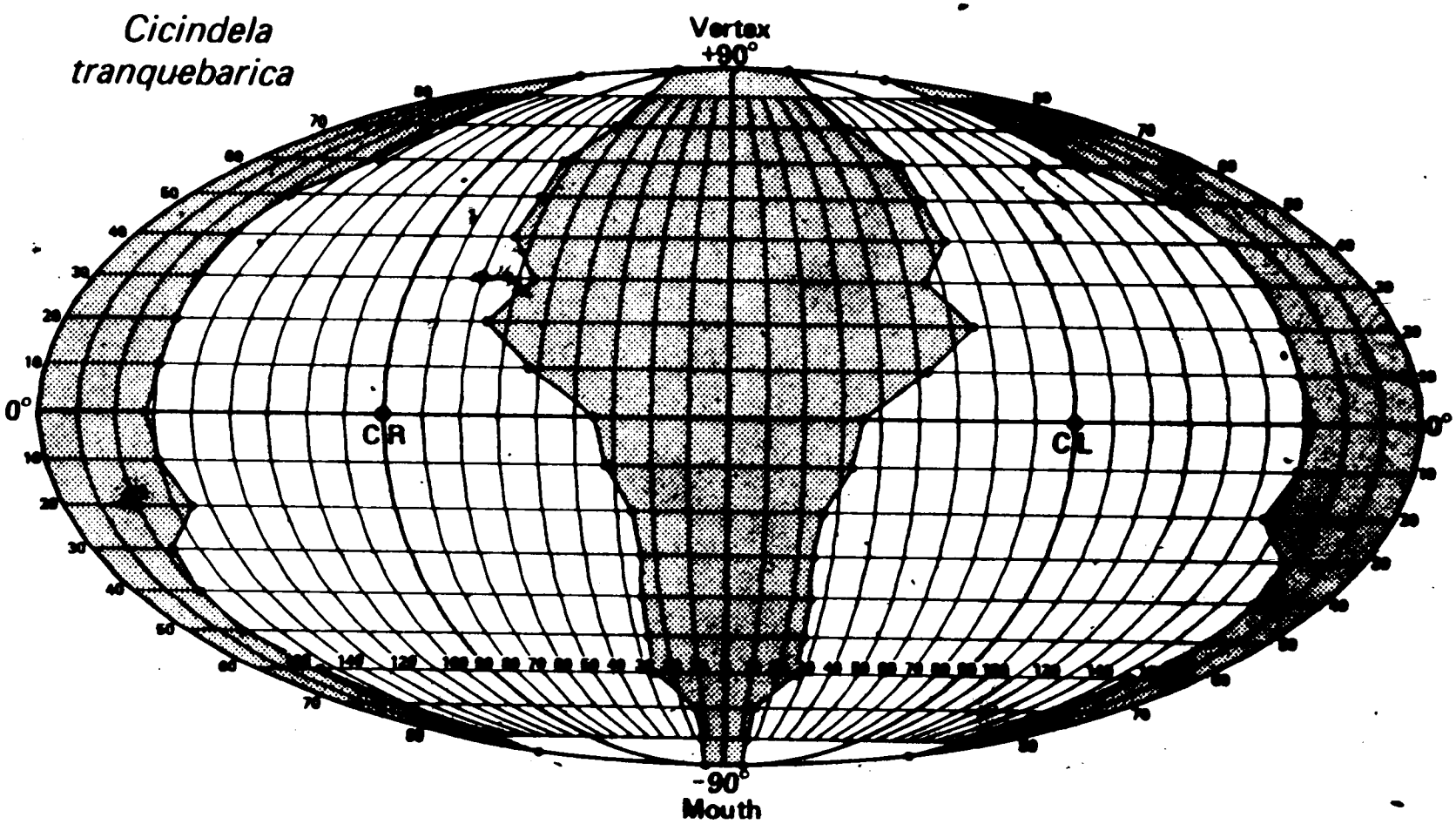

Table 4. Surface areas of the unit sphere homolographs of forward visual fields for each of the four cicindelid beetle eyes.

	Visual Field	Area of Steradians	Percent Area of Unit Sphere
	Amblycheila schwarzi		
One Eye	monoscopic	5.63	44.79
	stereoscopic frons	0.54	4.30
	stereoscopic behind	0.57	4.53
		6.74	53.62
Both Eyes	monoscopic X2	11.27	89.65
	stereoscopic frons	0.54	4.30
	stereoscopic behind	0.57	4.53
	blind frons	0.06	0.48
	blind behind	0.13	1.04
		12.57	100.00
	Omus californicus		
One Eye	monoscopic	5.46	43.43
	stereoscopic frons	1.29	10.26
	stereoscopic behind	0.33	2.63
		7.08	56.32
Both Eyes	monoscopic X2	10.92	86.87
	stereoscopic frons	1.29	10.26
	stereoscopic behind	0.33	2.63
	blind behind	0.03	0.24
		12.57	100.00

Table 4. Continued.

	Visual Field	Area in Steradians	Percent Area of Unit Sphere
	Megacephala carolina		
One Eye	monoscopic	4.51	35.88
	stereoscopic frons	1.91	15.19
	stereoscopic behind	1.64	13.06
		8.06	64.12
Both Eyes	monoscopic X2	9.02	71.76
	stereoscopic frons	1.91	16.19
	Stereoscopic behind	1.64	13.05
		12.57	100.00
	Cicindela tranquebarica		
One Eye	monoscopic	3.81	30.31
	stereoscopic frons	2.93	23.31
	stereoscopic behind	2.02	16.07
		8.76	69.69
Both Eyes	monoscopic X2	7.62	60.62
	stereoscopic frons	2.93	23.31
	stereoscopic behind	2.02	16.07
		12.57	100.00

$$= A_{\theta_1}^{\theta_1+10^\circ} = \left(\frac{\phi_1(\theta_1) + \phi_1(\theta_2)}{2} + \frac{\phi_2(\theta_1) + \phi_2(\theta_2)}{2} \right) \frac{\pi}{180}$$

$$\cdot (\sin \theta_2 - \sin \theta_1)$$

$$= \left(\frac{125 + 142}{2} + \frac{118 + 120}{2} \right) \frac{\pi}{180} \cdot (\sin 10^\circ - \sin 0^\circ)$$

$$= 4.4055 \cdot 0.1736$$

$$= 0.7648 \text{ Sr}$$

The surface area in steradians of the visual field of the left eye of Cicindela tranquebarica (Fig. 20) from -90° to +90°

$$= A_{-90}^{-80^\circ} + A_{-80^\circ}^{-70^\circ} \ldots + A_{+80}^{+90^\circ}$$

$$= \sum_{j=-90^\circ}^{-90^\circ} A_{(10_j)^\circ}^{(10_j+10)^\circ}$$

$$= 0.0554 + 0.1696 + 0.2874 + 0.3979 + 0.4859 + 0.5632 + 0.6438 + 0.7098 + 0.7345 + 0.7648 + 0.7906 + 0.7458 + 0.6716 + 0.5891 + 0.4886 + 0.3607 + 0.2184 + 0.0750$$

$$= 8.7521 = 8.76 \text{ (from Table 4 due to summation of three visual areas)}$$

The surface area of the visual field of the left eye of Cicindela tranquebarica as a percentage of the unit sphere surface is (Table 4):

$$= \frac{100}{4\pi} \sum_{j=-90^\circ}^{+90^\circ} A_{(10_j)^\circ}^{(10_j+10)^\circ}$$

$$= \frac{100}{4\pi} (8.76)$$

$$= 69.69\%.$$

In this way each visual field area was calculated for each eye (Tables 4 and 6).

From forward visual field homolographs (Figs. 21-24) and Table 4, adults of the two nocturnal genera have larger monoscopic and smaller stereoscopic areas of the visual field, and also exhibit some blind areas. A. schwarzi adults are blind above the mouth and like individuals of O. californicus, also are blind in the posterior lateral direction. Both adults of M. carolina and C. tranquebarica do not have blind areas in their forward visual field. Stereoscopic areas in the forward, lateral, and posterior directions increase as monoscopic decreases as a percentage of surface area of the visual field. C. tranquebarica adults have the largest total stereoscopic area of the visual field of any of the beetles examined.

Table 5 tabulates mean dorsal visual field angles for

Table 5. Mean dorsal visual field angles for the left compound eye of one species of each of the four North American genera of cicindelid beetles.

Degrees of Rotation	Angles of the Visual Field for One Eye								Degrees of Rotation
	← ϕ_1 →				← ϕ_2 →				
	Neck								
	A.	O.	M.	C.	C.	M.	O.	A.	
0	80	94	110	118	118	110	94	80	0
+10	89	89	114	120	120	111	96	97	+10
+20	97	92	114	120	125	113	90	94	+20
+30	99	94	118	119	112	111	89	93	+30
+40	112	98	116	119	110	106	92	92	+40
+50	113	101	113	121	109	109	96	88	+50
+60	122	104	126	133	112	106	93	86	+60
+70	127	111	134	132	113	102	94	83	+70
+80	126	115	144	138	111	105	99	86	+80
90	128	122	148	143	102	106	102	93	90
-80	117	118	145	142	103	105	101	90	-80
-70	116	117	140	143	104	97	104	85	-70
-60	111	117	146	153	118	95	107	86	-60
-50	108	115	146	153	117	95	107	85	-50
-40	111	112	154	155	116	92	96	88	-40
-30	106	111	142	146	114	95	111	89	-30
-20	102	101	134	156	116	98	116	90	-20
-10	97	106	123	142	122	104	110	92	-10
0	92	103	106	125	125	106	103	92	0
	Mouth								

(vertex)

A. = Amblycheila schwarzi

O. = Omus californicus

M. = Megacephala carolina

C. = Cicindela tranquebarica

ϕ_1 = longitude to the left of 0°

ϕ_2 = longitude to the right of 0°

s. 25-28. Mollweide homolographs of dorsal visual fields of both compound eyes of cicindelid beetles. Centres of right (CR) and left eyes (CL) are indicated. Stereoscopic visual field area stippled; blind area black; and remaining area monoscopic.

. 25. Amblycheila schwarzi.

. 26. Omus californicus.

. 27. Megacephala carolina.

. 28. Cicindela tranquebarica.

Amblycheila schwarzi

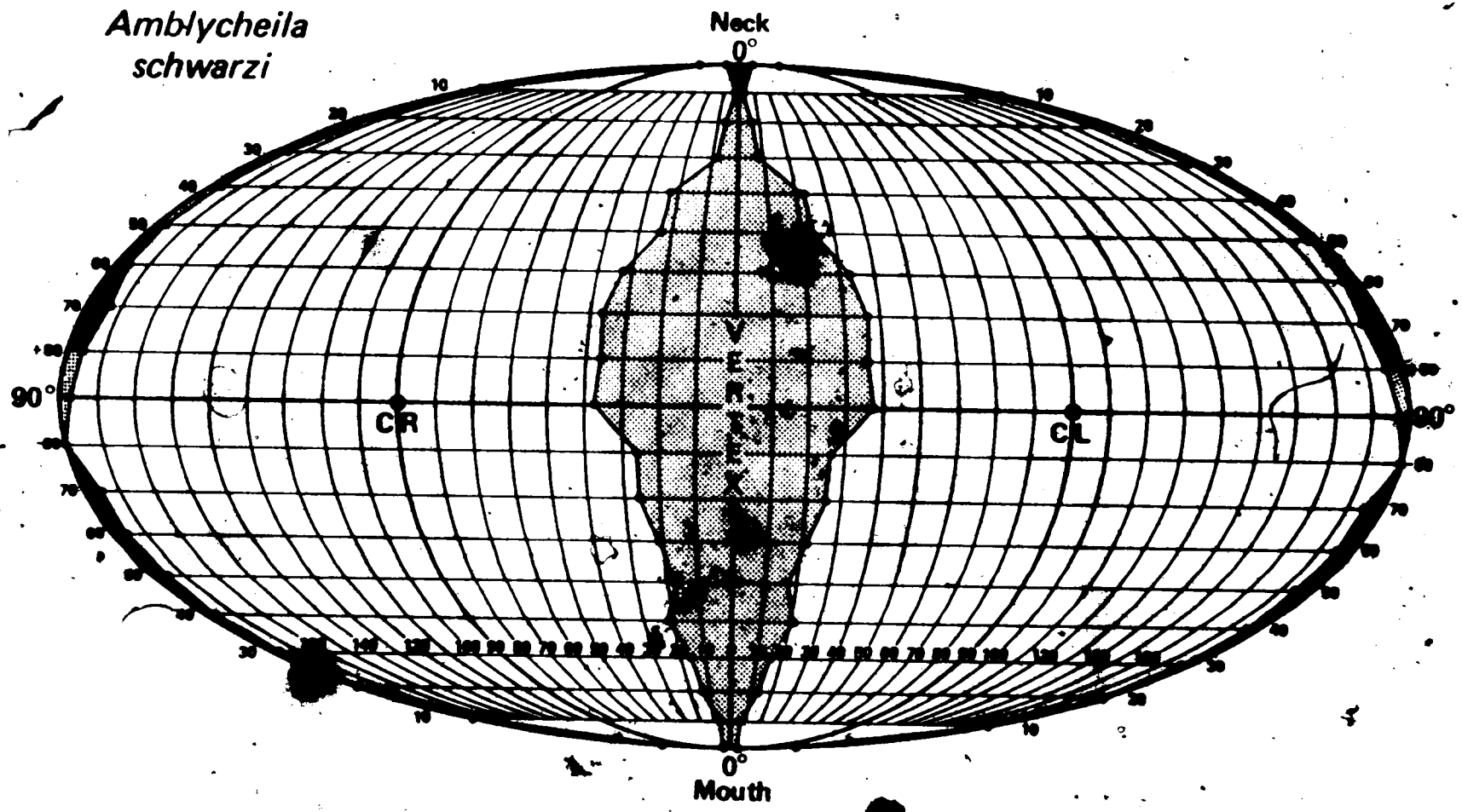

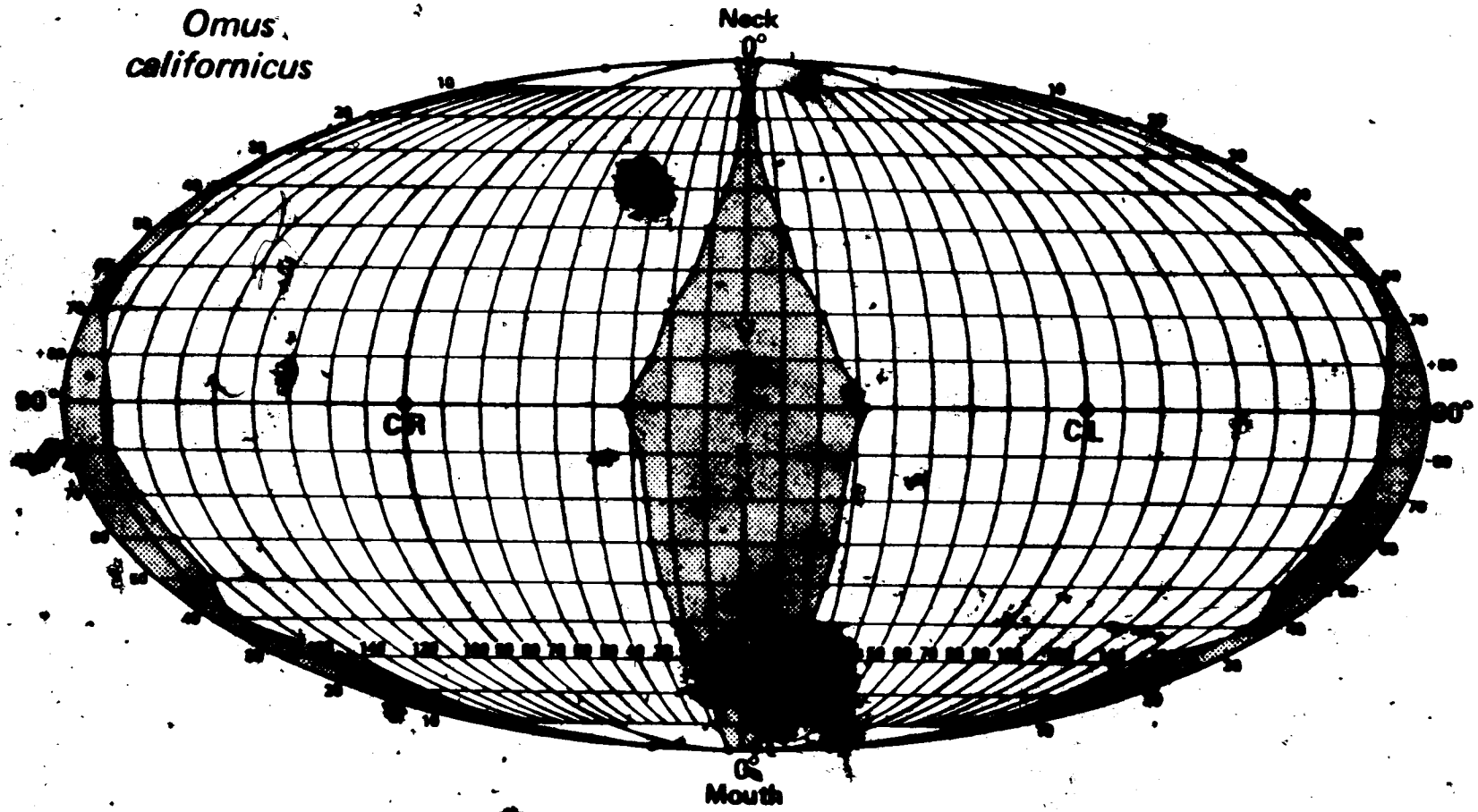
Omus californicus
Neck
0°
CR
CL
0°
Mouth

Megacephala carolina

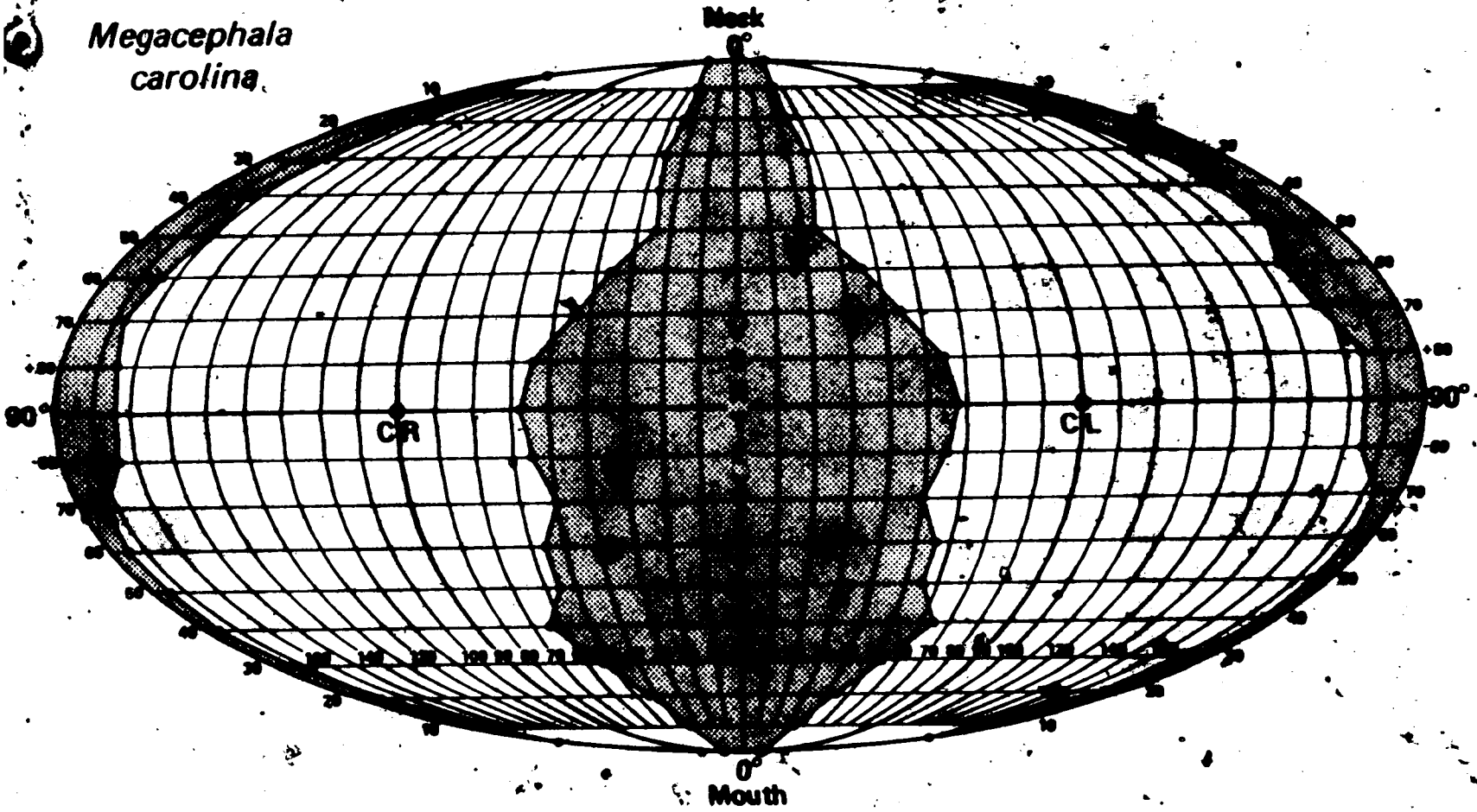

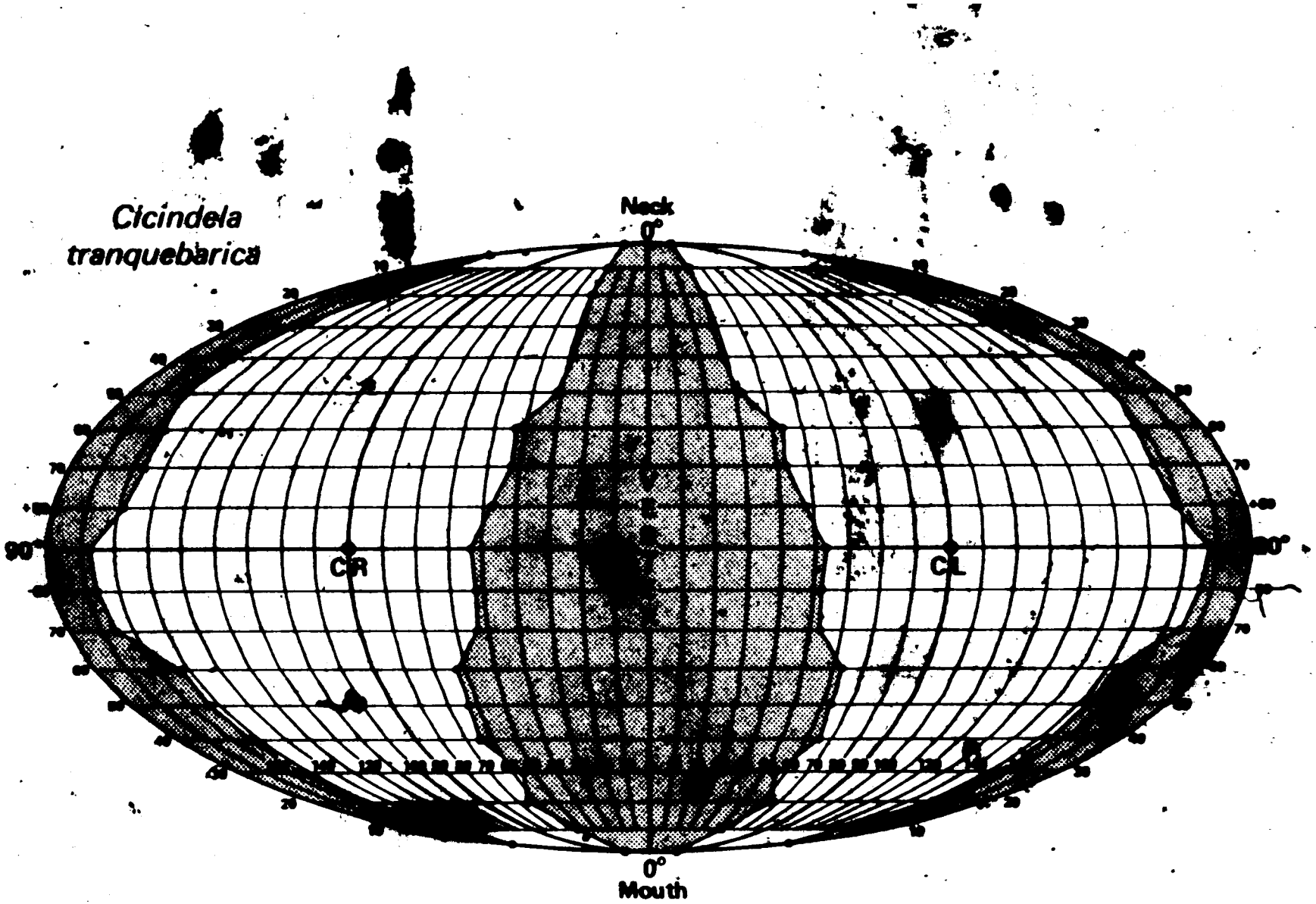
Cicindela
tranquebarica
Neck
0°
CR
CL
0°
Mouth

Table 6. Surface areas of the unit sphere homolographs of dorsal visual fields for each of the four cicindelid beetle eyes.

	Visual Field	Area in Steradians	Percent Area of Unit Sphere
	Amblycheila schwarzi		
One Eye	monoscopic	5.63	44.79
	stereoscopic vertex	1.03	8.19
	stereoscopic mouth to neck	0.08	0.64
		6.74	53.62
Both Eyes	monoscopic X2	11.27	89.65
	stereoscopic vertex	1.03	8.19
	stereoscopic mouth to neck	0.08	0.64
	blind vertex	0.04	0.33
	blind mouth to neck	0.15	1.19
		12.57	100.00
	Omus californicus		
One Eye	monoscopic	5.46	43.43
	stereoscopic vertex	0.91	7.24
	stereoscopic mouth to neck	0.71	5.65
		7.08	56.32
Both Eyes	monoscopic X2	10.92	86.87
	stereoscopic vertex	0.91	7.24
	stereoscopic mouth to neck	0.71	5.65
	blind vertex	0.02	0.16
	blind mouth to neck	0.01	0.08
		12.57	100.00

Table 6. Continued.

	Visual Field	Area in Steradians	Percent Area of Unit Sphere
	Megacephala carolina		
One Eye	monoscopic	4.51	35.88
	stereoscopic vertex	2.60	20.68
	stereoscopic mouth to neck	0.95	7.56
		8.06	64.12
Both Eyes	monoscopic X2	9.02	71.76
	stereoscopic vertex	2.60	20.68
	stereoscopic mouth to neck	0.95	7.56
		12.57	100.00
	Cicindela tranquebarica		
One Eye	monoscopic	3.81	30.31
	stereoscopic vertex	3.13	24.90
	stereoscopic mouth to neck	1.82	14.48
		8.76	69.69
Both Eyes	monoscopic X2	7.62	60.62
	stereoscopic vertex	3.13	24.90
	stereoscopic mouth to neck	1.82	14.48
		12.57	100.00

the left compound eye of three individuals of each genus. These data were obtained by a 90° rotation of each visual field angle given in Table 3 so that, for example, data for 90° in Table 3 now are angular measurements for 0° in Table 5. These data from Table 5 were plotted on Mollweide homolographic projections to show dorsal areas of the visual field (Figs. 25-28). Table 6, like Table 4, quantifies dorsal visual field areas in steradians and also as a percentage surface area of the unit sphere.

Figs. 25-28 and Table 6 provide data to prove that adults of both A. schwarzi and O. californicus have large lateral monoscopic areas of the visual field. Stereoscopic vision at the vertex and between the mouth and neck are limited. These beetles have blind areas at the vertex and between the mouth and neck. Dorsal visual field areas for adult M. carolina and C. tranquebarica show they have smaller lateral monoscopic areas of the visual field than the nocturnal beetles, but increased stereoscopic vision at the vertex and between the mouth and neck. No blind areas are indicated. Visual fields between mouth and neck are impossible and their appearance in the homolographs must be assumed to be the result of plotting non-spherical eyes. This blind area is presumably small.

3.4 Discussion and Conclusions

Unlike fast flying diurnal adults of Cicindela tranquebarica or crepuscular Megacephala carolina adults,

both flightless nocturnal adults of Omus californicus and Amblycheila schwarzi have small eyes. I conclude that nocturnal cicindelids have not used the strategy of increased eye size to enhance visual perception in darkness since eye size is larger in diurnal beetles. Number of ommatidia is larger in adults of A. schwarzi than of O. californicus; of M. carolina than C. tranquebarica adults, which shows that ommatidial number is not linked to the phylogeny of these beetles. A. schwarzi adults have relatively long antennae as do adult M. carolina compared to O. californicus or C. tranquebarica adults. Since the visual ability of A. schwarzi adults is extremely weak (Willison, 1877; Snow, 1877; Gissler, 1879; and Horn, 1908-1915), these authors suggest that these beetles have an acute sense of touch, chiefly concentrated in their long and constantly vibrating antennae. My field observations support this hypothesis as these beetles appear to feel and smell their environment (Kuster, 1976). The ratio of antennal length to ommatidial number shows that there are comparatively fewer ommatidia per mm antennal length in those beetles with long antennae.

Adaptation for diurnal activity, flight, and fast running behaviour has required an expansion in the visual field. Eyes of C. tranquebarica and M. carolina adults occupy more of the head width and exceed the head height permitting larger horizontal and vertical visual fields than in adults of O. californicus or A. schwarzi. Although none

of these beetles have the capacity to see behind their elytra, adults of both C. transwabarica and M. carolina can see behind their pronota. The list of ratios (Table 2) does not, however, indicate the absolute limits of vision. Tiger beetles display an alert behavioural stance by rearing up on the prothoracic legs so that the abdomen is pressed to the substrate (Swiecimski, 1957; Willis, 1967). Such a stance may permit the beetles to see more of their environment in the lateral and posterior directions. The more anterior position and bulbous shape of eyes of adult C. transwabarica and M. carolina allows for larger stereoscopic areas of the visual field in the forward, posterior, and dorsal directions than is demonstrated for the lateral flatter small eyes of either O. californicus or A. schwarzi adults.

Other workers have measured visual fields of representatives of Cicindela adults. Using eye scalps Friedrichs (1931), calculated the total visual field of C. campestris L. to be 206° in the horizontal direction; 172° vertically. Approximately 90° of the forward visual field is binocular. Bauers (1933) computed the vertical visual field of C. hybrida L. to be 159.5° of which 93.5° are for vision above and 66.0° for vision below the central axis of the eye. [redacted] field is transformed into a spherical representation as done here, the horizontal visual field of C. transwabarica Horbst is 243° with a vertical visual field of 245° (Table 3).

Ommatidia bordering the vertex [redacted] of S. [redacted] L. have an acceptance angle of 3°. [redacted] cervically and posteriorly have acceptance angles greater than 3°. Central ommatidia have acceptance angles of less than 2° (Prosvirina, 1958). The [redacted] received by [redacted] with [redacted] acceptance angles is composed of fewer points of a mosaic and hence the image cannot be as clearly resolved. From my visual field experiments, these ommatidia appear to function in depth (stereoscopsis) and possibly movement perception from stimuli received by symmetrical ommatidia in both eyes. In the central region of the eye used for monoscopic vision, the ommatidia have smaller acceptance angles. Since more ommatidia per eye function in perception of the incident light rays, these ommatidia may be capable of resolving a more detailed image of the objects lateral to the insect but these ommatidia may not function in depth perception. Also, because of their keener power of resolution, movement perception would not be an efficient use of these ommatidia.

With reference to habitat and diel activity, a comparative ethological discussion follows. This concerns the roles of sight and distance localization of these beetles for prey capture, finding a mate, and escape response.

Little is known of nocturnal hunting behaviors of adults of [redacted]. They seem to stumble upon their food as if by accident and cannot sight their prey from a distance (Snow, 1907). However, [redacted] of gut contents

by Horn (1908-1915) and Larochelle (1974a) indicate that they capture some insects and they may have an unusual paralyzing capability for food capture (Zweifel, in Vaurie, 1955). Predators include skunks, nocturnal birds (Williston, 1877), and spiders (Vaurie, 1955). It would seem that their limited visual field areas are of little value in either predatory or escape behaviours. They make no attempt to escape from their human captors, allowing themselves to be picked up as though they were entirely blind (Snow, 1877; Williston, 1877). I do not know if visual cues are involved in finding a mate.

Adults of Omus are attracted to meaty baits (Schaupp, 1883; Horn, 1908-1915; and Larochelle, 1974a), but little else is known of their predatory capabilities. They are prey of several species of birds and mammals (Horn, 1908-1915; Larochelle, 1974a). Skunks (Mephitis mephitis Schreber, and Spilogale putorius L.) eat vulnerable teneral adults, but visual cues seem not to be of value in sighting this potential danger since the beetles seldom elicit an appropriate escape response into their burrows (Maser, 1973). Since adults of Omus become diurnal during the mating season (Horn, 1908-1915), vision may be involved in seeking a mate.

Adults of Megacephala run quickly and erratically, but often crawl on to a stick or other prominence to take flight (Mitchell, 1905). They have evolved good visual abilities since they capture a large variety of terrestrial and aerial insects (Horn, 1908-1915; Larochelle, 1974a). Spe-

cific predators of adults of Megacephala are not documented in the literature. However, because of their large eye size it is suggested that vision is used to initiate escape behaviour as is presumably used to locate potential mates.

Literature is voluminous on diet and prey finding of adults of Cicindela. These carnivores actively hunt a variety of insects in all stages of metamorphosis and include some crustaceans in their diet (Mitchell, 1905; Horn, 1908-1915; Moore, 1906; Wallis, 1961; and Larochelle, 1974a). Moore (1906) recorded that distance localization of C. purpurea Oliv. adults for formicids was 10 to 13 cm; C. repanda Dejean, 8 to 13 cm. Balduf (1925) observed adults of C. punctulata Oliv. detect Blissus leucopterus Say (Lygaeidae), from a distance of 5 to 8 cm. C. hybrida L. adults attack creeping maggots, 8 to 12 mm in length, from a distance of 10 cm (Friedrichs, 1931). Distance localization for adults of C. campestris and C. hybrida was shown to be 20 to 30 cm (Faasch, 1968). Considering field of vision, perception of direction, shape, and movement, Swiecimski (1957) investigated prey capture behaviour of C. hybrida L. When prey is stalked, adult beetles assume the alert stance, align their body to the long axis of their prey, thus placing the prey directly in their stereoscopic visual field, then run and attack the victim. Males seek females using similar aggressive behaviour (Faasch, 1968). From prey capture experiments involving changes in light intensity, Bauer et al. (1977) reported that a decrease of

light intensity reduces hunting success of adults of the diurnal carabid, Notiophilus biguttatus. This discovery may also apply to diurnal cicindelids for which the optimal physiological response of their eyes has been selected to correspond to their diurnal activity during periods of bright light.

Despite their keen eyesight, adults of Cicindela are under extreme predation pressures from many sources: asilids (Wallis, 1913; Bromley, 1914; Graves, 1962; Lavigne, 1977), formicids (Larochelle, 1972), arachnids (Day, 1969); also amphibians and reptiles (Larochelle, 1972; 1974b), birds (Maser, 1973; Larochelle, 1975a), and mammals (Larochelle, 1975b). However, beetles in this genus have adapted several strategies to survive in their vulnerable diurnal niche. When frightened by sudden movement or by a shadow, or ground vibration from one to two meters away (Moore, 1906; Friedrichs; 1931), a beetle assumes its alert stance and if stimulation continues, it flies downwind. From my observations, upon landing, a beetle faces upwind with both eyes now directed at the danger. Using its stereoscopic forward visual field it assesses the approximate distance of the attacker. If danger ensues, it flies and hides in nearby vegetation where its elytral markings provide cryptic colouration (Shelford, 1917). When attacked from above, as is the case with the collector's net, it can be concluded that the bulbous eyes extending above the vertex provide adequate visual perception since these beetles often escape

capture through rapid flight initiation.

The evolution of increased eye size and larger stereoscopic visual abilities have apparently been selected in the cicindelids as an adaptive strategy for crepuscular and diurnal activity in open niches where predation pressures are severe.

4. Comparative Structure and Function of cicindelid and carabid Beetle Compound Eyes

4.1 Introduction

On the basis of ecological correlations, Exner (1891) classified compound eyes of insects into two structural and functional categories: apposition eyes characteristic of diurnal insects active in bright sunlight, and superposition eyes characteristic of crepuscular and nocturnal insects. In an ommatidium of an apposition eye, the retinula is in contact with the apex of the crystalline cone and a dense layer of secondary pigment granules surrounds the cone permitting only light transmitted through that cone to stimulate the underlying rhabdom. Pigment migrations are not pronounced during light and dark adaptation. Therefore, the image formed by an apposition eye is a mosaic composed of apposed light from each individual ommatidium (Müller, 1879). In an ommatidium of a superposition eye, the rhabdom is not in contact with the apex of the cone, the two structures being separated by a transparent clear zone. Secondary pigment granules are capable of migration. At night the pigment migrates distally to expose the cone apices permitting incident light entering one ommatidium to scatter over the clear zone to stimulate adjacent rhabdoms (Exner, 1891). In this way, a superposi-

tion mosaic image is formed with increased brightness but at the expense of image resolution (Müller, 1879). Trachae between retinula cells act as a tapetum to reflect light, thus further increasing light intensity within the eye (Bugnion and Popoff, 1914).

Recently (Goldsmith and Bernard, 1974), terms for the functional categories of insect compound eyes have been borrowed from cone and rod visual systems of the vertebrate retina. Apposition and superposition eyes are now termed "photopic" and "scotopic" respectively. A good example of the function of a photopic eye is given by Varela and Wiitanen (1970) for adults of Apis mellifica L. (= A. mellifera L., Apidae). Parallel light rays in the corneal lens are brought to focus at a point about two-thirds of the way down the crystalline cone. As light penetrates beyond the focal point the rays diverge, lateral rays are absorbed by secondary pigment granules, and only the central rays proceed to the rhabdom for phototransduction. Therefore, in this optical arrangement, each ommatidium collects light through a narrow angle and less than 1 percent of the light striking a rhabdom is received through neighbouring corneal lenses (Shaw, 1969).

In scotopic eyes, the transparent clear zone or "crystalline tract" is formed either as an extension of Semper's cells (Horridge, 1968; 1969a), or by the distal non-rhabdomeric portions of the retinula cells (Kuiper, 1962; Miller et al., 1968; and Døving and Miller, 1969).

An alternative hypothesis to the superposition mosaic theory of Müller (1870), postulates that in dark-adapted scotopic eyes the crystalline tract functions as a wave guide since it has a higher refractive index than the surrounding cells (de Bruin, 1957). This hypothesis suggests that only the light focused in the tract is effective in stimulating individual retinulae and that light enters the rhabdom only in a perpendicular direction. However, Horridge (1971) showed that in clear zone scotopic eyes, light entering many facets is scattered upon several rhabdoms thus increasing light intensity received by each (Horridge, Ninham, and Diesendorf, 1972; and Horridge, 1975b). Structural changes including shortening of the crystalline tract, organelle movement in retinula cells, and pigment migrations for photopic and scotopic eyes during light adaptation are reviewed by Walcott (1975).

In this chapter, the structure of eyes of one representative species from each of the four North American genera of Cicindelidae is described using light microscopy. Since adults of Cicindela lepida Dejean exhibit a bimodal diurnal and crepuscular activity, specimens collected at twilight were examined to determine whether these beetles have secondarily evolved scotopic eyes for vision in near darkness. The cellular organization for vision of crepuscular, flightless adults of Cicindela (Dromochorus) belfragei Sallé is also analyzed because of their diel activity, and because of the ranking of this taxon as a

separate genus by some taxonomists (Chapter 2). To ascertain cellular changes in eyes caused by light deprivation, histological features of eyes of C. tranquebarica Herbst and C. limbata nympha Casey adults are described following dark adaptation. Eyes of specimens of C. leptda collected during daylight are also to describe diel activity changes in these eyes. Eyes of two carabini, the sister group to cicindelids (Arnett, 1968) are also studied to determine if there are similarities in [redacted]ture and function based on diel activity. Carabids examined were adults of nocturnal Pterostichus melanarius Illiger, and diurnal Elaphrus americanus Dejean.

Eye size groups and functional photopic and scotopic categories for these beetle eyes are determined from measurements of structures. These groups and categories are related to diel activity and discussed in relation to cellular organization in other insect eyes. From a reconstructed phylogeny of these beetles, an hypothesis is proposed concerning a course of evolution of compound eye structure and function and visual ability of cicindelid and carabid beetles.

4.2 Materials and Methods

Tissues used for SEM were prepared as described in Section 3.2. Histological material for light microscopy (LM) was fixed in hot 80 percent ethanolic Bouin's Duboscq (Pantin, 1962). Excised eyes were dehydrated in tertiary

butanol then double embedded using Peterfi's celloidin-paraffin technique (Pantin, 1962). To facilitate sectioning of these hard beetle heads, the knife and wax blocks were chilled. Sections were cut at 10 to 12 µm using a Leitz Wetzlar rotary microtome. The knife was grounded to prevent build up of static electricity. Longitudinal and transverse sections were treated in saturated mercuric chloride containing 5 percent acetic acid mordant solution (Pantin, 1962). Precipitations of mercurous chloride and metallic mercury were removed using Gram's variation of Lugol's iodine solution. A 5 percent sodium thiosulfate solution removed Lugol's solution (Humason, 1962). Sections were stained with Mallory's triple stain (Pantin, 1962) and mounted with Canada balsam. Representative photographs were taken using a Carl Zeitz Ultraphot II microscope on Kodak Plus-X, Pan Professional, 10.2 x 12.7 cm sheet film. Unstained sections were examined using a polarizing petrographic microscope and the Becke line (Bloss, 1961) was observed to move into eye structures with the higher refractive index. Using a Carl Zeitz Photomicroscope II with Nomarski interference optics (NIM), some relative refractive indices (n) of structures were determined. Dark-adapted beetles were deprived of light for five days before fixation.

The retinula was assumed to be a cylinder consisting of three portions: the clear zone, rhabdom zone, and basal zone. These volumes and volumes of the rhabdom zone of the basal retinula cell were calculated as cylinders. Volumes

of the rhabdom of the retinula rhabdom zone were calculated as a solid rectangle. Comparative measurement data were statistically analyzed using computer programs for One-Way Analysis of Variance and Duncan's New Multiple Range Test of Means (Sokal and Rohlf, 1969).

4.3 Results

4.3.1 Structure of Eyes of One Species of Each of the Four North American Genera of cicindelid Adults

4.3.1.1 General Features

Ommatidia of compound eyes of insects are organized into two distinct structural and functional regions; the light receiving or dioptric apparatus, with associated pigment cells, and the light perceiving apparatus, the retinula, with associated pigment cells. Figs. 79-82 are diagrammatic representative longitudinal sections of ommatidia. Figs. 29-32 illustrate longitudinal sections through compound eyes of one species from each of the four North American genera of Cicindelidae. These figures show the distal corneal lenses (l) having a thin corneal layer (t), and crystalline cones (c). Normally, the dioptric apparatus of eucone eyes (sensu Grenacher, 1879) consists solely of these two structures. However, in cicindelid beetle eyes, a third layer has been discovered between lens and cone. This layer is termed the "subcorneal layer" (cl) because of its position and structural similarity to the corneal

Figs. 29-32. LM of longitudinal sections of compound eyes of cicindelid beetles. Shown are: thin corneal layer (t); corneal lens (l); subcorneal layer (cl); crystalline cone (c); retinula (rt); rhabdom (r); basal retinula cell (b); basement membrane (bm); axons (a); lamina ganglionaris (lg); secondary pigment cells (2p); and basal pigment cells (bp). Note pigment accumulation (pa) in Fig. 32.

Scale = 200 µm

Fig. 29. Amblycheila schwarzi.

Fig. 30. Omus californicus.

Fig. 31. Megacephala carolina.

Fig. 32. Cicindela tranquebarica.

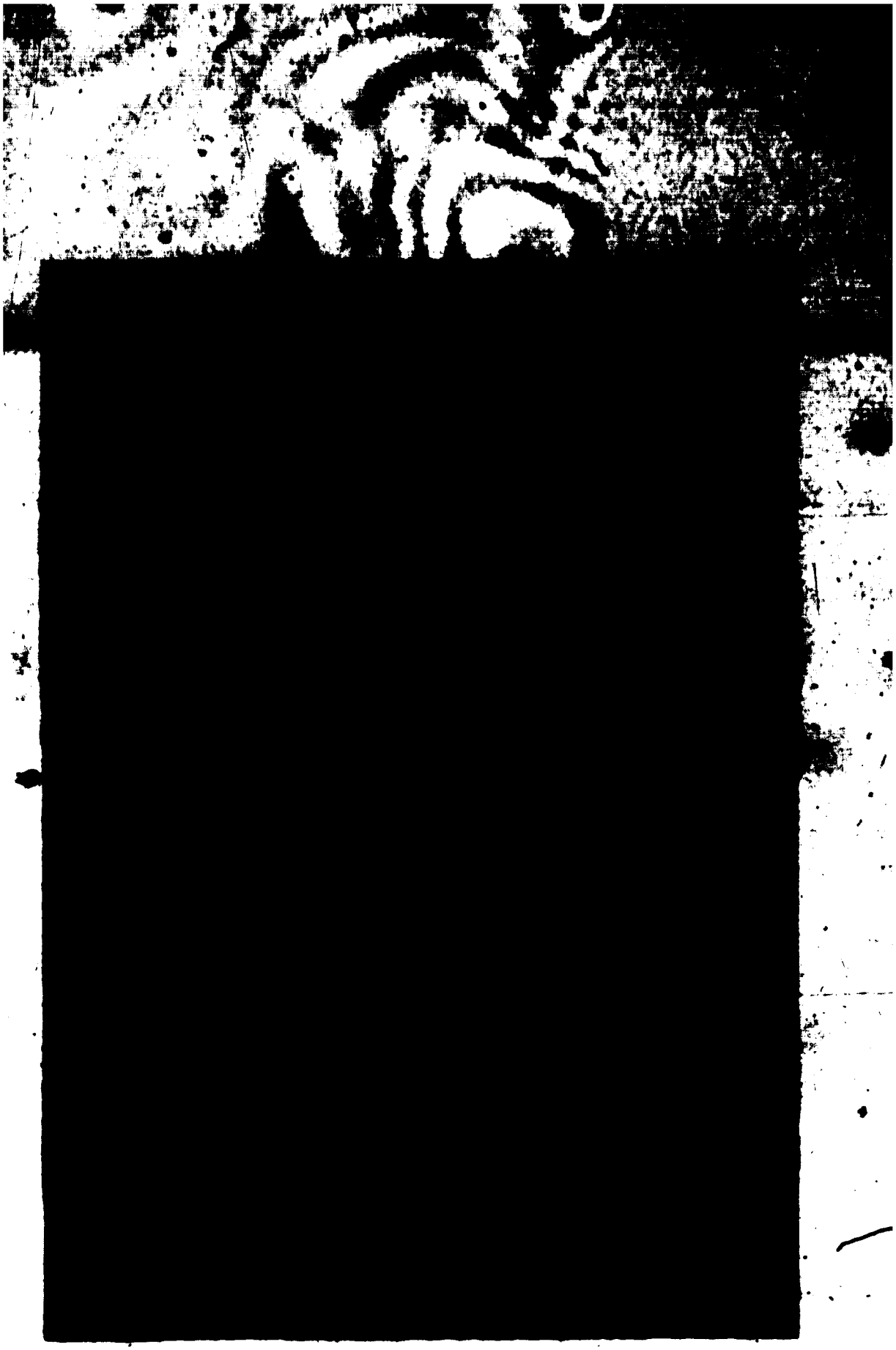

lens. These beetles therefore, have a three layered dioptric apparatus. Although not visible in these figures, two primary pigment cells (also termed principal pigment cells, Hauptpigmentzellen, corneagenous pigment cells, and primary iris cells; Goldsmith, 1964), which are devoid of pigment granules surround each crystalline cone. Oblique rays entering the eye, which cannot be focused by the dioptric apparatus, are absorbed laterally by pigment granules in secondary pigment cells (2p) (also termed Nebenpigmentzellen, secondary iris cells, iris pigment cells, and outer pigment cells; Goldsmith, 1964). In longitudinal section of the whole eye, most of the pigment appears as an opaque distal arch (2p) surrounding the crystalline cones. Secondary pigment granules are more densely aggregated and appear black in eyes of nocturnal A. schwarzi and O. californicus adults, compared to the less dense brown pigment granules in eyes of M. carolina and C. tranquebarica. The dioptric apparatus is connected to the retinula by a crystalline thread which is shrouded by secondary pigment cells. This thread is an extension from each of the four Semper's cells which surround the quadrants of the crystalline cone.

The retinula (rt) extends proximally from the tip of the crystalline thread to the basement membrane (bm). A cluster of seven neurons or retinula cells constitute the retinula. Microvilli of individual retinula cells constitute a rhabdomere. Rhabdomeres of the retinula cells interdidgitate to form a central rhabdom (r) which appears

as a solid line running centrally through the vertical axis of each retinula. Distal to the basement membrane, each ommatidium has an eighth or basal retinula cell (b) having a separate rhabdomere. Basal pigment cells (bp) containing pigment granules surround this basal retinula cell. Phototransduction occurs at the rhabdoms (Höglund et al., 1973). Each of the eight retinula cells extends an axon (a) to interneurons in the lamina ganglionaris (lg).

Tables 7 and 8 provide measurement data and some volumes of eye structures. Measurements were taken randomly from five different ommatidia.

4.3.1.2 Dioptric Apparatus and Interfacetal Pegs

The dioptric apparatus consists of the corneal lens, subcorneal layer, and crystalline cone. In eyes of nocturnal adults of A. schwarzi and O. californicus, it occupies approximately half the ommatidial length and is longer than the retinula. In crepuscular and diurnal eyes of M. carolina and C. tranquebarica adults it is approximately one-third of the ommatidial length and is shorter than the retinula (Table 7).

4.3.1.2.1 Corneal Lens

Scanning electron micrographs (Figs. 33-36) show that corneal lenses (l) of these beetle eyes are apparently convex distally and hexagonal. Longitudinal sections (Figs. 39,40,41,42) show that lenses are proximally convex so that

Table 7. Measurements of structures of compound eyes of cicindelid beetles. The values are $\bar{x}$ + SE for n = 5 for each species. 0 indicates no such structure exists for that species.

Structural Component (μm)	*Amblycheila schwarzi*	*Omus californicus*	*Megacephala carolina*	*Cicindela tranquebarica*
Diel activity:	Nocturnal	Nocturnal	Crepuscular	Diurnal
Thickness of thin corneal layer	2.27 ± 0.16	1.70 ± 0.15	3.95 ± 0.18	1.65 ± 0.17
Length of corneal lens	111.60 ± 1.63	106.95 ± 1.54	74.40 ± 1.62	67.43 ± 1.63
Diameter of corneal lens	22.73 ± 1.58	20.45 ± 1.65	22.73 ± 1.58	25.00 ± 1.73
Thickness of subcorneal layer	2.33 ± 0.16	2.33 ± 0.16	2.33 ± 0.16	3.49 ± 0.18
Height of interfacetal peg	0	0	3.08 ± 0.17	3.12 ± 0.16
Diameter of interfacetal peg	0	0	2.28 ± 0.16	2.32 ± 0.18

Table 7. Continued.

Structural Component (μm)	*Amblycheila schwarzi*	*Omus californicus*	*Megacephala carolina*	*Cicindela tranquebarica*
Length of crystalline cone	60.45 ± 1.63	34.58 ± 1.58	55.80 ± 1.61	53.48 ± 1.65
Diameter of crystalline cone	18.60 ± 1.54	17.44 ± 1.68	16.28 ± 1.63	16.28 ± 1.63
Total length of dioptric apparatus	176.65 ± 1.63	145.56 ± 1.65	136.48 ± 1.61	126.05 ± 1.65
Length of crystalline cone	23.25 ± 1.62	13.95 ± 1.68	60.45 ± 1.62	51.15 ± 1.60
Length of retinula				
(a) clear zone	44.18 ± 1.63	0	111.60 ± 1.63	0
(b) rhabdom zone	58.13 ± 1.62	86.03 ± 1.61	102.30 ± 1.68	186.00 ± 1.63
(c) basal zone	20.93 ± 1.63	16.28 ± 1.65	18.60 ± 1.63	18.60 ± 1.63

Table 7. Continued.

Structural Component (μm)	*Amblycheila schwarzi*	*Omus californicus*	*Megacephala carolina*	*Cicindela tranquebarica*
Total length of retinula	123.24 ± 1.63	102.31 ± 1.63	232.50 ± 1.65	204.60 ± 1.63
Total length of ommatidium	323.14 ± 1.63	261.82 ± 1.58	429.43 ± 1.61	381.80 ± 1.65
Dimensions of retinula				
(a) Diameter of clear zone	4.63 ± 1.62	0	5.55 ± 1.63	0
(b) Diameter of rhabdom zone	12.79 ± 1.63	11.63 ± 1.61	12.79 ± 1.63	12.95 ± 1.65
(c) Diameter of basal zone	13.95 ± 1.63	13.95 ± 1.63	13.95 ± 1.63	11.63 ± 1.61

Table 7. Continued.

Structural Component (μm)	*Amblycheila schwarzi*	*Omus californicus*	*Megacephala carolina*	*Cicindela tranquebarica*
Dimensions of rhabdom				
(a) Rhabdom zone				
Length	9.30 ± 1.31	6.98 ± 1.28	11.63 ± 1.30	5.00 ± 1.32
Width	8.14 ± 1.30	5.81 ± 1.30	8.14 ± 1.30	4.00 ± 1.32
(b) Diameter of basal zone	4.65 ± 1.30	4.65 ± 1.30	6.95 ± 1.30	5.79 ± 1.31
% length of dioptric apparatus / Length of ommatidium	54.67 ± 0.22	55.59 ± 0.26	31.78 ± 0.25	53.01 ± 0.28

Table 7. Continued.

Structural Component (μm)	*Amblycheila schwarzi*	*Omus californicus*	*Megacephala carolina*	*Cicindela tranquebarica*
% length of crystalline thread / Length of ommatidium	7.20 ± 0.46	5.33 ± 0.58	14.08 ± 0.33	13.40 ± 0.37
% length of retinula / Length of ommatidium	38.13 ± 0.31	39.08 ± 0.38	54.14 ± 0.17	53.59 ± 0.20

Table 8. Volumes of the retinula and rhabdom of compound eyes of cicindelid beetles. The values are $\bar{x} \pm SE$ for n = 5 for each species. 0 indicates no such volume exists for that species.

Volume $(\mu m)^3$	*Amblycheila schwarzi*	*Omus californicus*	*Megacephala carolina*	*Cicindela tranquebarica*
Volume of retinula				
(a) clear zone	743.84 ± 80.01	0	2,699 ± 197.96	0
(b) rhabdom zone	7,468.46 ± 399.26	9,139.01 ± 428.74	13,143.37 ± 543.58	24,498.66 ± 829.93
(c) basal zone	3,198.95 ± 323.59	2,488.24 ± 306.99	2,842.83 ± 315.26	1,975.89 ± 228.42
Total volume of retinula / Ommatidium	11,411.25 ± 802.80	11,627.25 ± 735.73	18,686.05 ± 1056.77	26,474.55 ± 1058.32
Total volume of retinula / Compound eye	$(19.40 \pm 1.50)(10^6)$	$(17.44 \pm 1.20)(10^6)$	$(78.48 \pm 4.90)(10^6)$	$(105.90 + 4.74)(10^6)$
Volume of rhabdom				
(a) Rhabdom zone	4,400.56 ± 288.47	3,488.84 ± 262.03	9,684.56 ± 483.36	3,720.00 ± 305.31

Table 8. Continued.

Volume $(\mu m)^3$	*Amblycheila schwarzi*	*Omus californicus*	*Megacephala carolina*	*Cicindela tranquebarica*
(b) Basal zone	355.44 ± 52.86	276.47 ± 47.34	705.62 ± 95.11	489.73 ± 70.72
Surface area of rhabdom in rhabdom zone $(\mu m)^2$	75.70 ± 2.84	40.55 ± 2.08	94.67 ± 3.19	20.00 ± 1.46
Total volume of rhabdom / Ommatidium	4,756.00 ± 341.13	3,765.31 ± 309.15	10,390.18 ± 578.69	4,209.73 ± 376.01
Total volume of rhabdom / Compound eye	$(8.09 \pm 0.63)(10^6)$	$(5.65 \pm 0.50)(10^6)$	$(43.64 \pm 2.69)(10^6)$	$(16.84 \pm 1.58)(10^6)$
% rhabdom volume / Retinula volume	41.68 ± 0.06	32.38 ± 0.66	55.60 ± 0.05	15.90 ± 0.78

Figs. 33-36. SEM of convex distal surfaces of hexagonal corneal lenses (l) of ommatidia, showing the scratched thin corneal layer (t). Note cuticular pegs (cp) between some lenses of eyes of M. carolina (Fig. 35) and C. tranquebarica (Fig. 36).

Scale = 10 µm.

Fig. 33. Amblycheila schwarzi.

Fig. 34. Omus californicus.

Fig. 35. Megacephala carolina.

Fig. 36. Cicindela tranquebarica.

Figs. 37-38. Same, of cuticular pegs (cp) of interfacetal mechanoreceptors of adult eyes of M. carolina (Fig. 37) and C. tranquebarica (Fig. 38). Note ecdysial scar (es).

Scale = 1 µm

Figs. 39,40,41,42. Longitudinal sections of lamellated (lm) corneal lenses (l) and crystalline cones (c). Note variations in length and slope of cone sides. Surrounding the cones are two Semper cells (s) shrouded by secondary pigment cells (2p). The subcorneal layer (cl) is also shown.
Scale = 20 µm

Fig. 39. Amblycheila schwarzi.

Fig. 40. Omus californicus.

Fig. 41. Megacephala carolina.

Fig. 42. Cicindela tranquebarica.

Figs. 43,44. Same, of the extension of four Semper's cells which form the crystalline thread (ct).
Scale = 20 µm

Fig. 43. Megacephala carolina.

Fig. 44. Cicindela tranquebarica.

close contact is made with the distal concavity of the underlying crystalline cone (c). Lenses consist of horizontal lamellae (Fig. 41). Although not calculated, these lamellae have a variety of refractive indices under Nomarski interference optics. Lengths and diameters of lenses are given in Table 7. Eyes of the nocturnal beetles have the longest lenses and represent larger percentages of ommatidial lengths (Table 7).

None of the corneal lenses of these beetle eyes have corneal nipples (Bernhard et al., 1965). Particularly on eyes of nocturnal adults of A. schwarzi and those of crepuscular adults of M. carolina, is a thin corneal layer (t) over the surface of the lenses (Figs. 33-36). Histochemically, the thin corneal layer is acidophilic since it stains with phosphomolybdic acid. The surface of the thin corneal layer is scratched (Figs. 33-35). Table 7 lists the thickness of this layer.

Thin films of transparent substances such as magnesium fluoride (MgF_2: n = 1.38), applied to camera lenses reduce reflection from the lens surface by interference. Attempts were made here to determine if this thin corneal layer acts as such a thin film. Knowing the refractive index (assuming fixation and dehydration did not induce any changes) and thickness of the thin corneal layer, the possible interference ability can be calculated (Fig. 45: modified after Halliday and Resnick, 1970). If light strikes the lens at near normal incidence (θ), a phase change of 180° is associ-

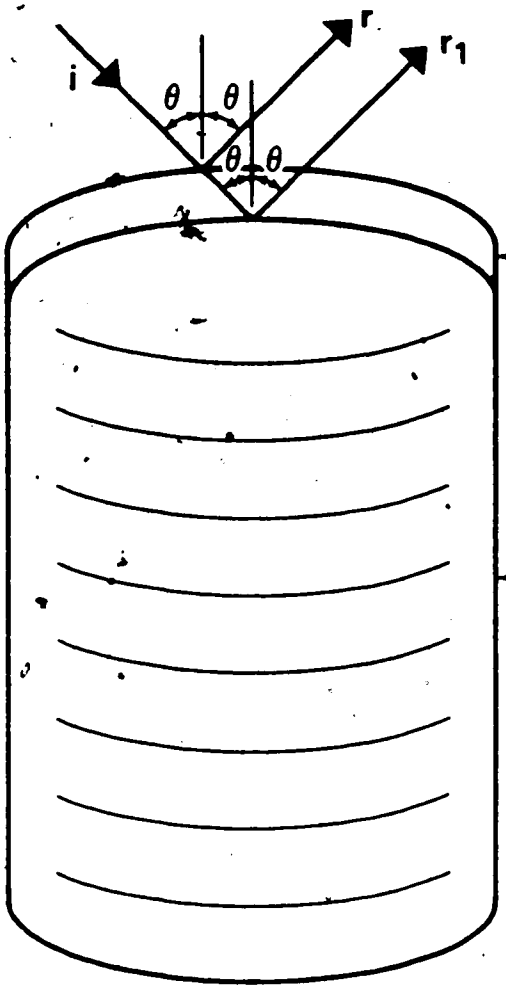

i = incident ray

r = reflected ray

r_1 = reflected ray

θ = angle of incidence and angle of reflection

45

ated with each ray since at the upper and lower surfaces of the film the reflection is from a medium of greater refractive index. There is no net change in phase produced by the two reflections (r, r_1) which indicates that the optical path difference for destructive interference is $(m = 1/2)\tau$ leading to:

$$2dn = (m + 1/2)\tau$$

where d = thickness of thin corneal layer

n = refractive index of thin corneal layer

m = 0,1,2,...(minima)

τ = wavelength of light

Table 9 lists the wavelengths of light which would produce minimum reflection if the thin corneal layer functions as an antireflecting layer (see discussion; Section 4.4.1).

4.3.1.2.2 Interfacetal Pegs

Scattered between lenses (facets) of adult eyes of M. carolina (fig. 37) and C. tranquebarica (Fig. 38) are triangular cuticular pegs (cp). There is approximately one peg per 20 ommatidia with a total of approximately 210 per eye in adults of M. carolina and one peg per 15 ommatidia (total of 260) on eyes of C. tranquebarica adults. Pegs are slightly taller and wider in eyes of C. tranquebarica (Table 7). These structures are not present on eyes of either

Table 9. Wavelengths of light required to produce minimum reflection within the thin corneal layer of compound eyes of cicindelid beetles.

Measurement	*Amblycheila schwarzi*	*Omus californicus*	*Megacephala carolina*	*Cicindela tranquebarica*
Thickness of thin corneal layer (d) in nm	2,275.0	1,703.0	3,958.0	1,655.0
Refractive index of thin corneal layer (n)	1.34	1.35	1.34	1.35
τ for minimum reflection in nm	12,194.0	9,196.2	21,214.9	8,937.0

adults of A. schwarzi or O. californicus (Figs. 33,34). Since the pegs appear to lie on a cuticular articulating membrane and since there is no hole at the apex, it is assumed that these structures function as mechanoreceptors. However in Fig. 37, a pit is clearly evident on the side of the peg. From its position it is likely the ecdysial scar (es) of the dendritic sheath (McIver, 1975).

4.3.1.2.3 Subcorneal Layer

The subcorneal layer (cl) is attached to the proximal surface of the corneal lens (Figs. 39,40,41,42). This layer is acidophilic, staining with phosphomolybdic acid. Its thickness varies (Table 7) from 2.33 µm in eyes of adult A. schwarzi, O. californicus, and M. carolina to 3.49 µm in eyes of C. tranquebarica. The subcorneal layer is thicker in the diurnal cicindelid than in the nocturnal and crepuscular tiger beetle eyes. Using a polarized petrographic microscope and following the Becke line into media of higher refractive index, the subcorneal layer was observed to have a higher refrattive index than the corneal lens, but a lower value than the distal portion of the crystalline cone. This layer then refracts incident light toward the centre of the underlying cone.

4.3.1.2.4 Crystalline Cone

All eyes considered here are eucone type. Cones consist of four quadrants in transverse section. In longi-

tudinal section (Figs. 39,40,41,42), they are conical but vary in length, width (Table 7), and acuteness. A transparent, thin, Semper cell surrounds each of the four quadrants of the crystalline cone. Nuclei of Semper's cells (s) are located beneath the subcorneal layer. These four cells surround the crystalline cone and are themselves enveloped by secondary pigment cells (2p) (Figs. 39,40,41, 42). From Becke line movements, the crystalline cone can be shown to have a higher refractive index than the corneal lens and therefore functions in bending the incident light rays toward the medially situated crystalline thread. Figs. 46-49 show optical paths into the compound eyes. Light was transmitted through histological longitudinal sections of the dioptric apparatus.

4.3.1.3 Crystalline Thread

Elongations of four transparent Semper cells, which extend proximally to the distal tip of the retinula cells, form the crystalline thread (ct). In longitudinal section (Figs. 43,44), it appears as a thread and has a higher refractive index than that of the surrounding tissue. In eyes of adults of the nocturnal genera, it is very densely surrounded by secondary pigment granules. In transverse section, 16 secondary pigment cells (2p) form a stellar arrangement around the four quadrants of the threads (ct) (Figs. 50-53). In Fig. 53 two primary pigment cells (1p) are also visible. Crystalline threads are longer in eyes of diurnal and

Figs. 46-49. Optical paths through longitudinal sections of the dioptric apparatus. Light is transmitted into the corneal lens (l), through the crystalline cone (c) and along the crystalline thread (ct). Oblique rays are absorbed by pigment granules in secondary pigment cells (2p). Light was transmitted antidromically through these sections. Scale = 50 μm.

Fig. 46. Amblycheila schwarzi.

Fig. 47. Omus californicus.

Fig. 48. Megacephala carolina.

Fig. 49. Cicindela tranquebarica.

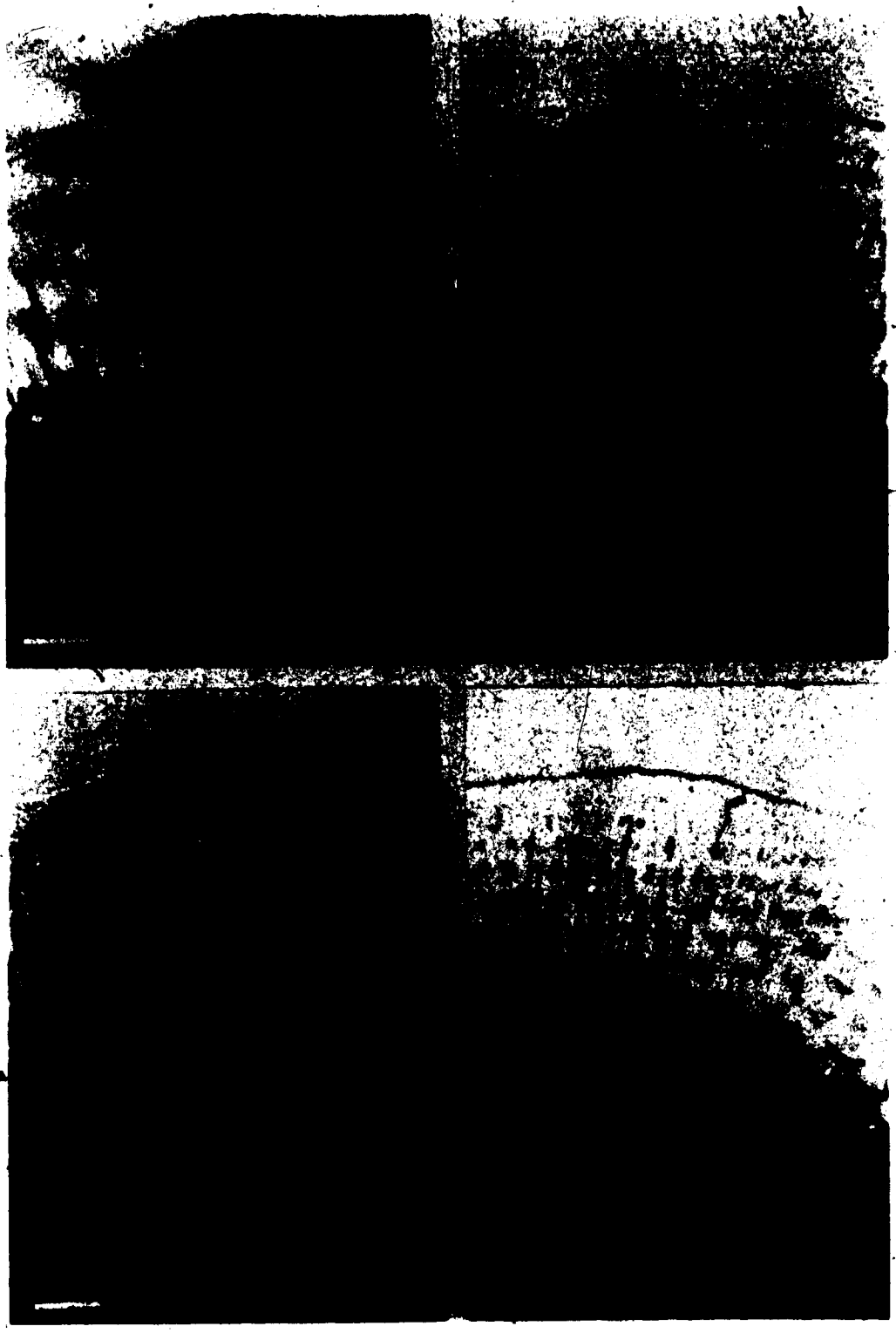

Figs. 50-53. Transverse sections through crystalline threads (ct), showing secondary pigment cells (2p) and in C. tranquebarica (Fig. 53), two primary pigment cells (1p).

Scale = 20 µm

Fig. 50. Amblycheila schwarzi.

Fig. 51. Omus californicus.

Fig. 52. Megacephala carolina.

Fig. 53. Cicindela tranquebarica.

Figs. 54-57. Same, through distal tips of retinula cells, showing seven retinula cell nuclei (n) and central fused rhabdoms (r).

Scale = 20 µm

Fig. 54. Amblycheila schwarzi.

Fig. 55. Omus californicus.

Fig. 56. Megacephala carolina.

Fig. 57. Cicindela tranquebarica.

crepuscular beetles (Table 7).

4.3.1.4 Retinula Cells

Distal transverse sections of the retinula cells (Figs. 54-57) reveal seven nuclei (n) of retinula cells. The seven retinula cells of ommatidia of A. schwarzi adults (Fig. 58) and of M. carolina (Fig. 60) consist of a clear zone (cr) and a rhabdom zone (rr). Retinulae of eyes of adult O. californicus (Fig. 59) and of C. tranquebarica (Fig. 61) consist only of a rhabdom zone (rr). All have a basal retinula zone (br). Transverse sections through the rhabdom zone show rectangular, fused rhabdoms (r) in the centre of the retinula cells (Figs. 62,63,65,66). Two retinula cells contribute microvilli to form the rhabdom on the long sides; one cell on each short side. The rhabdom occupies a greater percentage of retinula cell surface area and volume in eyes of adult A. schwarzi (Fig. 62) and M. carolina (Fig. 65) than in O. californicus (Fig. 63) or C. tranquebarica (Fig. 66). In eyes of C. tranquebarica the retinula cytoplasm is distinctly visible (Fig. 66), and the rhabdom appears as the centre of a "flower" surrounded by seven "petals", the retinula cells. Fig. 64 is a transverse section through the clear retinula zone of eyes of M. carolina adults. In all four beetle eyes, the seventh retinula cell (7) does not contribute to the rhabdom at this level. This highly vacuolated cell (Fig. 66) is positioned lateral to the rhabdom. Fig. 65 is a transverse

Figs. 58-61. Longitudinal sections of retinulae, showing clear zone of retinula (cr); rhabdom zone (rr); basal zone (br); and rhabdom (r).
Scale = 50 μm

Fig. 58. Amblycheila schwarzi.

Fig. 59. Omus californicus.

Fig. 60. Megacephala carolina.

Fig. 61. Cicindela tranquebarica.

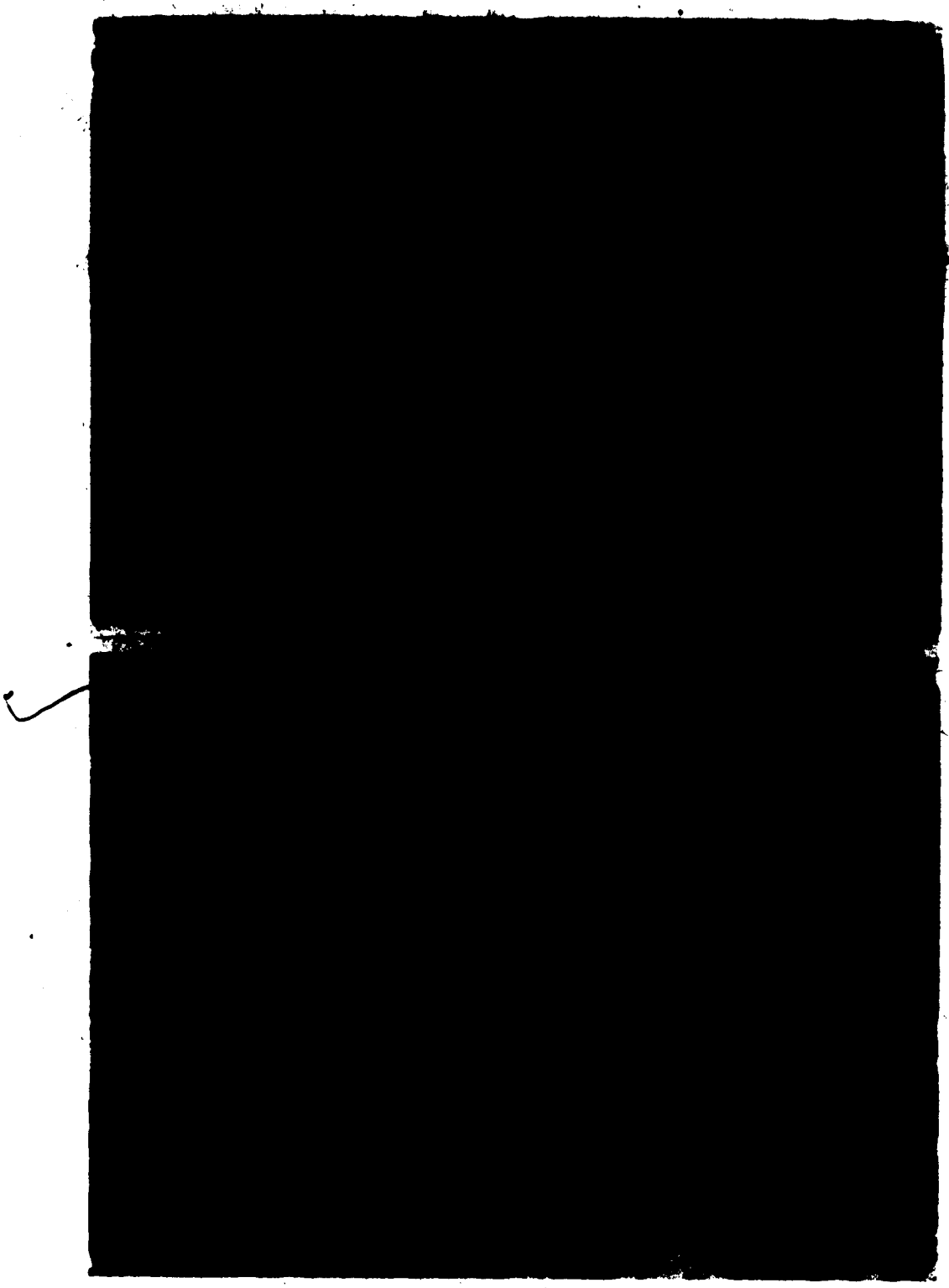

Figs. 62-66. Transverse sections through clear retinula zone (cr) of M. carolina (Fig. 64) and rhabdom zone of the four beetle eyes. The rectangular, fused rhabdom (r) of nocturnal and crepuscular eyes have large surface areas with limited retinula cytoplasm compared to the small rhabdom (r) of the diurnal eye. Note retinula cell seven (7).

Scale = 20 µm

Fig. 62. Amblycheila schwarzi.

Fig. 63. Omus californicus.

Fig. 64. Megacephala carolina.

Fig. 65. Megacephala carolina.

Fig. 66. Cicindela tranquebarica.

Figs. 67-70. Same, through basal, eighth retinula cells, showing central spherical rhabdom (r) surrounded by basal pigment cells (bp). Note basement membrane (bm) in Fig. 70.

Scale = 20 µm

Fig. 67. Amblycheila schwarzi.

Fig. 68. Omus californicus.

Fig. 69. Megacephala carolina.

Fig. 70. Cicindela tranquebarica.

section through the clear retinula zone of eyes of M. carolina adults. The clear zone of eyes of A. schwarzi also consists of seven retinula cells without a rhabdom. An eighth or basal retinula cell is distal to the basement membrane (bm) and contains a separate rhabdom (r) (Figs. 67-70). Retinulae of all these beetle eyes are shrouded by secondary pigment cells along their lengths. Basal retinula cells are also surrounded by four basal pigment cells (bp). Dimensions of retinula cells and their rhabdoms are listed in Table 7. Data in Table 7 show that retinulae of eyes of nocturnal beetles occupy about 40 percent of the ommatidial length; 50 percent in diurnal beetle eyes. Therefore, both ommatidia and retinulae are longer in diurnal cicindelid beetles. Table 8 shows retinula and rhabdom volumetric relationships, discussed in Section 4.3.5.

4.3.1.5 The Visual Peripheral Nervous System and the Central Nervous System

Each of the eight retinula cell axons synapse with an interneuron in the optic lobe. The eight axons from each ommatidium penetrate a single circular fenestration in the tracheole-rich basement membrane (bm), and are aggregated with axons of six adjacent ommatidia in the form of axonal bundles (ab) distal to the lamina ganglionaris (lg) (Figs. 71-74). Between axonal bundles are haemolymph channels (hc) (Shaw, 1977). Evident from these figures, axons of eyes of A. schwarzi adults are much longer than those in other beetle

Figs. 71-74. Longitudinal sections through axonal bundles (ab) of eight axons from eight adjacent ommatidia as they exit the basement membrane (bm) and enter the lamina ganglionaris (lg). Note length of axonal bundles of A. schwarzi (Fig. 71). Pigment granules (p) surround adjacent axons. Between axonal bundles are haemolymph channels (hc).

Scale = 40 µm

Fig. 71. Amblycheila schwarzi.

Fig. 72. Omus californicus.

Fig. 73. Megacephala carolina.

Fig. 74. Cicindela tranquebarica.

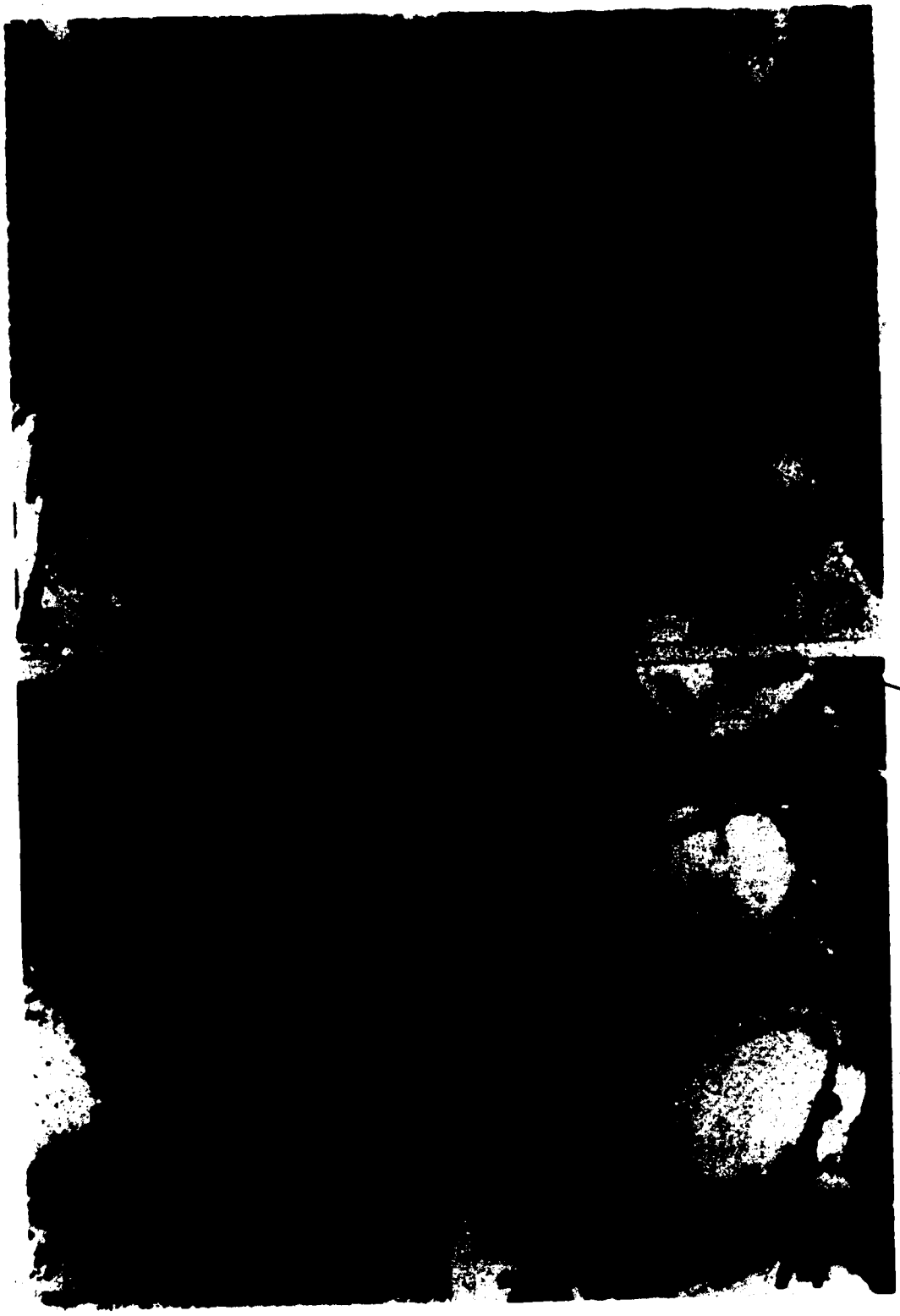

eyes. Pigment granules (p) in glial cells surround adjacent axons.

The neuronal pathway through the brain is suggested in Figs. 75-78. Following synapsis with lamina interneurons, axons are extended to the lamina and cross over at the first optic chiasmata (1c), then extend to the medulla (md), the second synaptic site of the optic lobe. Visual axons again cross over at the second optic lobe. Visual (2c), followed by proximal synapsis in the third region of the optic lobe, the lobula (lo). Glial cells (gl) surround the axons. Optic lobes consist of a connective tissue sheath, the neurilemma (nl), an underlying cellular perineurium (pn) with glial and neuronal cell bodies, and a central neuropile of axons and dendrites. A large pigment accumulation (pa) is on the ventral aspect of the interface of the lamina and medulla of the optic lobe (see also Fig. 32).

4.3.1.6 Summary of Structural Components

Structures of representative ommatidia are summarized diagrammatically in Figs. 79-82.

4.3.2 Structure of Eyes of *Cicindela lepida* and *Cicindela belfragei* Adults

Tables 10 and 11 include measurement and volumetric data of structures of these beetle eyes.

Fig. 83 of the head of a *C. lepida* adult collected at

Figs. 75-78. Frontal sections through optic lobes, showing axonal bundles (ab); lamina ganglionaris (lg); first optic chiasmata (1c); medulla (md); second optic chiasmata (2c); lobula (lo); glial cells (gl); neurilemma (nl); and perineurium (pn). Note dense pigment accumulation (pa) on the ventral aspect of optic lobes.

Scale = 100 µm

Fig. 75. Amblycheila schwarzi.

Fig. 76. Omus californicus.

Fig. 77. Megacephala carolina.

Fig. 78. Cicindela tranquebarica.

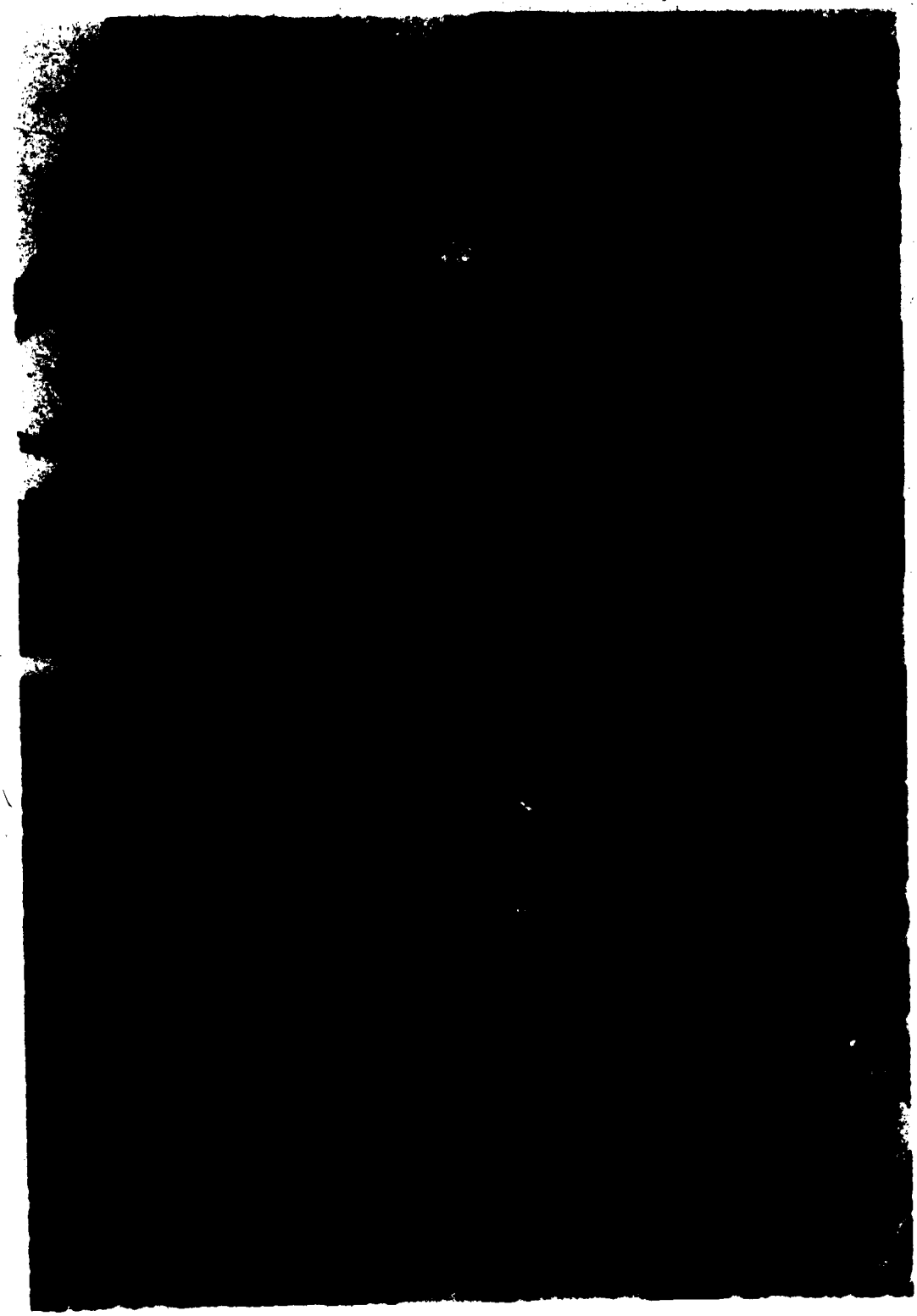

Figs. 79-82. Diagrammatic longitudinal sections of representative ommatidia and transverse sections of proximal rhabdoms of four cicindelid beetles, showing thin corneal layer (t); corneal lens (l); subcorneal layer (cl); cyrstalline cone (c); Semper cells (s); crystalline thread (ct); distal rhabdom (dr) of retinula cell seven (7); clear retinula zone (cr); proximal rhabdom (pr) of six retinula cells; basal retinula cell (b) with rhabdomere (br); secondary pigment cells (2p); basal pigment cells (bp); basement membrane (bm); and eight axons (a).

Longitudinal section scale = 50 μm

Transverse section scale = 20 μm

Fig. 79. Amblycheila schwarzi (Scotopic A).

Fig. 80. Omus californicus (Scotopic B).

Fig. 81. Megacephala carolina (Scotopic A).

Fig. 82. Cicindela tranquebarica (Photopic).

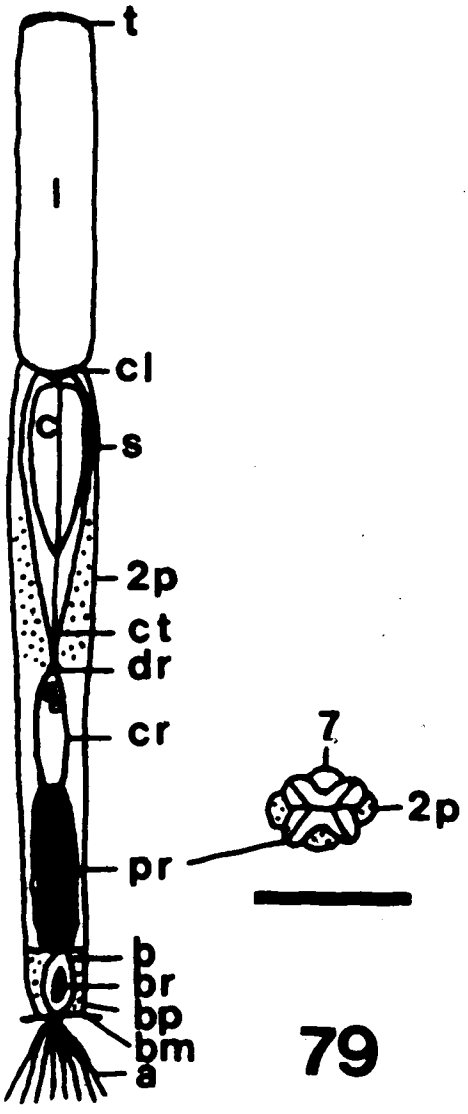
t
l
cl
c
s
2p
ct
dr
cr
pr
b
br
bp
bm
a
7
2p

79

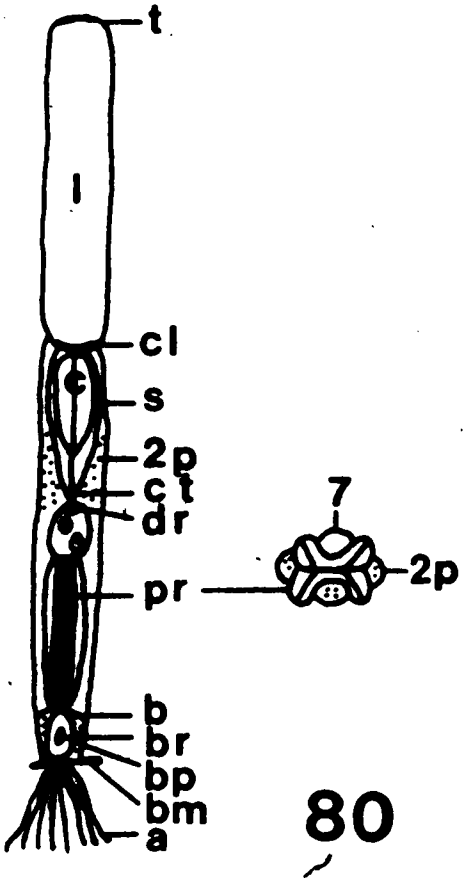
t
l
cl
c
s
2p
ct
dr
pr
b
br
bp
bm
a
7
2p

80

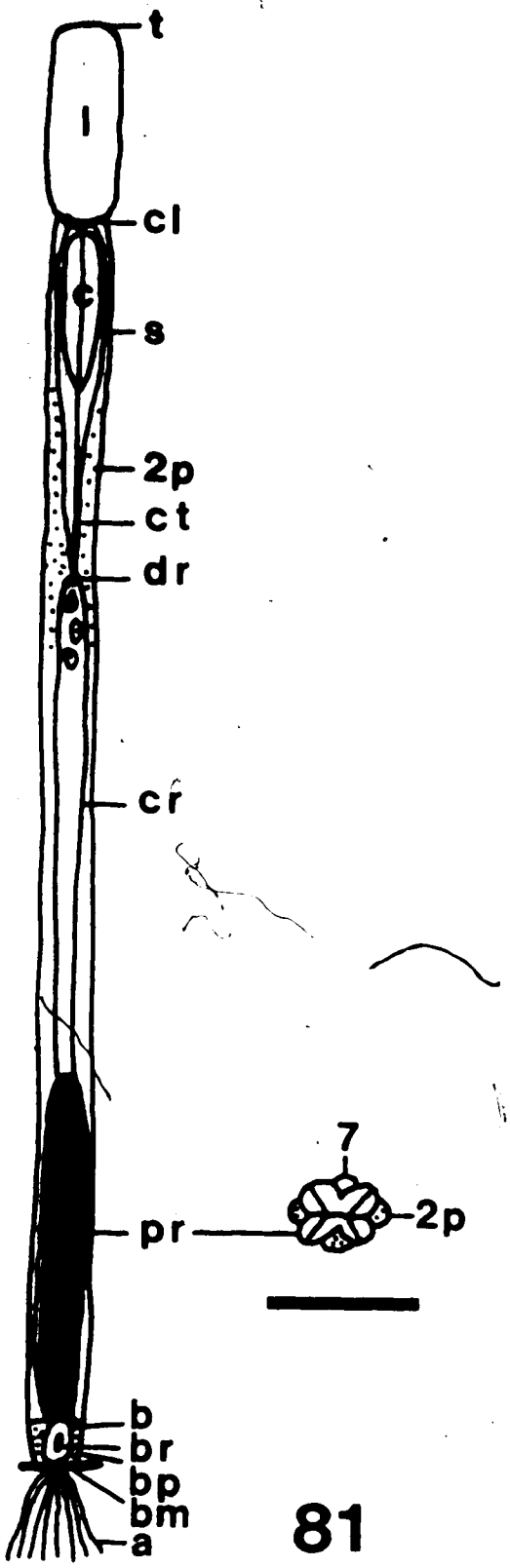
t
l
cl
c
s
2p
ct
dr
cr
pr
7
2p
b
br
bp
bm
a

81

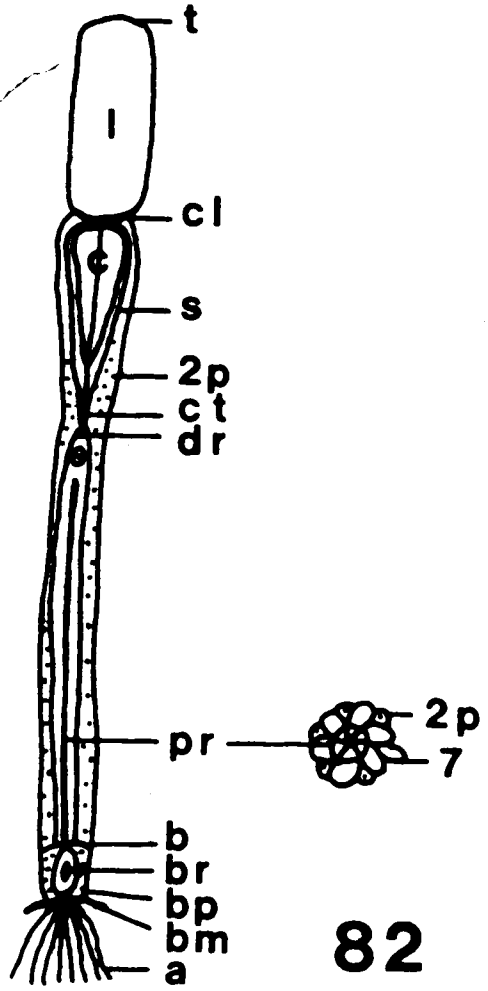
t
l
cl
c
s
2p
ct
dr
pr
2p
7
b
br
bp
bm
a

82

Table 10. Measurements of structures of compound eyes of two cicindelid and two carabid beetles.

The values are $\bar{x} \pm SE$ for $n = 5$ for each species. 0 indicates no such structure exists for that species.

Structural Component (μm)	*Cicindela lepida*	*Cicindela belfragei*	*Pterostichus melanarius*	*Elaphrus americanus*
Diel activity	Crepuscular	Crepuscular	Nocturnal	Dirunal
Number of ommatidia	3,200 ± 22.00	3,800 ± 27.00	1,420 ± 11.00	1,770 ± 9.00
Thickness of thin corneal layer	1.58 ± 0.16	1.36 ± 0.15	2.27 ± 0.16	0.75 ± 0.14
Length of corneal lens	47.67 ± 1.60	56.75 ± 1.68	63.56 ± 1.62	56.75 ± 1.63
Diameter of corneal lens	24.97 ± 1.63	24.97 ± 1.62	24.97 ± 1.65	22.70 ± 1.68
Thickness of subcorneal layer	2.27 ± 0.13	2.27 ± 0.14	1.70 ± 0.15	2.27 ± 0.13
Height of interfacetal peg	2.45 ± 0.11	2.54 ± 0.12	0	2.31 ± 0.16

Table 10. Continued.

Structural Component (μm)	Cicindela lepida	Cicindela belfragei	Pterostichus melanarius	Elaphrus americanus
Diameter of interfacetal peg	1.91 ± 0.14	2.00 ± 0.11	0	1.54 ± 0.11
Length of crystalline cone	47.67 ± 1.64	40.86 ± 1.68	47.67 ± 1.61	22.70 ± 1.59
Diameter of crystalline cone	16.08 ± 1.67	15.46 ± 1.58	13.62 ± 1.72	11.80 ± 1.58
Total length of dioptric apparatus	99.19 ± 3.58	101.24 ± 4.55	115.20 ± 1.67	82.47 ± 1.61
Length of crystalline thread	7.08 ± 1.68	9.08 ± 1.64	29.51 ± 1.63	13.62 ± 1.65
Length of retinula				
(a) Clear zone	76.50 ± 1.69	0	0	0

Table 10. Continued.

Structural Component (μm)	Cicindela lepida	Cicindela belfragei	Pterostichus melanarius	Elaphrus americanus
(b) Rhabdom zone	90.00 ± 1.78	121.50 ± 1.61	97.61 ± 1.60	95.34 ± 1.65
(c) Basal zone	18.00 ± 1.61	13.50 ± 1.61	18.16 ± 1.48	9.08 ± 1.51
Total length of retinula	184.50 ± 4.88	135.00 ± 3.25	115.77 ± 1.59	104.42 ± 1.60
Total length of ommatidium	290.77 ± 8.69	245.32 ± 7.83	260.48 ± 1.65	200.51 ± 1.62
Dimensions of retinula				
(a) Diameter of clear zone	6.65 ± 1.63	0	0	0
(b) Diameter of rhabdom zone	11.35 ± 1.64	9.08 ± 1.63	11.10 ± 1.57	10.22 ± 1.61
(c) Diameter of basal zone	10.22 ± 1.61	6.81 ± 1.65	9.25 ± 1.62	9.08 ± 1.59

Table 10. Continued.

Structural Component (μm)	Cicindela lepida	Cicindela belfragei	Pterostichus melanarius	Elaphrus americanus
Dimensions of rhabdom				
(a) Rhabdom zone				
Length	9.08 ± 1.36	3.41 ± 0.98	9.25 ± 1.30	2.72 ± 1.24
Width	6.81 ± 1.63	3.41 ± 1.26	8.33 ± 1.31	2.72 ± 1.22
(b) Diameter of basal zone	4.54 ± 1.61	2.72 ± 0.69	4.65 ± 1.32	2.27 ± 1.26
% length of dioptric apparatus / Length of ommatidium	34.12 ± 0.22	41.27 ± 0.57	44.23 ± 0.33	41.13 ± 0.48

Table 10. Continued.

Structural Component (µm)	Cicindela lepida	Cicindela belfragei	Pterostichus melanarius	Elaphrus americanus
% length of crystalline thread / Length of ommatidium	2.43 ± 0.02	3.70 ± [illegible]	11.33 ± 0.56	6.79 ± 0.61
% length of retinula / Length of ommatidium	63.45 ± 0.20	55.03 ± 0.52	44.44 ± 0.36	52.08 ± 0.39

Table 11. Volumes of the retinula and rhabdom of compound eyes of two cidindelid and two carabid beetles.

Values are $\bar{x} \pm$ SE for n = 5 for each species. 0 indicates no such volume exists for that species.

Volume $(\mu m)^3$	Cicindela lepida	Cicindela belfragei	Pterostichus melanarius	Elaphrus americanus
Volume of retinula				
(a) Clear zone	2,657.02 ± 186.82	0	0	0
(b) Rhabdom zone	9,105.93 ± 425.88	7,867.62 ± 338.92	9,445.61 ± 437.23	7,821.08 ± 382.70
(c) Basal zone	1,476.60 ± 180.58	491.72 ± 83.11	1,220.36 ± 152.60	587.96 ± 126.78
Total volume of retinula Ommatidium	13,239.55 ± 793.26	8,359.24 ± 421.41	10,665.97 ± 589.81	8,409.04 ± 509.45
Total volume of retinula Compound eye	$(42.37 \pm 0.28)(10^6)$	$(31.77 \pm 1.82)(10^6)$	$(15.15 \pm 0.95)(10^6)$	$(14.88 \pm 0.97)(10^6)$
Volume of rhabdom				
(a) Rhabdom zone	5,564.70 ± 329.23	1,413.04 ± 154.32	7,521.09 ± 404.87	705.36 ± 97.25

Table 11. Continued.

Volume $(\mu m)^3$	*Cicindela lepida*	*Cicindela belfragei*	*Pterostichus melanarius*	*Elaphrus americanus*
(b) Basal zone	291.39 ± 47.58	78.44 ± 19.21	308.40 ± 49.57	36.75 ± 12.23
Surface area of rhabdom in rhabdom zone $(\mu m)^2$	61.83 ± 2.53	11.63 ± 1.11	77.05 ± 2.86	6.17 ± 0.81
Total volume of rhabdom / Ommatidium	5,856.09 ± 376.79	1,491.48 ± 173.48	7,829.49 ± 454.39	742.11 ± 109.44
Total volume of rhabdom / Compound eye	$(18.74 \pm 1.33)(10^6)$	$(5.67 \pm 0.70)(10^6)$	$(11.12 \pm 0.73)(10^6)$	$(1.31 \pm 0.20)(10^6)$
% rhabdom volume / Retinula volume	44.23 ± 0.19	17.84 ± 1.17	73.41 ± 0.20	8.83 ± 0.75

Fig. 83. SEM of the frontal aspect of the head of a Cicindela lepida adult, showing large bulbous eyes.

Scale = 500 µm

Fig. 84. Same, of a lateral view of the left compound eye, showing hexagonal corneal lenses (l) and ocular sclerite (os). Vertex positioned at the left.

Scale = 200 µm

Fig. 85. Same, of convex distal surfaces of hexagonal corneal lenses (l). Note cuticular pegs (cp) between some lenses.

Scale = 10 µm

Fig. 86. Same, of a cuticular peg (cp) of an interfacetal mechanoreceptor. Note ecdysial scar (es).

Scale = 1 µm

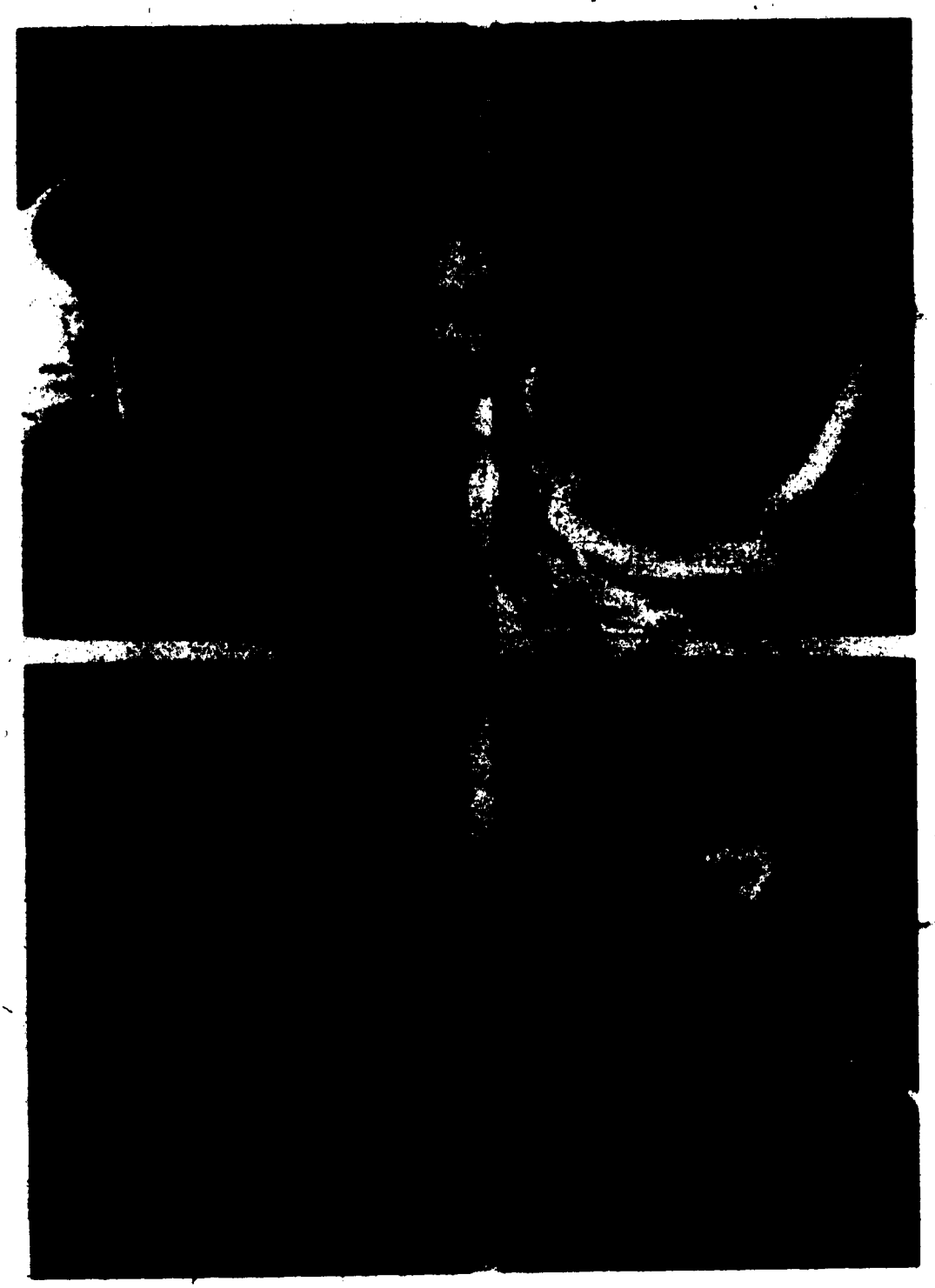

twilight shows large bulbous eyes, similar in shape (Fig. 84) to those of C. tranquebarica adults (Fig. 16). Because of their eye size, large stereoscopic visual fields can be inferred for these eyes. Corneal lenses (l) (Fig. 85) and interfacetal pegs (cp) (Fig. 86) are typical of Cicindela adults. The thin corneal layer (t) is relatively thin (Table 10). From longitudinal (Fig. 87) and transverse sections (Fig. 88) of the eye, the cellular organization is similar to that of eyes of M. carolina adults (Fig. 31). A clear retinula zone (cr) is present. The surface area of the rhabdom (r) (Fig. 89) (Table 11) is moderately large.

Eye shape (Figs. 90,91), corneal lenses (l) (Fig. 92) and cuticular pegs (cp) (Fig. 93) of eyes of C. belfragei adults are similar to those of other Cicindela adults. Cellular organization for vision (Figs. 94,95) is similar to that of C. tranquebarica eyes (Fig. 32). There is no clear retinula zone. The surface area of the rhabdom (r) (Fig. 96) (Table 11) is small.

4.3.3 Structure of Dark-Adapted Eyes of Cicindela tranquebarica and Cicindela limbata nympha Adults, and Light-Adapted Eyes of Cicindela lepida Adults

After dark adaptation for five days, structures of the eyes of C. tranquebarica and C. limbata nympha adults were examined. Only minor changes occurred when compared to light-adapted eyes. In both beetle eyes, pigment granules

Fig. 87. LM of longitudinal section of the eye of a Cicindela lepida adult. Shown are: thin corneal layer (t); corneal lens (l); subcorneal layer (cl); crystalline cone (c); clear retinula zone (cr); retinula rhabdom zone (rr); basal retinula zone (br); basement membrane (bm); axons (a); lamina ganglionaris (lg); secondary pigment cells (2p); and basal pigment cells (bp).

Scale = 100 µm

Fig. 88. LM of transverse section of the eye. Structural component abbreviations as above.

Scale = 200 µm

Fig. 89. Same, through the retinula rhabdom zone, showing retinula cells (rt) and rhabdom (r).

Scale = 10 µm

Fig. 90. SEM of the frontal aspect of the head of a Cicindela belfragei adult, showing large bulbous eyes.

Scale = 500 µm

Fig. 91. Same, of a lateral view of the left compound eye, showing hexagonal corneal lenses (l) and ocular sclerite (os). Vertex positioned at the left.

Scale = 200 µm

Fig. 92. Same, of convex distal surfaces of hexagonal corneal lenses (l). Note cuticular pegs (cp) between some lenses.

Scale = 10 µm

Fig. 93. Same, of a cuticular peg (cp) of an interfacetal mechanoreceptor.

Scale = 1 µm

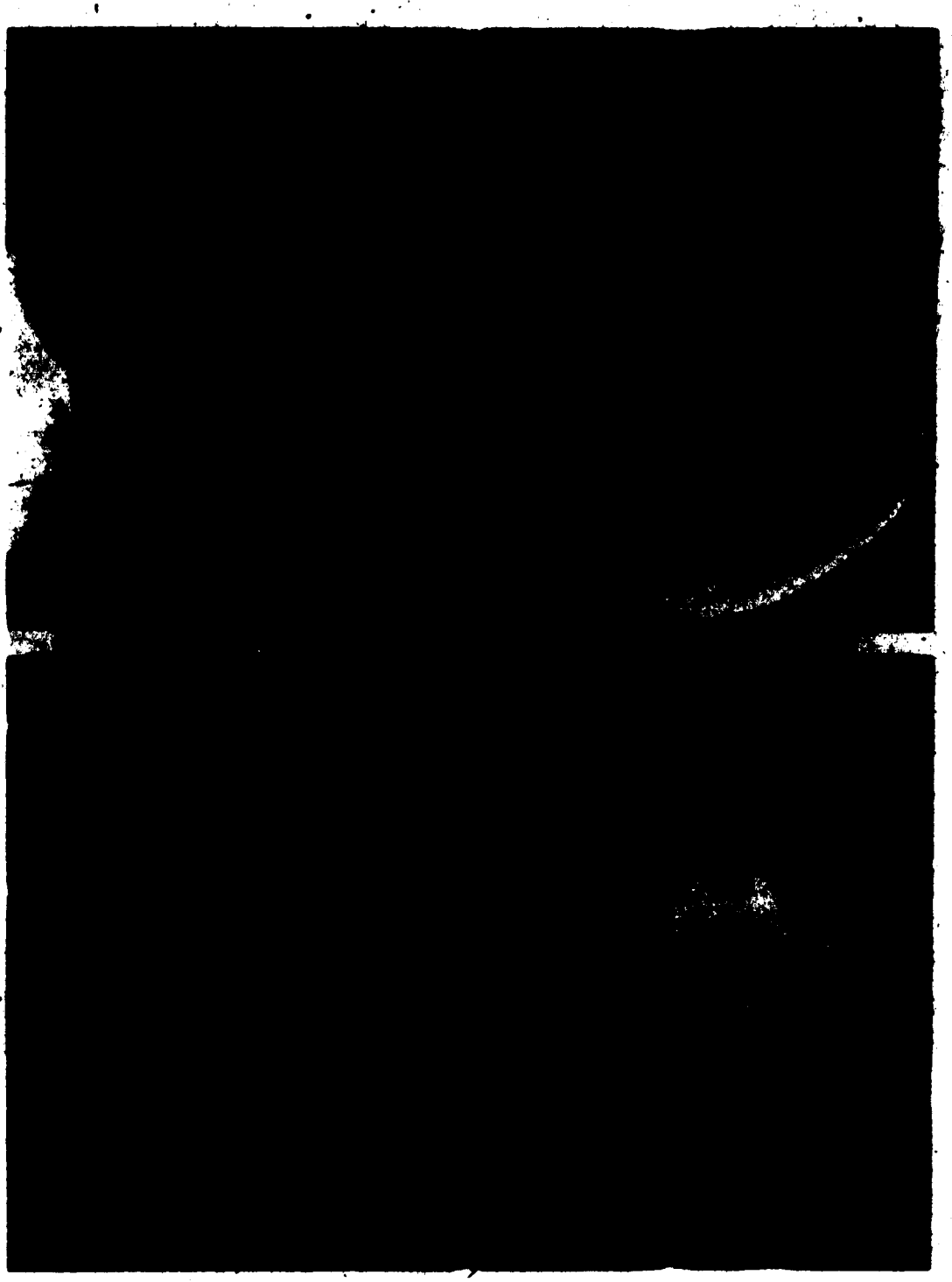

Fig. 94. LM of longitudinal section of the eye of a Cicindela belfragei adult. Shown are: thin corneal layer (t); corneal lens (l); subcorneal layer (cl); crystalline cone (c); retinula rhabdom zone (rr); rhabdom (r); basal retinula zone (br); basement membrane (bm); axons (a); lamina ganglionaris (lg); secondary pigment cells (2p); and basal pigment cells (bp).

Scale = 100 µm

Fig. 95. LM of transverse section of the eye. Structural component abbreviations as above.

Scale = 200 µm

Fig. 96. Same, through the retinula rhabdom zone, showing retinula cells (rt) and rhabdom (r).

Scale = 10 µm

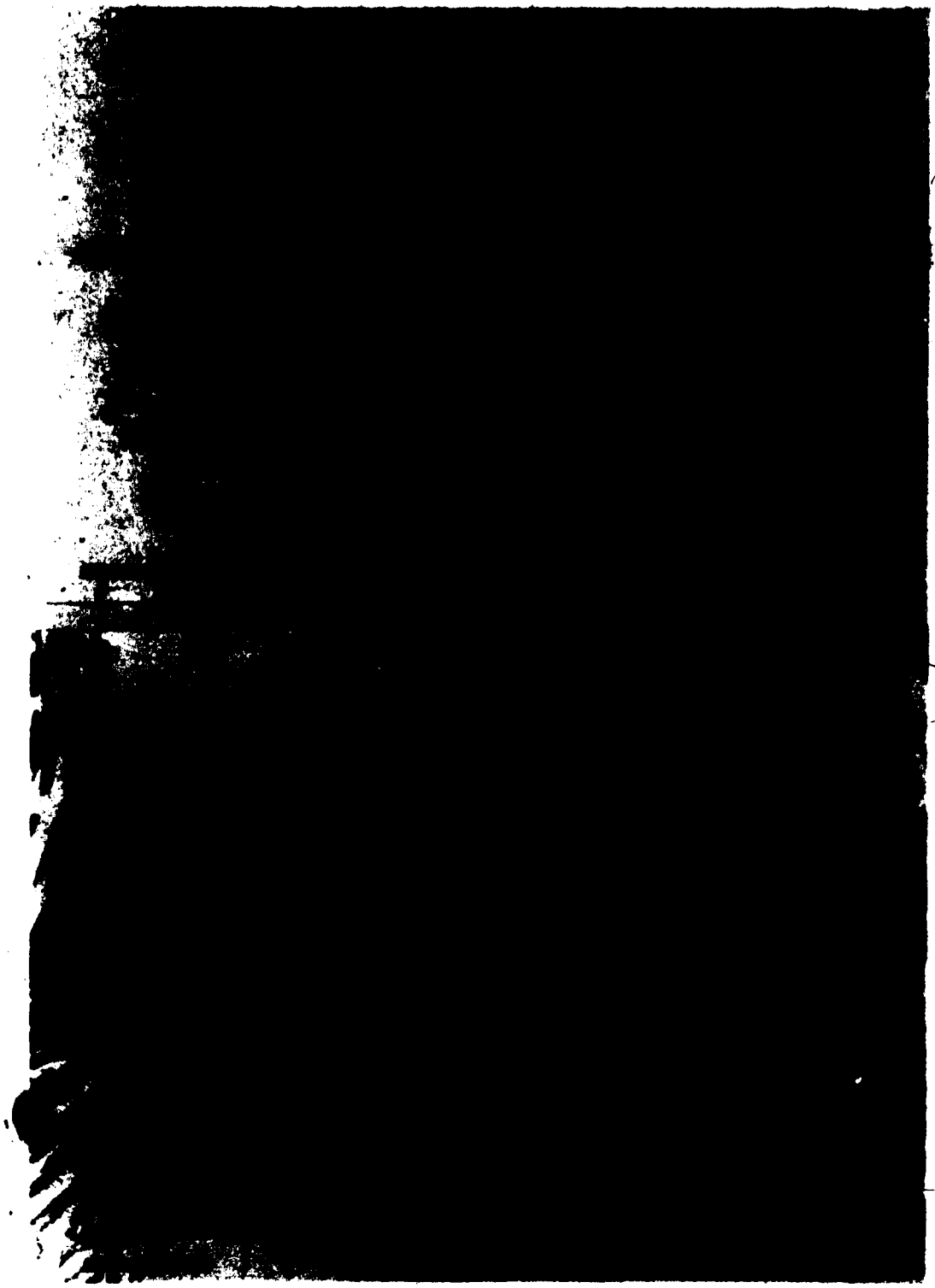

in secondary pigment cells (2p) migrated distally around crystalline cones and proximally around basal retinula cells leaving little pigmentation surrounding retinulae. One is assuming that the same pattern of orientation of pigment is not altered by fixation and dehydration. Shortening of the crystalline threads (ct) (Fig. 97) to approximately half their length in the light-adapted state (Fig. 32) was the most striking change. No clear retinula zone was observed after dark adaptation.

Light-adapted eyes of C. lepida adults (Fig. 98) show lengthening of crystalline threads (ct), shortening, but not disappearance, of the clear retinula zone (cr). A more even distribution of pigment granules in secondary pigment cells (2p) also occurred along the length of retinulae compared to dark-adapted C. lepida eyes collected at twilight (Fig. 87).

4.3.4 Structure of Eyes of Pterostichus melanarius and Elaphrus americanus carabid Adults

The head of a P. melanarius adult (Fig. 99) has a convex vertex like that of A. schwarzi and of O. californicus adults (Figs. 6,7). Eyes are small and spherical (Fig. 100) as are those of A. schwarzi adults (Fig. 10). Presumably these eyes have large monoscopic areas of the visual field. Hexagonal, convex corneal lenses (1) (Fig. 101) have a thin corneal layer (Table 10), but no interfacetal pegs. Material (x) secreted from dermal

Fig. 97. LM of longitudinal section through the dark-adapted eye of a Cicindela tranquebarica adult. Note shortening of crystalline threads (ct) and migration of secondary pigment granules (2p) distally around the crystalline cones (c) (contrast Fig. 32). There is no clear retinula zone.

Scale = 100 µm

Fig. 98. Same, of the light-adapted eye of a Cicindela lepida adult. Note lengthening of crystalline threads (ct), more even distribution of secondary pigment cells (2p), shortening of clear retinula zone (cr) (contrast Fig. 87).

Scale = 100 µm

Fig. 99. SEM of the frontal aspect of the head of a *Pterostichus melanarius* adult, showing relatively flat eyes.

Scale = 500 µm

Fig. 100. Same, of a lateral view of the left compound eye, showing hexagonal corneal lenses (l) and ocular sclerite (os). Vertex at the top.

Scale = 200 µm

Fig. 101. Same, of convex distal surfaces of hexagonal corneal lenses (l). No interfacetal pegs are present.

Scale = 10 µm

Fig. 102. Same, of dermal glands surrounding the eye. Glands secrete a material (x) which spreads over the ocular sclerite (os) and some corneal lenses (l).

Scale = 10 µm

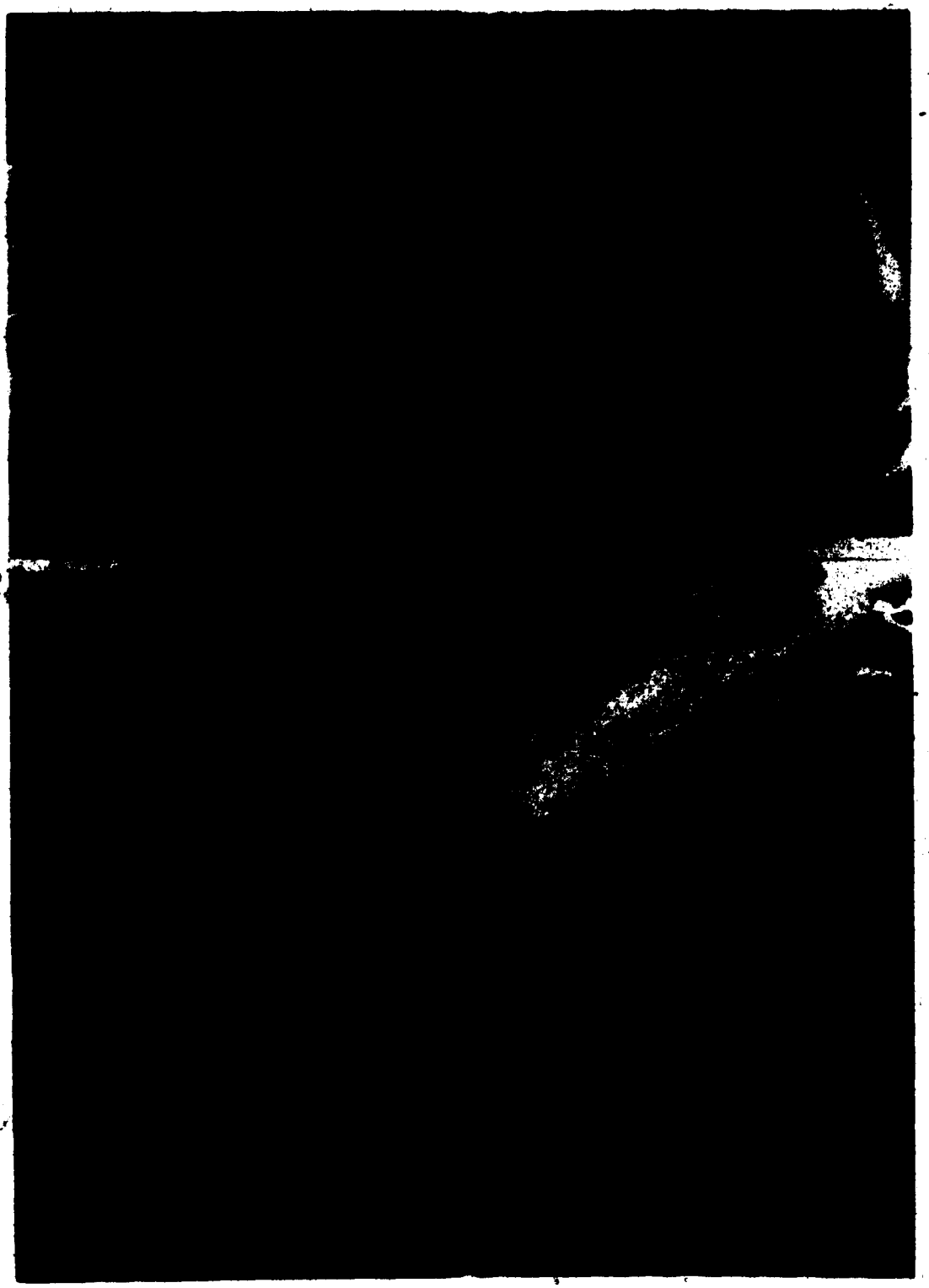

glands (Fig. 102) may be used as grooming lubricant to clean the eye, or may contribute to the composition of the thin corneal layer. These eyes have no clear retinula zone (Figs. 103,104) like eyes of O. californicus adults (Fig. 30), but the rhabdom (r) has a large cross-sectional surface area (Fig. 105) (Table 11) to that of the rabdom of A. schwarzi eyes (Fig. 66).

Although vertices of E. americanus adults are convex, their eyes are bulbous and extend above the vertex (Fig. 106). They are similar in shape (Fig. 107) to eyes of M. carolina adults (Fig. 8), and those of other Cicindela adults (Figs. 9,83,90). It is therefore inferred that these beetles have large stereoscopic areas of the visual field. Hexagonal corneal lenses (l) are well defined (Fig. 108) due to their degree of convexity, and similar to those of other Cicindela adults (Figs. 38,85,92). Interfacetal pegs (cp) (Fig. 109) are present. There is no clear retinula zone (Figs. 110,111) and these eyes have a similar cellular organization to eyes of C. tranquebarica (Fig. 32) and C. belfragei (Figs. 94,95). The rhabdom (r) (Fig. 112) has a small surface area (Table 11).

4.3.5 Eye Size Groups and Functional Categories of cicindelid Beetle Eyes Based on Measurements of Structures

From statistical inference using One-Way Analysis of Variance and Duncan's New Multiple Range Test of Means, measurement data (Tables 7,8,10,11) were grouped either into eye size or eye functional categories.

Fig. 103. LM of longitudinal section of the eye of a Pterostichus melanarius adult. Shown are: thin corneal layer (t); corneal lens (l); subcorneal layer (cl); crystalline cone (c); retinula rhabdom zone (rr); rhabdom (r); basal retinula zone (br); basement membrane (bm); axons (a); lamina ganglionaris (lg); secondary pigment cells (2p); and basal pigment cells (bp).

Scale = 100 µm

Fig. 104. LM of transverse section of the eye. Structural component abbreviations as above.

Scale = 200 µm

Fig. 105. Same, through the retinula rhabdom zone, showing retinula cells (rt) and rhabdom (r).

Scale = 10 µm

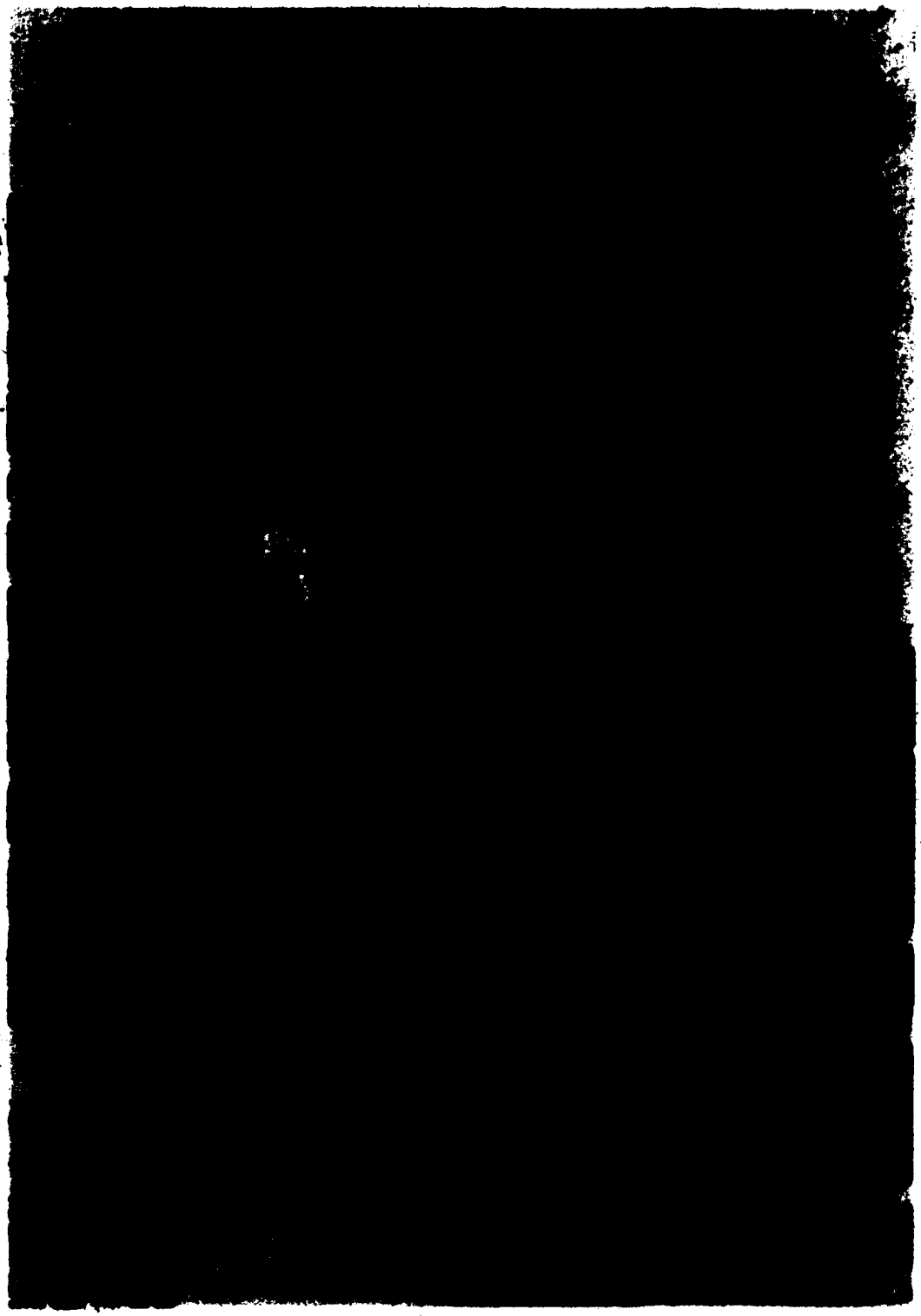

Fig. 106. SEM of the frontal aspect of the head of an *Elaphrus americanus* adult, showing large bulbous eyes.

Scale = 200 µm

Fig. 107. Same, of a lateral view of the left compound eye, showing hexagonal corneal lenses (l) and ocular sclerite (os). Vertex positioned at the left.

Scale = 100 µm

Fig. 108. Same, of convex distal surfaces of hexagonal corneal lenses (l). Note cuticular pegs (cp) between some lenses.

Scale = 10 µm

Fig. 109. Same, of a cuticular peg (cp) of an interfacetal mechanoreceptor.

Scale = 1 µm

Fig. 110. LM of longitudinal section of the eye of an Elaphrus americanus adult. Shown are: thin corneal layer (t); corneal lens (l); subcorneal layer (cl); cyrstalline cone (c); retinula rhabdom zone (rr); rhabdom (r); basal retinula zone (br); basement membrane (bm); axons (a); lamina ganglionaris (lg); secondary pigment cells (2p); and basal pigment cells (bp).

Scale = 100 µm

Fig. 111. LM of transverse section of the eye. Structural component abbreviations as above.

Scale = 200 µm

Fig. 112. Same, through the retinula rhabdom zone, showing retinula cells (rt) and rhabdom (r).

Scale = 10 µm

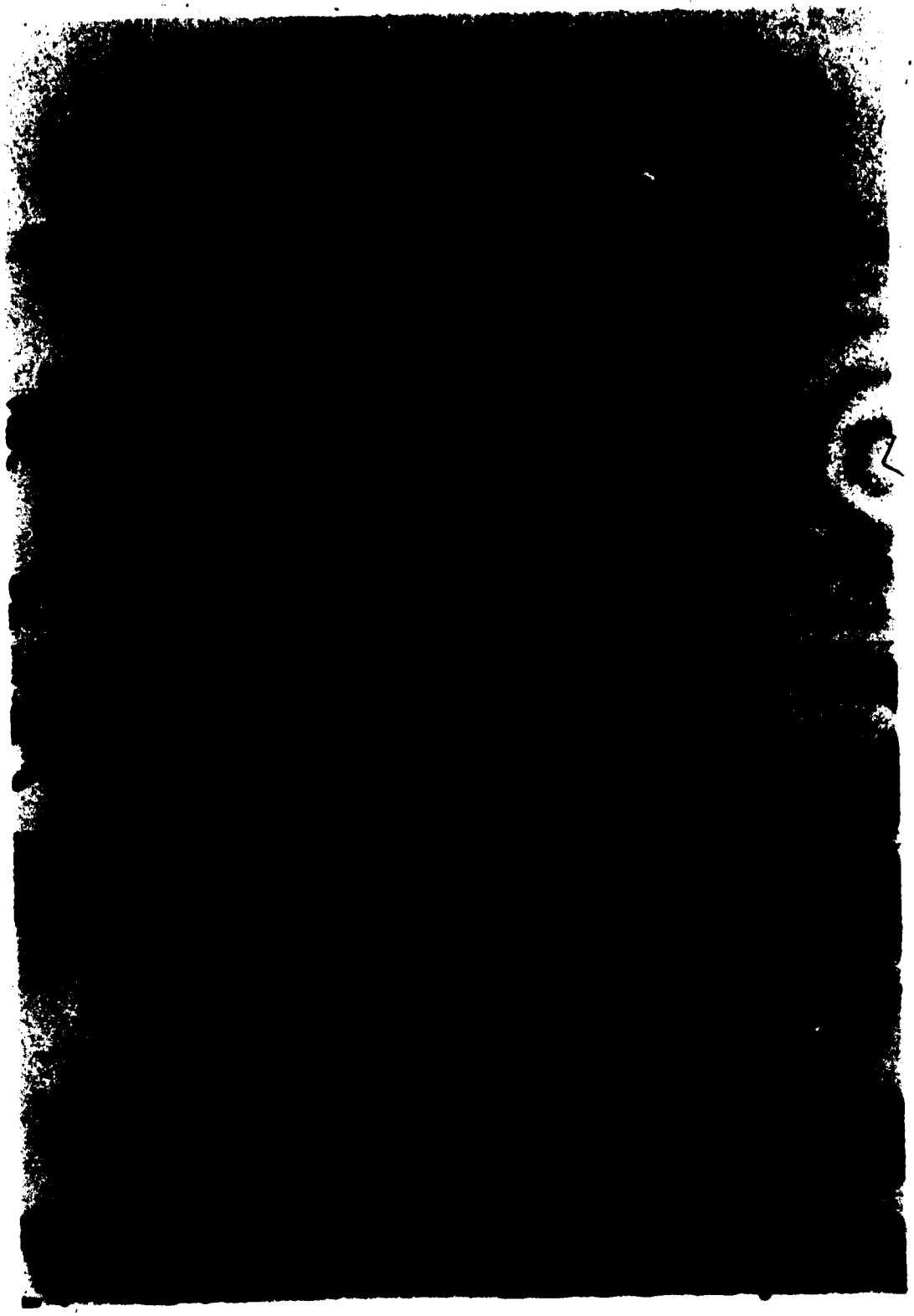

4.3.5.1 Eye Size Groups

When structural measurements are related to eye size, adults of the four North American genera of Cicindelidae can be divided into two groups (Table 12): Small Eye Group: eyes of representative adults of: Amblycheila schwarzi; Omus californicus. Large Eye Group: eyes of representative adults of: Megacephala carolina; Cicindela tranquebarica; Cicindela lepida; Cicindela belfragei.

For clarification of eye size relationships of cicindelid taxa, the similarity matrix (Table 13) is included. The data for Table 13 are summations of similar structures from Table 12. Based on these totals, there are trends in similarities within eye size groups and differences between these two groups among the cicindelids. Note that of 39 characters, small eyes of nocturnal A. schwarzi and O. californicus share 21 characters; large eyes of crepuscular M. carolina and diurnal C. tranquebarica adults share 16 characters. Also, eyes of the adults of Cicindela spp. share several attributes.

Unlike the diurnal and crepuscular beetles, nocturnal cicindelids possess small eyes with fewer ommatidia and no interfacetal pegs. Smaller areas of visual fields are characteristic of these small beetle eyes as demonstrated by head, thorax, and elytral ratios, and from forward and dorsal Mollweide homolographic projections (Chapter 3). Corneal lenses are long in these beetle eyes, while

Table 12. Arrangement of six cicindelid beetles into two groups based on eye size.

The values are $\bar{x}$ for n = 5 for each species. Solid underscore represents no statistically significant difference at $\alpha = 0.05\%$. Dashed underscore represents no statistically significant difference at $\alpha = 0.01\%$. Absence of an underscore indicates statistical difference. 0 indicates no such structure exists for that species and — indicates no measurement was determined.

Measurement (see previous tables for units)	*Amblycheila schwarzi*	*Omus californicus*	*Megacephala carolina*	*Cicindela tranquebarica*	*Cicindela lepida*	*Cicindela belfragei*
Eye size group	Small	Small	Large	Large	Large	Large
Diel activity	Nocturnal	Nocturnal	Crepuscular	Diurnal	Crepuscular	Crepuscular
Number of ommatidia	1,700	1,500	4,200	4,000	3,200	3,800
$\frac{\text{Number of ommatidia}}{\text{Antennal length}}$	89.60	167.17	323.79	498.53	—	—
$\frac{\text{Eye width}}{\text{Head width}}$	23.70	26.88	41.50	55.10	—	—
$\frac{\text{Eye height}}{\text{Head height}}$	91.18	92.58	105.54	112.60	—	—
$\frac{\text{Head width}}{\text{Pronotum width}}$	84.30	85.80	104.70	108.48	—	—

Table 12. Continued.

Measurement (see previous tables for units)	Amblycheila schwarzi	Omus californicus	Megacephala carolina	Cicindela tranquebarica	Cicindela lepida	Cicindela belfragei
Head width* / Elytra width	66.90	66.10	76.20	63.90	—	—
Mollweide projection of forward visual field areas (n = 3).						
Monoscopic	89.65	86.87	71.76	60.62	—	—
Stereoscopic frons	4.30	10.26	15.19	23.21	—	—
Stereoscopic behind	4.53	2.63	13.05	16.07	—	—
Total stereoscopic	8.83	12.89	28.24	39.38	—	—
Blind frons	0.48	0	0	0	—	—
Blind behind	1.04	0.24	0	0	—	—
Total blind	1.52	0.24	0	0	—	—

Table 12. Continued.

Measurement (see previous tables for units)	Amblycheila schwarzi	Omus californicus	Megacephala carolina	Cicindela tranquebarica	Cicindela [illegible]	Cicindela belfragei
Mollweide projection of dorsal visual field areas (n = 3).						
Monoscopic	89.65	86.87	71.76	60.62	—	—
Stereoscopic vertex	8.19	7.24	20.68	24.90	—	—
Stereoscopic mouth to neck	0.64	5.65	7.56	14.48	—	—
Total stereoscopic	8.83	12.89	28.24	39.38	—	—
Blind vertex	0.33	0.16	0	0	—	—
Blind mouth to neck	1.19	0.08	0	0	—	—
Total blind	1.59	0.24	0	0	—	—

Table 12. Continued.

Measurement (see previous tables for units)	Amblycheila schwarzi	Omus californicus	Megacephala carolina	Cicindela tranquebarica	Cicindela lepida	Cicindela hoffmani
Length of corneal lens	111.60	106.95	74.40	67.43	47.67	56.75
Height of interfacetal peg	0	0	3.08	3.12	2.45	2.54
Diameter of interfacetal peg	0	0	2.28	2.32	1.91	2.00
Length of crystalline cone	60.45	34.58	55.80	53.48	47.67	40.8

Table 12. Continued.

Measurement (see previous tables for units)	Amblycheila schwarzi	Omus californicus	Megacephala carolina	Cicindela tranquebarica	Cicindela lepida	Cicindela belfragei
Diameter of crystalline cone	18.60	17.44	16.28	16.28	16.08	16.46
Total length of dioptric apparatus	176.65	145.56	136.48	126.05	99.19	101.24
Length of crystalline thread	23.25	13.95	60.45	51.15	7.08	9.08
Length of retinula						
(b) Rhabdom zone	58.13	86.03	102.30	186.00	90.00	121.50
(c) Basal zone	20.93	16.28	18.60	18.60	18.00	13.50
Total length of retinula	123.24	102.31	232.50	204.60	184.50	135.00

Table 12. Continued.

Measurement (see previous tables for units)	Amblycheila schwarzi	Omus californicus	Megacephala carolina	Cicindela tranquebarica	Cicindela lepida	Cicindela belfragei
Total length of ommatidium	323.14	261.82	429.43	381.80	290.77	245.32
Dimensions of rhabdom						
(b) Diameter of basal zone	4.65	4.65	6.95	5.79	4.54	2.72
Length of dioptric apparatus	54.67	55.59	31.78	33.01	34.12	41.27
Length of ommatidium						
Length of crystalline thread	7.20	5.33	14.08	13.40	2.43	3.70
Length of ommatidium						

Table 12. Continued.

Measurement (see previous tables for units)	Amblycheila schwarzi	Omus californicus	Megacephala carolina	Cicindela tranquebarica	Cicindela lepida	Cicindela belfragei
Length of retinula / Length of ommatidium	38.13	39.08	54.14	53.59	63.45	55.03
Volume of retinula						
(b) Rhabdom zone	7468.46	9139.01	13143.37	24498.66	9105.93	7867.62
Volume of retinula / ommatidium	11411.25	11627.25	18686.05	26474.55	13239.55	8359.24
Volume of retinula / Compound eye	19.40(10^6)	17.44(10^6)	78.48(10^6)	105.90(10^6)	42.37(10^6)	31.79(10^6)
Volume of rhabdom / Compound eye	8.09(10^6)	5.65(10^6)	43.64(10^6)	16.84(10^6)	18.74(10^6)	5.67(10^6)

Table 13. Similarity matrix for six cicindelid beetles based on eye size groups. For A. schwarzi, O. californicus, M. carolina, C. tranquebarica there are 39 characters. When all six beetles are compared there are 20 characters.

Tiger Beetle	Omus californicus	Megacephala carolina	Cicindela tranquebarica	Cicindela lepida	Cicindela belfragei
Amblycheila schwarzi	21	3	3	2	3
Omus californicus		6	4	6	7
Megacephala carolina			16	4	5
Cicindela tranquebarica				8	5
Cicindela lepida					11

crystalline cones of diurnal-crepuscular large beetle eyes occupy a larger percentage of dioptric apparatus lengths. The dioptric apparatus occupies over half the ommatidial length in small-eyed beetles; but only approximately one-third the ommatidial length in the large eye group. Characteristic of large cicindelid eyes are crystalline threads almost twice as long as in the small eye group. Retinulae extend only slightly over one-third the ommatidial length of the small eye group but over half this length in the large-eyed beetles. Basal retinula zones are longer in the small eye group. There is also a similarity in nocturnal beetles concerning rhabdom zone volume and retinula and rhabdomeric volumes of ommatidia and compound eyes, all of which are smaller than volumes of the long retinulae and rhabdoms of large eyes.

4.3.5.2 Eye Functional Categories

When structures involved with function of cicindelid compound eyes are statistically analyzed, three functional categories can be inferred (Table 14):

Functional Eye Category

Scotopic A: eyes of representative adults of:

Amblycheila schwarzi

Megacephala carolina

Cicindela lepida

Scotopic B: eyes of representative adults of:

Omus californicus

Table 14. Arrangement of six cicindelid beetles into three categories based on eye function. The values are $\bar{x}$ for n = 5 for each species. Solid underscore represents no statistically significant difference at α = 0.05%. Dashed underscore represents no statistically significant difference at α = 0.01%. Absence of an underscore indicates statistical difference. 0 indicates no such structure exists for that species and — indicates no measurement was determined.

Measurement (see previous tables for units)	Amblycheila schwarzi	Megacephala carolina	Cicindela lepida	Omus californicus	Cicindela belfragei	Cicindela tranquebarica
Functional eye category	Scotopic A	Scotopic A	Scotopic A	Scotopic B	Photopic	Photopic
Eye size group	Small	Large		Small	Large	Large
Diel activity	Nocturnal	Crepuscular		Nocturnal	Crepuscular	Diurnal
Antennal length	18.98	12.98	—	8.98	—	8.00
Thickness of thin corneal layer	2.27	3.95	1.58	1.70	1.36	1.65
Diameter of corneal lens	22.73	22.73	24.97	20.45	24.97	25.00
Thickness of subcorneal layer	2.33	2.33	2.27	2.33	2.27	3.49

Table 14. Continued.

Measurement (see previous tables for units)	Amblycheila schwarzi	Megacephala carolina	Cicindela lepida	Omus californicus	Cicindela belfragei	Cicindela tranquebarica
Length of retinula						
(a) Clear zone	44.18	111.60	76.50	0	0	0
Dimensions of retinula						
(a) Diameter of clear zone	4.63	5.55	6.65	0	0	0
(b) Diameter of rhabdom zone	12.79	12.79	11.53	11.63	9.08	12.96
(c) Diameter of basal zone	13.96	13.95	10.22	13.95	6.81	11.63

Table 14. Continued.

Measurement (see previous tables for units)	Amblycheila schwarzi	Megacephala carolina	Cicindela lepida	Omus californicus	Cicindela belfargei	Cicindela tranquebarica
Dimensions of rhabdom						
(a) Rhabdom zone						
Length	9.30	11.63	9.08	6.98	3.41	5.00
Width	8.14	8.14	6.81	5.81	3.41	4.00
Volume of retinula						
(a) Clear zone	743.84	2695.85	2657.02	0		0
(b) Basal zone	3198.95	2842.83	1467.60	2488.24	491.72	1975.89

Table 14. Continued.

Measurement (see previous tables for units)	Amblycheila schwarzi	Megacephala carolina	Cicindela lepida	[illegible] californicus	Cicindela belfragei	Cicindela tranquebarica
Volume of rhabdom						
(a) Rhabdom zone	4400.56	9684.56	5564.70	3488.84	1413.04	3720.00
(b) basal zone	355.44	705.62	291.39	276.47	78.44	489.72
Surface area of rhabdom in rhabdom zone	75.70	94.67	61.83	40.55	11.63	20.00
Total volume of rhabdom ommatidium	4756.00	10390.18	5856.09	3765.31	1491.48	4209.73
Rhabdom volume Retinula volume	41.68	55.60	44.23	32.38	17.84	15.90

Table 15. Similarity matrix for six cicindelid beetles based on eye function. For A. schwarzi, O. californicus, M. carolina, C. tranquebarica there are 17 characters. When all six beetles are compared there are 16 characters.

Tiger Beetle	Omus californicus	Megacephala carolina	Cicindela tranquebarica	Cicindela lepida	Cicindela belfragei
Amblycheila schwarzi	8	6	5	6	2
Omus californicus		4	9	6	7
Megacephala carolina			4	3	2
Cicindela tranquebarica				4	8
Cicindela lepida					4

Photopic: eyes of representative adults of:

Cicindela tranquebarica,

Cicindela belfragei

For verification of functional eye categories of cicindelid taxa, the similarity matrix (Table 15) is included. The data for Table 15 are summations of similar structures from Table 14. Based on these totals, there are trends in similarities within eye functional categories and differences among these three categories among the cicindelids.

Beetles included in the scotopic A functional category have relatively long antennae which may permit increased touch and olfactory stimulation in addition to sight. The thin corneal layers of these eyes are relatively thick, but the subcorneal layers are relatively thin. Eyes of adult A. schwarzi, M. carolina, and C. lepida have clear retinula zones and although less than half these retinula lengths are rhabdomeric, these rhabdoms have very large surface areas. Volume of rhabdom zones are greater in eyes of A. schwarzi than those of O. californicus, its small-eyed counterpart; as it is larger in eyes of M. carolina than its large-eyed counterparts, C. tranquebarica, C. lepida, and C. belfragei. Percentage rhabdom zone volume of retinulae are smaller in scotopic A eyes due to the presence of clear retinula zones. However, total volume of the rhabdom per ommatidium is larger in scotopic A eyes as is percentage of rhabdom volume to retinula volume since the rhabdom has such a large surface area.

Eyes of O. californicus adults are scotopic B. Individuals of this species have short antennae and although their eyes possess many small-eyed structural similarities with those of A. schwarzi adults (Table 14), they can be grouped into a separate functional category. Like scotopic A eyes, these eyes have thin subcorneal layers, but thinner, thin corneal layers. Unlike the scotopic A eyes, there is no clear retinula zone. Although almost twice the retinula lengths are occupied by the rhabdom zone, surface areas and volumes of the rhabdom are smaller as is percentage volume of the rhabdom to retinula volume in scotopic B than scotopic A eyes. Consequently, percentage volume of the retinula around the rhabdom and percentage volume of the rhabdom are larger in scotopic B ommatidia, but total retinula and rhabdom volumes are less in the whole scotopic B eye.

C. tranquebarica and C. belfragei adults have photopic eyes. Like adults of O. californicus, these beetles have short antennae. But based on eye size, these eyes share structural similarities to eyes of M. carolina adults since they are in the large eye group (Table 12). Photopic eyes of C. tranquebarica and C. belfragei adults have thick subcorneal layers, but like scotopic B eyes, have thin, thin corneal layers, no clear retinula zone, and rhabdoms occupying almost the complete retinula length. Surface areas of rhabdom are the smallest and rhabdom volumes are small considering retinulae lengths. Percentage rhabdom volume to retinula volume is very small but percentage of retinula volume sur-

rounding the rhabdom is very large.

4.3.6 Eye Size Groups and Functional Categories of carabid Beetle Eyes Based on Measurements of Structures

4.3.6.1 Eye Size Groups

In Section 4.3.5, cicindelid beetle eyes were placed into two groups based on eye size and into three functional categories. To test convergence of eye structure and function based on eye size, eyes of two carabid adults were statistically compared to four cicindelid sister taxa.

According to the eye size, cicindelid and carabid adults have similar eye structures (Table 16). Eyes of P. melanarius fit the small eye group; E. americanus, the large eye group. For clarification of eye size groups of carabid taxa, the similarity matrix (Table 17) is included.

The data for Table 17 are summations of similar structures from Table 16. Based on these totals, there are trends in similarities within eye size groups and differences between these two groups among the cicindelids and carabids.

Although eyes of the carabids have fewer ommatidia, eyes of diurnal E. americanus adults have more than eyes of nocturnal P. melanarius. Corneal lenses and crystalline cones are longer and no interfacetal pegs are present in the nocturnal small carabid eyes. Lengths of crystalline threads of eyes of O. californicus and E. americanus are similar, and crystalline threads of P. melanarius, and M. carolina eyes are similar in lengths. Basal retinula zone lengths

Table 15. Arrangement of four cicindelid and two carabid beetles into two groups based on eye size. The values are $\bar{x}$ for n = 5 for each species. Solid underscore represents no statistical significant difference using Duncan's multiple range test means at $\alpha = 0.05\%$. Dashed underscore represents no statistical significant difference at $\alpha = 0.01\%$. Absence of an underscore indicates statistical difference. 0 indicates no such structure exists for that species.

Measurement (see previous tables for units)	Amblycheila schwarzi	Omus californicus	Pterostichus melanarius	Megacephala carolina	Cicindela [illegible]ca	Elaphrus [illegible]
Eye size group	Small	Small	Small	Large	Large	Large
Diel activity	Nocturnal	Nocturnal	Nocturnal	Crepuscular	Diurnal	Diurnal
Number of ommatidia	1,700	1,500	1,420	4,200	4,000	1,770
Length of [illegible]	111.60	106.95	63.56	74.40	67.43	56.75
Height of interfacetal peg	0	0	0	3.08	3.12	2.31
Diameter of interfacetal peg	0	0	0	2.28	2.32	1.54
Length of crystalline [illegible]	60.45	34.58	47.67	55.80	53.92	22.70
Diameter of crystalline [illegible]	18.60	17.44	13.62	16.28	16.28	11.00

Table 16. Continued.

Measurement (see previous tables for units)	Amblycheila schwarzi	Omus californicus	Pterostichus melanarius	Megacephala carolina	Cicindela tranquebarica	Elpharus americanus
Total length of dioptric apparatus	176.65	145.56	115.20	136.48	126.05	82.47
Length of crystalline thread	23.25	13.95	29.51	60.45	51.15	13.62
Length of retinula						
(b) Rhabdom zone	58.13	86.03	97.61	102.30	186.00	95.34
(c) Basal zone	20.93	16.28	18.16	70.60	18.60	9.08
Total length of retinula	123.24	102.31	115.77	232.50	204.60	104.42
Total length of ommatidium	323.14	261.82	260.48	429.43	381.80	200.51

Table 16. Continued.

Measurement (see previous tables for units)	Amblycheila schwarzi	Omus californicus	Pterostichus melanarius	Megacephala carolina	Cicindela tranquebarica	Elaphrus americanus
Dimensions of rhabdom						
(b) Diameter of basal zone	4.65	4.65	4.65	6.95	5.79	2.27
Length of dioptric apparatus / Length of ommatidium	54.67	55.59	44.23	31.78	33.01	41.13
Length of crystalline thread / Length of ommatidium	7.20	5.33	11.33	14.08	13.40	6.75
Length of retinula / Length of ommatidium	38.13	39.08	44.44	54.14	53.59	52.08

Table 16. Continued.

Measurement (see previous tables for units)	Amblycheila schwarzi	Omus californicus	Pterostichus melanarius	Megacephala carolina	Cicindela tranquebarica	Elaphrus americanus
Volume of retinula (b) Rhabdom zone	7468.46	9139.01	9445.61	13143.37	24498.66	7821.08
Volume of retinula / Ommatidium	11411.25	11627.25	10665.97	18686.05	26474.55	8409.04
Volume of retinula / Compound eye	19.40(10^6)	17.44(10^6)	15.15(10^6)	78.48(10^6)	105.90(10^6)	14.88(10^6)
Volume of rhabdom / Compound eye	8.09(10^6)	5.65(10^6)	11.12(10^6)	43.64(10^6)	16.84(10^6)	1.31(10^6)

Table 17. Similarity matrix for four cicindelids and two carabid beetles based on eye size. There are 20 characters.

Beetle	Amblycheila schwarzi	Omus californicus	Megacephala carolina	Cicindela trans[illegible]erica	Pterostichus melan[illegible]
Pterostichus melanarius	8	8	4	4	20
Elaphrus americanus	5	6	2	1	15

and [illegible] are similar in all these beetle taxa except in those of E. americanus where they are small as large. Eyes of P. melanarius adults have longer retinulae similar to these of Q. californicus adults. Volume of the rhabdom zone of the retinula and rhabdom volume per eye are similar in Q. californicus and P. melanarius adults, and adults of E. americanus, A. schwarzi, and C. californica since all these eyes have relatively short retinulae. Indicative of small eyes and nocturnal behaviour, both adults of A. schwarzi and P. melanarius have similar rhabdom volumes per eye but the carabid has a statistically similar volume to eyes of C. tranquebarica adults because retinulae of this carabid are so short. Rhabdom volume of E. americanus adults is exceedingly small.

4.3.6.2 Eye Fuctional Categories

Comparisons of functional aspects of the cellular organization for vision of cicindelid and carabid beetles show similarities (Table 18). Eyes of P. melanarius adults are grouped with eyes of Q. californicus adults in the scotopic B category; eyes of E. americanus adults in the photopic category with C. tranquebarica adults. For clarification of functional eye categories of carabid taxa, the similarity matrix (Table 19) is included. The data for Table 19 are summations of similar structures from Table 18. Based on these totals, there are trends in similarities within the eye functional categories and differences among these

Table 18. Arrangement of four cicindelid and two carabid beetles into three categories based on eye function.

The values are $\bar{x}$ for n = 5 for each species. Solid underscore represents no statistical significant difference at $\alpha = 0.05\%$. Dashed underscore represents no statistical at $\alpha = 0.01\%$. Absence of an underscore indicates statistical differ[illegible] 0 indicates no such structure exists for that species.

Measurement (see previous tables for units)	Amblycheila schwarzi	Megacephala carolina	Omus californicus	Pterostichus melan[illegible]	Cicindela trans[illegible]	[illegible]
Functional eye category	Scotopic A	Scotopic A	Scotopic B	Scotopic B	Photopic	[illegible]
Eye size group	Small	Large	Small	Small	Large	[illegible]
Diel activity	Nocturnal	Crepuscular	Nocturnal	Nocturnal	Diurnal	[illegible]
Thickness of thin corneal layer	2.27	3.95	1.70	2.27	1.[illegible]	[illegible]
Diameter of corneal lens	22.73	22.73	20.45	24.97	2[illegible]	[illegible]
Thickness of subcorneal layer	2.33	2.33	2.33	1.70	3.49	[illegible]
Length of retinula						
(a) Clear zone	44.18	111.60	0	0	[illegible]	[illegible]

Table 18. Continued.

Measurement (see previous tables for units)	Amblycheila schwarzi	Megacephala carolina	Omus californicus	Pterostichus melanarius	Cicindela transbaicalica	Elaphrus americanus
Dimensions of retinula						
(a) Diameter of clear zone	4.63	5.55	0	0		0
(b) Diameter of rhabdom zone	12.79	12.79	11.63	11.10	[illegible]95	10.22
(c) Diameter of basal zone	13.95	13.95	13.95	9.25	11.63	9.08
Dimensions of rhabdom						
(a) Rhabdom zone						
Length	9.30	11.63	6.98	9.25	5.00	2.72
Width	8.14	8.14	5.81	8.33	4.00	2.72

Table 18. Continued.

Measurement (see previous tables for units)	Amblycheila schwarzi	Megacephala carolina	Omus californicus	Pterostichus melanarius	Cicindela tranquebarica	Elaphrus americanus
Volume of retinula						
(a) Clear zone	743.84	2699.85	0	0	0	0
(c) Basal zone	3198.85	2842.83	2488.24	1220.36	1975.89	587.96
Volume of rhabdom						
(a) Rhabdom zone	4400.56	9684.56	3488.84	[illegible]	3720.00	705.36
(b) Basal zone	355.44	705.62	276.47	308.40	489.73	36.75
Surface area of rhabdom in rhabdom zone	75.70	94.67	40.55	[illegible]77.05	20.00	6.17

Table 18. Continued.

Measurement (see previous tables for units)	Amblycheila schwarzi	Megacephala carolina	Omus californicus	Pterostichus melanarius	Cicindela tranquebarica	Elaphrus americanus
Total volume of rhabdom / Ommatidium	4756.00	10390.18	3765.31	7829.49	4209.73	742.11
Rhabdom volume / Retinula volume	41.68	55.60	32.38	73.41	15.90	8.83

Table 19. Similarity matrix for four cicindelid and two carabid beetles based on eye function.

There are 16 characters.

Beetle	*Amblycheila schwarzi*	*Omus californicus*	*Megacephala carolina*	*Cicindela tranquebarica*	*Pterostichus melanarius*
Pterostichus melanarius	6	7	2	5	16
Elaphrus americanus	1	5	2	4	6

three categories among the cicindelids and carabids.

Thickness of the thin corneal layer places eyes of P. melanarius close to those of A. schwarzi while the subcorneal layer of eyes of E. americanus adults, though thicker than that of P. melanarius is similar to that in eyes of adult representatives of A. schwarzi, Q. californicus, and M. carolina. Diameters of retinulae of P. melanarius eyes are similar to those of Q. californicus, while basal zone diameters of the two carabid eyes are similar. Both lengths and widths of rhabdoms of P. melanarius eyes are similar to those of A. schwarzi adults, but the rhabdom of E. americanus, like that of C. tranquebarica adults, is exceedingly small with minimum surface area and volume.

4.4 Discussion and Conclusions

4.4.1 Dioptric Apparatus

Adult eyes of representative species of North American genera of Cicindelidae and Carabidae have a eucone three layered dioptric apparatus. Although Gissler (1879) observed corneal lens of adult Omus sp. and Cicindela sp. to be biconvex, and the cornea of adult Amblycheila sp. to be convex only interiorly, I have shown that adult eyes of species of these genera to have biconvex lenses. Confusion regarding corneal lens shape possibly resulted because the lenses of A. schwarzi, M. carolina have relatively thick corneal layers which externally appear smooth. Thickness

of this layer may be important in understanding differences in eye function. A thick layer of septate filament light over many lenses so that light is shared by adjacent ommatidia. Because this corneal layer is thinner in eyes of [redacted] adults, individual lenses are more distinctly separated and optical isolation is maintained between adjacent ommatidia, possibly resulting in enhanced visual acuity. Scratches on this layer may result from burrowing or less likely from grooming activities. None of the thin corneal layers act as anti-reflecting coatings (Table 9) within the probable visible spectrum of 325 nm to 625 nm (Menzel, 1975b).. The films are too thick, and if they were to function as anti-reflecting layers, they should be from 606.3 nm to 1,166.0 nm thick for eyes of A. schwarzi and M. carolina; 812.5 nm to 1,187.4 nm for eyes of O. californicus and C. tranquebarica adults.

I introduced the term "subcorneal layer" for a structural component of some insect ommatidia. An extension of the corneal lens often termed the "corneal process" (processus corneae) is observed in many diurnal lepidopteran eucone eyes (Eltringham, 1919; 1933; Nowikoff, 1931; and Yagi and Koyama, 1963a). Confusion in terms has led Goldsmith (1964) to state that in exocone compound eyes (sensu Grenacher, 1879), the "cone" is an inward projection of the corneal process and is therefore an extracellular secretion of the corneal lens, unlike the intracellular

secretion from four Semper cel[illegible]
eyes. Cones of [illegible] (Coleoptera) [illegible]
example (Horridge, [illegible] Seitz, [illegible]
[illegible] uses the term corneal process [illegible]
cone beetle compound eyes. In [illegible] eyes of [illegible]
Creophilus erythrocephalus and [illegible] (Staphylinidae) Meyer-Rochow (1972) describes the proximal convexity of the corneal lens as the "corneal cone". Meyer-Rochow and Horridge (1975) continue to use the term corneal cone in describing eucone eyes of _Anoplognathus pallidicollis_ Blanch (Scarabaeidae). Using a light microscope, a true subcorneal layer has been observed by Yagi and Koyama (1963a) in lepidopteran eyes which appears to be similar to the layer described here. Eyes of adult _Notiophilus biguttatus_ F. and _Loricera pilicornis_ F. (Carabidae) also have a subcorneal layer which Home (1976) terms the "proximal corneal layer".

Because of the confusion in terms of these components of corneal lenses, I use the terms in the following manner:

corneal process (_processus corneae_): the extracellular extension of the corneal lens to form the "cone" in exocone eyes (_sensu_ Goldsmith, 1964; Meyer-Rochow, 1975).

corneal cone: the proximal convexity of the corneal lens of eucone eyes (_sensu_ Meyer-Rochow, 1972; Meyer-Rochow and Horridge, 1975).

subcorneal layer: the structurally distinct layer between the corneal lens and crystalline cone of eucone eyes. Pre-

viously termed the processus corneae (Eltringham, 1919; 1933; Nowikoff, 1931; and Yagi and Koyama, 1963a), and the proximal corneal layer (Home, 1976).

The fine structure of this subcorneal layer is described in Section 5.3.2.2.

4.4.2 Interfacetal Pegs

Both crepuscular and diurnal adult cicindelids and the diurnal carabid have interfacetal pegs between some corneal lenses. Nocturnal flightless cicindelids and the nocturnal carabid do not have these. Other adult beetles, capable of flight, such as Creophilus erythrocephalus F. and Sartallus signatus Sharp (Staphylinidae) also have interfacetal pegs (Meyer-Rochow, 1972) similar in size and shape to those described here. According to Nesse (1965; 1966) for Apis mellifica (= A. mellifera), Chi and Carlson (1976) for Musca domestica (Muscidae), and Honegger (1977) for Gryllis campestris L. (Gryllidae), these interfacetal hairs function as mechanoreceptors to sense the direction and relative velocity of wind passing over the eyes during flight. See Section 5.3.4 for a description of the fine structure of these pegs, and Section 5.4.2 for a discussion of their probable mechanoreceptor function as revealed by electron microscopy.

4.4.3 Retinula Cells and Rhabdoms

It is important to emphasize that the difference in

retinula and rhabdom structure of the cicindelid and carabid eyes investigated is not one of a change in cell number, but is a difference in cellular organization which results in varied functional abilities of these eyes.

4.4.3.1 Scotopic A Eyes -

Retinulae of eyes of adults of A. schwarzi, M. carolina and C. lepida have a distal clear retinula zone or crystalline tract (sensu Døving and Miller, 1969), consisting of seven retinula cells which do not have a rhabdom at this level. Proximally, the retinula broadens and has a rectangular fused rhabdom composed of six rhabdomeres. A third level of retinula organization, the eighth or basal rhabdomere-bearing retinula cell, is located just distal to the basement membrane. Such a scotopic A retinula organization has also been observed in adult carabid beetle eyes such as those of Carabus auratus L. (Kirchoffer, 1905; 1908; Bernard, 1932; Hasselmann, 1962), Steropus madidus Fab., and Eutrichomerus terricola Herbst (Bernard, 1932); Dytiscus sp. and Cybister sp. adults (Dytiscidae) (Grenacher, 1879; Exner, 1891; Kirchoffer, 1908; and Horridge, 1969a). These proximal fused rhabdoms are so large they occupy almost the complete proximal surface area of the eye. Evolution of such a rhabdomeric layer is an adaptation for reception of light from neighbouring ommatidia. From intraretinular electrophysiological recordings, Horridge et al. (1970) showed that dytiscid ommatidia have wide angles of acceptance.

Ray tracing in corneal lenses and crystalline cones show that visual acuity is poor in Cybister sp. adults, but summation of scattered light across the clear zone could confer a high sensitivity (Meyer-Rochow, 1973). Eyes of cryptophilus adults of Notonomus sp. (Carabidae) and aquatic adults of Hydrophilus sp. (Hydrophilidae) have a similar tiered retinula like dytiscids (Horridge and Giddings, 1971a). Like these other beetle eyes, ommatidia of cicindelid adults do have a distal rhabdomere associated with the seventh retinula cell. However it was not possible to photograph it using light microscopy (see Section 5.3.5.1).

Scarab adults, Melontha vulgaris F. (Kirchoffer, 1908), Oryctes rhinoceros (Bugnion and Popoff, 1914), and others (Grenacher, 1879) also have scotopic A functional eyes. Based on research on Repsimus manicatus Lea adults (Scarabaeidae), Horridge and Giddings (1971a) define the "neuropteran" type of compound eye as having a crystalline thread in the light-adapted state only, with retinula cell bodies extending to the tip of the cone only in the dark-adapted state. Eyes of Anoplognathus pallidicollis Blanch are also scotopic A and have a basal retinula cell (Meyer-Rochow and Horridge, 1975). Although dark and light adaptation experiments were not performed on scotopic A cicindelid beetle eyes, it is possible to assume that eyes of A. schwarzi, M. carolina and C. lepida adults are of the neuropteran

type (sensu Horridge and Giddings, 1971a). Clear retinula zones in these cicindelid eyes probably function as suggested by Horridge, Ninham, and Djesendorf (1972) to permit a further increase in sensitivity in the dark-adapted state by allowing an increase in the acceptance angle of lenses and in the cross-sectional area of the rhabdoms, without prejudice to acuity of the light-adapted eye. Optical mechanisms of summation of scattered light in clear zone compound eyes are reviewed by Horridge, 1971; Kunze, 1972; Horridge, Ninham, and Diesendorf, 1972; Diesendorf and Horridge, 1973; Horridge, 1972; 1974; and 1975b.

A clear retinula zone is not confined to coleopteran compound eyes. Adults of Cloeon sp. (Ephemeroptera) (Horridge, 1976), and Chrysopa spp. (Neuroptera) (Ast, 1919; Horridge and Henderson, 1976) also have this retinula organization, as do some Lepidoptera: Heliothis zea Boddie (Agee, 1971), Heliothis virescens (Noctuidae) (Agee, 1972); Ephestia spp. (Pyralidae) (Umbach, 1934; Horridge and Giddings, 1971b; and Fischer and Horstmann, 1971), and some hesperiids (Yagi, 1951; Yagi and Koyama, 1963a; and Horridge, Giddings and Stange, 1972).

4.4.3.2 Scotopic B Eyes

Like eyes of adults of the closely-related genus Amblycheila sp. in the same subtribe Omina, scotopic B eyes of O. californicus adults are eucone and have a thick dioptric apparatus and a crystalline thread, but importantly,

they have no clear retinula zone. Instead, the rhabdom extends the full length of the retinula to the proximal eighth basal retinula cell. Although adephagans usually have a neuropteran type of scotopic eye as defined by Horridge and Giddings (1971a), these authors state that some adephagan eyes have long fused rhabdoms. In longitudinal section, ommatidia of P. melanarius (Section 4.3.4), Procrustes coriaceus L., Carabus glabratus Payk., and Broscus cephalotes L. (Carabidae) (Kirchoffer, 1908) also have broad fused rhabdoms and no clear retinula zones. Dorsal and ventral divided eyes of Gyrinus nator subtriatus Steph. (Bott, 1928), Gyrinus subtriatus (Wachmann and Schröer, 1975), Gyrinus natator L. (Burghause, 1976), and dorsal eyes of Dineutes assimilis adults (Gyrinidae) (Pappas and Larsen, 1973) are also of the scotopic B functional category. Ommatidia of Necrophorus sp. (Silphidae) (Grenacher, 1879), and acone eyes of Creophilus erythrocephalus F. adults (Staphylinidae) (Meyer-Rochow, 1972); eucone eyes of Attagenus megatoma Fab. (Dermestidae) (Butler et al., 1970); and Anthonomus grandis Boheman (Curculionidae) (Agee and Elder, 1970) also do not have a clear retinula zone, but have a long fused rhabdom composed of various numbers of retinula cells.

4.4.3.3 Photopic Eyes

Other adult carabid eyes have rhabdoms extended the full retinula length (Bernard, 1932; Home, 1976). These

eyes have three levels of rhabdom organization similar to those of Dytiscus marginalis adult eyes (Horridge, 1969a). However, like eyes of O. californicus adults, there is no clear retinula zone but, importantly, the rhabdoms have less surface area. A greater reduction of rhabdomeric surface area and volume occurs in photopic eyes of diurnal cicindelid adults of the genus Cicindela. From histological examination of adult eyes of C. campestris L., C. sylvatica Latr., and C. hybrida L., Kirchoffer (1905) described these eyes, and in 1908 figured ommatidia of the first two species. Further examination of eyes of C. campestris by Friedrichs (1931) and Home (1976) confirmed the slender fused cruciform rhabdom structure. Swiecimski (1957) reported a similar retinula organization in eyes of C. hybrida adults, and I have also observed this cellular organization in eyes of adults of the following diurnal cicindelids: C. tranquebarica Herbst, C. belfragei Salle, C. limbalis Klug, C. longilabris Say, C. limbata nympha Casey, and C. repanda repanda Dejean. Since these ommatidia do not have a clear retinula zone or a broad fused rhabdom, light is not scattered over adjacent rhabdoms and the eyes are photopic. Eyes of E. americanus also are photopic and although E. cupreus are active in the shade they have photopic eyes (Kirchoffer, 1908; Bauer, 1974; and Home, 1976) as do heliophilus adults of E. riparius (Bauer, 1974).

Rhabdom structure of these photopic eyes is similar to that of other diurnal insect eyes. Compound eyes of

damselflies Ischnura senegalensis and Cercion calamorum (Minemiya et al., 1969), and the dorsal sector of the dragon-fly divided eye Aeschna cyanea Müll. (Eguchi, 1971) have a small fused rhabdom as do most diurnal lepidoptera (Yagi and Koyama, 1963a; Meyer-Rochow, 1971). Within the Hymenoptera, day-flying Apis mellifica (= A. mellifera) workers (Skrzipek and Skrzipek, 1971a) and drones (Perrelet, 1970) have a slender fused rhabdom composed of eight retinula cells with a basal nineth retinula cell. Formica polyctena (Menzel, 1972) and Cataglyphis bicolor F. (Formicidae) (Brunnert and Wehner, 1973) also have the hymenopteran cellular organization for vision. These photopic eyes have a greater spectral sensitivity than scotopic eyes (review: Menzel, 1975) and have the ability to detect polarized light (reviews: Snyder, 1973; Wehner, 1976). Some hemimetabolous adults also have eyes having a slender central fused rhabdom composed of eight retinula cells: Locusta sp. (Locustidae) (Horridge and Barnard, 1965), Pteronemobius heydeni Fisch. (Gryllidae) (Wachmann, 1970), and Periplaneta americana L. (Blattidae) (Butler, 1973b).

4.4.4 Pigment Cells

In dark-adapted scotopic A eyes of A. schwarzi adults, pigment is concentrated in distal portions of the secondary pigment cells surrounding the crystalline cones and retinulae extend to the cone tips. The clear retinula zone is devoid of pigment, allowing light to be scattered

on adjacent rhabdoms for increased light intensity. Such a cellular organization corresponds to the dark-adapted scotopic eye of the neuropteran type (sensu Horridge and Giddings, 1971a). Light-adapted scotopic A eyes of M. carolina and C. lepida have crystalline threads to direct light to individual rhabdoms, but the long clear zones are not surrounded by secondary pigment granules which suggests that light is scattered over adjacent rhabdoms. Dark-adapted scotopic B eyes of O. californicus and P. melanarius and light-adapted photopic eyes of C. tranquebarica, C. belfragei, and E. americanus adults have distal aggregations of pigment granules surrounding crystalline cones and threads. Like photopic eyes of Apis mellifica L. (Kolb and Autrum, 1972), C. tranquebarica and C. belfragei eyes also have pigment granules along the retinula length. As postulated for these apid eyes (Varela and Wiitanen, 1970), I suggest that parallel light entering photopic cicindelid and carabid eyes is directed to the rhabdom for photo-transduction and oblique rays are absorbed at the level of the dioptric apparatus by secondary pigment granules. Optical isolation at the retinula level is maintained by an envelope of pigment along its length which prevents stimulation of the rhabdom by light coming from adjacent ommatidia. This presumably results in finer resolution of the image seen.

Photomicrographs of optical paths through histological sections of these beetle eyes, indicate that light intensity

in clear zone eyes of A. schwarzi (Fig. 46) and M. carolina adults (Fig. 48) is brighter than light at tips of crystalline cones of eyes of O. californicus (Fig. 47) and C. tranquebarica (Fig. 49). The difference in light intensity may be due to the ability of the former two eyes to scatter incident light over adajcent rhabdoms.

Large pigment aggregations on the ventral aspect of the lamina ganglionaris and medulla interface are postulated to be reminants of six larval stemmata similar to that in other adult insect eyes (Weber, 1933). To prove this, an analysis of tissue organization of the pharate pupa would be required. Functionally, this pigment and glial cell pigment may prevent stimulation of retinulae by light entering the eye antidromically through thin cuticular regions.

4.4.5 Retinula Cell Axons

I did not determine from light microscope studies if axons of similar colour sensitivity in an axonal bundle synapse in the same lamina cartridge as observed by Braitenberg (1967) in eyes of Musca domestica Meig. (Muscidae). Why the axons are comparatively longer in eyes of A. schwarzi is not understood, but a similar arrangement is also observed in nocturnal scotopic B eyes of P. melanarius and in Steropus madidus Fab. adults (Carabidae) (Bernard, 1932). Axons of the other cicindelid and carabid beetle eyes are shorter, and these eyes have a lamina, medulla, and lobula grossly similar to photopic eyes of the

honey bee Apis mellifera L. (Ribi, 1975a), ant, Cataglyphis bicolor F. (Ribi, 1975b), and cockroach, Periplaneta americana L. (Ribi, 1977). To determine exact neural connections, Golgi silver impregnation (Ribi, 1974), cobalt chloride filling (Strausfeld and Obermayer, 1976), or procion yellow infiltration (Dvorak et al., 1975) into axons and interneurones would be required.

4.4.6 Significance of Evolution of Character States of cicindelid and carabid Beetle Compound Eyes

Significance of differences in structure and function of compound eyes is approached through a phylogenetic analysis of tiger beetles. This is followed by consideration of taxa representing other families of adephagans. A general pattern is sought and its outlines are explained in terms of the relationship between ecology and diversification of evolutionary lineages.

Evolution of character states of cicindelid and carabid bettle compound eyes are related to the reconstructed phylogeny (Fig. 113). For readers interested in keys, descriptions, and diagnoses of character states of tiger beetle taxa, see Schaupp (1883); Leng (1902;1920); Bradley (1930); and Arnett (1968). For a discussion of character states determining cleavage points between tribes, see Horn (1908-1915; 1926); Bradley (1930); and Arnett (1968); for subtribes, see Thompson (1857); Horn (1908-1915); Leng (1920); and Wallis (1961); for genera within the subtribe

Reconstructed Phylogeny of North American Genera of Cicindelidae Based on Horn, 1926 and Compound Eye Structure and Function

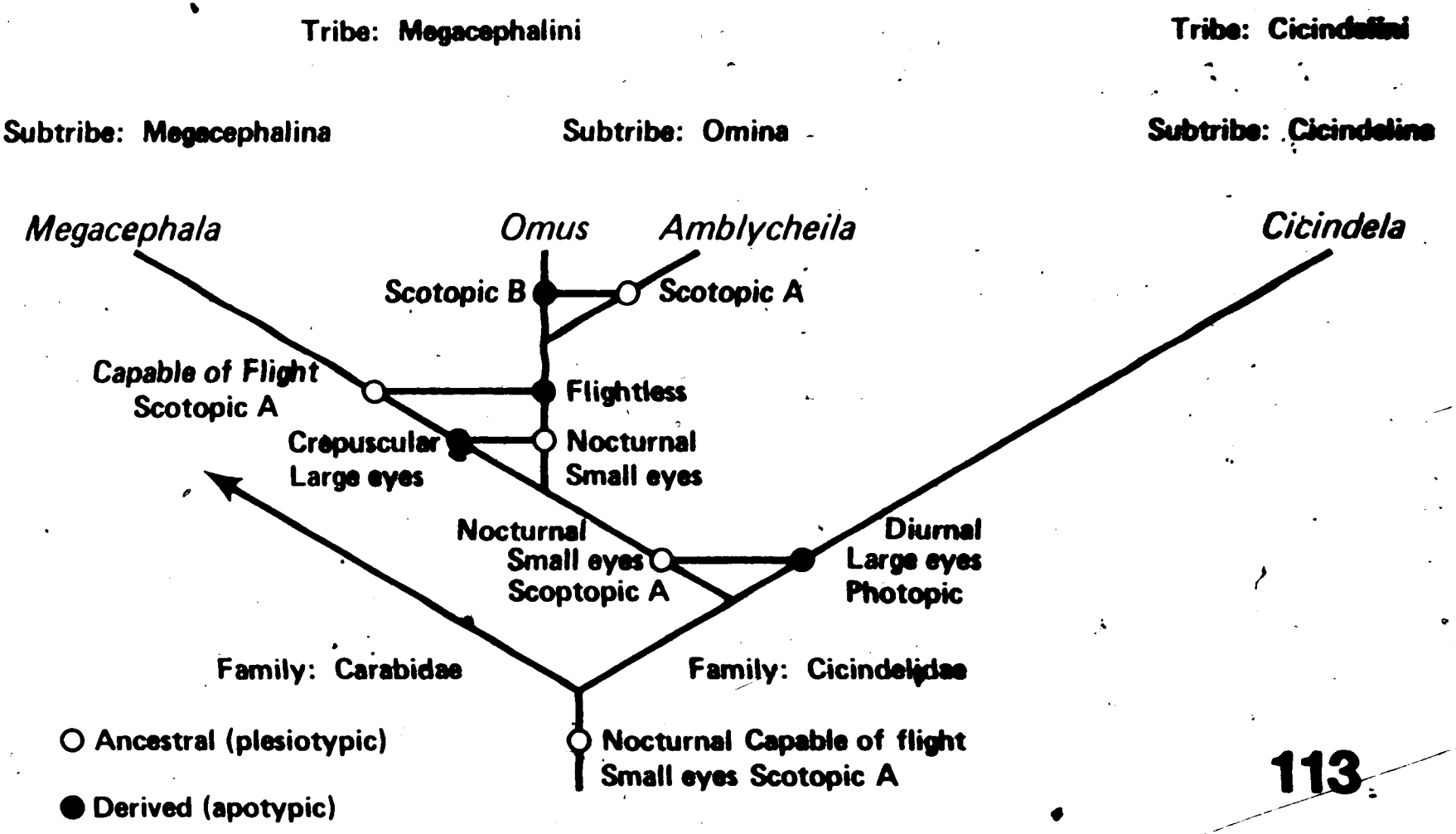

Omina, see Lacordaire (1843); Thompson (1857); Breus (1877); Schaupp (1883); Casey (1897); Leng (1902); Bradley (1930); Arnett (1946;1968); and Vaurie (1955); the genus Megacephala, see Thompson (1857); Schaupp (1883); Horn (1908-1915); Arnett (1946); and Willis (1969); the genus Cicindela, see Leconte (1857); Schaupp (1883); Leng (1902; 1920); Horn (1908-1915); Bradley (1930); Arnett (1946;1968); Rivalier (1954); Wallis (1961); and Willis (1968).

Ancestral stock of the Cicindelidae were probably related to Carabini of the family Carabidae. These primitive cicindelines invaded an ecological zone probably involving hunting of relatively large, active, heavily sclerotized prey, and larvae seizing prey from a fixed hiding place. Adults were probably nocturnal hunters and basically ground beetle-like in behaviour. They did not fly actively. Early divergence produced two lines, one of which initially retained the plesiotypic small, scotopic A eyes and nocturnal behaviours (the Megacephalini); the other acquired large eyes (ancestors of the Cicindelini).

Within the Megacephalini, two major lineages developed: the Omina, whose adults retained small eyes, and mainly nocturnal behaviour; and the Megacephalina, whose adults became crepuscular, acquired large eyes for stereopsis, but remained functionally scotopic A. Within the Omina, adults are secondarily flightless. Adults of Amblycheila plesiotypically have small scotopic A eyes. However, eyes of Omus adults have evolved scotopic B eyes

capable of finer image resolution for vision during more frequent diurnal activity periods.

The Cicindelini became divergent and probably initially diversified in the shade of tropical forests, where representatives of many cicindeline genera now live. Early lineages were probably crepuscular. Probably one of the more recent lineages moved into more open areas (initially, perhaps, along stream margins), developed quick flight, which could have been a correlate of the superior binocular vision afforded by large eyes. A lineage with such properties could have been ancestral to Cicindela, whose species became diurnal, and adapted for life in open areas. This taxon underwent an evolutionary flowering that produced an abundance of species on all continents (except Antarctica).

Among the species of Cicindela whose eyes I examined, I found two functional types: the plesiotypic scotopic A; and the apotypic photopic. Given only this information, one would be tempted to think that the taxa with scotopic A eyes were ancestral to those with the photopic eyes. However, I believe that the reverse is true, based on the following consideration. Photopic eyes and diurnal activity are characteristic of groups characterized by more primitive male genitalia, and hence believed to represent more primitive lineages of the genus. These species and the groups to which they belong (indicated by numbers (Freitag, 1974), based on Rivalier (1954)) are: Group 1A - C. repanda and C. limbata; Group 1B - C. longilabris; Group 1C - C.

[illegible] Group III - C. [illegible]. On the other hand, adults of some taxa characterized by highly derived genitalia are crepuscular as well as diurnal, and have either photopic or scotopic A eyes. These are: Group I, C. [illegible], eyes photopic; Group XII - C. [illegible], eyes scotopic A. [illegible] C. [illegible] (Group X) and C. lemniscata (Group XI) are active both in full light and in dim light, but their eyes have not been examined histologically.

Because of the nature of the correlations, I infer that diurnal activity and photopic eyes are plesiotypic in Cicindela, and that crepuscular activity and scotopic A eyes are apotypic. Therefore, presence of the latter type of eyes in Cicindela represents an evolutionary reversal.

Basically this phylogenetic framework provides a satisfactory continuity of evolution of eye function through nocturnal to crepuscular, and diurnal to crepuscular diel activity transitions. However, one abrupt change from nocturnal to diurnal is involved in the divergence of the Cicindelini from the Megacephalini. It must be mentioned that within the Cicindelini there are four subtribes containing a total of 16 genera which are more primitive than Cicindela (Horn, 1926). Eyes of adults of these genera may provide a smooth transition from ancestral small scotopic A eyes through large scotopic A eyes to still larger photopic eyes of Cicindela adults.

Based on earlier classification (Lacordaire, 1843;

1854; and Thompson, 1857), an alternative reconstructed phylogeny can be provided. This places the crepuscular Megacephalina as the sister group of the diurnal Cicindelini. One can then propose that the ancestors of these two taxa were crepuscular, like the extant members of the Megacephalina. Thus a smooth transition is provided for evolution of photopic eyes as suggested above. I believe that Horn's hypothesis is more correct and suggest that in the strict sense ancestors of Cicindelini had crepuscular eyes. This hypothesis should be tested by examination of eyes of the more primitive taxa of Cicindelini.

Using Horn's classification, several assumptions are required for the following events of evolution of cicindelid compound eyes: divergence in eye size; divergence in eye function; divergence in eye size and function; parallel acquisition of enlarged eyes; and reversion in function (but not in eye size) to an ancestral condition. Divergence in eye size alone is exhibited by evolution of large eyes in the Megacephalina; divergence in function alone, by acquisition of scotopic B eyes in adults of Omus; divergence in eye size and function by evolving eyes of ancestral Cicindelini. Parallel evolution of eye size is exhibited by independent acquisition of large eyes in both Megacephalina and Cicindelini. Reversal in function is exhibited by evolution of scotopic A eyes by a highly derived lineage of Cicindela, C. lepida. Also, in other highly derived Cicindela, C. belfragei, there is a reversal from diurnal

to crepuscular diel activity, without change in eye function.

Table 20 shows that based on my three functional categories, cellular organization in adephagan beetle eyes has undergone parallel evolution. Parallelism in function is identified in independent acquisition of scotopic B eyes among Cicindelidae (Omus spp.), Carabidae (Pterostichus melanarius and other taxa), and Gyrinidae (Gyrinus spp.). Parallelism in eye size and function related to diurnal activity is shown by Cicindelidae (Cicindela spp.) and Carabidae (Elaphrus spp.). All families but Gyrinidae have living taxa with ancestral scotopic A eyes. The impression is that parallel acquisition of the derived types of eyes occurred many times. Reversion to an ancestral functional condition might be common, through probably less frequent than parallelism.

It is important to recapitulate that modifications are based on eye size and on an alteration of cellular organization not on a change in cell number in ommatidia. Coadapted to nocturnal activity are small scotopic A eyes, scotopic B eyes to nocturnal but more frequent diurnal activity; to crepuscular activity, large scotopic A eyes (exception, large photopic eyes of C. belfragei); and to diurnal activity, large photopic eyes.

The mechanism used to evolve large eyes from small eyes is addition of number of ommatidia with an accompanying shortening of the dioptric apparatus and increased retinula

Table 20. Functional eye categories of adephagan beetle adults.

Family	Functional Eye Category	References
Cicindelidae	Scotopic A	Section 4.3.5.2
	Scotopic B	Sections 4.3; 5.3
	Photopic	Kirchoffer, 1905; 1908 Friedrichs, 1931 Swiecimski, 1957 Home, 1976 Section 4.3.5.2
Carabidae	Scotopic A	Kirchoffer, 1905; 1908 Bernard, 1932 Hasselmann, 1962
	Scotopic B	Grenacher, 1879 Kirchoffer, 1905; 1908 Bernard, 1932 Section 4.3.6.2
	Photopic	Kirchoffer, 1905; 1908 Horridge and Giddings, 1971a Bauer, 1974; 1977 Home, 1976 Section 4.3.6.2
Dytiscidae	Scotopic A	Grenacher, 1879 Exner, 1891 Kirchoffer, 1905; 1908 Horridge, 1969a Horridge et al., 1970 Meyer-Rochow, 1973; 1975
Gyrinidae	Scotopic B	Kirchoffer, 1905; 1908 Horridge and Giddings, 1971a Pappas and Larsen, 1973 Wachmann and Schröer, 1975 Burghause, 1976

length. The transition from scotopic A to scotopic B eyes involves elimination of the clear retinula zone by extension of the rhabdom the complete retinula length. Such a structural modification only involves shortening of the retinula cells. Changes involved with elimination of the clear retinula zone and reduction of rhabdom surface area and volume evolve photopic eyes from large scotopic A eyes and converse relationships are required for the opposite transition.

Because slight changes in internal structure have profound effects on function, it is fairly easy for evolving groups to move from one adaptive zone to another, and back again. Such shifts are generally correlated with speciation. This means an increase in diversity when such shifts occur, and ultimately they involve change in eye function. Therefore, it seems likely that the ability of eyes to respond quickly to selection is an integral component of evolution of diversity among the Adephaga in particular, and perhaps among insects in general.

5. Fine Structure of Photopic Eyes of Males of *Cicindela tranquebarica* Herbst

5.1 Introduction

Chapter 5 describes the fine structural cellular organization in eyes of males of *Cicindela tranquebarica* Herbst and discusses the functional morphology of this derived photopic eye. Also suggestions for further research are made. As reported in Section 4.4.3.3, other authors have histologically examined adult eyes of various *Cicindela*. Kirchoffer (1905) gave a general description of eyes of *C. campestris* L., *C. silvatica* Latr., and *C. hybrida* L., and in 1908 amplified his descriptions to include figures of eyes of the first two species. From observations of structure of eyes of *C. campestris* and *C. hybrida* adults, Friedrichs (1931) corrected Kirchoffer's (1908) inaccurate description on the following three points: the nucleus of the eighth retinula cell lies proximal, not distal to the basement membrane; there are seven not six axons surrounding each basal retinula cell, and there appears to be 16 not 17 secondary pigment cells. Swiecimski (1957) examined the eye structure of *C. hybrida* adults and analyzed the role of vision in prey capture behaviour (Section 3.4).

I have examined the cellular organization in eyes of adults of *C. limbata nympha* Casey, *C. limbalis*

Klug, C. repanda repanda Dejean, C. longilabris Say (Section 4.4.3.3); C. lepida Dejean, and C. belfragei Sallé (Section 4.3.2). Home (1976) has examined some aspects of the fine structure of the eyes of C. campestris adults. Her description deals mainly with the retinulae of this insect and she does not give a detailed account of other eyes structures. In the following treatment, structures between the corneal lens and lamina ganglionaris of the eyes of C. tranquebarica males are described.

5.2 Materials and Methods

For light microscopy (LM) wax sections 10 to 12 µm thick, were prepared as in Section 4.2. Araldite sections 1.5 µm thick, were stained at 80°C with 1% periodic acid then with 1% Mallory's Azur II containing an equal volume of 1% methylene blue in 1% borax solution (Richardson et al., 1960), or at room temperature in saturated Sudan III in 70% ethanol (de Martino et al., 1968). Slides were mounted with Permount and with glycerine respectively. Representative photographs were taken with a Carl Zeitz Ultraphot II on Kodak Plus-X, Pan Professional, 10.2 x 12.7 cm sheet film.

Eyes to be observed by Nomarski interference microscopy (NIM) were fixed, dehydrated, embedded, sectioned, and photographed as in Section 4.2.

For SEM examination of their cellular organization, eyes were fixed in 3% glutaraldehyde for 2 h and post-fixed for 1 h in 1% osmium tetroxide, at pH 7.4 in Millonig's

phosphate buffer with sucrose (Millonig, 1961). They were dehydrated through a graded series of ethanols then transferred to 100% amyl acetate for critical point drying with carbon dioxide in a Denton Vacuum DCP-1 dryer. After drying, eyes were fractured with a razor blade (Carlson and Larsen, 1972a and b; Carlson and Chi, 1974; and Chi and Carlson, 1975). An alternate method used was to cryofracture eyes in liquid nitrogen (Nei, 1974). After critical point drying, eyes were exposed to osmium tetroxide vapours overnight. Fractured eyes were carbon and gold coated to a thickness of 15 to 20 nm using an Edwards 12E vacuum evaporator and were then examined using a Cambridge Stereoscan S4, scanning electron microscope (SEM) at accelerating voltages of 20 to 30 kV. Representative photographs were taken on Kodak Plus-X, Pan Professional, PXP-120 roll film.

For transmission electron microscopy (TEM), eyes were fixed in 3% glutaraldehyde for 4 h and post-fixed for 1 1/2 h in 2% osmium tetroxide in Millonig's (Millonig, 1961) phosphate buffer with sucrose at pH 7.4 (Perrelet, 1970). After ethanolic dehydration and propylene oxide treatment, eyes were embedded in araldite 502 (Luft, 1961). Longitudinal and transverse sections were cut at a thickness of approximately 60 nm using glass knives in a Reichert OmU_2 ultramicrotome. Sections were transferred to 200 mesh copper grids having a 0.25% formvar (polyvinal formal) in ethylene dichloride support film (Hayat, 1970). Sections were stained for 5 h in saturated aqueous uranyl acetate followed by a

3 min. stain in 0.02% aqueous lead citrate (Venable and Coggeshall, 1965). Grids were examined using a Phillips EM 201C at 60 kV accelerating voltage. Photomicrographs were taken on Kodak Fine Grain Positive 35 mm film.

Eye tissue to be freeze-etched was fixed for 2 h in 3% glutaraldehyde in Millonig's phosphate buffer with sucrose and then transferred to 30% aqueous glycerine. Tissue was then rapidly frozen in freon (dichlorodifluoromethane) at its fusion point of -155°C (Moor, 1971). Frozen material was then placed on the pre-cooled stage at -150°C of a Balzers BA 360M high vacuum freeze-etch unit, then fractured and evaporated with carbon and platinum (Perrelet et al., 1972). Tissue from thawed preparations was digested using a 40% solution of chromic acid. Ajax ^{R} detergent-washed replicas were placed on 0.25% formvar-coated, 200 mesh copper grids and examined using a Phillips EM 201C.

5.3 Results

5.3.1 General Features

Figs. 114-117 show the general organization of the eye of Cicindela tranquebarica males. Fig. 114 is a frontal section through a left eye. Ommatidia near the frons (fo) which function in stereoscopic vision (Section 3.3), are longest; followed by the cervical ommatidia (co), which also function in binocular vision (Section 3.3). Shortest are the medial ommatidia (mo) used for monocular vision (Section 3.3). Figs. 115-117, illustrate the organization of the

Figs. 114-117. Longitudinal sections of eyes of *Cicindela tranquebarica* adults. Shown are: corneal lens (l); subcorneal layer (cl); crystalline cone (c); crystalline thread (ct); retinula rhabdom zone (rr); rhabdom (r); basal retinula zone (br); basement membrane (bm); axons (a); lamina ganglionaris (lg); secondary pigment cells (2p); basal pigment cells (bp); frontal ommatidia (fo); medial ommatidia (mo); and cervical ommatidia (co).

Fig. 114. LM of a wax section.
Scale = 250 µm

Fig. 115. LM of an araldite section.
Scale = 100 µm

Fig. 116. NIM of a wax section.
Scale = 100 µm

Fig. 117. SEM cryofracture.
Scale = 100 µm

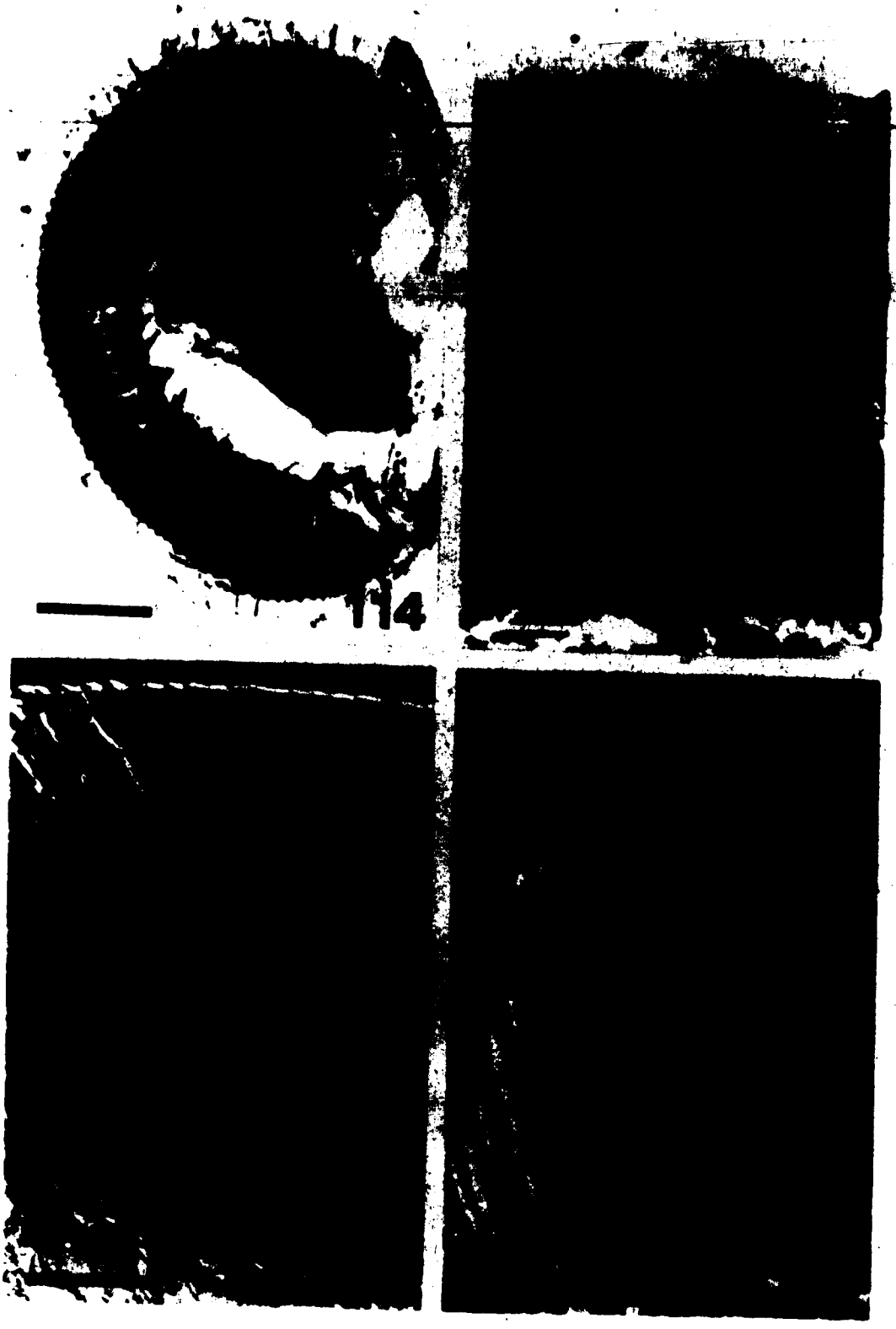
114

compound eye of this cicindelid beetle. The fine structure of this eye is described in detail in the following sections and is summarized in Fig. 193.

5.3.2 Dioptric Apparatus

The dioptric apparatus consists of a biconvex, hexagonal, corneal lens (l), subcorneal layer (cl), and a crystalline cone (c) (Fig. 118). The thin corneal layer (t) is only 1.65 µm thick (Table 7; Section 4.3.1.1).

5.3.2.1 Corneal Lens

The corneal lens is 50.6 µm long, and 18.7 µm in diameter and consists of lamellae (lm) of exocuticle (Fig. 118) which are best seen in freeze-etch preparations (Fig. 119). Thin transverse sections through the lens reveal a spiral conformation of lamellae (lm) (Fig. 120). The spiral is tighter in the centre of each lens. Lamellae have differing refractive indices since phase changes in polarized light transmitted through unstained sections can be observed using NIM.

5.3.2.2 Subcorneal Layer

The subcorneal layer (cl) as defined in Section 4.4.1 is situated between the corneal lens (l) and crystalline cone (c) (Fig. 121). It is approximately 11.7 µm in diameter and 0.6 µm thick. Cryofracture SEM observations of this layer (Figs. 122, 123), show that both its distal (Fig. 122),

Fig. 118. SEM cryofracture of longitudinal section of dioptric apparatus, showing biconvex hexagonal corneal lenses (l); lamellae of exocuticle (lm); thin corneal layer (t); subcorneal layer (cl); crystalline cone (c); and secondary pigment cells (2p).

Scale = 10 μm

Fig. 119. TEM freeze-etch of longitudinal section of corneal lens, showing exocuticular lamellae (lm).

Scale = 0.5 μm

Fig. 120. TEM of transverse section through corneal lenses, showing spiral conformation of lamellae (lm).

Scale = 1 μm

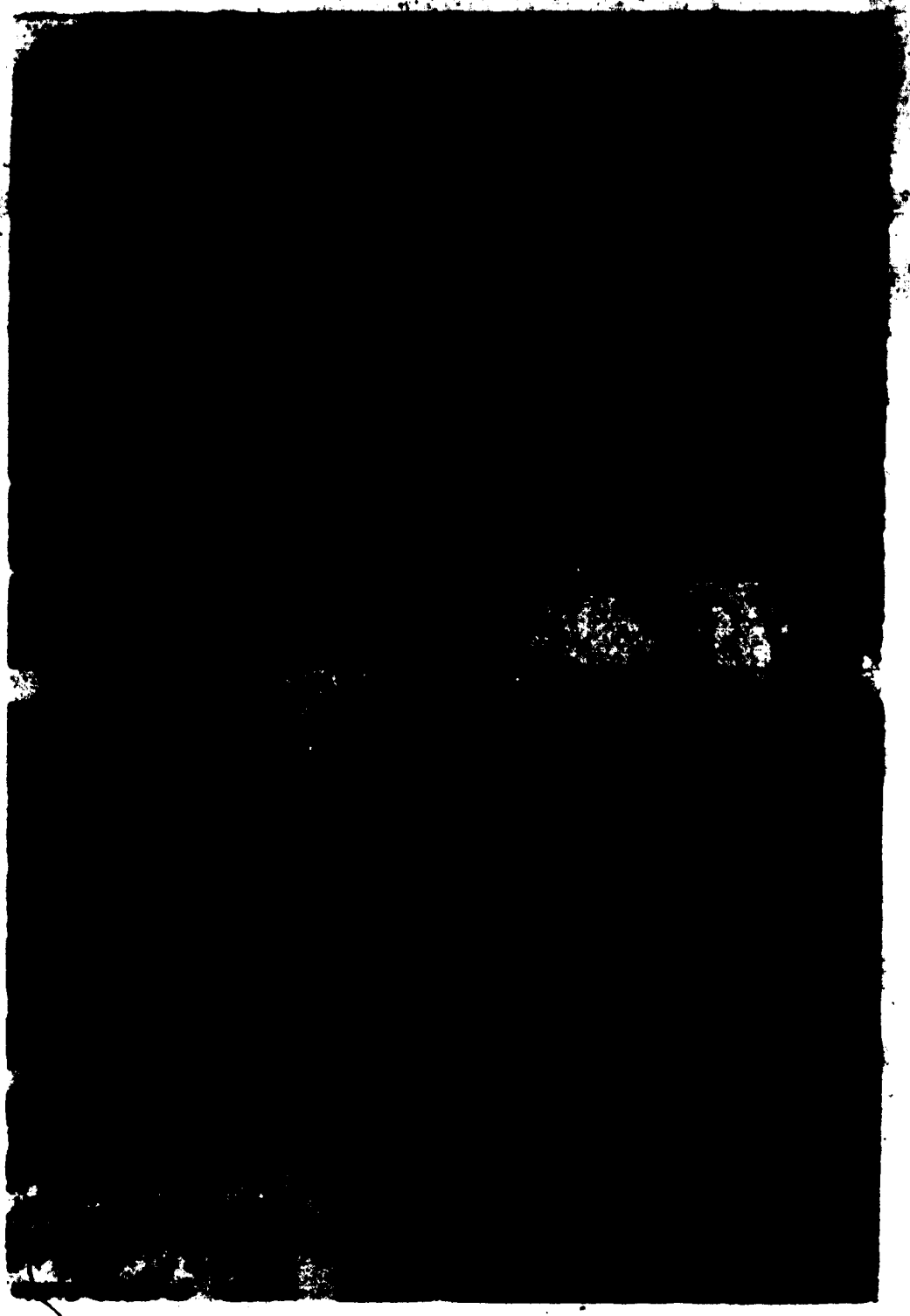

Fig. 121. LM of longitudinal section through dioptric apparatus, showing corneal lens (l); subcorneal layer (cl); crystalline cone (c); crystalline thread (ct); primary pigment cell nucleus (n); and secondary pigment cells (2p).

Scale = 10 µm

Fig. 122. SEM cryofracture of distal surfaces of subcorneal layer, showing polygons (po) of endocuticle.

Scale = 5 µm

Fig. 123. Same, of subcorneal layer, showing polygons (po); crystalline cone (c); Semper's cells (s); and secondary pigment cells (2p).

Scale = 2 µm

Fig. 124. Same, of subcorneal layer, showing lamellae of endocuticle (lm); crystalline cone (c); Semper's cells (s); primary pigment cells (1p); and secondary pigment cells (2p).

Scale = 1 µm

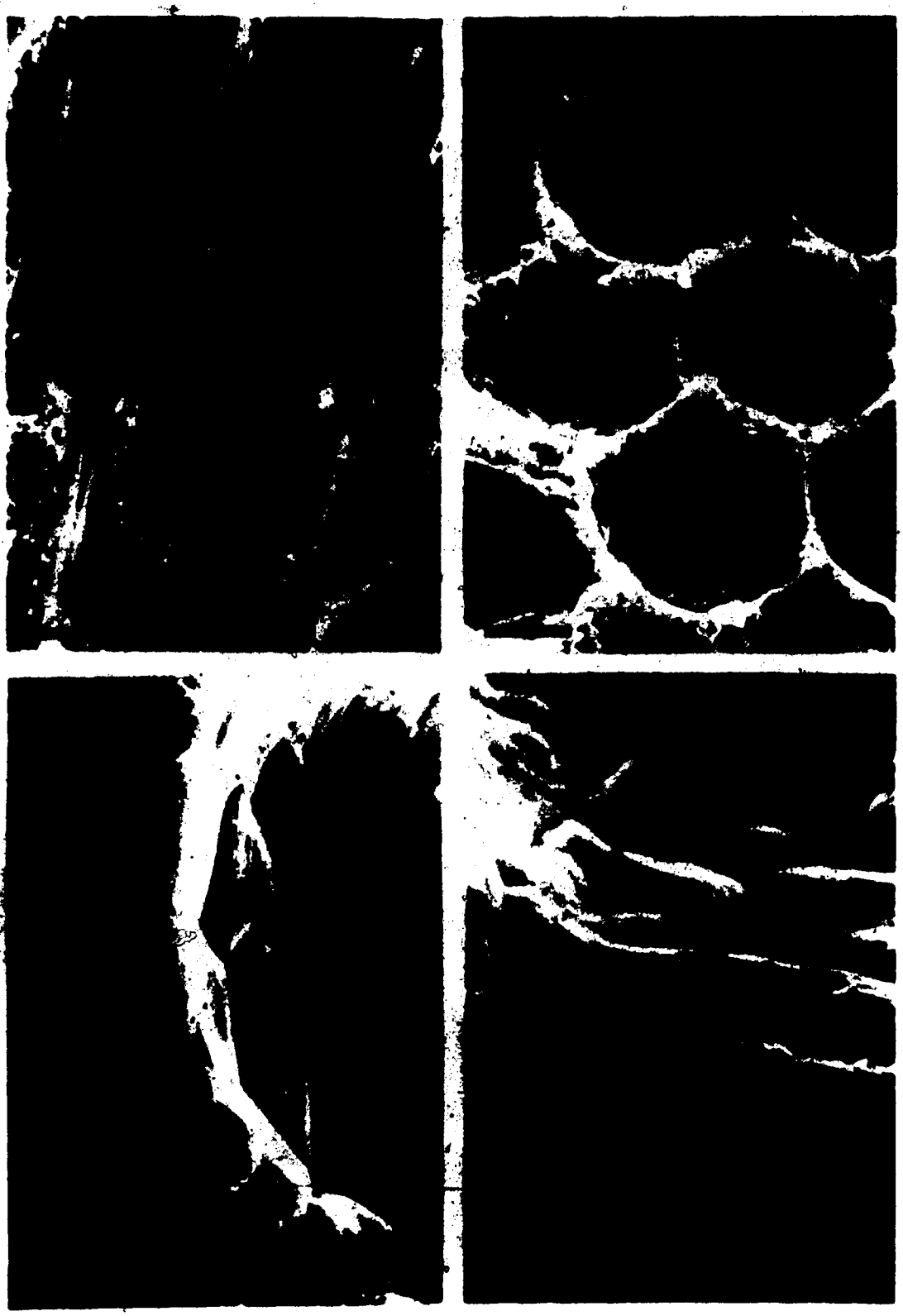

and proximal (Fig. 123) surfaces consist of the outlines of 11 "cellular" polygons (po) each approximately 5 µm across. The subcorneal layer is lamellated (Fig. 124). In section these lamellae appear to consist of parabolae of endocuticular microfibrils (mf) (Figs. 125-127). Towards the corneal lens (l) (Fig. 125), the lamellae are thicker and their microfibrils (mf) have what may be protein (pr) deposits (Neville, 1975) along their lengths (Fig. 127).

5.3.2.3 Crystalline Cone

The crystalline cone (c) is concave distally (Fig. 128). It is approximately 53.5 µm long and has a maximum diameter of 25.8 µm. Four equal-sized quadrants form the cone, each of which is separated from its neighbour by a transparent Semper cells (s) (Figs. 123, 124, 128, 129). The nuclei (n) of these Semper cells lie beneath the lens (l) (Fig. 125). Thin sections (Fig. 129), show the crystalline cone to be granular, particularly peripherally. The central region of each cone quadrant is less electron-dense than their peripheral region. The four Semper cells surrounding the cone contain mitochondria (m), and microtubles (mt), while primary pigment cells (lp) contain mainly polysomes (arrows) and a few mitochondria (m) (Fig. 130). A freeze-etched preparation (Fig. 131) of a section similar to that of Fig. 130 shows stippling (arrows) of the primary pigment cell (lp) unit membranes. This stippling of protein on the "protoplasmic face" (pf) (Branton et al., 1975) could

Fig. 125. TEM of longitudinal section of dioptric apparatus, showing lamellated corneal lens (l); lamellated subcorneal layer (cl); two quadrants of the crystalline cone (c); nuclei (n) of Semper cells; primary pigment cells (1p); and secondary pigment cells (2p).

Scale = 2 µm

Fig. 126. Same, of subcorneal layer, showing lamellae (lm) consisting of parabolic endocuticular microfibrils (mf).

Scale = 2 µm

Fig. 127. Same, of lamellae of endocuticle, showing microfibrils (mf) of endocticular lamellae with protein (pr) deposits along their lengths.

Scale = 1 µm

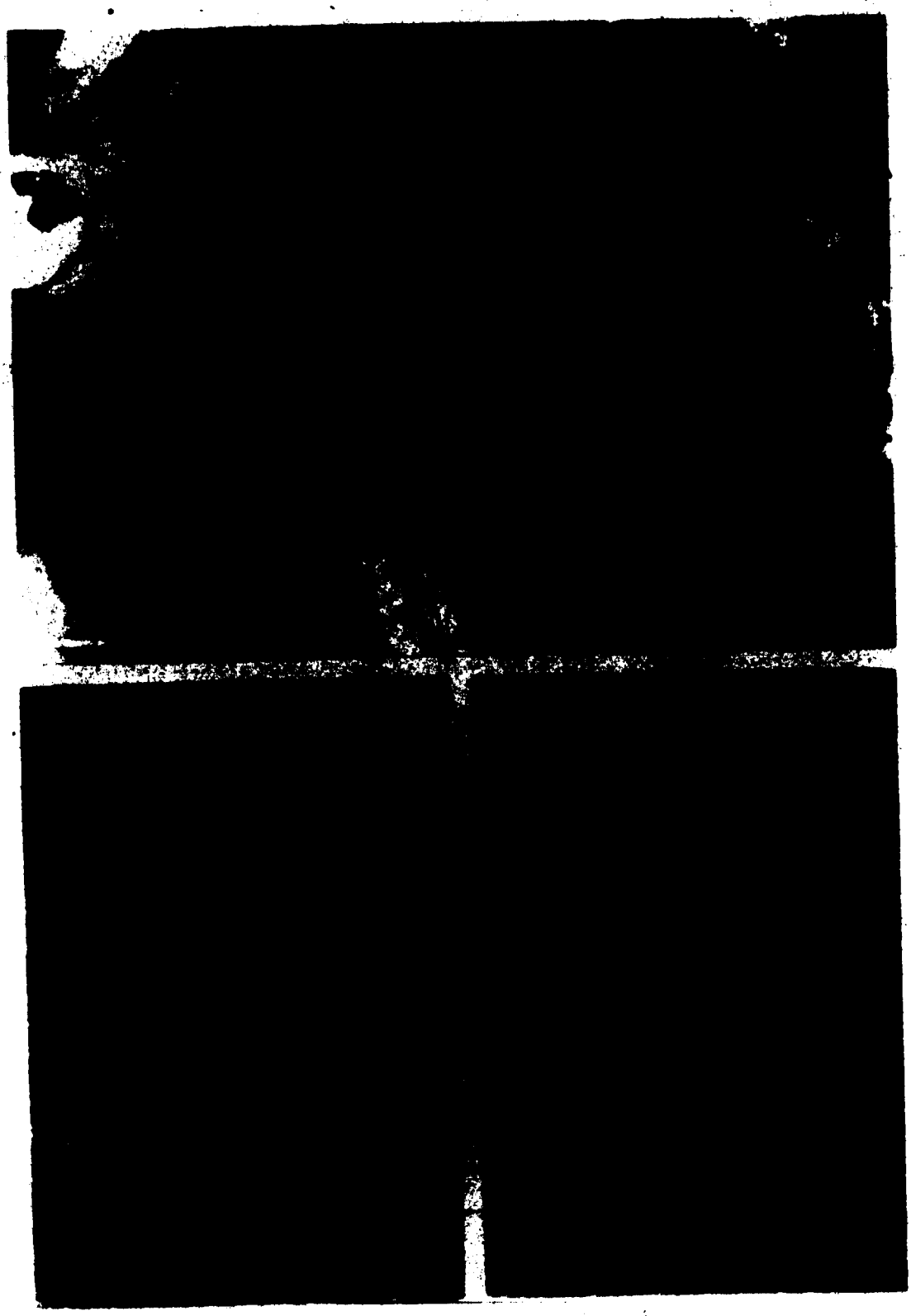

Fig. 128. SEM cryofracture of a crystalline cone (c), showing concave distal surface, and four quadrants limited by four Semper cells (s).

Scale = 5 µm

Fig. 129. TEM of transverse section through a crystalline cone (c), showing the granular appearance of the four quadrants; Semper cells (s); primary pigment cells (1p); and secondary pigment cells (2p).

Scale = 2 µm

Fig. 130. Same, showing Semper cells (s) containing mitochondria (m) and microtubules (mt); and primary pigment cells (1p) containing polysomes (arrows); and mitochondria (m).

Scale = 1 µm

Fig. 131. Same, freeze-etch. Note granular appearance of crystalline cone (c) surrounded by Semper cells (s) and protein (arrows) on the pf face of the primary pigment cell (1p) unit membrane.

Scale = 1 µm

be intramembranal manifestations of some kind of desmosome.

5.3.3 Crystalline Thread and Primary Pigment Cells

Closely applied, proximal extensions of the four Semper cells form the crystalline thread. Fig. 132 shows a transverse cryofracture section through the crystalline thread (ct) with surrounding primary pigment cells (1p). Approximately 16 secondary pigment cells (2p) radiate to form a stellate pattern around these cells. Transverse sections of the thread (ct) examined by TEM (Fig. 133) show it to be of four parts. The surrounding primary pigment cells (1p) contain nuclei (n) at the proximal level of the thread (see also Fig. 121). Septate desmosomes (d) (Locke, 1965) occur between primary pigment cells (Fig. 133). Primary pigment cells do not contain pigment granules. Fig. 134 indicates that the cytoplasm of these cells is rich in rough endoplasmic reticulum (rer), which suggests that they are active in protein synthesis. Examination of the crystalline thread (ct) at higher magnification (Fig. 135), shows that microtubules (mt) are its major cellular inclusion. Longitudinal sections (Fig. 136) show these microtubules to be aligned parallel to the vertical axis of the thread. The crystalline thread is approximately 1.2 µm in diameter. The four strands of the crystalline thread separate and extend proximally to form inter-retinular fibers (f) (Waddington and Perry, 1963) between retinula cells: 1/2, 3/4, 5/6, and 7/1 (Fig. 137). Microtubules (mt)

Fig. 132. SEM cryofracture of transverse section through a crystalline thread (ct) surrounded by primary pigment cells (1p) and a stellate arrangement of 16 secondary pigment cells (2p).

Scale = 2 µm

Fig. 133. TEM of transverse section through a crystalline thread (ct), showing four quadrants surrounded by two primary pigment cells (1p) each containing a nucleus (n) and cytoplasm rich in rough endoplasmic reticulum (rer). Note septate desmosomes (d) between primary pigment cell membranes. Secondary pigment cells (2p) containing nuclei (n) and pigment granules (p) surround these structures.

Scale = 2 µm

Fig. 134. Same, through a crystalline thread (ct) and primary pigment cells (1p) rich in rough endoplasmic reticulum (rer).

Scale = 1 µm

Fig. 135. Same, through four crystalline thread quadrants, showing microtubules (mt).

Scale = 200 nm

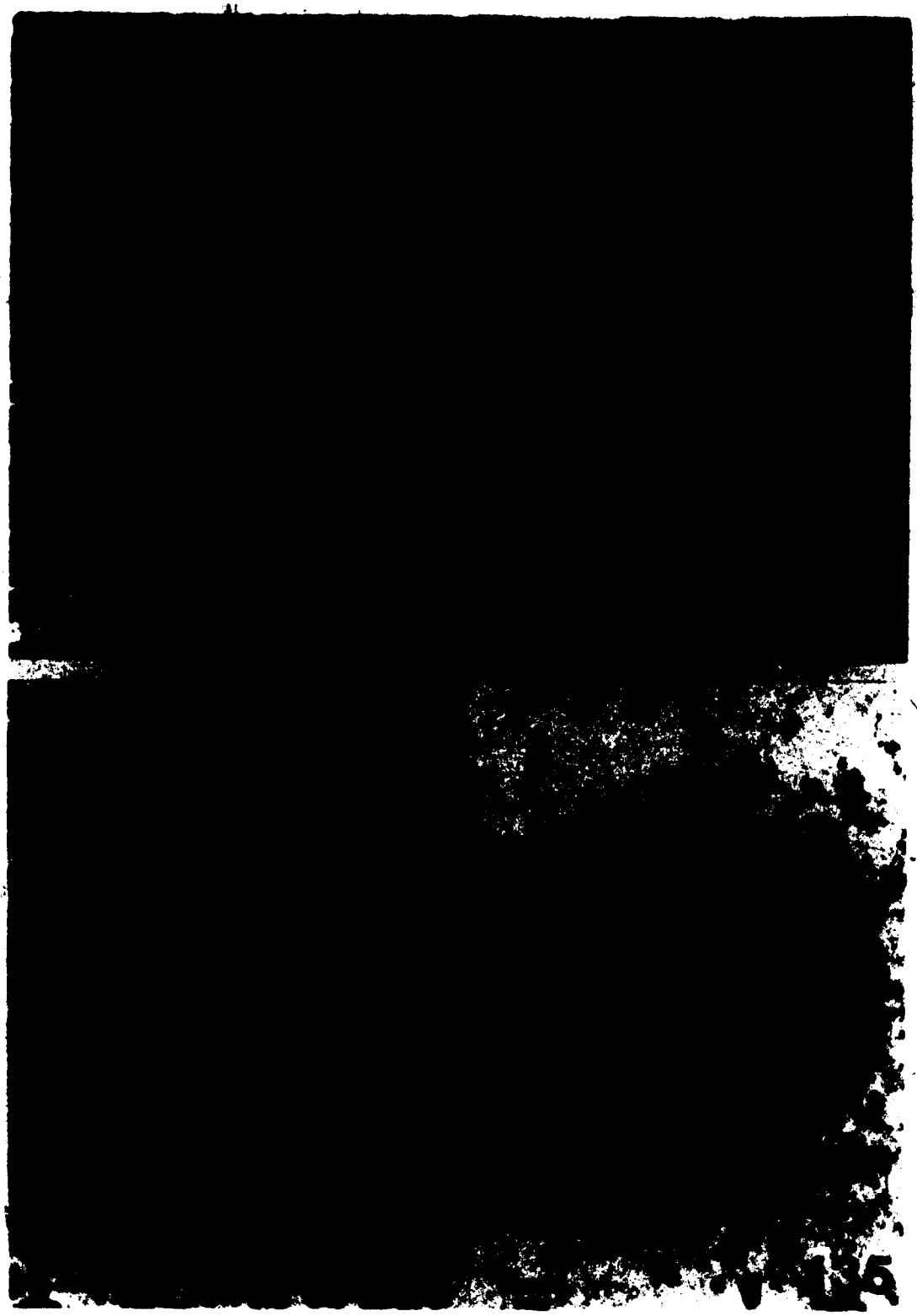

Fig. 136. TEM of longitudinal section through crystalline thread (ct), showing microtubules (mt). The thread is surrounded by primary pigment cells (1p) containing rough endoplasmic reticulum (rer). Secondary pigment cells (2p) envelope primary pigment cells.

Scale = 1 µm

Fig. 137. Same, of transverse section through distal rhabdom (r), showing inter-retinular fibers (f) between retinula cells 1/2, 3/4, 5/6, and 7/1.

Scale = 1 µm

Fig. 138. Same, through an inter-retinular fiber, showing microtubules (mt) within its cytoplasm. Note spot desmosome (d) near the rhabdom (r).

Scale = 250 nm

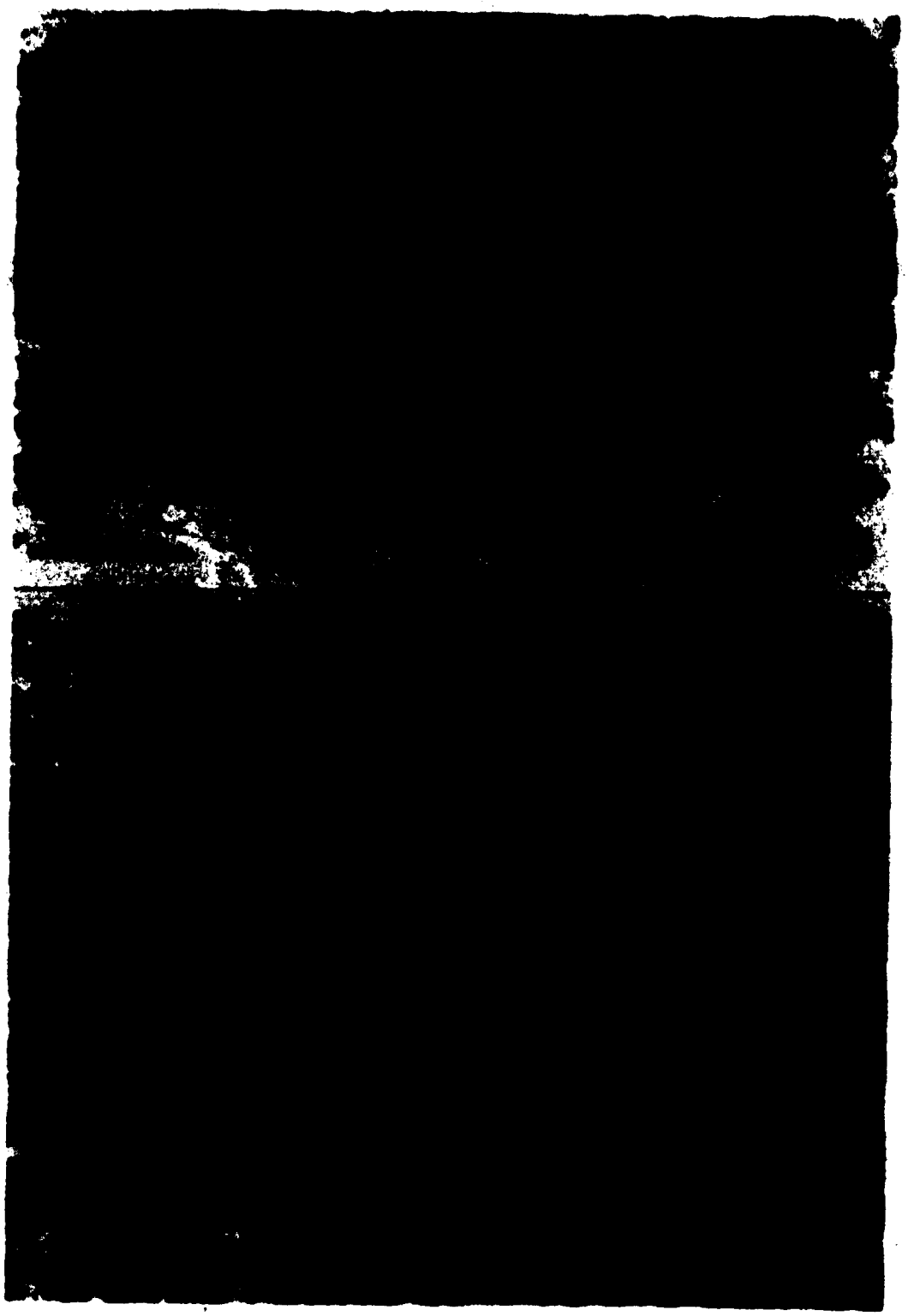

are still present in the thread at this level. Spot desmosomes (d) of retinula cells are medial to these interretinular fibers (Fig. 138).

5.3.4 Interfacetal Pegs

Scattered between some corneal lenses (l) are interfacetal cuticular pegs (cp) (Fig. 139) conical in shape and approximately 2.3 µm in diameter and 3.1 µm high. In longitudinal section (Fig. 140) these pegs (cp) can be seen to have a cuticular socket (so) which sits on an articulating cutucular membrane (mb). The location of this is speculated. Fig. 147 shows a dendritic sheath (ds) (=cuticular sheath, scolopale) and in Fig. 142, nuclei (n) of the inner (=trichogen) (i) and outer sheath cells (=tormogen) (o) (inner and outer sheath terminology from personal communication with R.Y. Zacharuk). Transverse sections of the distal portion show the cuticular peg (cp) and socket (so). Suspension fibers (sf) connect the peg and socket (Fig. 143). Distally, the dendritic sheath (ds) is surrounded by the cuticular peg (cp) and socket (sp) (Fig. 144). This sensillum has a single bipolar neuron. Fig. 145 shows a distally located tubular body (tb), approximately 630 nm in diameter, surrounded by the dendritic sheath (ds). These structures are surrounded by corneal lenses (l) (Fig. 145). The tubular body consists of numerous longitudinally oriented microtubules (mt) interspersed with electron-dense substance, and is surrounded by a large lumen (lu) (Fig. 146). More proximally is a cilium (ci) (Figs. 147, 148)

Fig. 139. SEM of a cuticular peg (cp) of an interfacetal mechanoreceptor situated between corneal lenses (l).

Scale = 2 µm

Fig. 140. LM of longitudinal section of a cuticular peg (cp) and socket (so) which sits on an articulating membrane (mb).

Scale = 10 µm

Fig. 141. Same, of the dendritic sheath (ds) of an interfacetal mechanoreceptor.

Scale = 10 µm

Fig. 142. Same, of the inner (i) and outer sheath cells (o), showing nuclei (n).

Scale = 10 µm

Fig. 143. TEM of transverse section through a cuticular peg (cp) and socket (so).

Scale = 1 µm

Fig. 144. Same, through dendritic sheath (ds) surrounded by the cuticular peg (cp) and socket (so). Note suspension fibers (sf).

Scale = 1 µm

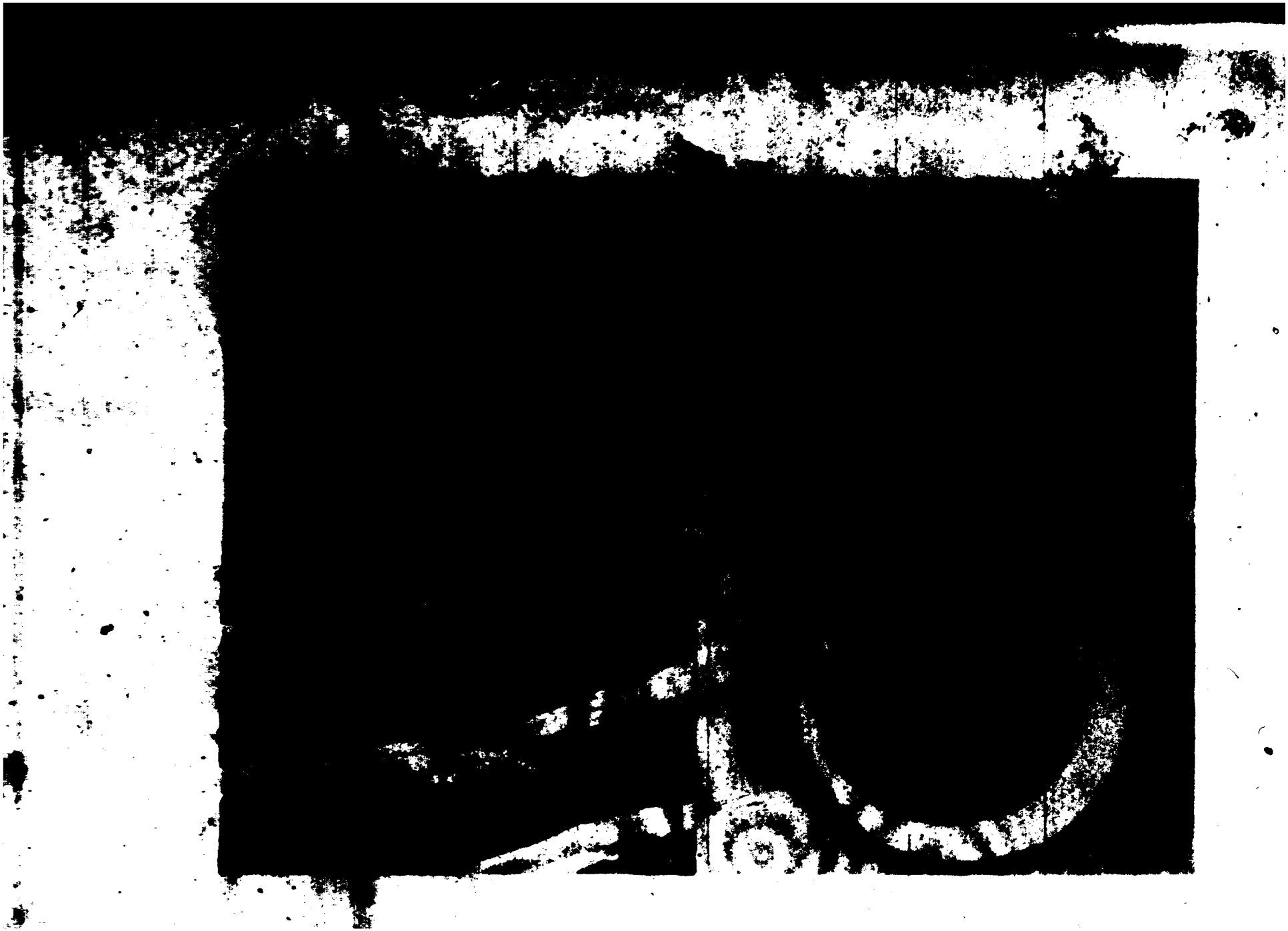

Fig. 145. TEM of transverse section through a tubular body (tb) surrounded by a dendritic sheath (ds). Corneal lenses (l) surround these structures.

Scale = 1 µm

Fig. 146. Same, showing longitudinally oriented microtubules (mt) and electron-dense substance. A lumen (lu) surrounds the tubular body.

Scale = 500 nm

Fig. 147. Same, through cilium (ci) surrounded by a dendritic sheath (ds) and sheath cells (sc). Note corneal lenses (l) and secondary pigment cells (2p).

Scale = 2 µm

Fig. 148. Same, showing cilium (ci) containing 11 peripheral microtubular doublets and five central singlets. Note dendritic sheaths (ds); inner (i) and outer sheath cells (o); four accessory eipthelial cells (e); microtubules (mt); mitochondria (m); septate desmosomes (arrows); and lumen (lu).

Scale = 1 µm

Fig. 149. Same, through a basal body (bb) of cilium. Note that the dendritic sheath (ds) only partially surrounds this structure.

Scale = 2 µm

Fig. 150. Same, through nucleus (n) of neuron (largest cell) and inner and outer sheath cells. Cells contain mitochondria (m) and rough endoplasmic reticulum (rer).

Scale = 2 µm

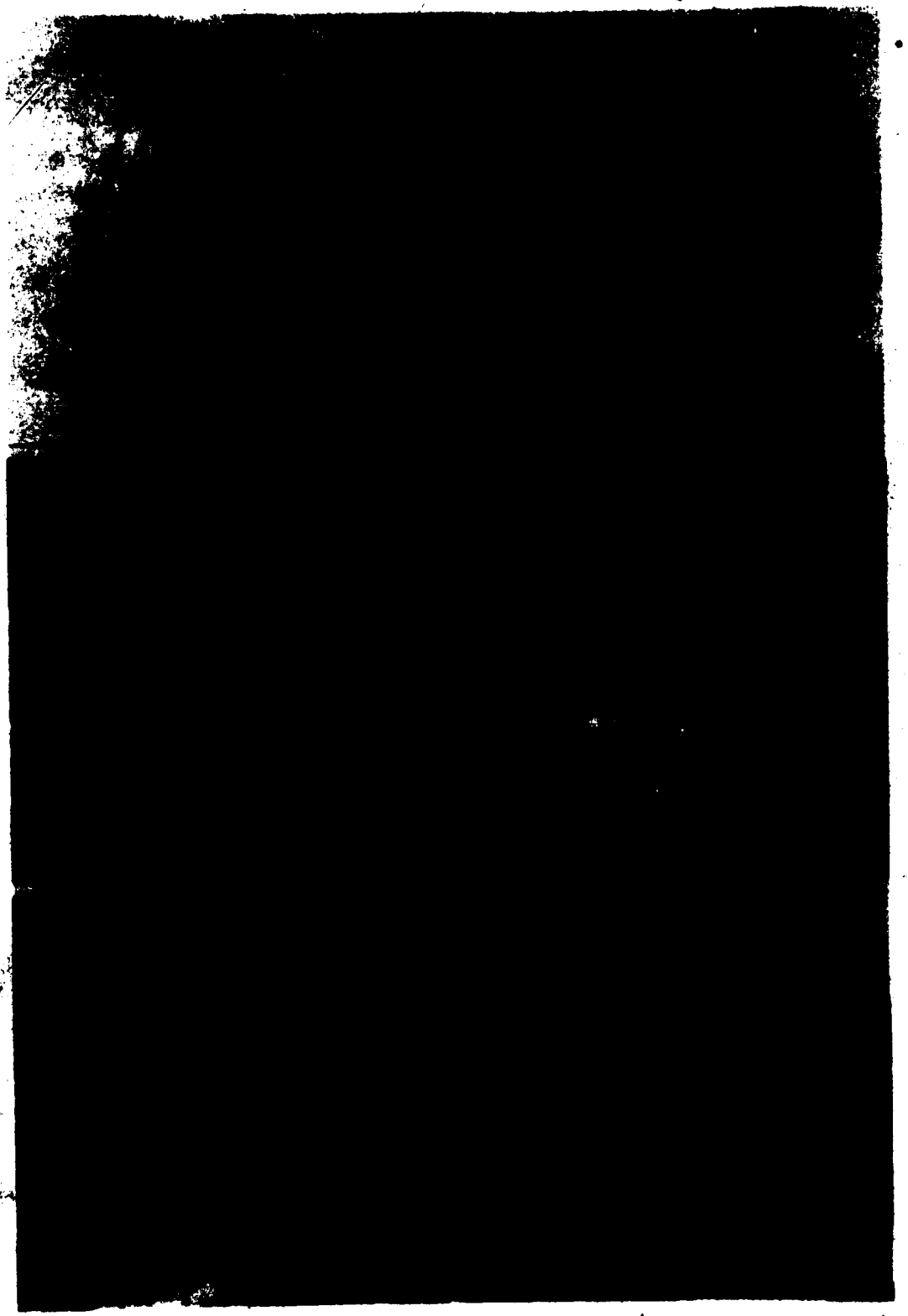

containing 11 peripheral microtubular doublets and five central singlets. The cilium is approximately 625 nm in diameter and is enclosed by the dendritic sheath (ds). This dendritic sheath is surrounded by an inner (i) and outer sheath cell (o), and four accessory sheath cells (e). Septate desmosomes (arrows) are present between the sheath cell membranes and microtubules (mt) and mitochrondria (m) are within their cytoplasm. Sheath cells are adjacent to a large lumen (lu), and corneal lenses (l) and secondary pigment cells (2p) are also seen at this level. The cilium has a basal body (bb) (= centriole, kinetosome; Wolfe, 1972) which lies parallel to the vertical axis of the interfacetal mechanoreceptor (Fig. 149). The dendritic sheath (ds) only partially surrounds this structure. Nuclei (n) of the sheath cells and neuron are more proximally located (Figs. 150, 151). Neurotubules are present in the cytoplasm of the neuron. Sheath cells contain: mitochondria (m) and rough endoplasmic reticulum (rer). There are no septate desmosomes between sheath cells at this level (Figs. 150, 151). Figs. 151, 152 show the axon (a). The axon (Fig. 153) contains: mitochondria (m), rough endoplasmic reticulum (rer), neurotubules (arrows), and what may be a vacuole (v) or a fixation artifact. Three sheath cells surround the axon; the third is probably the basal or neurilemma cell (nu). All sheath cells contain pigment granules (p) at this level. Because of the density of pigment granules in secondary pigment cells (2p) of the eyes, it

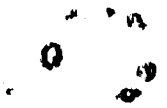

Fig. 151. TEM of transverse section through nucleus (n) of one sheath cell and lumen (lu) of the other. Note axon (a).

Scale = 2 µm

Fig. 152. Same, through lumina (lu) of sheath cells and axon (a) of neuron.

Scale = 2 µm

Fig. 153. Same, through axon, showing mitochondria (m); rough endoplasmic reticulum (rer); and neurotubules (arrows); and vacuole (v). Note inner (i) and outer sheath cells (o) and the neurilemma sheath cell (nu). All sheath cells contain mitochondria (m); microtubules (mt); rough endoplasmic reticulum (rer); and pigment granules (p). The axon is also surrounded by secondary pigment cells (2p).

Scale = 1 µm

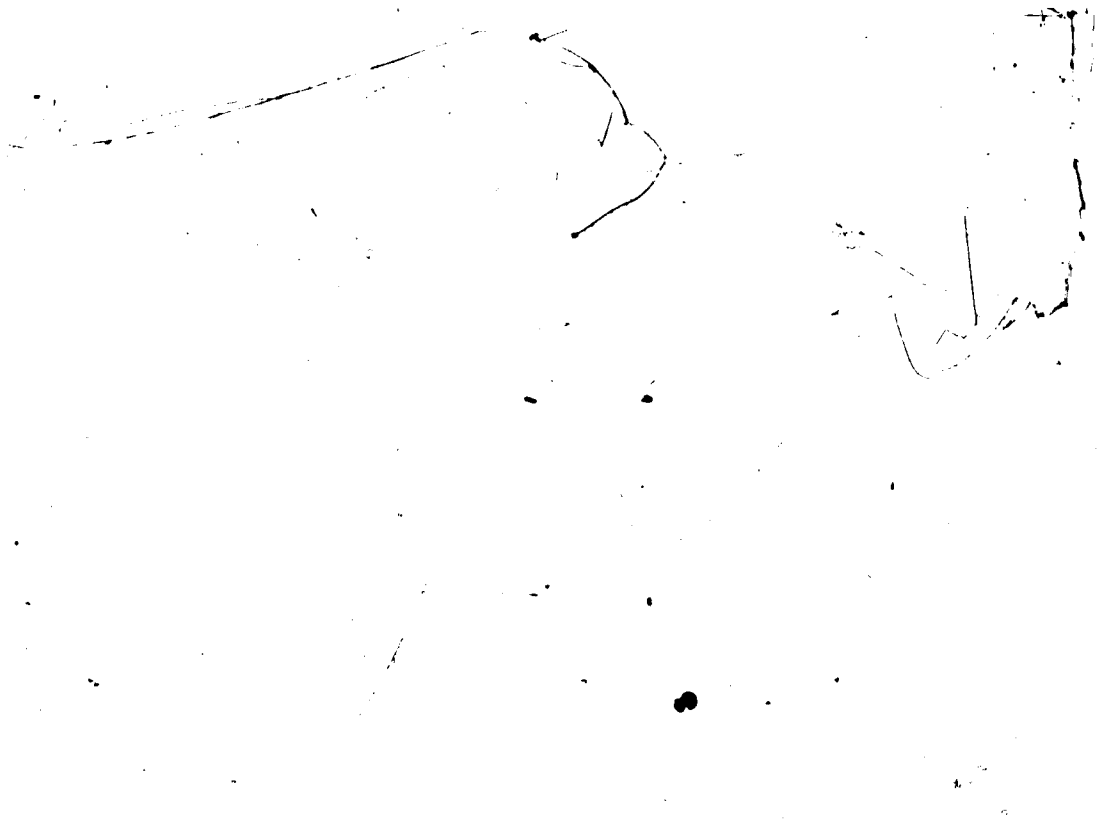

Fig. 154. Diagrammatic longitudinal section of an interfacetal mechanoreceptor of Cicindela tranquebarica, showing cuticular peg (cp); socket (so); articulating membrane (mb); tubular body (tb); dendritic sheath (ds) enclosing a cilium (ci); basal bodies (bb) of cilium; nucleated inner (i) and outer sheath cells (o); axon (a); neurilemma sheath cell (nu); corneal lens (l); subcorneal layer (cl); crystalline cone (c); Semper's cells (s); and secondary pigment cells (2p).

Scale = 20 µm

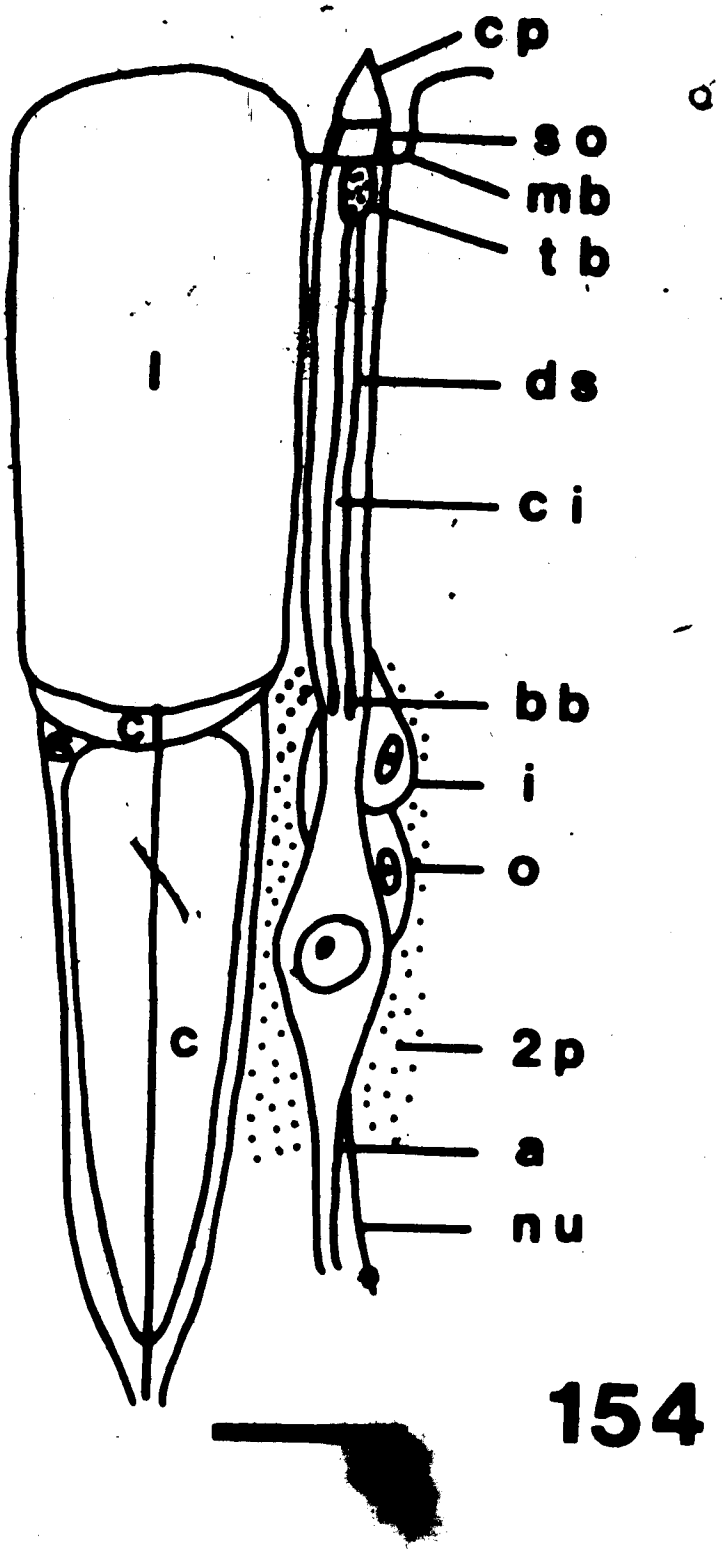

154

was not possible to trace the axon of the neuron to the central nervous system. Fig. 154 shows the principal structural components of the interfacetal mechanoreceptor sensillum.

5.3.5 Retinula and Secondary Pigment Cells

5.3.5.1 Distal Retinula Cells

The crystalline thread (ct) connects the dioptric apparatus to seven long retinula cells. Nuclei (n) of these cells are located distally (Fig. 156). Transverse cryofracture sections through the retinula at this level (Fig. 156) show seven retinula cells with nuclei (n) enclosing a central, distal rhabdom (r). The retinula is surrounded by secondary pigment cells (2p). The seventh retinula cell (7) appears to be vacuolated. A thin section at this level (Fig. 157) shows that the distal rhabdom (r) consists of microvilli from only retinula cell seven. Distances between spot desmosomes (d) of adjacent retinula cells, indicate that retinula cell seven is wider than the other six at this level (Fig. 158). Fig. 159 shows a freeze-etch section through the distal retinula showing pf and ef ("extracellular or exoplasmic face" of the membrane revealed by the fracture process; Branton et al., 1975), of the microvilli of the rhabdom. TEM shows the cytoplasm of retinula cell seven to be rich in mitochondria (m) suggestive of a cell active in oxidative phosphorylation (Fig. 160). This part

Fig. 155. LM of longitudinal section of junction between crystalline thread (ct) and seven retinula cells, showing their distal nuclei (n).

Scale = 10 µm

Fig. 156. SEM cryofracture of transverse section through distal retinula zone, showing seven retinula cells, some with nuclei (n), enclosing a central rhabdom (r). The seventh retinula cell (7) appears vacuolated. Secondary pigment cells (2p) surround the retinula.

Scale = 5 µm

Fig. 157. Same, TEM.

Scale = 5 µm

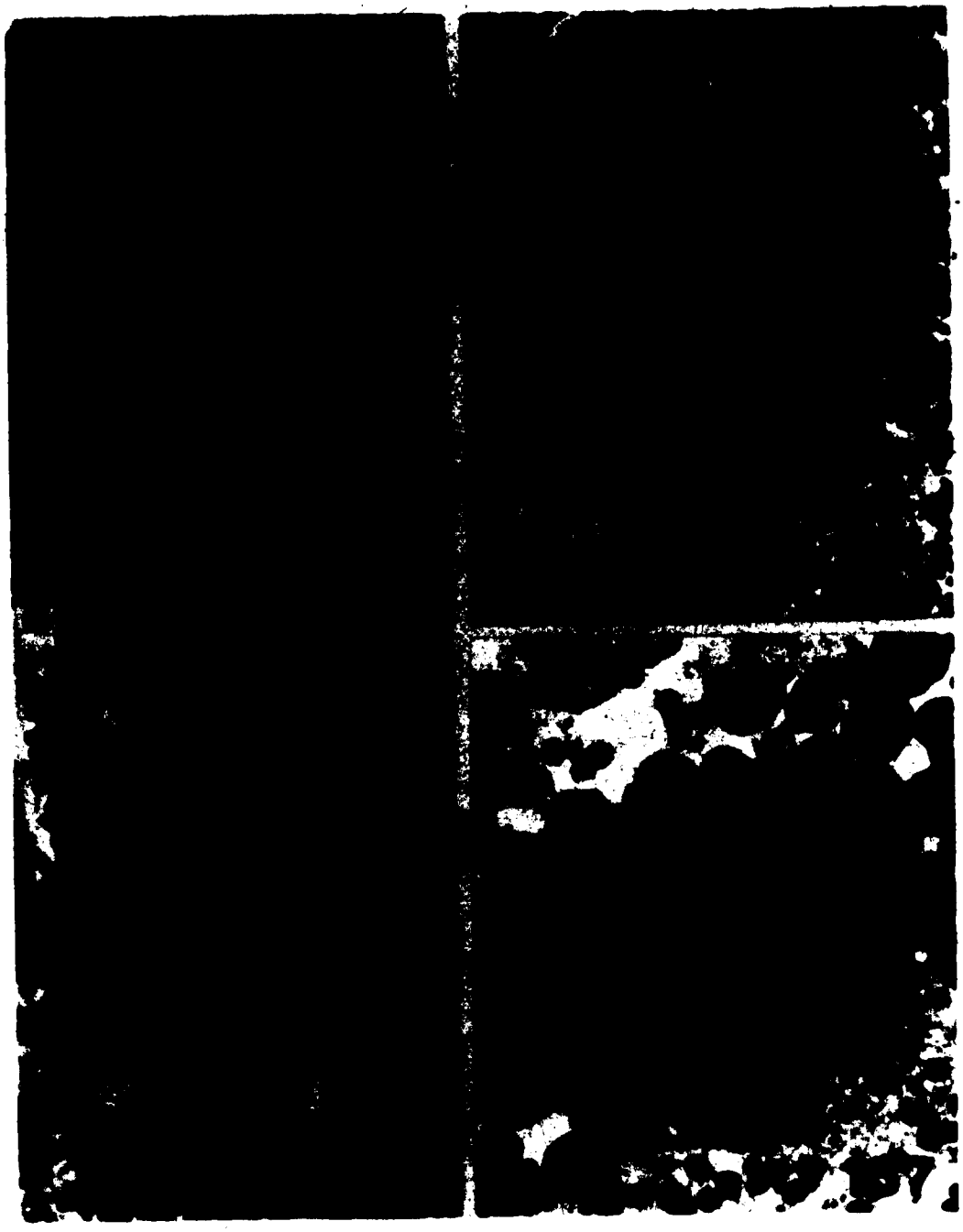

Fig. 158. TEM of transverse section through distal rhabdom (r), showing spot desmosomes (d) between adjacent retinula cells. Note that retinula cell 7 is larger than the others and that it alone forms the rhabdom.

Scale = 1 µm

Fig. 159. Same, freeze-etch, showing pf and ef faces of rhabdom microvilli and nuclei (n) and mitochondria (m) of retinula cells.

Scale = 1 µm

Fig. 160. TEM of transverse section through distal rhabdom (r). Note mitochondria (m) within retinula cell 7.

Scale = 1 µm

Fig. 161. Same, freeze-etch, showing microvilli of rhabdom (r); nucleus (n) of retinula cell; and inter-retinular fibers (f).

Scale = 1 µm

of the distal rhabdom has its microvilli aligned parallel to the longitudinal axis of the retinula (Figs. 158, 160, 161) and these are approximately 900 nm long and 80 nm in diameter. They contain amorphous material in their lumina.

5.3.5.2 Proximal Retinula Cells

Transverse sections through the proximal, fused rhabdom reveal seven retinula cells: six of similar structure, but a dissimilar seventh retinula cell positioned laterally (Fig. 162). Each of the six normal retinula cells are rich in mitochondria (m), rough endoplasmic reticulum, polysomes, and Golgi lacunae (la) are dispersed throughout their cytoplasm. Spot desmosomes are located between adjacent retinula cells. Some pigment granules (p) are located near the periphery of these cells, and the retinula is enveloped by secondary pigment cells (2p) (Fig. 163). At higher magnification, this proximal rhabdom (r) (Fig. 164) is rectangular in transverse section. Microvilli of two retinula cells (i.e., 1, 2) each contribute a rhabdomere to a long side of the rhabdom; but only one (i.e., 6) makes up each short side. Microvilli of the two short sides are arranged perpendicular to the four rhabdomeres of the long sides. Microvilli are approximately 2 µm long and 80 nm in diameter. Retinula cells twist along their length such that individual cells change position along the length of an ommatidium. Retinula cell seven (Fig. 165) does not contribute to the rhabdom at this level. Cytoplasmic inclusions in these cells

Fig. 162. TEM of transverse section through proximal rhabdom zone. Shown are six retinula cells enclosing a central fused rhabdom (r) with the seventh retinula cell positioned laterally.

Scale = 5 µm

Fig. 163. Same, through proximal retinula cells, showing rhabdom (r); mitochondria (m); Golgi lacunae (la); pigment granules (p); and secondary pigment cells (2p).

Scale = 2 µm

Fig. 164. Same, through proximal, rectangular rhabdom (r). Microvilli of two retinula cells contribute a rhabdomere on each long side of the rhabdom and one on each short side. Retinula cells are numbered 1-6.

Scale = 1 µm

Fig. 165. Same, through seventh retinula cell, showing mitochondria (m); possible polysomes (arrows); and vacuoles (v). This cell does not contribute to the rhabdom at this level.

Scale = 200 nm

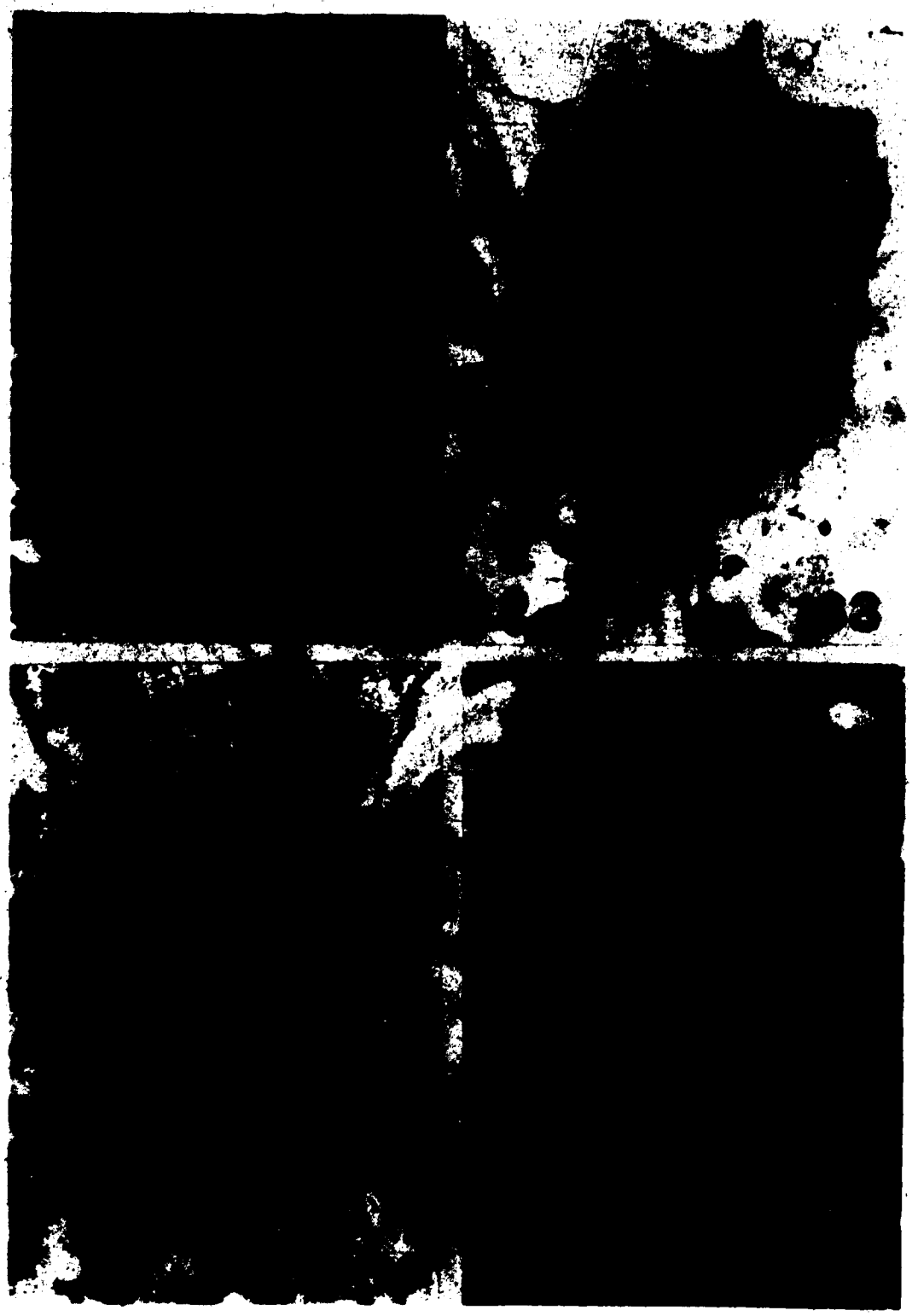

include: mitochondria (m), possible polysomes (arrows), and vacuoles (v). Fig. 166 is a longitudinal section through the proximal rhabdom (r), showing a perpendicular arrangement of adjacent microvilli. Near the rhabdom (r), multivesicular bodies (mvb) about 0.5 µm in diameter and consisting of a single unit membrane enclosing a variable number of small membrane-bound vesicles are present (Fig. 167). There are extracellular spaces (esp) between the bases of microvilli. Also present in the retinula cytoplasm are spherical lamellar or onion bodies (on) approximately 1.2 µm in diameter containing concentric membrane whorls (Fig. 168). These membranes are also found in extracellular spaces between retinula cells associated with modified secondary pigment cells (2p) (Fig. 169).

5.3.5.3 Ciliary Structures

Proximal to the nucleus of each retinula cell are two basal bodies (bb) (= centriole, kinetosome) (Fig. 170). These are aligned perpendicular to each other with the distal basal body (Fig. 171) at right angles to the longitudinal axis of the ommatidium and the proximal basal body parallel to it (Fig. 172). The proximal basal body consists of nine microtubular triplet sets enclosing a central hub. Eighteen electron-dense tubules (arrows) surround the triplet sets. This basal body is approximately 281 nm in diameter. Two fibrillar feet (ft) extend from the proximal basal body and fuse proximally, appearing in transverse section as an open

Fig. 166. TEM of longitudinal section through proximal rhabdom (r), showing perpendicular arrangement of adjacent microvilli.

Scale = 1 µm

Fig. 167. TEM of transverse section through a multivesicular body (mvb) containing small membrane-bound vesicles near the rhabdom (r). Note extracellular spaces (esp) at the bases of microvilli.

Scale = 250 nm

Fig. 168. Same, through a spherical lamellar or onion body (on) within the retinula cytoplasm. These structures contain concentric membrane whorls.

Scale = 1 µm

Fig. 169. Same, through an onion body (on) in an extracellular space between retinula cells. Shown also are modified secondary pigment cells (2p).

Scale = 1 µm

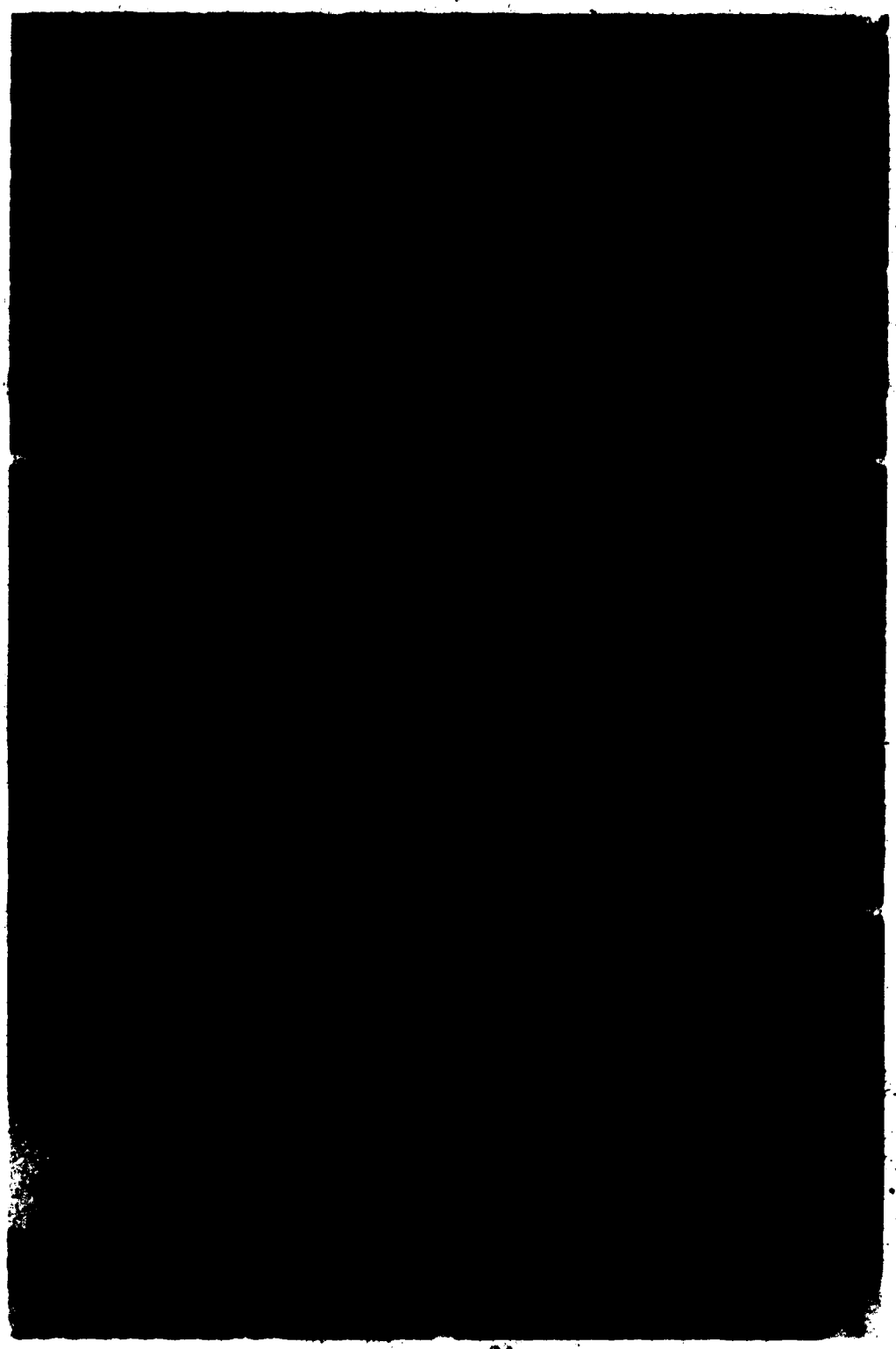

Fig. 170. TEM of transverse section through distal retinula cell basal bodies (bb) aligned perpendicularly. Also shown are seven retinula cells and the distal rhabdom (r).

Scale = 1 μm

Fig. 171. Same, of a distal basal body (bb), showing microtubules aligned perpendicular to the ommatidial vertical axis.

Scale = 250 nm

Fig. 172. Same, of a proximal basal body (bb), aligned parallel to the ommatidial axis. The proximal basal body contains nine microtubular triplet sets (arrows) enclosing a central hub. 18 electron-dense tubules surround the triplet sets (arrows).

Scale = 250 nm

circle with less microtubular definition than the basal bodies (Fig. 173). Shortly after entering the proximal rhabdom region, a striated ciliary rootlet (cr) is formed from the ffbrillar feet. The rootlet is solid in transverse section and is approximately 150 nm in diameter (Fig. 174). It extends the length of the retinula cells peripheral to the rhabdom (Fig. 175). Although not shown here, the rootlet is banded horizontally.

5.3.5.4 Secondary Pigment Cells

Approximately 16 secondary pigment cells (2p) surround the cone and retinula. Nuclei (n) lie at differing levels between the cone region and the middle of the retinula. Pigment granules (g) vary in size but are approximately 600 nm in diameter (Fig. 176). Some cells contain onion bodies (on) which, perhaps through the process of pinocytosis, liberate the onion bodies found in extracellular spaces between adjacent cells (2p) (Fig. 177). Some secondary pigment cells contain vesicles (v) (Fig. 178) while others or portions of the same cells are devoid of pigment, but contain numerous smaller vesicles (v). Microtubules (mt) are located within these cells which could function in transporting these vesicles within the cytoplasm of these cells (Fig. 179).

5.3.6 Basal Retinula Cells and Basal Pigment Cells

The eighth or basal retinula cell (b) is positioned distal to the fenestrated, mucopolysaccharide, basement me

Fig. 173. TEM of transverse section through fused fibrillar feet (ft) within the cytoplasm near the proximal rhabdom (r).

Scale = 250 nm

Fig. 174. Same, through a ciliary rootlet (cr) within the cytoplasm near the proximal rhabdom (r) proximal to level shown in Fig. 173.

Scale - 250 nm

Fig. 175. TEM of longitudinal section through a ciliary rootlet (cr) parallel to the proximal fused rhabdom (r).

Scale = 1 µm

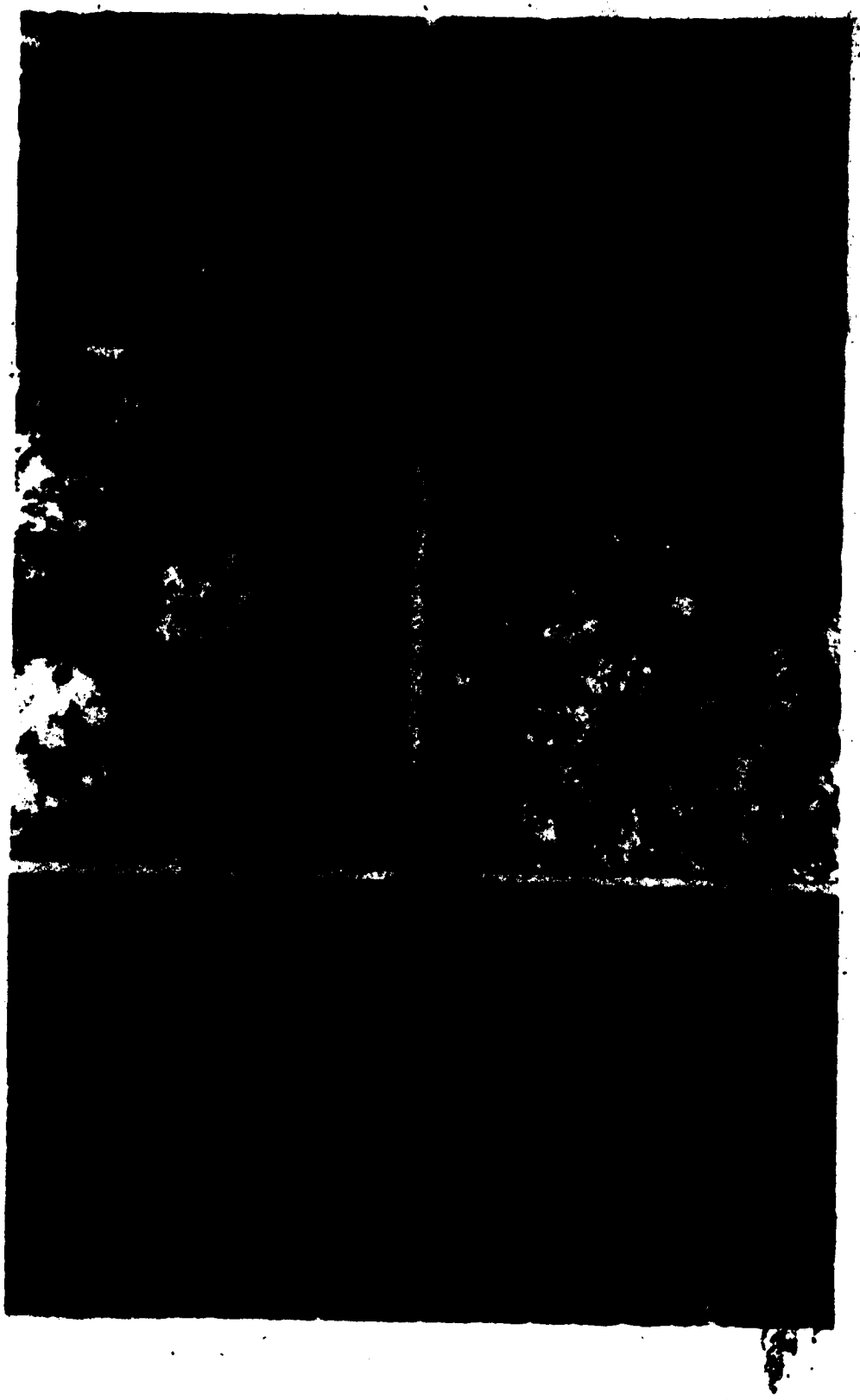

Fig. 176. TEM of transverse section through secondary pigment cells (2p), showing nuclei (n) and pigment granules (p).

Scale = 2 µm

Fig. 177. Same, through onion bodies (on) within secondary pigment cells (2p) in the process of pinocytosis to become located in the extracellular spaces between them.

Scale = 1 µm

Fig. 178. Same, through secondary pigment cells (2p) containing vesicles (v).

Scale = 1 µm

Fig. 179. Same, through secondary pigment cells (2p) devoid of pigment granules but containing microtubules (mt) and vesicles (v) of unknown chemical composition.

Scale = 500 nm

198

brane (bm). This cell contains a spherical rhabdomere (r) surrounded by pigment granules (p) (Fig. 180). In transverse section, the basal retinula cell is seen to be approximately 6 µm in diameter and to contain a distal nucleus (n) and a spherical fused rhabdomere (r) approximately 3 µm in diameter. The basal retinula cell cytoplasm is rich in mitochondria (m) and pigment granules (p). The seven axons (a) of the other retinula cells surround the basal retinula cell. They are sheathed by four basal pigment cells (bp) containing pigment granules (p) (Fig. 181). The rhabdomere consists of microvilli approximately 125 nm in diameter which are oriented parallel to the long axis of the ommatidium. Axons (a) contain pigment granules (p). Tracheoles (tr) are present at this level of the ommatidium (Fig. 182).

5.3.7 The Visual Peripheral Nervous System and the Central Nervous System

Each basal retinula cell (b) axon surrounded by seven retinula axons (a) penetrates the basement membrane (bm) together and emerge as a bundle of eight axons (a) (Fig. 183). In transverse section the fenestrations of the basement membrane (bm) are clearly visible (Figs. 184, 185). Fig. 186 shows a transverse section through the eight retinula axons (a) from one ommatidium. Axons containing neurotubules (nt) are surrounded by glial cells (gl) which are in intimate contact with tracheoles (tr). From cryofracture SEM analysis of these tracheoles (Fig. 187), their epicuti-

Fig. 180. LM of longitudinal section through basal retinula zone, showing basal retinula cell (b); rhabdomere (r); basement membrane (bm); and pigment granules (p).

Scale = 10 µm

Fig. 181. TEM of transverse section through basal retinula cells, showing distal nuclei (n); fused spherical rhabdomere (r); mitochondria (m); pigment granules (p); seven axons (a); and four basal pigment cells (bp) containing pigment granules (p).

Scale = 5 µm

Fig. 182. Same, through a basal retinula cell, showing rhabdomere (r) and retinula cell axons (a) containing mitochondria (m); neurotubules (nt); and pigment granules (p). Note tracheoles (tr).

Scale = 2 µm

Fig. 183. TEM of longitudinal section through basal retinula cells (b) and basement membrane (bm), showing bundles of eight axons (a) emerging from each ommatidium. Note tracheoles (tr).

Scale = 5 µm

Fig. 184. LM of transverse section through basement membrane (bm), showing bundles of eight axons (a) penetrating fenestrations.

Scale = 10 µm

Fig. 185. Same, TEM.

Scale = 5 µm

Fig. 186. Same, through bundle of eight axons (a), containing neurotubules (nt), surrounded by glial cells (gl). Note tracheoles (tr).

Scale = 2 µm

Fig. 187. SEM cryofracture of longitudinal section of a tracheole (tr), showing epicuticular foldings forming taenidia (td) and spherical bodies (sb) on their lumen surface.

Scale = 1 µm

Fig. 188. TEM of longitudinal section proximal to the basement membrane (bm) showing, glial cells (gl) with nuclei (n); mitochondria (m); and pigment granules (p). Note nucleus (n) of a large monopolar neuron (mn) and tracheoles (tr).

Scale = 2 µm

cular lining can be seen to be folded into taenidia (td) approximately 258 nm in diameter, with their luminal surface covered with spherical bodies (sb) approximately 103 nm in diameter. The function of these bodies is unknown. Glial cells contain nuclei (n), mitochondria (m), and pigment granules (p). They are surrounded by large monopolar neurons (mn) (Fig. 188) (Ribi, 1976).

Glial cells (gl), large monopolar neurons and axons (a) of a lamina cartridge are more clearly seen in Fig. 189. Within the lamina ganglionaris (lg), these cartridges (oc) are aligned parallel to the long axis of the ommatidium and twist at the first optic chiasmata (lc) before entering the medulla (Fig. 190).

5.3.8 Adipose Tissue and Lipid Within the Compound Eye

Within the head capsule lateral to the ocular sclerite (os), is a large accumulation of adipose tissue (at) which stains with Sudan III (Fig. 191). Lipid deposits (ld) are also found between the axonal bundles (ab) of the eyes (Fig. 192). As previously mentioned, some secondary pigment cells contain vesicles (Figs. 178, 179). The significance of this adipose tissue, lipid deposits, and vesicles is discussed in relation to storage and transport of the visual pigment chromophore derived from vitamin A_1.

5.3.9 Summary of Structural Components

Fig. 193 shows the principal structural components in

Fig. 189. TEM of transverse section through lamina ganglionaris, showing cartridges of axons (a) surrounded by glial cells (gl), and large monopolar neurons (mn).

Scale = 2 µm

Fig. 190. LM of longitudinal section of axonal bundles (ab) of six ommatidia entering the lamina ganglionaris (lg) in optic cartridges (oc). Optic cartridges twist at the first chiasmata (1c).

Scale = 100 µm

Fig. 191. LM of oblique section through a compound eye stained with Sudan III, showing adipose tissue (ap) lateral to the ocular sclerite (os).

Scale = 100 µm

Fig. 192. LM of longitudinal section through proximal portion of an eye, showing lipid deposits (ld) between axonal bundles (ab) and lamina ganglionaris (lg).

Scale = 20 µm

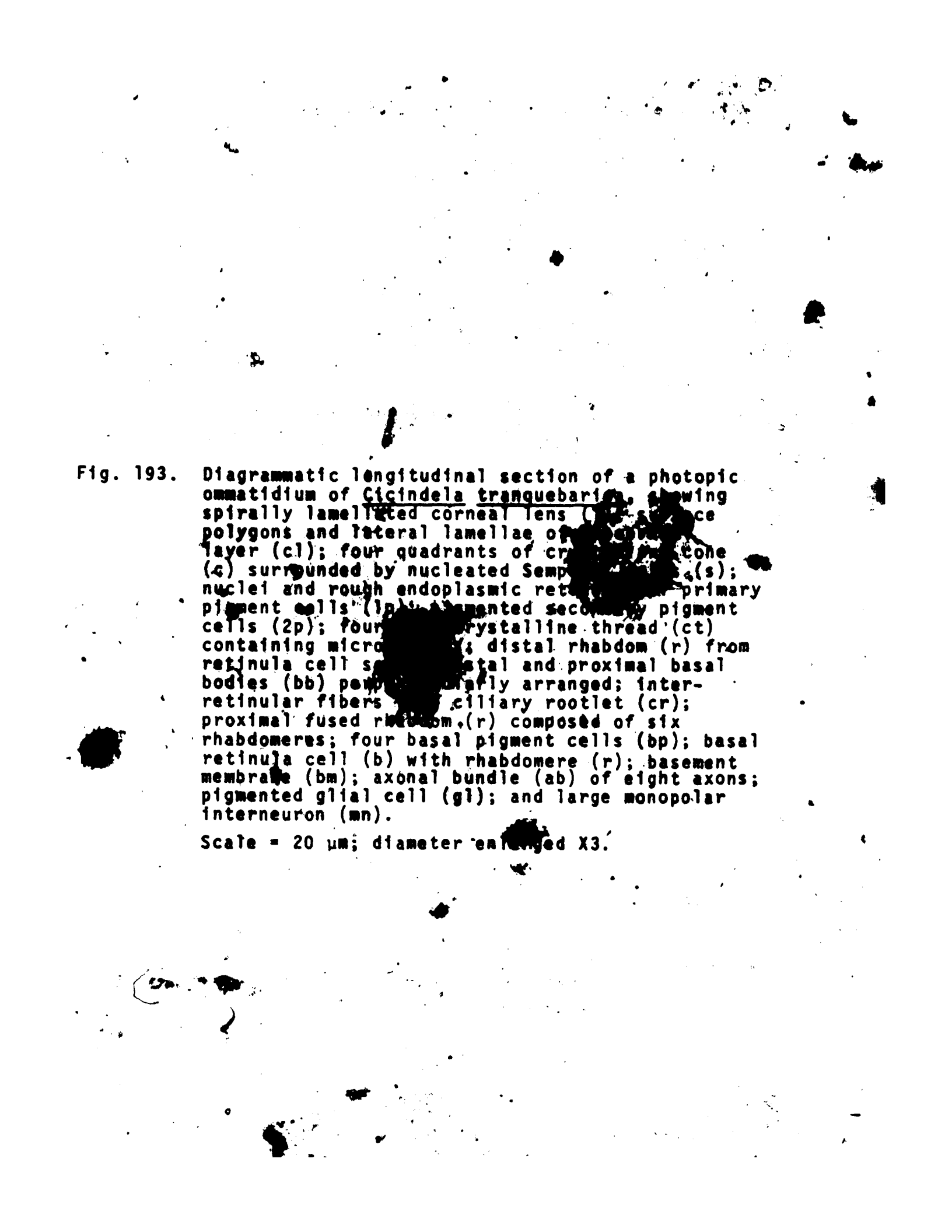

Fig. 193. Diagrammatic longitudinal section of a photopic ommatidium of Cicindela tranquebarica, showing spirally lamellated corneal lens (l), surface polygons and lateral lamellae of [illegible] layer (cl); four quadrants of cr[illegible]tone (c) surrounded by nucleated Semp[illegible](s); nuclei and rough endoplasmic ret[illegible] primary pigment cells (1p); [illegible]mented secondary pigment cells (2p); four [illegible]rystalline thread (ct) containing micro[illegible]; distal rhabdom (r) from retinula cell s[illegible]tal and proximal basal bodies (bb) per[illegible]arly arranged; inter-retinular fibers [illegible] ciliary rootlet (cr); proximal fused rh[illegible]om (r) composed of six rhabdomeres; four basal pigment cells (bp); basal retinula cell (b) with rhabdomere (r); basement membrane (bm); axonal bundle (ab) of eight axons; pigmented glial cell (gl); and large monopolar interneuron (mn).

Scale = 20 µm; diameter enlarged X3.

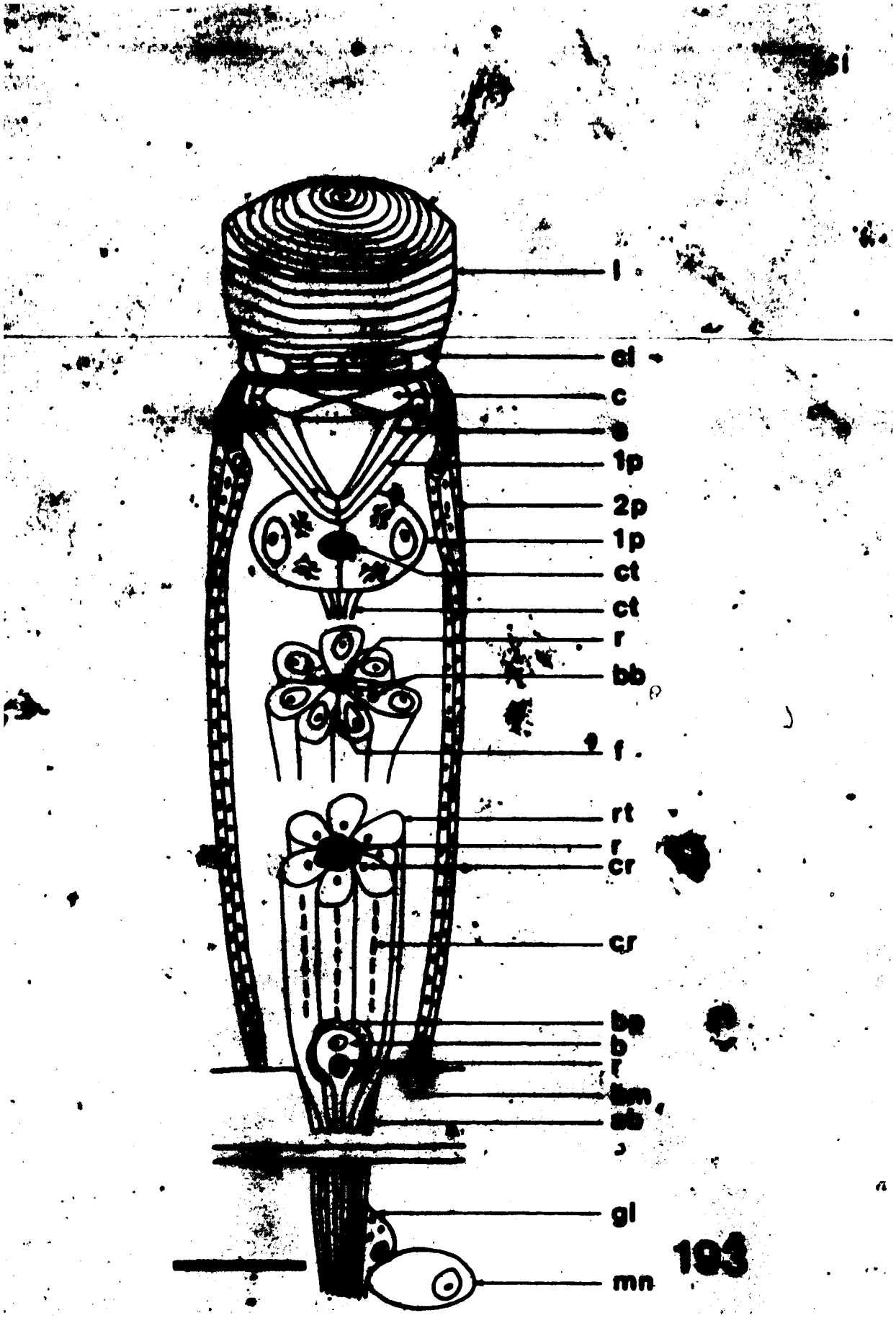
l
ol
c
1p
2p
1p
ct
ct
r
bb
f
rt
r
cr
cr
gl
mn

a photopic ommatidium of a Cicindela tranquebarica male.

5.4 Discussion and Conclusions

5.4.1 Dioptric Apparatus

The corneal lenses of C. tranquebarica adults have a thin corneal layer. This may be epicuticular, and formed from secretions from dermal glands (Home, 1974), which, although not figured here, surround the ocular sclerite (see Section 4.3.4, P. melanarius eyes). Corneal lenses consist of exocuticular lamellae of spirally arranged chitin-protein complexes (Neville, 1975).

Beneath each corneal lens lies the newly described subcorneal layer. I have also observed this layer in other cicindelid and carabid beetle eyes (Sections 4.3.1.2.3, 4.3.2 and 4.3.4). Although she did not describe it in detail, Home (1976) figured a proximal corneal layer, which can be termed the subcorneal layer, in eyes of adult Notiophilus biguttatus F. and Loricera pilicornis F. (Carabidae). This layer may be similar to the processes corneae described using a light microscope in eyes of adult diurnal Lepidoptera (Eltringham, 1919; 1933; Nowikoff, 1931; and Yagi and Koyama, 1963a) (see Section 4.4.1).

Thin sections through this subcorneal layer of C. tranquebarica eyes show parabolic lamellae. Bouligand (1965) presented a model for the structure of chitin and protein (arthropodin) complexes of arthropod lamellated endocuticle.

He postulated that the basic unit of the lamellae is the parabolic microfibril (micelle) consisting of a chitin core coated with protein. The subcorneal layer consists of such microfibrils. There is no evidence of pore canals (Locke, 1961; Neville et al., 1969) traversing this endocuticle. When examined by cryofracture SEM techniques, the surface of this subcorneal layer consists of polygons. I postulate that prior to the cuticular pharate adult, M of the 16 secondary pigment cells are positioned between the developing corneal lens and cystalline cone and they secrete extracellularly the subcorneal layer. These cells then migrate laterally and differentiate into secondary pigment cells. Cuticular deposition is differential; less cuticle being secreted about the periphery of the cells, leaving a surface consisting of polygons.

Several hypotheses can be generated to explain the function of this subcorneal layer. Since its refractive index is greater than that of the lens, but less than that of the crystalline cone, it could function to bend incident light towards the normal and hence towards the crystalline cone. This would maintain incident light intensity rather than permitting light rays to be absorbed by secondary pigment granules. Furthermore, since this layer is of intermediate refractive index, it would reduce reflection towards the lens. Because each polygon appears to have a concave distal surface, each may function as a small concave lens which would extend the focal length of incident light to a

point more proximal within the crystalline cone. Without precise measurement of refractive index such as those made for tracing rays of incident light through the lens and cone by Horridge (1975b) and Meyer-Rochow (1975), it is not known if this layer acts as a thin film for constructive or destructive interference of light entering the cone. Such investigations would be difficult to undertake since the surface of each endocuticular polygon is of variable thickness.

The material of the four cone quadrants is granular. Fyg (1961) located glycogen in cones of adult Apis mellifica L. (Apidae) as did Bara (1971) in those of adult Collembola. Developmental work by Kim (1964) showed that the granular nature of cones of eyes of Pieris rapae L. adults (Noctuidae) results from a polymerization of polysaccharides with proteins. From examination of thin sections and freeze-etch preparations, the chemical composition, cones of C. tranquebarica also appear to have depositions similar to the glycogen observed by these workers. Since the electron density of the glycogen is less dense in the central region of each cone quadrant, this could cause light rays to be concentrated centrally towards the underlying crystalline thread. There is no evidence of variation in electron density of the glycogen between adjacent cone quadrants. This is unlike cones of A. mellifera adult eyes which Skrzipek and Skrzipek (1971b) postulated to function in differential absorption of incident polarized light.

5.4.2 Interfacetal Mechanorecptors

Interfacetal mechanoreceptors are present between some lenses of *C. tranquebarica* eyes. Such hairs were first reported in eyes of *Apis mellifera* workers (Apidae) (Phillips, 1905), but Friza (1928) was first to observe a nerve fibril (neuron) from hairs of eyes of *Anacridium aegyptium* adults (Acrididae). Many adult lepidopteran eyes also have interfacetal hairs (Eltringham, 1933; Yagi and Koyama, 1963a; Koyama, 1971; and Koyama and Ogawa, 1972). Scott (1937) observed the presence of these hairs in adult nymphalids and worker apids (Hymenoptera), Perrelet (1970) described the external structure of drone *A. mellifera* interfacetal hairs, and Meyer-Rochow (197[illegible] of *Creophilus erythrocephalus* F. adults (Staphyl[illegible]). Nesse (1965) figured these sensilla for eyes of *A. mellifera*. He concluded that they were innervated by one neuron which enters a retinula cell at the level of a retinula cell body. Work with adult individuals of *Cataglyphis bicolor* F. (Formicidae), Brunnert and Wehner (1973) figured a thin section of an interfacetal dendrite wrapped in a single sheath cell. Fine structure of interfacetal hairs of *Musca domestica* Meig. adults (Muscidae) was examined by Chi and Carlson (1976). This sensillum is also innervated by a single bipolar neuron. The cilium, however, consists only of nine peripheral microtubular doublets. Basal bodies are not described, but there are nine ciliary rootlet microtubules and therefore presumably nine triplets comprising

the basal bodies (Pitelka, 1974). Axons of interfacetal hairs of Gryllus campestris L. adults (Gryllidae) extend forward into the trito- and deutocerebra, and into the subesophageal- and prothoracic ganglia via a branch of the nervus tegumentarius (Honegger, 1977).

From examination of interfacetal hair structure of nymphalids and apids, Scott (1937) concluded that these sensilla are chordotonal, i.e., function as modified auditory sense organs. Nesse (1965) studied flight behaviour following interfacetal hair removal in A. mellifera adults. His experiments provided evidence suggesting that they function in control of sidewind deviation arising during flight and in 1966 he postulated that they are involved in regulating flight velocity in honey bees. Absence of flight in adults of Gryllus campestris L. (Gryllidae) suggested to Honegger (1977) that these sensilla have a role in controlling eye cleaning behaviour.

Without behavioural and electrophysiological experiments, one must speculate on the function of interfacetal pegs of eyes of C. tranquebarica adults. However, from Sections 4.3.1.2.2, 4.3.2 and 4.3.4 it can be concluded that of the cicindelids and carabids studied, pegs are characteristic of diurnal beetles capable of flight. The only exception are C. belfragei Sallé adults, which are secondarily flightless, but have interfacetal pegs. Perhaps in cooperation with other mind sensitive sensilla on the body (Weis-Fogh, 1949; 1956), sensory input to brain centres

elicit effector responses leading to compensatory movements and hence to flight stability.

5.4.3 Retinula Cells and Rhabdoms

Based on criteria presented in Section 4.3.10, it is concluded here that eyes of C. tranquebarica adults are photopic and probably function similarly to photopic eyes of other diurnal insects (Varela and Wiitanen, 1970; Section 4.1). The rectangular, fused proximal portion of the rhabdom is similar to that of zygopterans (Ninomiya et al., 1969); blattids (Butler, 1973b); locustids (Horridge and Barnard, 1965); gryllids (Wachmann, 1970); other [illegible]rabids and cicindelids (Home, 1976; Sections 4.3.1.4, 4.3.2, and 4.3.4); and apids (selected references: Goldsmith, 1962; Varela and Porter, 1969; Perrelet, 1970; Skrzipek and Skrzipek, 1971a).

Some of the conclusions made by Snyder et al. (1973) from a review of the structure and function of the fused rhabdom of honey bees may be applicable to the rhabdom of C. tranquebarica. They showed that rhabdomeres joined tightly together have enhanced "optical coupling". Each rhabdomere functions as an absorption filter; the blue and ultraviolet rhabdomeres filter out these two wavelengths from green rhabdomeres, thus enhancing spectral sensitivity of the green retinula cell. There is no loss in absolute sensitivity since each filter acts as a photoelectric transducer. Therefore, due to this optical coupling, "each reti-

nula cell has a high absolute sensitivity while preserving its spectral [illegible]. Since all spectral cell types are together in one rhabdom, the insect has good hue discrimination in a small field of view.

It would be particularly interesting to determine the spectral [illegible] curve for retinula cells of T. ornamentarica using intracellular electrophysiological recordings. Following such experiments, one could stimulate single retinula cells sensitive to a particular wavelength. Gribakin (1972; 1975) showed that following differential stimulation, osmium tetroxide fixation caused the photoproduct to stain more intensely in stimulated cells, such that he could distinguish two types of retinula cells in A. mellifera, each specific to a wavelength maximum of either 340 nm (ultraviolet) or 530 nm (green).

Horridge and Barnard (1965) showed that in dark-adapted eyes of Locusta migratoria L. (Locustidae), cisternae of the endoplasmic reticulum collect near the rhabdom forming a "pallisade" of lower refractive index. Light transmitted through this region is reflected internally to increase rhabdom sensitivity. Under light adapted conditions, the pallisade disperses to form lacunae (vacuoles) of endoplasmic reticulum within the cytoplasm, and mitochondria migrate to surround the rhabdom. Other insect eyes show similar changes: blattids (Snyder and [illegible], 1972); grillids (Wachmann, 1970); staphylinids (Mayer-Rochow, 1972); calliphorids (freeze-etch study, Seitz, 1970); and

formicids (Menzel, 1972; Brunnert and Wehner, 1973); review: Walcott (1975). Kolb and Autrum (1972) showed similar changes in eyes of A. mellifera, but also observed pigment migration medially towards the rhabdom during light adaptation. Since mitochondria closely surround the rhabdom and because endoplasmic reticulum lacunae are dispersed within the cytoplasm, the rhabdom of eyes of C. tranquebarica adults examined here can be considered as being similarly light-adapted. The position of mitochondria in this light-adapted state is essential as an ATP energy source for isomerization of visual pigment during phototransduction.

Desmosomes between retinula cell membranes are adhesive and possibly assist in maintaining microvillar interdidgitation (Eley and Shelton, 1976). Extracellular spaces between bases of microvilli may be channels through which the flow of current responsible for depolarization of the retinula cell passes through the membranes of the microvilli (Perrelet and Bauman, 1969).

5.4.4 Multivesicular Bodies, Onion Bodies, and Their Roles in Visual Protein Metabolism

The retinula cytoplasm of C. tranquebarica contains multivesicular bodies (mvb's) and onion bodies. Both structures are characteristic of invertebrate photoreceptor cells (Fernández-Morán, 1958; Trujillo-Cenóz, 1966; Eguchi and Waterman, 1967; White, 1968; and Eakin, 1972). Onion bodies are also found in some secondary pigment cells.

Exposure to light induces the formation of mvb's in the spider crab Libinia sp. (Eguchi and Waterman, 1967); in the cricket, Pteronemobius heydeni Fischer (Gryllidae) (Wachmann, 1969); in the toad bug Gelastocoris oculatus (Gelastocoridae) (Burton and Stockhammer, 1969); in larval mosquito stemmata (Culicidae) (White, 1968); and in the wood louse, Oniscus asellus L. (Isopoda) (Puurala and Lehtinen, 1971).

Multivesicular bodies are probably the main organelles involved in protein hydrolysis (Locke and Collins, 1967). Working with eyes of the lobster, Homarus vulgaris (Rutherford and Horridge, 1965), and the spider crab, Libinia emarginata (Eguchi and Waterman, 1967) these authors studied the pathway by which metabolic products of phototransduction are transported away from rhabdom microvilli. They conclude that cisternae of microvilli produce vesicular spheroids which are enveloped by Golgi membranes, which in turn give rise to mvb's. Multivesicular bodies are converted into onion bodies by the incorporation of lytic enzymes from Golgi cisternae. Ferritin, a water soluble protein, can be traced through this pathway in larval mosquito stemmata (White, 1968). Following phototransduction in eyes of C. tranquebarica, opsin proteins probably are hydrolyzed via the mvb-onion body sequence similar to that proposed by these authors. Furthermore, here, onion bodies seem to be incorporated into some secondary pigment cells and are then released via pinocytosis into the extracellular space be-

tween them. This suggests that proteins incorporated into mvb's may not be recycled to the rhabdom microvilli.

I postulate that opsin components of visual pigments (presuming a dichromatic visual system) are synthesized in the primary pigment cells of C. tranquebarica eyes since there is a larger accumulation of rough endoplasmic reticulum there. Using tritiated leucine in drone eyes, Perrelet (1972) concluded that labelled proteins are first associated with polysomes, and rough endoplasmic reticulum. Later they appear at the microvilli. Although he concluded that these proteins contribute to the renewal of photoreceptor membranes, I suggest this may represent the pathway for opsins synthesis in these eyes.

Linking of opsins to the chromophore may occur in Golgi cisternae prior to transport of visual pigments to the microvilli. Clearly autoradiographic experiments are required to prove this postulate. Proposed storage and transport mechanisms for the chromophore are discussed in Section 5.4.8.

5.4.5 Ciliary Structures

Photoreceptive cells have increased surface area from proliferation and folding of plasma membranes. For the animal kindgom, Eakin (1966; 1972) proposed a dichotomy in the evolutionary origin of photoreceptive cell membranes:

1. Ciliary type (coelenterate-echinoderm-chordate line) in which the photoreceptive membranes are usually deve-

loped from tubular or lamellar outgrowths of a cilium.

2. Rhabdomeric type (annelid-arthropod-molluscan line) having increased surface area arising through microvillus extensions of the plasma membrane, and which may or may not show traces of a ciliary process. When present, the cilium is not involved in rhabdom formation.

When Eakin published (1966; 1972) insect eyes were not known to have ciliary structures. However, proximal to the nucleus in each retinula cell of eyes of C. tranquebarica adults, two basal bodies are aligned perpendicular to each other with the distal basal body at right angles to the longitudinal axis of the ommatidium. The proximal basal body has two basal fibrillar feet which unite to form a horizontally banded ciliary rootlet extending the retinula length. Similar ciliary structures are found in eyes of Megachile rotunda F. adults (Megachilidae) (Wachmann et al., 1973); four species of coccinelids, Hyphydrus ovatus L. (Dytiscidae), and Phyllobius pamaceus Gyllenhal (Curculionidae) (Home, 1972); some carabid beetles, and the cicindelid, C. campestris L. (Home, 1976). Developmental studies by Wachmann and Hennig (1974) using M. rotunda and by Home (1975) using Coccinella septempunctata L. (Coccinelidae) did not provide evidence for ciliary involvement in rhabdom formation. Therefore, insect eyes cannot be classified as ciliary (sensu Eakin, 1966; 1972). Further developmental studies should be undertaken since Munoz-Cuevas (1975) demonstrated ciliary involvement in the development of micro-

villi in the eye of Ischyropsalis luteipes (Arachnida: Opiliones). Such a conclusion caused Vanfleteren and Coomans (1976) to emphasize the risk of assuming that close phyletic relationships infer a similarity in photoreceptor design.

In invertebrate and vertebrate ciliary photoreceptors, membranous surfaces containing visual pigments are restricted to the distal or outer segment and are consequently associated with the microtubular cilium which extends distally from the distal basal body (Eakin, 1972). In these bipolar cell types, cilia may have a role in transmission of a generator potential and since ATP-ase activity has been reported in the ciliary rootlet of human retinal rods (Matsusaka, 1967), the rootlet may have a conductive function. However, insect retinula cells are monopolar and cannot function similarly since there is no distal cilium and the ciliary rootlet is associated with the photoreceptive membrane, not proximal to it and proximal, not distal to the nucleus.

Home (1975) concluded that ciliary structures in eyes of C. septempunctata (Coccinelidae) are not involved in cellular reorganization during light-dark adaptation.

Since the basal bodies are not associated with a distal cilium, they possibly are remnants of the basal bodies responsible for differentiative mitoses. Ciliary rootlets may provide cytoskeletal support to maintain rhabdomeric interdidgitations.

5.4.6 Basal Retinula Cells and Basal Pigment Cells

The basal eighth retinula cells of eyes of C. tranquebarica adults are similar to the ninth retinula cells of A. mellifera (Skrzipek and Skrzipek, 1974). In both insects, the rhabdomere has microvilli oriented parallel to the ommatidial longitudinal axis.

Possibly the four basal pigment cells are basal swellings of Semper's cells which have also been reported distal to the basement membrane in adult eyes of Drosophila sp. (Drosophilidae) (Waddington and Perry, 1963); Creophilus erythrocephalus F. (Staphylinidae); and Megachile rotunda F. (Megachilidae) (Wachmann et al., 1973).

5.4.7 Polarized Light Detection by Fused Rhabdoms

Microvilli of eyes of C. tranquebarica adults form a proximal, rectangular, fused rhabdom with adjacent sides having microvilli perpendicularly arranged. Two retinula cells contribute microvilli to each long side; one to each short side. The rhabdom of the honey bee is similar in organization although it consists of eight retinula cells, two on each side (Skrzipek and Skrzipek, 1971a). Both eyes have a basal rhabdomere-bearing retinula cell. Because of similarity in microvillar orientation, and photopic organization, polarized light detection in diurnal cicindelids may be similar to that in honey bees.

It is well documented that many insect eyes detect polarized light due to the parallel configuration of their

microvilli (Goldsmith and Bernard, 1974). In eyes capable of polarized light detection, the chromophores of rhodopsin molecules lie parallel to the tangent planes of the microvilli. This particular [illegible] leads to polarized light detection when the E[illegible]es vibrating in one plane and moving in one direction = plane polarized light) is parallel to the microvilli (Moody and Parriss, 1961). However, such a geometry is not maintained along the retinula length in eyes of C. tranquebarica since retinulae twist along their lengths. Such twisting also occurs in eyes of adults zygopterans (Ninomiya et al., 1969); apids (Snyder, 1973; Wehner et al., 1975); and formicids (Menzel, 1975; Wehner, 1976). From electrophysiological recordings, Menzel and Snyder (1974) concluded that because of this twisting, only the basal ninth retinula cell of the honey bee functions as a polarized light detector.

The proximal rhabdom of scotopic A eyes of the adephagan Dytiscus marginalis L. (Dytiscidae) lacks sensitivity to plane polarized light (Horridge et al., 1970). However, these researchers did not record from either the seventh or eighth retinula cells and were not aware at that time of the possibility of retinula cell twisting. Although no electrophysiological experiments were performed, Wachmann and Schröer (1975) predicted polarized light detection by the basal eighth retinula cells of the dorsal and ventral eyes of the adephagan Gyrinus substriatus Steph. (Gyrinidae).

In view of these conclusions, if polarized light is

detected by tiger beetle eyes, perhaps the basal eighth or distal seventh retinula cells are involved.

5.4.8 Synthesis, Storage, Transport, and Metabolism of Visual Pigments

Retinal is reported to be the chromophore of insect visual pigments (Goldsmith, 1958; Briggs, 1961; review; Goldsmith, 1972). 11-cis retinal is combined with a visual protein, an opsin (Karplus, 1973). Photochemical reactions associated with transduction of a light stimulus via a chemical intermediate to an electrical response occur at receptor sites on rhabdomeric microvilli (Langer and Thorell, 1966; Höglund et al., 1973). A summary of the photochemical events (modified after Wald, 1968) involved in visual excitation follows:

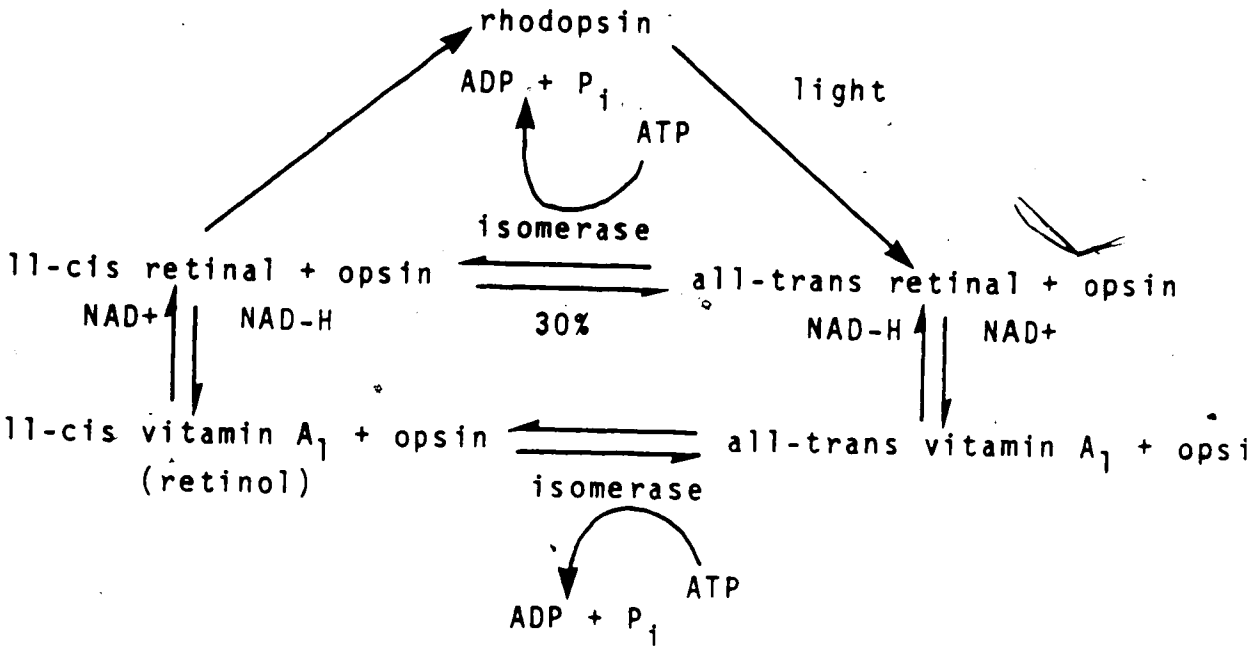

It is believed (Gilmour, 1961) that insects do not synthesize the fat-soluble vitamin A_1, but accumulate β-carotene primarily through dietary intake. This carotenoid is then oxidized to vitamin A_1. Inadequate amounts of vitamin A_1 in the diet induces pathological conditions in insect eyes (Aedes aegypti L. (Culicidae) (Brammer and White, 1969)); Manduca sexta Johannson (Sphingidae) (Carlson et al., 1967; 1969). Changes also occur in the threshold and spectral absorption of the rhabdom when the animal is deprived of vitamin A_1 (review: Goldsmith, 1972).

Little is known of storage, transport, or metabolism of fat-soluble vitamin A_1 in insect tissues (Rees, 1977). Perhaps the fat body serves as a storage organ and from histochemical examination of eyes of C. tranquebarica adults, it is postulated that the large adipose accumulation surrounding the eye and retinula cell axons may also store this vitamin. Also some secondary pigment cells in these eyes contain microtubules which may possibly be used for transport of vesicles within their cytoplasm. Perhaps these vesicles contain the chromophore (either the alcohol or aldehyde) which is released into the retinula cells via pinocytosis. Skrzpiek and Skrzipek (1971b) reported long cytoplasmic extensions of some secondary pigment cells between retinula cells of honey bee eyes. Vesicles were also observed in the tips of these extensions.

Following release of the chromophore, it could combine with opsin proteins via the smooth endoplasmic reticulum and

be transported to the microvilli via the Golgi cisternae. The possible synthesis site and hydrolysis of opsins have been discussed (Section 5.4.4). A proposed diagrammatic summary of synthesis, storage, transport, and metabolic pathways of visual pigments are represented in Fig. 194.

Questions involving visual pigment metabolism may be answered by tracing movements of labelled vitamin A_1 and amino acids using autoradiographic techniques and/or microprobe analysis. One such study has been done tracing tritiated vitamin A_1 acetate in the pulmonate snail Helix aspera (Eakin and Brandenburger, 1968; Brandenburger and Eakin, 1970). Vitamin A_1 (alcohol or aldehyde?) is incorporated by the smooth endoplasmic reticulum and conjugated with a protein. This visual pigment is sequestered into photic vesicles (80 nm in diameter and peculiar to snail eyes) which move distally where their contents are liberated close to the microvilli. Extrapolation from these experiments is difficult since the structural components of these eyes are quite different. More research is required on chromophore and opsin synthesis, storage, and transport before we can begin to understand the metabolism of insect visual pigments.

5.4.9 Summary

From examination of the fine structural cellular organization of C. tranquebarica compound eyes, it has been shown that more detailed conclusions can be made regarding

Fig. 194. Proposed diagrammatic summary of synthesis, storage, transport, and metabolic pathways of visual pigments within the compound eye.

a: Vitamin A_1 stored in adipose tissue surrounding ocular sclerite and between retinula cell axons.

b: Incorporation of vitamin A_1 into lipid vesicles in secondary pigment cells.

c: Vitamin A_1 alcohol (retinol) reduced to retinal in cytoplasm.

d: Transport of retinal vesicles into retinula cells via pinocytosis.

e: Incorporation of retinal into smooth endoplasmic reticulum, into Golgi cisternae, and transport to rhabdom microvilli.

f: Conjugation of retinal and opsins.

g: Phototransduction: Isomerization of 11-cis retinal to all-trans retinal plus opsin.

h: Isomerization of all-trans retinal to 11-cis retinal. Degradation pathway of retinal unknown.

Fig. 194. Continued.

a': Synthesis of opsins on rough endoplasmic reticulum in primary pigment cells.

b': Transport of opsins into retinula cells via pinocytosis.

c': Synthesis of opsins on rough endoplasmic reticulum in retinula cells.

d': Incorporation of opsins into smooth endoplasmic reticulum, into Golgi cisternae, and transport to rhabdom microvilli.

f: Conjugation of retinal and opsins.

g: Phototransduction: Isomerization of 11-cis retinal to all-trans retinal plus opsin.

h: Opsins recycled.

i: Transport of opsins into multivesicular bodies.

j: Opsin peptides hydrolyzed to amino acids in onion bodies.

k: Transport of onion bodies into secondary pigment cells via pinocytosis.

l: Pinocytosis of onion bodies into extracellular spaces.

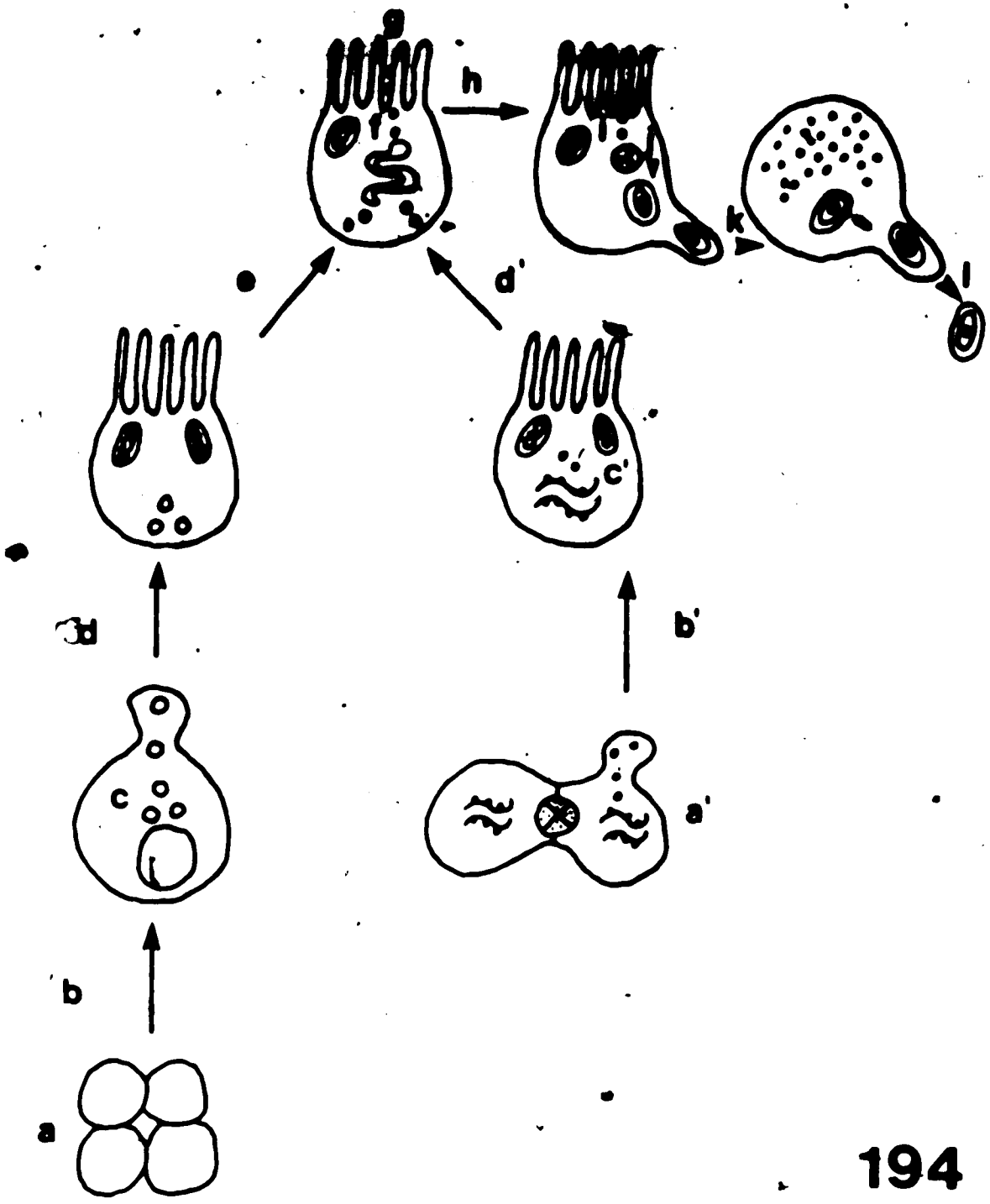
h
k
l
d'
c'
3d
b'
c
a'
b
a

the function of this derived photopic eye than were provided from light microscope studies (Chapter 4). Suggestions for further research have been presented which will provide more information to enhance our understanding of insect vision.

6. Concluding Statements

An investigation such as this one begins to fill the void in our understanding of evolution of insect compound eyes through studies of intergeneric, interspecific, and family sister group comparisons. These results show that the choice of studying cicindelid and carabid beetles has been a good one for examining compound eyes from an evolutionary approach. It is concluded that compound eye structure and function of these beetles have evolved parallel to their behavioural transformation series from nocturnal, crepuscular, to diurnal diel activity. Furthermore, the relative simplicity of increase in eye size and alteration of cellular organization from scotopy to photopy has permitted these beetles to increase their adaptive zones. If the origin of a species begins from the differences of the sense organs which perceives the mate (Yagi, 1953), it should be stressed that the plasticity of cicindelid and carabid beetle compound eyes is an integral component of their diversity.

From examination of the fine structure of photopic compound eyes of the derived genus Cicindela, it becomes apparent that structure and function are interdependent for the process of vision. It is from an appreciation of the complexity of the compound eye that even Darwin (1859) chose

the evolution of this sense organ as an example to substantiate his notion of natural selection within the animal kingdom.

7. References

Agee, H.R. 1971. Histology of the compound eye of Heliothis zea. Ann. Ent. Soc. Am. 64:85-88.

Agee, H.R. 1972. Histology of the compound eye of Heliothis virescens (Lepidoptera: Noctuidae). Ann. Ent. Soc. Am. 65:767-768.

Agee, H.R. and H.W. Elder. 1970. Histology of the compound eye of the boll weevil. Ann. Ent. Soc. Am. 63: 1654-1656.

Arnett, R.H. 1946. The family Cicindelidae. Syst. Nat. 2:i + 7 pp.

Arnett, R.H. 1968. The Beetles of the United States (a Manual for Identification). The American Entomological Institute, Ann Arbor, Michigan. xii + 1112 pp.

Ast, F. 1919. Über den feineren Bau der Facettenaugen bei Neuropteren. Zool. Jah. Ab. 41:411-458.

Autrum, H. and I. Wiedemann. 1962. Versuche über den Strahlengang im Insektenauge (Appositionsauge). Z. Naturforsch. 17b:480-482.

Balduf, W.V. 1925. The feeding of a common tiger beetle (Coleoptera: Cicindelidae). Ent. News 36:275-276.

Baldus, K. 1926. Experimentelle Untersuchungen über die Entfernungslokalization der Libellen (Aeschna cyanea). Z. Vergl. Physiol. 3:475-505.

Barra, J.A. 1971. Les photorécepteurs des Collemboles, étude ultrastructurale. I. L'appareil dioptrique. Z. Zellforsch. 117:322-353.

Barrós-Pita, J.C. and H. Maldonado. 1970. A fovea in the preying mantis eye. II. Some morphological considerations. Z. Vergl. Physiol. 67:79-92.

Bauer, T. 1974. Ethologische, autökologische und ökophysiologische Untersuchungen an Elaphrus cupreus Dft. und Elaphrus riparius L. (Coleoptera, Carabidae). Oecologica 14:139-196.

Bauer, T., U. Brauner, and E. Fischerleitner. 1977. The relevance of the brightness to visual acuity, predation, and activity of visually hunting ground-beetles (Coleoptera, Carabidae). Oecologica 30: 63-73.

Bauers, C. 1953. Der Fixierbereich des Insektenauges. Z. Vergl. Physiol. 34:589-605.

Baumgärtner, H. 1928. Der Formensinn und die Sehscarfe der Bienen. Z. Vergl. Physiol. 7:56-143.

Bernard, F. 1932. Comparison de l'oeil normal et de l'oeil régressé chez quelques carabiques. Bull. Biol. Fr. Belg. 66:111-148.

Bernhard, C.G. ed. 1965. The Functional Organization of the Compound Eye. Pergamon Press, London. xiii + 591 pp.

Bernhard, C.G., G. Gemme, and G. Seitz. 1972. Optical properties of the compound eye. In: M.G.F. Fuortes ed. Handbook of Sensory Physiology. Springer-Verlag, New York. 7(2):5-62.

Bernhard, C.G., W.H. Miller, and A.R. Møller. 1965. The insect corneal nipple array. Acta. Physiol. Scand. 63. Suppl. 243:79 pp.

Beveridge, W.I.B. 1950. The Art of Scientific Investigation. Vintage Books, New York. xiv + 239 pp.

Bloss, F.D. 1961. An Introduction to the Methods of Optical Crystallography. Holt, Rinehart, and Winston, New York. vii + 294 pp.

Bott, H.R. 1928. Beiträge zur Kenntnis von Gyrinis natator subtriatus Steph. II. Der Sehapparat. Zeit. Morph. Ökol Tiere. 10:252-305.

Bouligand, Y. 1965. Sur une architecture torsadée repondue dans de nombreuses cuticles d'arthropodes. C.R. Acad. Sci. Paris 261:3665-3668.

Bradley, J.C. 1930. A Manual of the Genera of Beetles of America North of Mexico. Daw Illston and Company, Ithaca, New York. x + 360 pp.

Braitenberg, V. 1967. Patterns of projection in the visual system of the fly. I. Retina-lamina projections. Exp. Brain Res. 3:271-298.

Brammer, J.D. and R.H. White. 1969. Vitamin A deficiency: Effect on mosquito eye ultrastructure. Science 163: 821-823.

Brandenburger, J.L. and R.M. Eakin. 1970. Pathway of incorporation of vitamin A $^{3}H_2$ into photoreceptors of a snail, Helix aspersa. Vision Res. 10:639-653.

Branton, D., S. Bullivant, N.B. Gilula, M.J. Karnovsky, H. Moor, K. Mühlethaler, D.H. Northcote, L. Packer, B. Satir, P. Satir, V. Speth, L.A. Staehlin, R.L. Steere, and R.S. Weinstein. 1975. Freeze-etching nomenclature. Science 190:54-56.

Briggs, M.H. 1961. Retinene-1 in insect tissues. Nature 192:874-875.

Bromley, S.W. 1914. Asilids and their prey. Psyche 21: 192-198.

Brous, H.A. 1877. Habits of Amblycheila cylindriformis. Trans. Kansas Acad. Sci. 5:11-12 + 1 fig.

Brunnert, A. and R. Wehner. 1973. Fine structure of light- and dark-adapted eyes of desert ants, Cataglyphis bicolor (Formicidae, Hymenoptera). J. Morph. 140: 15-30.

Buddenbrock, W. von. 1935. Die Physiologie des Facettenauges. Biol. Rev. 10:283-316.

Bugnion, E. and N. Popoff. 1914. Les yeux des insectes nocturnes. Arch. Anat. Microsc. Paris. 16:261-304.

Burghause, F. 1976. Adaptationserscheinungen in den Komplexaugen von Gyrinus natator L. (Coleoptera: Gyrinidae). Int. J. Insect Morphol. & Embryol. 5:335-348.

Burkhardt, D., B. Darnhofer-Demar, and K. Fischer. 1973. Zum binokularen Entfernungssehen der Insekten. I. Die Struktur des Sehraums von Synsekten. J. Comp. Physiol. 87:165-188.

Burkhardt, D., I. de la Motte, and G. Seitz: 1966. Physiological optics of the compound eye of the blowfly. In: C.G. Bernhard ed. The Functional Organization of the Compound Eye. Pergamon Press, Oxford. pp. 51-62.

Burton, P.R. and K.A. Stockhammer. 1969. Electron microscope studies of the compound eye of the toadbug, Gelastocoris oculatus. J. Morph. 127:233-258.

Butler, R. 1973a. The anatomy of the compound eye of Periplaneta americana L. 1) General features. J. Comp. Physiol. 83:223-238.

Butler, R. 1973b. The anatomy of the compound eye of Periplaneta americana L. 2: Fine structure. J. Comp. Physiol. 83:239-262.

Butler, L., R. Roppel, and J. Zeigler. 1970. Post emergence maturation of the eye of the adult black carpet beetle, Attagenus megatoma (Fab.): An electron microscope study. J. Morph. 130:103-128.

Carlson, S.D. and C. Chi. 1974. Surface fine structure of the eye of the housefly (Musca domestica): Ommatidia and lamina ganglionaris. Cell Tiss. Res. 149:21-41.

Carlson, S.D., G. Gemme, and W.E. Robbins. 1966. Ultrastructure of photoreceptor cells in a vitamin-A deficient moth (Manduca sexta). Experimentia 25: 175-177.

Carlson, S.D. and J.R. Larsen. 1972a. Scanning electron microscopy of the insect compound eye. I: The apposition eye (Sarcophaga bullata). Z. Zellforsch. 126:437-445.

Carlson, S.D. and J.R. Larsen. 1972b. Scanning electron microscopy of the insect compound eye. II. The superposition eye (Manduca sexta). Z. Zellforsch. 126:446-453.

Carlson, S.D., H.R. Steeves III, and J.S. VandeBerg. 1967. Vitamin A deficiency: Effect on retinal structure of the moth Manduca sexta. Science 158:268-270.

Casey, T.L. 1897. Coleopterological notices 7. Ann. New York Acad. Sci. IX:285-684.

Chi, C. and S.D. Carlson. 1975. The distal ommatidium of the compound eye of the housefly (Musca domestica): A scanning electron microscope study. Cell Tiss. Res. 159:379-385.

Chi, C. and S.D. Carlson. 1976. The housefly interfacetal hair: Ultrastructure of a presumed mechanoreceptor. Cell Tiss. Res. 166:353-363.

Darwin, C. 1859. On the Origin of Species by Means of Natural Selection, or, the Preservation of Favored Races in the Struggle for Life. Republished by The Modern Library, 1936. Random House, Inc., New York. xvi + 386 pp.

Davis, W.T. 1921. Cicindela tranquebarica and its habits. Bull. Brooklyn Ent. Soc. 16:111.

Day, E. 1969. Black widow spider victimizes tiger beetle. CICINDELA 1:8.

de Bruin, G.H.P. and D.J. Crisp. 1957. Influences of pigment migration on vision of higher crustaceans. J. Exp. Biol. 34:447-463.

de Martino, C., P.G. Natali, C.B. Bruni, and L. Accinni. 1968. Influence of plastic embedding media on staining and morphology of lipid bodies: A light and ultrastructural study. Histochemie 16:350-360.

Deetz, C.H. and O.S. Adams. 1945. Elements of Map Projection with Applications to Map and Chart Construction. 5th ed. U.S. Department of Commerce Coast and Geodetic Society Special Publication 68:226 pp. + xv plates.

Diesendorf, M.O. and G.A. Horridge. 1973. Two models of the partially focused clear zone compound eye. Proc. Roy. Soc. Lond. B. 183:141-158.

Døving, K.B. and W.H. Miller. 1969. Function of insect compound eyes containing cyrstalline tracts. J. Gen. Physiol. 54:250-267.

Dvorak, D.R., L.G. Bishop, and H.E. Eckert. 1975. On the identification of movement detectors in the fly optic lobe. J. Comp. Physiol. 100:5-23.

Eakin, R.M. 1966. Evolution of photoreceptors. Cold Spring Harbor Symp. Quant. Biol. XXX:363-370.

Eakin, R.M. 1972. Structure of invertebrate photoreceptors. In: J.A. Dartnall ed. Handbook of Sensory Physiology 7(1):625-684.

Eakin, R.M. and J.L. Brandenburger. 1968. Localization of vitamin A in the eyes of a pulmonate snail. Proc. Nat. Acad. Sci. Wash. 60:140-145.

Edwards, H. 1875. On the localities and habits of the various species of Omus. Psyche 1:73-76.

Eguchi, E. 1971. Fine structure and spectral sensitivities of retinular cells in the dorsal sector of compound eyes in the dragonfly Aeschna. Z. Vergl. Physiol. 71:201-218.

Eguchi, E. and T.H. Waterman. 1967. Changes in retinal fine structure induced in the crab Libinia by light and dark adaptation. Z. Zellforsch. 79:209-229.

Eheim, W.P. and R. Wehner. 1972. Die Sehfelder der zentralen Ommatidien in den Appositionsaugen von Apis mellifica und Cataglyphis bicolor (Apidae, Formicidae; Hymenoptera). Kybernetik 10:168-179.

Eley, S. and P.M.J. Shelton. 1976. Cell junctions in the developing compound eye of the desert locust Schistocerca gregaria. J. Embryol. Exp. Morph. 36: 409-423.

Eltringham, H. 1919. Butterfly vision. Trans. Ent. Soc. Lond. 67:1-49 + v plates.

Eltringham, H. 1933. The insect eye. In: Ibid. The Senses of Insects. Methuen and Co. Ltd., London. pp. 7-35.

Exner, S. 1891. Die Physiologie der Facettirten Augen von Krebsen und Insecten. Franz Deutricke, Leipsig und Wien. xviii + 206 pp., 76 figs., VII Taf.

Faasch, von H. 1968. Beobachtungen zur Biologie und zum Verhalten von Cicindela hybrida L. und Cicindela campestris L. und experimentelle Analyse ihres Beutefangverhaltens. Zool. Jb. Syst. 95:477-522.

Fernández-Morán, H. 1958. Fine structure of the light receptors in the compound eyes of insects. Exp. Cell Res. Suppl. 5:586-644.

Fischer, A. and G. Horstmann. 1971. Der Feinbau des Auges der Mehlmotte, Ephestia kuehniella Zeller (Lepidoptera, Pyralididae). Z. Zellforsch. 116:275-304.

Foelix, R.F. and I-Wu Chu-Wang. 1973. The morphology of spider sensilla. I. Mechanoreceptors. Tiss. & Cell 5:451-460.

Freitag, R. 1974. Selection for a non-genetalic mating structure in female tiger beetles of the genus Cicindela. Can. Ent. 106:561-568.

Friedrichs, H. 1931. Beiträge zur Morphologie und Physiologie der Sehorgane der Cicindeliden. Zeit. Morph. Ökol. Tiere. 21:1-172.

Friza, F. 1928. Zur Frage der Färbung und Zeichnung des Facettierten Insektenauges. Z. Vergl. Physiol. 8: 289-336.

Fyg, W. 1961. Über die Kristallkegel in den Komplexaugen der Honigbiene (Apis mellifera L.). Bull. Soc. Ent. Swisse XXXIII:185-194.

Ganguly, J. 1969. Absorption of vitamin A. Am. J. Clin. Nutr. 22:923-933.

Gaumer, G.C. and R.R. Murray. 1971. Checklist of the Cicindelidae of Texas with regional distributions. CICINDELA 3:9-12.

Gemminger, Dr. and B. de Harold. 1868. Cicindelidae. In: Ibid. Catalogus Coleopterorum: Hucusque descriptorum synonymicus et systematicus. Monachii, Paris. I:1-40.

Gilmour, D. 1961. The Biochemistry of Insects. Academic Press, Inc., New York. xii + 343 pp.

Gissler, C.F. 1879. The anatomy of Amblycheila cyclindriformis Say. Psyche 2:233-248.

Gokan, N. 1973. The compound eyes of the lamellicorn leaf-chafers and the relation between their structures and activities. Kôntyu 41:106-125 (in Japanese with English summary).

Goldsmith, T.A. 1958. The visual system of the honeybee. Proc. Nat. Acad. Sci. Wash. 44:123-126.

Goldsmith, T.A. 1962. Fine structure of the retinulae in the compound eye of the honeybee. J. Cell Biol. 14:489-494.

Goldsmith, T.A. 1964. The visual system of insects. In: M. Rockstein ed. The Physiology of Insecta. 1st ed. Academic Press, New York. I:397-462.

Goldsmith, T.A. 1972. The natural history of invertebrate visual pigments. In: J.A. Dartnall ed. Handbook of Sensory Physiology. Springer-Verlag, New York. 7(1):685-719.

Goldsmith, T.A. and G.D. Bernard. 1974. The visual system of insects. In: M. Rockstein ed. The Physiology of Insecta. 2nd ed. Academic Press, New York. II: 165-272.

Graves, R.C. 1962. Predation on Cicindela by a dragonfly. Can. Ent. 94:1231.

Graves, R.C. and D.L. Pearson. 1973. The tiger beetles of Arkansas, Louisiana, and Mississippi (Coleoptera: Cicindelidae). Trans. Am. Ent. Soc. 99:157-203.

Grenacher, H. 1879. Untersuchungen über das Sehorgan der Arthropoden inshesondere der Spinnen, Insecten und Crustaceen. Verlag von Vandenhoeck und Ruprecht, Göttingen. vii + 188 pp., 127 figs., xi plates.

Gribakin, F.G. 1969. The ultrastructural organization of the photoreceptors of insects. Inst. Evol. Physiol. Biochem. Acad. Sci. U.S.S.R. 53:238-273 (in Russian).

Gribakin, F.G. 1972. The distribution of the long wave photoreceptors in the compound eye of the honey bee as revealed by selective osmic staining. Vision Res. 12:1225-1230.

Gribakin, F.G. 1975. Functional morphology of the compound eye of the bee. In: G.A. Horridge ed. The Compound Eye and Vision of Insects. Clarendon Press, Oxford. pp. 154-176.

Guérin-Méneville, F.E. 1845. Note sur le Dromochorus (Cicindela) sur la Fulgora cyanirostris, et Ptilophylum Godeyi (Lucanide). Ann. Soc. Ent. Fr. Sér. 2. 3:95-98.

Halliday, D. and R. Resnick. 1970. Interference. In: Ibid. Fundamentals of Physics. John Wiley and Sons, Inc., New York. pp. 703-723.

Hasselmann, E-M. 1962. Über die relative spektrale Empfindlichkeit von Käfer- und Schmetterlingsaugen bei verschiedenen Helligkeiten. Zool. Jb. Physiol. 69:537-576.

Hatch, M.H. 1953. The Beetles of the Pacific Northwest. Part I: Introduction and Adephaga. University of Washington Press, Seattle. vii + 340 pp.

Hayat, M.A. 1970. Principles and Techniques of Electron Microscopy: Biological Applications. Van Nostrand Reinhold Co., New York. I:xv + 412 pp.

Hocking, B. 1964. Aspects of insect vision. Can. Ent. 96:320-334.

Höglund, G., K. Hamdorf, H. Langer, R. Paulsen, and J. Schwemer. 1973. The photopigments of an insect retina. In: H. Langer ed. Biochemistry and Physiology of Visual Pigments. Springer-Verlag, New York. pp. 167-174.

Hollenberg, M.J. and A.M. Erickson. 1973. The scanning electron microscope: Potential usefulness to biologists. J. Histochem. Cytochem. 21:109-130.

Homann, H. 1928. Beitrage zur Physiologie des Spinnenaugen I and II. Z. Vergl. Physiol. 7:201-268.

Home, E.M. 1972. Centrioles and associated structures in the retinula cells of insect eyes. Tiss. & Cell 4:227-234.

Home, E.M. 1975. Ultrastructural studies of development and light-dark adaptation of the eye of Coccinela septempunctata L., with particular reference to ciliary structures. Tiss. & Cell 7:703-722.

Home, E.M. 1976. The fine structure of some carabid beetle eyes, with particular reference to ciliary structures in the retinula cells. Tiss. & Cell 8:311-333.

Honegger, H.W. 1977. Interommatidial hair receptor axons extending into the ventral nerve cord in the cricket Gryllus campestris. Cell Tiss. Res. 182:281-285.

Horn, G.H. 1886. Some critical notes. Entomologica Americana. II:207-209.

Horn, G.H. 1903. List of the Cicindelidae of Mexico and on their relationship with the species of the United States, J. New York Ent. Soc. XI:213-221.

Horn, G.H. 1908-1915. Coleoptera, Family Carabidae, Subfamily Cicindelinae. Genera Insectorum. P. Wytsman, Brussels 82C:209-486.

Horn, G.H. 1926. Carabidae: Cicindelidae. In: S. Schenkling ed. Coleopterum Catalogus. W. Junk, Berlin I:1-486 pp. + 23 plates.

Horn, G.H. 1930. Notes on the races of Omus californicus and a list of the Cicindelidae of America north of Mexico. Trans. Am. Ent. Soc. 56:73-86.

Horridge, G.A. 1968. Pigment movements and the crystalline threads of the firefly eye. Nature 218:778-779.

Horridge, G.A. 1969a. The eye of Dytiscus (Coleoptera). Tiss. & Cell 1:425-442.

Horridge, G.A. 1969b. The eye of the firefly Photuris. Proc. Roy. Soc. Lond. B. 171:445-463.

Horridge, G.A. 1971. Alternatives to superposition images in clear-zone compound eyes. Proc. Roy. Soc. Lond. B. 179:97-124.

Horridge, G.A. 1972. Further observations on the clear zone eye of Ephestia. Proc. Roy. Soc. Lond. B. 181:157-173.

Horridge, G.A. 1974. Insect vision. In: The Insects of Australia Supplement. Melbourne University Press, Australia. pp. 1-6.

Horridge, G.A. ed. 1975a. The Compound Eye and Vision of Insects. Clarendon Press, Oxford. xviii + 595 pp.

Horridge, G.A. 1975b. Optical mechanisms of clear-zone eyes. In: G.A. Horridge ed. The Compound Eye and Vision of Insects. Clarendon Press, Oxford. pp. 255-298.

Horridge, G.A. 1976. The ommatidium of the dorsal eye of Cloeon as a specialization for photoreisomerization. Proc. Roy. Soc. Lond. B. 193:17-29.

Horridge, G.A. 1977a. Insects which turn and look. End. 1:7-17.

Horridge, G.A. 1977b. The compound eye of insects. Sci. Am. 237:108-120.

Horridge, G.A. and P.B.T. Barnard. 1965. Movement of palisade in locust retinula cells when illuminated. Quart. J. Micr. Sci. 106:131-135.

Horridge, G.A. and C. Giddings. 1971a. Movement on dark-light adaptation in beetle eyes of the neuropteran type. Proc. Roy. Soc. Lond. B. 179:73-85.

Horridge, G.A. and C. Giddings. 1971b. The retina of Ephestia (Lepidoptera). Proc. Roy. Soc. Lond. B. 179:87-95.

Horridge, G.A., C. Giddings, and G. Stange. 1972. The superposition eye of skipper butterflies. Proc. Roy. Soc. Lond. B. 182:457-469.

Horridge, G.A. and I. Henderson. 1976. The ommatidium of the lacewing Chrysopa (Neuroptera). Proc. Soc. Lond. B. 192:259-271.

Horridge, G.A., K. Mimura, and R.C. Hardie. 1976. Fly photoreceptors. III. Angular sensitivity as a function of wavelength and the limits of resolution. Proc. Roy. Soc. Lond. B. 194:151-177.

Horridge, G.A., B.W. Minham, and M.O. Diesendorf. 1972. Theory of the summation of scattered light in clear zone compound eyes. Proc. Roy. Soc. Lond. B. 181: 137-156.

Horridge, G.A., B. Walcott, and A.C. Ioannides. 1970. The tiered retina of Dytiscus: A new type of compound eye, Proc. Roy. Soc. Lond. B. 175:83-94.

Humason, G.L. 1962. Animal Tissue Techniques. W.H. Freeman and Co., San Francisco. xv + 468 pp.

Jones, A.W. 1884. Notes on the habits of Cicindelidae. Bull. Brooklyn Ent. Soc. VII:74-76.

Karplus, M. 1973. Theory of retinal and related moleculgs. In: H. Langer ed. Biochemistry and Physiology of Visual Pigments. Springer-Verlag, New York. pp. 17-18.

Kim, C.W. 1964. Formation and histochemical analysis of the crystalline cone of compound eye in Pieris rapae L. (Lepidoptera). Kor. J. Zool. VII:89-94.

Kirchoffer, O. 1905. Untersuchungen über eucone Käferaugen. Gesell. Nat. Freunde. 5:149-153.

Kirchoffer, O. 1908. Untersuchungen über die Augen der pentameren Käfer. Arch. Biontol. 2:1-32.

Kirschfeld, K. 1967. Die projektion der optischen Umwelt auf das Raster der Rhabdomere im Komplexauge von Musca. Exptl. Brain Res. 3:248-270.

Knaus, W. 1900. The Cicindelidae of Kansas. Can. Ent. XXXII:109-116.

Kolb, G. and H. Autrum. 1972. Die Feinstruktur im Auge der Biene bei Hell- und Dukeladaptation. J. Comp. Physiol. 77:113-125.

Koyama, N. 1964. Estimation of activities of Bombycid and Saturniid moths by the structure of compound eye. J. Sericul. Sci. Japan 33:24-27 (in Japanese with English summary).

Koyama, N. 1971. Notes on the compound eye of the lepidopterous insects. 2. Interfacetal hairs. New. Ent. 20:41-49 (in Japanese with English summary).

Koyama, N., N. Gokan, and M. Matsui. 1975. The compound eye of the longicorn beetles (Coleoptera: Cerambycidae) with estimation of the activities by its structure. J. Facul. Text. Sci. & Tech. Shinshu Univ. Ser. A. Biol. 18:1-16 (in Japanese with English summary).

Koyama, N. and K. Ogawa. 1972. Notes on the compound eye of the lepidopterous insects. 3. The interfacetal hair and the occipital structure in the two species belonging to the genus Neope, Satyridae. New. Ent. 21:23-30 (in Japanese with English summary).

Kuhn, T.S. 1970. The Structure of Scientific Revolutions. 2nd ed. The University of Chicago Press, Chicago. xii + 210 pp.

Kunze, P. 1972. Comparative studies of arthropod superposition eyes. Z. Vergl. Physiol. 76:347-357.

Kuster, J.E. 1973. Book Review: Wehner, R. ed. 1972. Information Processing in the Visual Systems of Arthropods. Springer, New York. xi + 334 pp., 263 figs. Quaest. Ent. X:257-258.

Kuster, J.E. 1975. Micrograph of the compound eye of Cicindela tranquebarica Herbst. Cover. CICINDELA 7(3).

Kuster, J.E. 1976. Collection of Amblycheila schwarzi W. Horn (Coleoptera: Cicindelidae) in Joshua Tree National Monument, California. CICINDELA 8:11-12.

Lacordaire, M.T. 1843. Révision de la famille des Cicindélides (Cicindelidae) de l'ordre des Coléoptères, accompagnée de la création de quelques genres nouveaux. Hist. Nat. des Insect IV:24-120.

Lacordaire, M.T. 1854. Histoire Naturelle des Insectes. Genera des Coléoptères. Librairie encyclopédique de Roret, Paris. I:486 pp.

Langer, H. ed. 1973. Biochemistry and Physiology of Visual Pigments. Springer-Verlag, New York. xiii + 366 pp.

Langer, H. and B. Thorell. 1966. Microspectrophotometry of single rhabdomeres in the insect eye. Exp. Cell Res. 41:673-677.

Lantz, D.E. 1905. Notes on collecting Cicindelidae. Trans. Kansas Acad. Sci. 19:252-260.

Larochelle, A. 1972. On some enemies of tiger beetles. CICINDELA 4:67-68.

Larochelle, A. 1974a. The food of Cicindelidae of the world. CICINDELA 6:21-39.

Larochelle, A. 1974b. North American amphibians and reptiles as predators of tiger beetles. CICINDELA 6:83-86.

Larochelle, A. 1975a. Birds as predators of tiger beetles. CICINDELA 7:1-7.

Larochelle, A. 1975b. North American mammals as predators of tiger beetles. CICINDELA 7:9-11.

Lavigne, R.J. 1977. Additional records of cicindelids as prey of robber flies (Diptera: Asilidae). CICINDELA 9:25-27.

Lawko, C.M. 1971. A double replica method for counting ommatidia in curved compound eyes. Can. Ent. 103: 1849-1850.

Lawton, J.K. 1972. Translation and condensation of Horn's notes on the habits of the world genera of Cicindelidae. CICINDELA 4:9-18.

LeConte, J.L. 1857. Revision of the Cicindelidae of the United States. Am. Phil. Soc. Trans. New Series. 11:27-62 + 1 plate.

Leng, C.W. 1902. Revision of the Cicindelidae of boreal America. Trans. Am. Ent. Soc. XXVIII:93-186 + iv plates.

Leng, C.W. 1920. Catalogue of the Coleoptera of America, North of Mexico. The Cosmos Press, Cambridge, Massachusettes. x + 470 pp.

Lévin, L. and H. Maldonado. 1970. A fovea in the preying mantis eye. III. The centering of the prey. Z. Vergl. Physiol. 67:93-101.

Lindroth, C.H. 1961. The ground-beetles (Carabidae, excl. Cicindelinae) of Canada and Alaska. Part 2. Opusc. Ent. (Lund) Suppl. 20:1-200.

Lindroth, C.H. 1963. Part 4. Opusc. Ent. (Lund) Suppl. 29:409-648.

Locke, M. 1961. Pore canals and related structures in insect cuticle. J. Biophys. Biochem. Cytol. 10: 589-618.

Locke, M. 1965. The structure of septate desmosomes. J. Cell Biol. 25:166-169.

Locke, M. 1974. The structure and formation of the integument in insects. In: M. Rockstein ed. The Physiology of Insecta. 2nd ed. Academic Press, New York. VI: 123-213.

Locke, M. and J.V. Collins. 1967. Protein uptake in multivesicular bodies in the molt-intermolt cycle of an insect. Science 155:467-469.

Luft, J.H. 1961. Improvements in epoxy resin embedding methods. J. Biophys. Biochem. Cytol. 9:409-414.

Mainwaring, J. 1942. An Introduction to the Study of Map Projections. Macmillan and Co. Ltd., London. 114 pp.

Maldonado, H. and J.C. Barrós-Pita. 1970. A fovea in the preying mantis eye. I. Estimation of the catching distance. Z. Vergl. Physiol. 67:58-78.

Maser, C. 1973. Notes on predators upon cicindelids. CICINDELA 5:21-23.

Maser, C. and F.M. Beer. 1971. Notes on the daily activity of Omus audouini and Omus dejeani. CICINDELA 3:52.

Matsusaka, T. 1967. ATPase activity in the ciliary rootlet of human retinal rods. J. Cell Biol. 33:203-208.

Mazokin-Porshnyakov, G.A. 1969. Insect Vision: translated from Russian by R. and L. Masironi, with T.H. Goldsmith ed. Plenum Press, New York, xiv + 306 pp.

McIver, S.B. 1975. Structure of cuticular mechanoreceptors of arthropods. Ann. Rev. Ent. 20:381-397.

Melluish, R.K. 1931. An Introduction to the Mathematics of Map Projections. Cambridge University Press, Cambridge. viii + 145 pp.

Menzel, R. 1972. Feinstruktur des Komplexauges der Roten Waldameise, Formica polyctena (Hymenoptera, Formicidae). Z. Zellforsch. 127:356-373.

Menzel, R. 1975a. Polarisation sensitivity in insect eyes with fused rhabdoms. In: A.W. Snyder, and R. Menzel eds. Photoreceptor Optics. Springer-Verlag, New York. pp. 372-387.

Menzel, R. 1975b. Colour receptors in insects. In: G.A. Horridge ed. The Compound Eye and Vision of Insects. Clarendon Press, Oxford. pp. 121-153.

Menzel, R. and A.W. Snyder. 1974. Polarized light detection in the bee, Apis mellifera. J. Comp. Physiol. 88: 247-270.

Meyer-Rochow, V.B. 1971. A crustacean-like organization of insect rhabdoms. Cytobiologie 4:241-249.

Meyer-Rochow, V.B. 1972. The eyes of Creophilus erythrocephalus F. and Sartallus signatus Sharp (Staphylinidae: Coleoptera) light-interference-scanning-electron- and transmission electron microscopy. Z. Zellforsch. 133:59-86.

Meyer-Rochow, V.B. 1973. The dioptric system of the eye of Cybister (Dytiscidae: Coleoptera). Proc. Roy. Soc. Lond. B. 183:159-178.

Meyer-Rochow, V.B. 1975. The dioptric system in beetle compound eyes. In: G.A. Horridge ed. The Compound Eye and Vision of Insects. Clarendon Press, Oxford. pp. 299-313.

Meyer-Rochow, V.B. and G.A. Horridge. 1975. The eye of Anoplognathus (Coleoptera, Scarabaeidae). Proc. Roy. Soc. Lond. B. 188:1-30.

Miller, W.H., G.D. Bernard, and J.L. Allen. 1968. Optics of insect compound eyes. Science 162:759-771.

Millonig, G. 1961. Advantages of a phosphate buffer for osmium tetroxide solutions in fixation. J. Appl. Physics 32:1637.

Mitchell, J.D. 1905. Observations on the habits of two Cicindelidae. Proc. Ent. Soc. Wash. 5:108-110.

Mollweide, K.B. 1806. Analytische Theorie der stereographische Porjektion. Monatliche Correspondenz zur Beförderung der Erd- und Himmeiskunde. 14.

Mollweide, K.B. 1807. Einige Projektions arten der Sphädroidischen Erde. Monatliche Correspondenz zur Beförderung der Erd- und Himmelskunde. 16.

Moody, M.F. and J.R. Parriss. 1961. The discrimination of polarized light by Octopus: A behavioural and morphological study. Z. Vergl. Physiol. 44:268-291.

Moor, H. 1971. Recent progress in the freeze-etching technique. Phil. Trans. Roy. Soc. Lond. B. 261: 121-131.

Moore, R. 1906. Notes on the habits of Cicindela. Ent. News 17:338-343.

Müller, J. 1879. Zur vergleichenden Physiologie des Gesichtssinnes des Menschen und Tiere. C. Cnobloch, Leipzig. xxxii + 462 pp., 8 plates.

Munoz-Cuevas, A. 1975. Modèle ciliare de développement du photorécepteur chez l'opilion Ischyropsalis luteipes (Arachnida). C.R. Acad. Sci. Paris 280: 725-727.

Nei, T. 1974. Cryotechniques. In: M.A. Hayat ed. Principles and Techniques of Scanning Electron Microscopy: Biological Applications. Van Nostrand Reinhold Co., New York. I:113-124.

Nesse, V. 1965. Zur Funktion der Augenborsten bei der Honigbiene. Z. Vergl. Physiol. 49:543-585.

Nesse, V. 1966. Zur Bedeutung der Augenborsten bei der Fluggeschwindigkeitsregulation der Bienen. Z. Vergl. Physiol. 52:149-154.

Neville, A.C. 1975. Biology of the Arthropod Cuticle. Springer-Verlag, New York. xvi + 448 pp.

Neville, A.C., M.G. Thomas, and B. Zelazny. 1969. Pore canal shape related to molecular architecture of arthropod cuticle. Tiss. & Cell 1:183-200.

Ninomiya, N., Y. Tominaga, and M. Kuwabara. 1969. The fine structure of the compound eye of a damsel-fly. Z. Zellforsch. 98:17-32.

Nowikoff, M. 1931. Untersuchungen über die Komplexaugen von Lepidopteran nebst einigen Bemerkungen über die Rhabdome der Arthropoden im allgemeinen. Zeit. Wiss. Zool. 138:1-67.

Pantin, C.F.A. 1962. Notes on Microscopical Techniques for Zoologists. 2nd ed. Cambridge University Press, Cambridge. viii + 77 pp.

Pappas, C.D. and J.R. Larsen. 1973. Fine structure of the light- and dark-adapted dorsal eyes of Dineutes assimilis Kirby (Coleoptera: Gyrinidae). Am. Zool. 13:1341.

Perrelet, A. 1970. The fine structure of the retina of the honey bee drone. Z. Zellforsch. 108:530-562.

Perrelet, A. 1972. Protein synthesis in the visual cells of the honey bee drone as studied with electron microscope radioautography. J. Cell Biol. 55:595-605.

Perrelet, A. and F. Baumann. 1969. Presence of three small retinula cells in the ommatidium of the honey-bee drone eye. J. Microscopie 8:497-502.

Perrelet, A., H. Bauer, and V. Fryder. 1972. Fracture faces of an insect rhabdome. J. Microscopie 13: 97-106.

Phillips, E.F. 1905. Structure and development of the compound eye of the honey bee. Proc. Acad. Nat. Sci. Phil. 57:123-157.

Pitelka, D.R. 1974. Basal bodies and root structures. In: M.A. Sleigh ed. Cilia and Flagella. Academic Press, New York. pp. 437-469.

Portillo, J. 1936. Beziehungen zwischen den Öffnunngs-winkeln der Ommatidien, Krümmung und Gestalt der Insekten-Augen und ihrer funktionellen Aufgabe. Z. Vergl. Physiol. 23:100-145.

Pritchard, G. 1966. On the morphology of the compound eyes of dragonflies (Odonata: Anisoptera), with speical reference to their role in prey capture. Proc. Roy. Ent. Soc. Lond. A. 41:1-8.

Rees, H.H. 1977. Insect Biochemistry. John Wiley and Sons, New York. 64 pp.

Ribi, W.A. 1974. Neurons in the first synaptic region of the bee, Apis mellifera. Cell Tiss. Res. 148:277-286.

Ribi, W.A. 1975a. The first optic ganglion of the bee. I. Correlation between visual cell types and their terminals in the lamina and medulla. Cell Tiss. Res. 165:103-111.

Ribi, W.A. 1975b. Golgi studies of the first optic ganglion of the ant, Cataglyphis bicolor. Cell Tiss. Res. 160:207-217.

Ribi, W.A. 1976. The first optic ganglion of the bee. II. Topographical relationships of the monopolar cells within and between cartridges. Cell Tiss. Res. 171: 359-373.

Ribi, W.A. 1977. Fine structure of the first optic ganglion (lamina) of the cockroach, Periplaneta americana. Tiss. & Cell 9:57-72.

Richardson, K.C., L. Jarett, and E.H. Finke. 1960. Embedding in epoxy resins for ultrathin sectioning in electron microscopy. Stain Tech. 35:313-323.

Rivalier, E. 1954. Démembrement du genre Cicindela Linné. II. Faune américaine. Rev. Franç., d'ent. 22: 249-268.

Ruck, P. 1964. Retinal structures and photoreception. Ann. Rev. Ent. 9:83-102.

Rutherford, D.J. and G.A. Horridge. 1965. The rhabdom of the lobster eye. Quart. J. Micr. Sci. 106:119-130.

Sallé, A. 1877. Communications: Seance du 10 Janvier. Ann. Soc. Ent. France Ser. 5. Bull. Seances. 7:4-6.

Schaupp, F.G. 1883. Synoptic tables of Coleoptera: Cicindelidae. Bull. Brooklyn Ent. Soc. VI:73-124 + v plates.

Schilder, F.A. 1953. Studien zur Evolution von Cicindela. Wiss. Z. Univ. Halle, Math.-Nat. 3:539-576.

Scott, E.A. 1937. The eyes of insects and their adaptation to habit and environment. J. Ent. Zool. XXIX:33-65.

Seitz, G. 1968. Der Strahlengang im Appositionsauge von Calliphora erythrocephala (Meig.). Z. Vergl. Physiol. 59:205-231.

Seitz, G. 1969. Untersuchungen am dioptrischen Apparat des Leuchtkäferauges. Z. Vergl. Physiol. 62:61-74.

Seitz, G. 1970. Nachweis einer Pupillenreaktion im Auge der Schmeissfliege. Z. Vergl. Physiol. 69:169-185.

Shaw, S.R. 1969. Interreceptor coupling in ommatidia of drone honeybee and locust compound eyes. Vision Res. 9:999-1030.

Shaw, S.R. 1977. Restricted diffusion and extracellular space in the insect retina. J. Comp. Physiol. 113: 257-282.

Shelford, V.E. 1917. Color and color-pattern mechanism of tiger beetles. Illinois Biol. Monographs. 111: 1-135 + 3 plates.

Sherk, T.E. 1978. Development of the compound eyes of dragonflies (Odonata). III. Adult compound eyes. J. Exp. Zool. 203:61-80.

Skrzipek, K.H. and H. Skrzipek. 1971a. Die Morphologie der Bienenretina (Apis mellifica L.) in electronenmikroskopischer und lichtmikroskopischer Sicht. Z. Zellforsch. 119:552-576.

Skrzipek, K.H. and H. Skrzipek. 1971b. Zur funktionellen Bedeutung der räumlichen Anordnung des Kristallkegels zum Rhabdom im Auge der Trachtbiene (Apis mellifica L.). Experimentia 27:409-411.

Skrzipek, K.H. and H. Skrzipek. 1974. The ninth retinula cell in the ommatidium of the worker honey bee (Apis mellifica L.). Z. Zellforsch. 147:589-593.

Snow, F.H. 1877. Hunting Amblycheila. Am. Nat. XI: 731-735.

Snyder, A.W. 1972. Angular sensitivity of the bee ommatidium. Z. Vergl. Physiol. 76:438-445.

Snyder, A.W. 1973. Polarization sensitivity of individual retinula cells. J. Comp. Physiol. 83:331-360.

Snyder, A.W. and G.A. Horridge. 1972. The optical function of changes in the medium surrounding the cockroach rhabdom. J. Comp. Physiol. 81:1-8.

Snyder, A.W. and R. Menzel eds. 1975. Photoreceptor Optics. Springer-Verlag, New York. x + 523 pp.

Snyder, A.W., R. Menzel, and S.B. Laughlin. 1973. Structure and function of the fused rhabdom. J. Comp. Physiol. 87:99-135.

Sokal, R.R. and F.J. Rohlf. 1969. Biometry: The Principles and Practice of Statistics in Biological Research. W.H. Freeman and Co., San Francisco. xxi + 776 pp.

Strausfeld, N.J. and M. Obermayer. 1976. Resolution of intraneuronal and transynaptic migration of cobalt in the insect visual and central nervous systems. J. Comp. Physiol. 110:1-12.

Swiecimski, J. 1957. The role of sight and memory in food capture by predatory beetles of the species Cicindela hybrida L. (Coleoptera, Cicindelidae). Polskie Pismo Ent. 26:205-232.

Thompson, M.J. 1857. Monographie des Cicindélides ou Exposé Méthodique et Critique des Tribus, Genres et Espèces de cette Famille. Société Entomologique de France, Paris. I:xvii + 66 pp. + x plates.

Trujillo-Cenóz, O. 1966. Some apsects of the structural organization of the arthropod eye. Cold Spring Harbour Symp. Quant. Biol. 30:371-382.

Trujillo-Cenóz, O. 1972. The structural organization of the compound eyes in insects. In: M.G. Fuortes ed. Handbook of Sensory Physiology. Springer-Verlag, New York. 7(2):5-62.

Trujillo-Cenóz, O. and J. Melamed. 1966. Compound eye of dipterans: Anatomical basis for integration. An electron microscope study. J. Ultrastruct. Res. 16:395-398.

Tunstall, J. and G.A. Horridge. 1967. Electrophysiological investigation of the optics of the locust retina. Z. Vergl. Physiol. 55:167-182.

Tuurala, O. and A. Lehtinen. 1971. Über die Einwirkung von Licht und Dunkel auf die Feinstruktur der Lichtsinneszellen der Assel Oniscus asellus L. Ann. Acad. Sci. Fenn. A. IV. Biol. 177:1-8.

Umbach, W. 1934. Entwicklung und bau des Komplexauges der Mehlmotte Ephestia kühniella Zeller nebst einigen Bemerkungen über die Entstehung der Optischen Ganglien. Z. Morph. Ökol. Tiere 28:561-594.

Vanfleteren, J.R. and A. Coomans. 1976. Photoreceptor evolution and phylogeny. Z. Zool. Syst. Evolut-forsch. 14:157-169.

Varela, F.G. and K.R. Porter. 1969. Fine structure of the visual system of the honeybee (Apis mellifera). I. The retina. J. Ultrastruct. Res. 29:236-259.

Varela, F.G. and W. Wiitanen. 1970. The optics of the compound eye of the honeybee (Apis mellifera). J. Gen. Physiol. 55:336-358.

Vaurie, P. 1955. A review of the North American genus Amblycheila (Coleoptera, Cicindelidae). Am. Mus. Nov. 1724:26 pp.

Venable, J.H. and R. Coggeshall. 1965. A simplified lead citrate stain for use in electron microscopy. J. Cell Biol. 25:407-408.

Wachmann, E. 1969. Multivesikuläre und andere Einschlusskörper in den Retinulazellen der Sumpfgrille Pteronemobius heydeni (Fischer). Z. Zellforsch. 99:263-276.

Wachmann, E. 1970. Zum Feinbau der Ommatidien von Pteronemobius heydeni (Fisch.) (Orthoptera, Gryllidae). Z. Zellforsch. 108:46-58.

Wachmann, E. and A. Hennig. 1974. Centriolen in der Entwicklung der Retinulazellen von Megachile rotundata (F.) (Hymenoptera, Apidae). Z. Morph. Tiere 77: 337-344.

Wachmann, E., S. Richter, and B. Schricker. 1973. Feinstrukturen im Komplexauge der Blattschneiderbiene Megachile rotundata (F.) (Hymenoptera, Apidae). Z. Morph. Tiere 76:109-128.

Wachmann, E. and W-D. Schröer. 1975. Zur Morphologie des Dorsal- und Ventralauges des Taumelkäfers Gryinus substriatus (Steph.) (Coleoptera, Gyrinidae). Zoomorphologie 82:43-61.

Wada, S. 1975. Morphological duality of the retinal pattern in flies. Experimentia 31:921-923.

Waddington, C.H. and M.M. Perry. 1963. Inter-retinular fibers in the eyes of Drosophila. J. Ins. Physiol. 9:475-478.

Wald, G. 1968. Molecular basis for visual excitation. Nature 219:800-807.

Walcott, B. 1975. Anatomical changes during light adaptation in insect compound eyes. In: G.A. Horridge ed. The Compound Eye and Vision of Insects. Clarendon Press, Oxford. pp. 20-33.

Wallis, J.B. 1913. Robber-fly and tiger beetle. Can. Ent. 45:135.

Wallis, J.B. 1961. The Cicindelidae of Canada. University of Toronto Press, Toronto. x + 74 pp.

Washizu, Y., D. Burkhardt, and P. Streck. 1964. Visual field of single retinula cells and interommatidial inclination in the compound eye of the blowfly, Calliphora erythrocephala. Z. Vergl. Physiol. 46: 413-428.

Weast, R.C. ed. 1975. Handbook of Chemistry and Physics. 56th ed. Chemical Rubber Publishing Co., Cleveland, Ohio.

Weber, H. 1933. Die Sinnesorgane. In: Ibid. Lehrbuch der Entomologie. Gustavfischer Verlag, Stuttgart, Germany. pp. 276-341.

Wehner, R. ed. 1972. Information Processing in the Visual Sytems of Arthropods. Springer-Verlag, New York. xi + 334 pp.

Wehner, R. 1976. Polarized light navigation by insects. Sci. Am. 235:106-115.

Wehner, R., G.D. Bernard, and E. Geiger. 1975. Twisted and nontwisted rhabdoms and their significance for polarization detection in the bee. J. Comp. Physiol. 104:225-245.

Weis-Fogh, T. 1949. An aerodynamic sense organ stimulating and regulating flight in locusts. Nature 164:873-874.

Weis-Fogh, T. 1956. Biology and physics of locust flight. IV. Notes on sensory mechanisms in locust flight. Phil. Trans. Roy. Soc. Lond. B. 239:553-584.

White, R.H. 1968. The effect of light and light deprivation upon the ultrastructure of the larval mosquito eye. III. Multivesicular bodies and protein uptake. J. Exp. Zool. 169:261-278.

Willis, H.L. 1967. Bionomics and zoogeography of tiger beetles of saline habitats in the central United States (Coleoptera: Cicindelidae). Univ. Kansas Sci. Bull. 47:145-313.

Willis, H.L. 1968. Artificial key to the species of Cicindela of North America north of Mexico (Coleoptera: Cicindelidae). J. Kansas Ent. Soc. 41:303-317.

Willis, H.L. 1969. Translation and condensation of Horn's key to world genera of Cicindelidae. CICINDELA 1:1-15.

Williston, S.W. 1877. Note on the habits of A. cylindriformis. Can. Ent. 9:163-165.

Wolken, J.J. 1968. The photoreceptors of arthropod eyes. Symp. Zool. Soc. Lond. 23:113-133.

Wolken, J.J. 1975. Photoprocesses, Photoreceptors, and Evolution. Academic Press, New York. xiii + 317 pp.

Yagi, N. 1951. Studies on the compound eyes of lepidoptera. 1. On the compound eyes of butterflies, especially on the pseudopupil and its meaning to the phylogeny of species. J. Fac. Tex. Sericult. Shinshu Univ. 1:131-173 (in Japanese with English summary).

Yagi, N. 1953. The taxonomic position of the Hesperiidae as derived from the morphology of the compound eye. Trans. Ninth Int. Congr. Ent. 1:76-78.

Yagi, N. and N. Koyama. 1963a. The Compound Eye of Lepidoptera: Approach from organic evolution. Shinkyo-Press and Co. Ltd. 319 pp.

Yagi, N. and N. Koyama. 1963b. Estimation of activities of moths by structures of the compound eyes. Jap. J. Appl. Ent. Zool. 7:316-320 (in Japanese with English summary).

8. Vita

I was born November 22, 1951 in Fort William, Ontario, the younger of two girls. My father is design and development engineering manager, rail division for Toronto Area Transit Operating Authority; my mother, a housewife and volunteer worker for community projects.

My elementary education was received both in Fort William and Dorval, Montreal. During those years, my major recreation was the Montreal Junior Ballet Company and gymnastics. My high school education was received at Selkirk Collegiate and Vocational Institute, Thunder Bay F, Ontario where I participated in a variety of intellectual and recreational pursuits including: secretary of the Biology Club, literary editor of the "Kaministigoyan" year book, vice-president of the Students' Council, and president of Canadian Girls in Training, Fort William Baptist Church; cheerleader and forward on the intercollegiate basketball team. In 1973 I graduated from Lakehead University, Thunder Bay, Ontario with a B.Sc. biology, receiving the dean of science gold medal and a Gulf Oil Canada Limited graduate student fellowship. I was funded in my third undergraduate year with a Lakehead University Alumni Scholarship.

During three summers in high school, I worked as a playground supervisor for the Board of Parks and Recreation,

Thunder Bay. While in first year university, I supply taught science subjects at my previous high school. Between my second and third university years, I was a research assistant for Dr. R. Freitag, entomologist. At this time, I began serious research pursuits in histology of cicindelid compound eyes and female genitalia. During my third undergraduate year, I demonstrated a tree morphology laboratory in forestry.

Upon receipt of my baccalaureate in 1973, I travelled west to the Department of Entomology, The University of Alberta, to further pursue my interests in cell biology and sensory physiology resulting in the research reported here. As part of my training, in 1974 I spent a month touring entomological laboratories and museums, and collecting cicindelids in California. During my graduate years I was a teaching assistant for the laboratories of the following courses: insect morphology, insect developmental morphology, entomology for biologists, and entomology for non-biologists. Also, I have participated in provincial, national, and international conferences.

This thesis represents my statement of intent to pursue a research career in the life sciences.

Publications:

Kuster, Janice E. 1973. Book Review: Wehner, R. (Editor). 1972. Information Processing in the Visual Systems of Arthropods. Springer, Berlin, New York. xi + 334 pp., 363 figs. Quaest Ent. X(4):257-258.

Kuster, Janice E. 1975. Micrograph of the compound eye of Cicindela tranquebarica Herbst. Cover. CICINDELA 7(3).

Kuster, Janice E. 1976. Collection of Amblycheila schwarzi W. Horn (Coleoptera: Cincindelidae) in Joshua Tree National Monument, California. CICINDELA 8(1):11-12.